



# Biomarqueurs solubles et tissulaires dans le cancer bronchique non à petites cellules traité par immunothérapie

Adrien Costantini

## ► To cite this version:

Adrien Costantini. Biomarqueurs solubles et tissulaires dans le cancer bronchique non à petites cellules traité par immunothérapie. Cancer. Université Paris-Saclay, 2024. Français. NNT : 2024UPASL090 . tel-04849309

HAL Id: tel-04849309

<https://theses.hal.science/tel-04849309v1>

Submitted on 19 Dec 2024

**HAL** is a multi-disciplinary open access archive for the deposit and dissemination of scientific research documents, whether they are published or not. The documents may come from teaching and research institutions in France or abroad, or from public or private research centers.

L'archive ouverte pluridisciplinaire **HAL**, est destinée au dépôt et à la diffusion de documents scientifiques de niveau recherche, publiés ou non, émanant des établissements d'enseignement et de recherche français ou étrangers, des laboratoires publics ou privés.

# Biomarqueurs solubles et tissulaires dans le cancer bronchique non à petites cellules traité par immunothérapie

*Soluble and tissue-based biomarkers in non-small cell lung cancer treated with immunotherapy*

## Thèse de doctorat de l'université Paris-Saclay

École doctorale n° 582, Cancérologie : biologie – médecine - santé (CBMS)

Spécialité de doctorat : Sciences du Cancer

Graduate School : Sciences de la vie et santé.

Référent : Université de Versailles Saint-Quentin-en-Yvelines

Thèse préparée dans l'unité de recherche **BECCOH** (UVSQ, Université Paris-Saclay, AP-HP), sous la direction de **Etienne GIROUX-LEPRIEUR**, PU-PH, (Université de Versailles SQY, Université Paris-Saclay)

Thèse soutenue à Boulogne-Billancourt, le 25 novembre 2024, par

**Adrien COSTANTINI**

### Composition du Jury

Membres du jury avec voix délibérative

**Jean-François EMILE**

PU-PH, Université de Versailles  
SQY, UFR Simone Veil, Université  
Paris-Saclay

Président

**Diane DAMOTTE**

PU-PH, Université Paris Cité

Rapporteur & Examinatrice

**Arnaud SCHERPEREEL**

PU-PH, Université de Lille

Rapporteur & Examinateur

**Charles TRUILLET**

Chercheur CEA, Université Paris-  
Saclay//CEA

Examinateur

**Titre :** Biomarqueurs solubles et tissulaires dans le cancer bronchique non à petites cellules traité par immunothérapie

**Mots clés :** cancer bronchique non à petites cellules, immunothérapie, biomarqueurs

**Résumé :** Le cancer du poumon est un problème majeur de santé publique au niveau mondial. Malgré des avancées thérapeutiques récentes avec l'avènement des inhibiteurs de point de contrôle immunitaire (ICIs) de type anticorps anti-PD1/PD-L1, le pronostic demeure sombre. Au stade métastatique, une majorité de patients vont présenter une résistance primaire ou acquise aux ICIs. Il est donc nécessaire de développer de nouveaux biomarqueurs prédictifs de réponse à l'immunothérapie afin de mieux sélectionner les patients qui vont en bénéficier, et d'autre part, découvrir de nouvelles voies de signalisation biologiques cibles afin de développer de nouvelles stratégies thérapeutiques personnalisées. Nos objectifs pour la réalisation de ce travail sont superposables à ces deux problématiques. Premièrement, nous avons effectué un travail de découverte de biomarqueurs plasmatiques en utilisant une technique de screening par ELISA multiplex. Deuxièmement, nous avons poursuivi notre étude autour du PD-L1 soluble (sPD-L1) afin de mieux caractériser son rôle de biomarqueur potentiel chez les patients présentant un cancer bronchique non à petites cellules (CBNPC) traité par ICIs seuls ou en association à la chimiothérapie (CT) en première ligne thérapeutique. Enfin, nous avons analysé par immunofluorescence quantitative multiplexée (mQIF) les composants du complexe de chargement des peptides (CCP). En effet, il est connu que la machinerie de présentation des antigènes est une cible préférentielle utilisée par les cellules cancéreuses afin de se soustraire à l'immunité anti-tumorale adaptative. Notre approche de découverte de biomarqueurs a été réalisée chez 35 patients traités par ICIs en première ou en deuxième ligne thérapeutique pour un CBNPC de stade avancé. Un échantillon de plasma prélevé avant initiation du traitement a été soumis à une analyse par ELISA multiplex analysant 48 cytokines. L'analyse a mis en évidence l'hepatocyte growth factor (HGF) comme biomarqueur prédictif de réponse aux ICIs. En effet, des taux élevés étaient associés à l'absence de bénéfice clinique, une progression précoce, une survie sans progression (SSP) et une survie globale

(SG) plus courtes.

Nous avons ensuite poursuivi notre étude du sPD-L1 chez des patients présentant un CBNPC de stade avancé traités par ICIs seuls ou en association à la CT en première ligne thérapeutique. Cette étude multicentrique a analysé trois cohortes de patients dont une traitée par CT seule. Notre analyse a pu confirmer le rôle pronostic du sPD-L1. En effet, les patients avec des taux élevés avant initiation du traitement présentaient un moins bon pronostic. En outre, nous avons montré que la variation du sPD-L1 pendant le traitement jouait un rôle majeur en termes de survie. Les patients avec un sPD-L1 augmentant entre l'initiation du traitement et la première évaluation tumorale avaient une SG significativement plus courte et ce, quelle que soit la modalité thérapeutique.

Enfin, nous avons analysé par mQIF l'expression de tapasin, calreticulin et ERp57 dans de multiples échantillons de patients représentés dans des tissus microarrays (TMAs) dans des cohortes prédéfinies en fonction des modalités thérapeutiques. Nous avons montré que la régulation négative par les cellules cancéreuses d'un ou plusieurs de ces composants est un événement fréquent, en particulier l'atteinte de tapasin seule ou en association avec d'autres composants. Nous avons montré que tapasin impacte l'infiltration lymphocytaire TCD8+ et que la régulation de tapasin semble être épigénétique. Nous avons montré que l'interleukin-8 (IL-8) semble jouer un rôle potentiel dans cette régulation et qu'il a la capacité d'inhiber l'action d'interféron gamma sur l'expression en surface de HLA-A/B/C suggérant l'existence d'une voie de signalisation cytokino-médiée.

L'ensemble de ces résultats ont un potentiel impact translationnel et apportent des données pertinentes pour la prise en charge future des patients atteints de CBNPC de stade avancé.

**Title:** Soluble and tissue-based biomarkers in advanced non-small cell lung cancer treated with immunotherapy

**Keywords :** non-small cell lung cancer, immunotherapy, biomarkers

**Abstract:** Lung cancer is a major global public health issue. Despite recent therapeutic advances with the advent of immune checkpoint inhibitors (ICIs) such as anti-PD1/PD-L1 antibodies, the prognosis remains bleak. At the metastatic stage, most patients exhibit primary or acquired resistance to ICIs. Therefore, it is necessary to develop new predictive biomarkers for immunotherapy response to ICIs and better select patients who will benefit, as well as to discover new targetable biologically relevant signaling pathways to develop personalized therapeutic strategies.

Our objectives for this work overlap with these two issues. First, we conducted a biomarker discovery study using a multiplex ELISA assay. Second, we continued our investigation of soluble PD-L1 (sPD-L1) to better characterize its potential role as a biomarker in patients with non-small cell lung cancer (NSCLC) treated with ICIs alone or in association with chemotherapy (CT) as first-line therapy. Finally, we analyzed the components of the peptide loading complex (PLC) using multiplexed quantitative immunofluorescence (mQIF). It is known that the antigen presentation machinery is a preferred target exploited by cancer cells to evade adaptive anti-tumor immunity.

Our biomarker discovery study was conducted in 35 patients treated with ICIs in the first or second line setting for advanced NSCLC. Pre-treatment plasma samples were analyzed using multiplexed ELISA assessing 48 cytokines. The analysis identified hepatocyte growth factor (HGF) as a predictive biomarker for ICI response. High HGF levels were associated with a lack of clinical benefit, early progression, shorter progression-free survival (PFS), and overall survival (OS).

We then continued our study of sPD-L1 in patients with advanced NSCLC treated with ICIs alone or in combination with CT in the first-line setting. This multicenter study analyzed three cohorts, one of which was treated with CT alone. Our analysis confirmed the prognostic role of sPD-L1. Patients with high levels before treatment initiation had a worse prognosis. Moreover, we demonstrated that the variation of sPD-L1 during treatment played a

major role in terms of survival. Patients with increasing sPD-L1 levels between treatment initiation and first tumor evaluation had significantly shorter OS, regardless of the treatment modality.

Finally, we analyzed the expression of tapasin, calreticulin, and ERp57 by mQIF in multiple patient samples represented in tissue microarrays (TMAs) in predefined cohorts based on treatment modalities. We showed that cancer-cell specific downregulation of one or more of these components is a frequent event, particularly the loss of tapasin alone or in combination with other components. We demonstrated that tapasin impacts CD8+ T-cell infiltration and that the regulation of tapasin appears to be epigenetic. We showed that interleukin-8 (IL-8) may play a potential role in this regulation and has the capacity to inhibit the action of interferon-gamma on the cell-surface expression of HLA-A/B/C, suggesting the existence of a cytokine-mediated signalling pathway.

Overall, these findings have potential translational impact and provide relevant data for the future management of patients with advanced NSCLC.

## **TABLE DES MATIERES**

FIGURES.....	7
TABLEAUX.....	8
LISTE DES ABBREVIATIONS.....	9
INTRODUCTION.....	11
I- Le cancer pulmonaire.....	11
1. Epidémiologie.....	11
a. Incidence du cancer du poumon.....	12
b. Mortalité du cancer du poumon.....	13
2. Anatomopathologie.....	14
a. Le CBNPC .....	14
b. Les néoplasies neuroendocrines.....	15
3. Classification TNM du cancer du poumon.....	17
4. Facteurs de risque et facteurs pronostiques.....	20
a. Tabagisme.....	20
b. Expositions environnementales et professionnelles.....	20
c. Facteurs pronostiques.....	21
4. Modalités thérapeutiques du CBNPC.....	23
a. Chirurgie.....	23
b. Radiothérapie stéréotaxique.....	24
c. Immunothérapie.....	24
d. Traitement péri-opératoire.....	26
d. Radio-chimiothérapie concomitante.....	28
e. Traitement de première ligne des CBNPC de stade avancé sans addiction oncogénique .....	28
f. Traitement des CBNPC avec addiction oncogénique.....	33
II- Les mécanismes de résistance à l'immunothérapie.....	40
1. Définition des mécanismes de résistance à l'immunothérapie.....	40
2. Altérations de la présentation antigénique.....	43
III- La présentation antigénique liée au complexe majeur d'histocompatibilité (CMH) de classe I.....	45
1. La formation des peptides.....	45
2. Le complexe de chargement des peptides (CCP) .....	47
a. Transporter associated with antigen processing (TAP).....	50
b. Tapasin.....	50
c. Erp57.....	51
d. Calreticulin.....	51
3. Présentation antigénique de type CMH-I et cancer.....	52
IV- Biomarqueurs solubles.....	56

1. Le PD-L1 soluble (sPD-L1).....	57
a. B7-H1 (PD-L1).....	57
b. Origine du sPD-L1.....	58
c. Fonction du sPD-L1.....	59
d. Le sPD-L1 comme biomarqueur.....	61
2. La voie de signalisation HGF/MET.....	64
a. Hepatocyte growth factor (HGF) .....	64
b. Le récepteur mesenchymal-épithelial transition (MET/c-MET) .....	64
c. La dérégulation de la voie HGF/MET.....	65
d. HGF comme biomarqueur.....	69
e. Ciblage thérapeutique de la voie HGF/MET.....	70
 OBJECTIFS.....	72
 RESULTATS.....	73
Article #1: Plasma biomarkers screening by multiplex ELISA assay in patients with advanced non-small cell lung cancer treated with immune checkpoint inhibitors.....	73
Article #2: Soluble PD-L1 (sPD-L1) as a biomarker of durable response and survival for first-line immune checkpoint inhibitor (ICI) treatment in advanced non-small cell lung cancer (NSCLC).....	86
Article #3: Role of HLA class-I antigen peptide loading complex (PLC) components in immune evasion and treatment sensitivity in human lung cancer.....	120
Article #4: A brief report evaluating the role of IL-8 on MHC class-I molecule expression.....	120
 DISCUSSION GLOBALE.....	157
 PERSPECTIVES.....	163
 CONCLUSION.....	165
 ANNEXES.....	166
Annexe #1: Role of the HGF/c-MET pathway in resistance to immune checkpoint inhibitors in advanced non-small cell lung cancer.....	167
Annexe #2: Predictive role of plasmatic biomarkers in advanced non-small cell lung cancer treated by nivolumab,.....	197
Annexe #3: Plasma Biomarkers and Immune Checkpoint Inhibitors in Non-Small Cell Lung Cancer: New Tools for Better Patient Selection?.....	209
 BIBLIOGRAPHIE.....	224

## **REMERCIEMENTS**

Je tiens à remercier chaleureusement le Pr. Giroux-Leprieur qui, très tôt a su me donner le goût de la recherche clinique et translationnelle. Merci pour ton soutien, tes conseils avisés et tes encouragements.

Je tiens à remercier le Pr. Jean-François Emile qui me fait l'honneur de présider mon jury.

Je remercie également le Pr. Diane Damote, le Pr. Arnaud Scherpereel et le Dr. Charles Truillet d'avoir accepté de siéger en tant que membres du jury.

Je tiens tout particulièrement à remercier le Dr. Paul Takam Kamga avec qui je travaille depuis de nombreuses années. Ton aide est inestimable et ta bonne humeur est à la hauteur de tes connaissances scientifiques.

Je remercie l'ensemble des membres du laboratoire BECCOH.

Je souhaite également remercier le Pr. Kurt Schelper qui m'a accueilli au sein de son laboratoire ainsi que tous les membres du Schelper Lab : Maria, Vivi, Angelo, Nikki, Janie, Noe, Jassim, Kerryan, Shruti, Miguel, Juan, Barani avec une mention spéciale pour Kishu Ranjan.

Merci à tous mes collègues du service de Pneumologie, Assya, Coraline, Ferréol, Jamila, Jennifer, Julia, Louise, Violaine, Xavier.

Enfin, je dédié cette thèse à ma famille. Merci à mes parents, Kerstin et Pascal et à ma sœur, Emma, qui ont toujours su me soutenir et m'encourager.

Maxyne, Soazig, si un jour vous lisez ces mots, j'espère qu'ils vous inspireront et vous donneront la curiosité de chercher à comprendre, toujours comprendre, douter, surmonter les difficultés et enfin, pendant ne serait-ce qu'un infime instant, savoir ce qu'aucun autre être humain n'a su avant vous.

Merci Caroline pour ta bonne humeur, ton énergie positive et pour tout le reste.

“If I have seen further it is by standing on the shoulders of Giants”

## **FIGURES**

Figure 1. Taux d'incidence et de mortalité du cancer du poumon en France entre 1990 et 2018 chez les hommes et les femmes (échelle logarithmique) [Defossez et al. 2019].....	13
Figure 2. Illustration des points de contrôle immunitaires CTLA-4/B7 et PD-L1/PD-1 et leur inhibition par des inhibiteurs de points de contrôle immunitaires [cancer.gov].....	25
Figure 3. Algorithme de prise en charge de première ligne des patients présentant un CBNPC métastatique sans addiction oncogénique [Couraud et al. 2024].....	32
Figure 4. Fréquence des altérations moléculaires dans le CBNPC de type adénocarcinome [Tan et al. 2022].....	34
Figure 5. Mécanismes de résistance primaire et acquise à l'immunothérapie.....	41
Figure 6. Représentation schématique de la machinerie de présentation antigénique dans les cellules tumorales [Yang et al. 2023].....	46
Figure 7. Composition et architecture du CCP humain [Blees et al. 2017].....	49
Figure 8. Le sPD-L1 d'origine tumorale induit l'apoptose des CD4+ et non des CD8+ [Frigola et al. 2011].....	60
Figure 9. Illustration des différentes voies de dérégulation de la voie de signalisation HGF/MET [Ref. Moosavi et al. 2019].....	68

## **TABLEAUX**

Tableau 1. Classification TNM du cancer pulmonaire (8 <sup>ème</sup> édition).....	19
Tableau 2. ECOG-PS et indice de Karnofsky.....	22
Tableau 3. Résumé des études évaluant les composants de la machinerie de présentation des antigènes dans le cancer pulmonaire.....	53
Tableau 4. Résumé des principales études évaluant le rôle du PD-L1 soluble (sPD-L1) dans le CBNPC de stade avancé.....	63

## **LISTE DES ABBREVIATIONS**

ADC: antibody drug conjugate

ADP: adenosine diphosphate

ALK: anaplastic Lymphoma Kinase

AJCC: American joint commitee on cancer

ANSM: Agence nationale de sécurité du medicament et des produits de santé

ATP: adenosine triphosphate

AQUA: automated quantitative analysis

BRAF: B-Raf prot-oncogene

CBNPC: cancer bronchique non à petites cellules

CBPC: cancer bronchique à petites cellules

CCP: complexe de chargement des peptides

CK: cytokératine

CMH: complexe majeur d'histocompatibilité

CTLA-4: cytotoxic T lymphocyte-associated antigen-4

DAPI: dye 40 ,6- diamidino-2-phenylindole

ECOG-PS: eastern cooporeitive oncology group-performance status

EGF: epidermeal growth factor

EGFR: epidermal growth factor receptor

ELISA: enzyme-linked immunosorbent assay

FDA: Food and Drug Administration

FDG: fluorodésoxyglucose

FEVG: fraction d'éjection du ventricule gauche

HGF: hepatocyte growth factor

HLA: human leucocyte antigen

IASLC: International Association for the study of lung cancer

ICI: immune checkpoint inhibitor/inhibiteur de point de contrôle immunitaire

IFNG : interféron gamma

IHC: immunohistochimie

ITK: inhibiteur de tyrosine kinase

JAK: janus kinase

MET: MET proto-oncogene

mQIF: multiplexed quantitative immunofluorescence

NUT: nuclear protein in testis

NSCLC: non-small cell lung cancer

NUT: nuclear protein in testis

OMS: Organisation Mondiale de la Santé

OR: Odds ratio

OS: overall survival

PD-L1: programmed death ligand 1

PFS: progression free survival

PPS: projet personnalisé de soins

PHA : phytohemagglutinin

PS : performance status

RE : reticulum endoplasmique

ROS1: c-ROS-oncogene 1

SG: survie globale

SITC: Society for immunotherapy of cancer

SMARCA4: SWI/SNF Related, Matrix Associated, Actin Dependent Regulator Of Chromatin, Subfamily A, Member 4

sPD-L1: soluble PD-L1/PD-L1 soluble

SSP: survie sans progression

TAP: transporter associated with antigen presentation

TEP: tomographie par émission de positons

TDM: tomodensitométrie

TMA: tissue microarray

TTF1: thyroid transcription factor 1

VEMS: volume expiratoire maximal par seconde

WNT: wingless-integration stie

β2M: beta-2-microglobuline

## **INTRODUCTION**

### **I- Le cancer pulmonaire**

#### **1. Epidémiologie**

Le cancer représente la deuxième cause de mortalité dans le monde après les maladies cardio-vasculaires avec autour de 10 millions de morts annuels estimés en 2019 [[ourworldindata.org/cancer](https://ourworldindata.org/cancer)].

##### *a. Incidence du cancer du poumon*

A l'échelle mondiale, il est estimé en 2020, tous sexes confondus, que le cancer du poumon représente le deuxième cancer le plus incident derrière le cancer du sein avec 2 206 771 nouveaux cas annuels, soit 11,4% des nouveaux cas de cancer. Le cancer du sein demeure le cancer le plus incident avec 2 261 41 nouveaux cas annuels soit 11,7% des nouveaux cas.

Il s'agit du cancer le plus incident chez l'homme (14,3% des nouveaux cas) et le troisième plus incident chez la femme (8,4% des nouveaux cas) derrière le cancer du sein (24,5%) et le cancer colorectal (9,4%).

En France, le cancer du poumon représente le deuxième cancer le plus incident chez l'homme derrière le cancer de la prostate avec respectivement 59 800 (estimation 2018, estimation 2023 non disponible) et 33 000 (estimation 2023) nouveaux cas annuels. Chez la femme, il s'agit du troisième cancer le plus incident avec 19 000 nouveaux cas annuels, derrière le cancer du sein et le cancer colorectal avec 61 000 et 21 000 nouveau cas annuels, respectivement [[santepubliquefrance.fr](https://santepubliquefrance.fr)].

### *b. Mortalité du cancer du poumon*

Le cancer du poumon représente la première cause de mortalité par cancer dans le monde tous sexes confondus avec 1 796 144 décès estimés en 2020. Cela représente 18% de la mortalité de tous les cancers, loin devant le cancer colorectal qui représente 9,4% de l'ensemble des décès, soit 935 173 décès annuels.

Chez l'homme, il s'agit de la première cause de mortalité par cancer avec 1 188 679 décès annuels soit 21,5% de tous les décès par cancer. Chez la femme, il s'agit de la deuxième cause de mortalité par cancer avec 607 465 décès annuels soit 13,7% de tous les décès par cancer, derrière le cancer du sein (684 996 décès annuels soit 15,5% de tous les décès par cancer) [gco.iarc.fr].

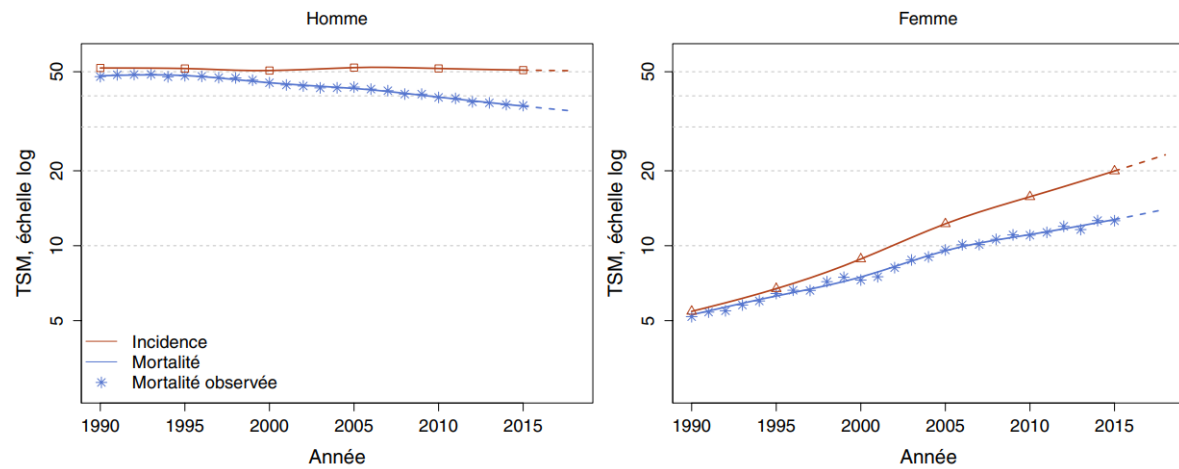
En France, il s'agit de la première cause de mortalité par cancer chez l'homme avec 23 000 décès annuels et la deuxième cause de mortalité par cancer chez la femme, derrière le cancer du sein avec respectivement 10 000 et 12 000 décès annuels.

Le cancer du poumon demeure un problème majeur de santé publique aussi bien à l'échelle nationale que mondiale. En effet, malgré une survie à 5 ans qui s'améliore : 3% en 1989-1993, 17% en 2005-2010 et 20% en 2010-2015, le pronostic du cancer du poumon reste sombre. Plusieurs facteurs doivent être pris en compte pour l'expliquer, d'une part le caractère intrinsèquement agressif des cancers pulmonaires, l'absence de programme de dépistage de masse organisé et standardisé entraînant, de fait, des diagnostics plus tardifs avec 70-80% des cancers diagnostiqués à des stades avancés. Cela s'explique aussi par l'évolution souvent insidieuse de ces tumeurs du fait de l'absence d'innervation nociceptive du parenchyme pulmonaire. Ces éléments contribuent à retarder le diagnostic initial de cancer pulmonaire et rendent son traitement plus complexe et difficile.

Une autre source d'inquiétude est la forte progression de l'incidence et de la mortalité du cancer du poumon chez la femme depuis 1990 alors qu'elles se stabilisent chez l'homme. Aux Etats-Unis, et dans de nombreux pays européens, la mortalité par cancer du poumon a dépassé la mortalité par cancer du sein [Siegel et al. 2023] avec 59 910 (21%) et 43 170 (15%) décès annuels pour les cancers du poumon et du sein, respectivement en 2023. Cette tendance est la même en France.

La Figure 1. récapitule l'évolution de l'incidence et de la mortalité du cancer du poumon en France entre 1990 et 2018.

**Figure 1. Taux d'incidence et de mortalité du cancer du poumon en France entre 1990 et 2018 chez les hommes et les femmes (échelle logarithmique) [Defossez et al. 2019]**



## 2. Anatomopathologie du cancer du poumon

L'Organisation Mondiale de la Santé (OMS) publie de manière régulière une classification des tumeurs pulmonaires. La dernière édition, datant de 2015 a été mise à jour en 2021. Cette classification repose sur l'analyse morphologique, l'immunohistochimie (IHC) et, enfin, l'analyse moléculaire.

Le cancer bronchique se divise de manière classique en deux grandes catégories, à savoir le cancer bronchique non à petites cellules (CBNPC) et le cancer bronchique à petites cellules (CBPC). Pour notre description, nous adopterons la distinction entre CBNPC et les néoplasies neuroendocrines dont le CBPC fait partie.

### *a. Le CBNPC*

Le CBNPC représente la forme histologique la plus fréquente de cancer pulmonaire (85 % des cas). On décrit plusieurs sous-types histologiques de CBNPC.

- L'adénocarcinome bronchique représente 40% des cas de CBNPC. Il correspond à une tumeur maligne épithéliale présentant une différenciation glandulaire, sécrétant des mucines ou exprimant un marqueur pneumocytaire (*thyroid transcription factor 1, TTF1*). Les adénocarcinomes invasifs sont par ailleurs divisés en adénocarcinomes avec invasion minime, adénocarcinomes invasifs non mucineux, adénocarcinomes invasifs mucineux, adénocarcinomes colloïdes, adénocarcinomes fœtaux et adénocarcinomes de type entérique. Les lésions glandulaires précurseurs (anciennement pré-néoplasiques), sont l'hyperplasie adénomateuse atypique (HAA) et l'adénocarcinome *in situ* (AIS).
- Le carcinome malpighien (ou épidermoïde) représente 30% des cas de CBNPC. Il correspond à une tumeur maligne épithéliale caractérisée par la présence de kératinisation, de ponts d'union intercellulaires, ou par la présence de marqueurs immunohistochimiques de différenciation malpighienne (comme p40). Il regroupe plusieurs sous-types histologiques tels que le carcinome malpighien kératinisant, non kératinisant ou basaloïde.

- Le carcinome à grandes cellules représente entre 5 - 10% des cas de CBNPC. Lors de la révision de la classification en 2015, cette catégorie avait connu des modifications majeures. Selon la définition en vigueur, le carcinome à grandes cellules correspond à un carcinome non à petites cellules qui ne présente pas de critères cytologiques, architecturaux ou immunohistochimiques de différenciation neuroendocrine, glandulaire ou malpighienne.
- Le carcinome sarcomatoïde est une tumeur rare qui représente moins de 1% des tumeurs malignes pulmonaires. Les carcinomes sarcomatoïdes comportent les carcinomes pléomorphes, eux-mêmes divisés en carcinomes à cellules fusiformes et carcinomes à cellules géantes, le carcinosarcome et le blastome pulmonaire.
- Les autres sous-types histologiques sont encore plus rares et correspondent au carcinome adénosquameux, au carcinome mucoépidermoïde, aux tumeurs thoraciques indifférenciées SMARCA4 (SWI/SNF Related, Matrix Associated, Actin Dependent Regulator Of Chromatin, Subfamily A, Member 4) déficientes et aux carcinome NUT (Nuclear protein in testis).

#### *b. Les néoplasies neuroendocrines*

Les néoplasies neuroendocrines pulmonaires sont, depuis 2021, regroupées comme un unique groupe de tumeurs, qui comprend d'une part les tumeurs neuroendocrines, comportant les tumeurs carcinoïdes typiques (de bas grade) et les tumeurs carcinoïdes atypiques (de grade intermédiaire), et d'autre part les carcinomes neuroendocrines, comportant les carcinomes neuroendocrines à grandes cellules et les carcinomes neuroendocrines à petites cellules.

- Le carcinome neuroendocrine à petites cellules représente 15% des cancers pulmonaires. Il s'agit d'une prolifération en nappes de cellules de petite taille, au cytoplasme indistinct, sans limites nettes. Ces cellules n'excèdent pas en taille celle de trois lymphocytes. Les noyaux sont typiques, allongés ou ovalaires, hyperchromatiques, à chromatine poivre et sel, sans nucléole proéminent. On dénombre en moyenne 10 mitoses par champ au grossissement 40 et les corps apoptotiques sont nombreux. On retrouve souvent de vastes plages de nécrose.

L'analyse immunohistochimique montre une expression des cytokératines, une différenciation neuroendocrine (chromogranine A, synaptophysine) et une positivité pour TTF1.

- Le carcinome neuroendocrine à grandes cellules est un carcinome non à petites cellules de morphologie endocrine dont l'index mitotique est supérieur à 10 mitoses/2 mm<sup>2</sup> et qui exprime un ou plusieurs marqueurs neuroendocrines. Il comporte une morphologie endocrine définie par les caractéristiques architecturales suivantes : agencement organoïde d'amas, îlots, travées, cordons ou pseudoglandes, présence de rosettes, agencement palissadique de noyaux. Les caractéristiques cytologiques sont proches de celles des carcinomes neuroendocrines non à petites cellules, avec des cellules de grande taille (> 3 lymphocytes), un nucléole généralement proéminent (mais parfois absent), une chromatine le plus souvent fine/granulaire (parfois vésiculeuse), et un cytoplasme abondant éosinophile avec fréquemment une membrane cytoplasmique bien visible. En immunohistochimie, ils peuvent exprimer les marqueurs neuroendocrines standards (chromogranine A, synaptophysine, CD56). L'expression de TTF1 est positive dans environ 50% des cas.
- Le carcinome mixte correspond à un carcinome neuroendocrine à grandes cellules qui présente une composante non neuroendocrine, fréquemment un adénocarcinome mais tous les sous-types histologiques peuvent s'observer (carcinome épidermoïde, carcinome sarcomatoïde). Il peut également exister une composante neuroendocrine de type carcinome neuroendocrine à petites cellules, on parle alors de carcinome à petites cellules combiné si ce contingent représente au moins 10 % de la tumeur.
- Les tumeurs carcinoïdes sont des tumeurs rares qui représentent moins de 2 % des tumeurs pulmonaires neuroendocrines ayant une architecture bien différenciée, organoïde dont il existe deux sous-types : les tumeurs carcinoïdes typiques et les tumeurs carcinoïdes atypiques.

Une avancée majeure du début du XXI<sup>ème</sup> siècle correspond à la découverte et l'utilisation systématique de l'analyse moléculaire, dans les CBNPC de type non-épidermoïde, afin de proposer des traitements ciblés et personnalisés. L'analyse moléculaire des adénocarcinomes bronchiques a permis de mettre en évidence un grand nombre

d'altérations moléculaires dont certaines sont très spécifiques des adénocarcinomes bronchiques comme les mutations d'Epidermal Growth factor (*EGFR*) (de type délétion de l'exon 19 ou les mutations ponctuelles situées au niveau de l'exon 21), et les translocations *EML4-ALK*. De nombreuses altérations moléculaires peuvent être ciblées par des thérapies spécifiques, comme les altérations d'*EGFR*, *ALK*, *BRAF*, *RET*, *ROS1*, *MET*, *KRAS* (G12C). Ces anomalies (a minima *EGFR*, *ALK*, *ROS1*, *RET*, mais extension rapide des indications thérapeutiques pour les autres anomalies moléculaires qui sont de plus en plus souvent recherchées d'emblée) doivent être recherchées systématiquement au diagnostic dans les CBNPC de stade avancé, dans les histologies non épidermoïdes, ou dans les rares épidermoïdes chez le sujet petit ou jamais fumeur. La recherche de mutation *EGFR* doit également être réalisée pour les stades précoces, car des inhibiteurs de tyrosine-kinase (ITK) sont disponibles en péri-opératoire dans ces indications. D'autres anomalies moléculaires ne sont actuellement pas la cible de thérapies spécifiques comme les mutations de *TP53*, *STK11* ou *KEAP1*, mais sont associées à un mauvais pronostic. Il est recommandé de réaliser une recherche de ces altérations moléculaires par séquençage de nouvelle génération (NGS) ADN et ARN.

Il est par ailleurs courant de réaliser une IHC pour évaluer l'expression de Programmed Death-Ligand 1 (PD-L1) (*tumour proportion score*, TPS) des cellules tumorales et de rechercher une surexpression des kinases *ALK* et *ROS1* par la même technique.

### 3. Classification TNM du cancer du poumon

La classification TNM (pour *Tumour*, *Node*, *Metastasis* ou Tumeur, Ganglions lymphatiques, Métastases), est une classification utilisée pour évaluer l'étendue de la propagation d'un cancer chez un patient. L'association des trois éléments permet de définir un stade qui guide la prise en charge thérapeutique.

L'International Association for the Study of Lung Cancer (IASLC) met régulièrement à jour la classification pour les différents sous-types histologiques de cancer. L'évaluation clinoco-radiologique initiale permet de fournir une classification cTNM. En cas de chirurgie thoracique, les tumeurs seront classées en pTNM pour le rendu des résultats anatomopathologiques et en ypTNM en cas de traitement néo-adjuvant. L'IASLC a publié cette dernière mise à jour en

2021 (8<sup>e</sup> classification TNM) et une proposition de neuvième édition a été publiée en 2023 [Rami-Porta et al. 2024]. La huitième édition de la classification TNM ainsi que les stades tumoraux sont représentés dans le Tableau 1.

**Tableau 1. Classification TNM du cancer pulmonaire (8<sup>ème</sup> édition)**

**A. Classification TNM**

**B. Stade TNM [Couraud et al. 2024]**

T (primary tumor)	
T0	No primary tumor
Tis	Carcinoma in situ (squamous or adenocarcinoma)
T1	Tumor $\leq 3$ cm
T1mi	Minimally invasive adenocarcinoma
T1a	Superficial spreading tumor in central airways*
T1a	Tumor $\leq 1$ cm
T1b	Tumor $> 1$ but $\leq 2$ cm
T1c	Tumor $> 2$ but $\leq 3$ cm
T2	Tumor $> 3$ but $\leq 5$ cm or tumor involving: visceral pleura,† main bronchus (not carina), atelectasis to hilum‡
T2a	Tumor $> 3$ but $\leq 4$ cm
T2b	Tumor $> 4$ but $\leq 5$ cm
T3	Tumor $> 5$ but $\leq 7$ cm or invading chest wall, pericardium, phrenic nerve; or separate tumor nodule(s) in the same lobe
T4	Tumor $> 7$ cm or tumor invading: mediastinum, diaphragm, heart, great vessels, recurrent laryngeal nerve, carina, trachea, esophagus, spine; or tumor nodule(s) in a different ipsilateral lobe
N (regional lymph nodes)	
N0	No regional node metastasis
N1	Metastasis in ipsilateral pulmonary or hilar nodes
N2	Metastasis in ipsilateral mediastinal or subcarinal nodes
N3	Metastasis in contralateral mediastinal, hilar, or supraclavicular nodes
M (distant metastasis)	
M0	No distant metastasis
M1a	Malignant pleural or pericardial effusion‡ or pleural or pericardial nodules or separate tumor nodule(s) in a contralateral lobe
M1b	Single extrathoracic metastasis
M1c	Multiple extrathoracic metastases (1 or $> 1$ organ)

	N0	N1	N2	N3	M1a-b Tout N	M1c Tout N
T1a	IA-1	IIB	IIIA	IIIB	IV-A	IV-B
T1b	IA-2	IIB	IIIA	IIIB	IV-A	IV-B
T1c	IA-3	IIB	IIIA	IIIB	IV-A	IV-B
T2a	IB	IIB	IIIA	IIIB	IV-A	IV-B
T2b	IIA	IIB	IIIA	IIIB	IV-A	IV-B
T3	IIB	IIIA	IIIB	IIIC	IV-A	IV-B
T4	IIIA	IIIA	IIIB	IIIC	IV-A	IV-B

#### 4. Facteurs de risque et facteurs pronostiques

##### *a. Tabagisme*

Le tabagisme est le principal facteur de risque de cancer du poumon. Selon les estimations, il est responsable de près de 90% des cancers du poumon. Le tabagisme augmente le risque de développer un cancer du poumon d'un facteur de 10 et ce risque est corrélé à la durée d'exposition au tabac, à l'âge de début de l'intoxication tabagique, et à la quantité de tabac consommé [Doll et al. 1994]. La fumée issue de la combustion du contenu d'une cigarette contient un grand nombre de produits chimiques connus pour leur caractère cancérogène : 4-(N-méthylnitrosoamino)-1-(3-pyridyl)-1-butanone, arsenic, benzène, Benzo[a]pyrène, Cadmium, chromium hexavalent, formaldéhyde, nickel...) [Smith et al. 2003] expliquant la relation de cause à effet entre tabagisme et apparition de cancer, en particulier pulmonaire. Cette exposition chronique à des carcinogènes connus entraîne des mutations somatiques, des inactivations de gènes suppresseurs de tumeurs et enfin le développement progressif de cellules cancéreuses.

Le tabagisme passif, définit comme une exposition aux fumées de tabac dans son environnement, constitue également un facteur de risque de développer un cancer du poumon et serait la cause d'environ 25% des cancers pulmonaires du non-fumeur avec une augmentation du risque de 30% de développer un cancer bronchique. [Besaratinia et al. 2008]. On notera que le cannabis constitue un facteur de risque surajouté au tabagisme. Lors de sa combustion, le cannabis émet une fumée dont la concentration en hydrocarbures aromatiques polycycliques et en carcinogènes est plus importante que la fumée émise par la combustion du tabac. A tabagisme égal, le cannabis multiplie par deux le risque de cancer pulmonaire avec un âge de survenue plus précoce et une association fréquente à l'emphysème pulmonaire témoignant d'une toxicité majeure pour les structures alvéolaires [Callaghan et al. 2013]

##### *b. Expositions environnementales et professionnelles*

Des expositions environnementales, liées ou non à la pratique d'un métier constituent également des facteurs de risque de développer un cancer bronchique. Au niveau professionnel, l'amiante est le carcinogène le plus fréquemment retrouvé. L'exposition à l'amiante seule augmente le risque relatif de développer un cancer pulmonaire de 7 et de 99 en cas d'association au tabagisme [Klebe et al. 2019]. Il existe d'autres expositions professionnelles, moins fréquentes mais que l'on doit également rechercher comme l'exposition à certains métaux lourds (oxyde de fer, nickel, arsenic, houille) ou aux radiations ionisantes. [Marant Micallef et al. 2018]. Hors du cadre professionnel, il existe également de nombreux carcinogènes environnementaux comme les particules fines liées à la pollution atmosphérique, le radon ou les radiations ionisantes thérapeutiques. Il a en effet été montré une association entre le niveau de pollution de l'air et la survenue de cancers pulmonaires présentant des addictions oncogéniques telles que des mutations d'*EGFR* [Hill et al. 2023].

#### c. Facteurs pronostiques

On distinguera les facteurs pronostiques liés au patient tels que l'âge physiologique, le sexe, les comorbidités, et les facteurs pronostiques liés au cancer tel que le stade et les caractéristiques histo-moléculaires. Deux facteurs liés au patient constituent des facteurs pronostiques majeurs. Il s'agit de l'état nutritionnel et de l'état général. La dénutrition, évaluée cliniquement par une perte de poids récente (et notamment supérieure à 5% en moins de 6 mois), ou biologiquement par un dosage bas de l'albumine et/ou de la pré-albumine plasmatiques, constitue un facteur de mauvais pronostic. L'état général du patient est habituellement évalué par deux échelles : l'Eastern Cooporative Oncology Group-Performance Status (ECOG-PS) et l'indice de Karnofsky (Tableau 2.). Ces échelles permettent d'évaluer la capacité fonctionnelle de chaque patient à un instant donné. L'échelle ECOG-PS est utilisée de manière courante et s'échelonne de 0 à 4 (5 étant le décès). Plus le score est élevé moins le patient présente un état général conservé et plus un traitement anti-cancéreux présente des risques de toxicité et de mauvaise tolérance clinique et biologique. De manière habituelle, un traitement sans limitation est proposé aux patients présentant un PS 0 – 1 alors que les patients présentant un PS 3- 4 se voient proposer une prise en charge palliative. Les patients présentant un PS intermédiaire, à 2, peuvent se voir proposer un

traitement dont on adaptera les modalités.

**Tableau 2. ECOG-PS et indice de Karnofsky**

**A. ECOG-PS [ECOG-ACRI]**

**B. Indice de Karnofsky [santé.gouv.fr]**

GRADE	ECOG PERFORMANCE STATUS
0	Fully active, able to carry on all pre-disease performance without restriction
1	Restricted in physically strenuous activity but ambulatory and able to carry out work of a light or sedentary nature, e.g., light house work, office work
2	Ambulatory and capable of all selfcare but unable to carry out any work activities; up and about more than 50% of waking hours
3	Capable of only limited selfcare; confined to bed or chair more than 50% of waking hours
4	Completely disabled; cannot carry on any selfcare; totally confined to bed or chair
5	Dead

Capable de mener une activité normale	100 %	normal, pas de signe de maladie
	90 %	peut mener une activité normale, symptômes mineurs de la maladie, totalement autonome
	80 %	peut mener une activité normale, mais avec effort, symptômes ou signes mineurs, totalement autonome
Incapable de travailler, capable de vivre chez lui et d'assumer ses besoins personnels, une assistance variable est nécessaire	70 %	peut se prendre en charge, incapable de mener une activité normale, autonome mais à stimuler
	60 %	nécessite une aide occasionnelle mais peut prendre en charge la plupart des besoins, semi-autonome
	50 %	nécessite une aide suivie et des soins médicaux fréquents, semi-autonome
	40 %	handicapé, nécessite une aide et des soins particuliers
	30 %	sévèrement handicapé, dépendant
Incapable de s'occuper de lui-même, nécessite des soins hospitaliers ou l'équivalent	20 %	très malade soutien actif, absence totale d'autonomie
	10 %	moribond, processus fatal progressant rapidement

## 5. Modalités thérapeutiques du CBNPC

Le traitement du cancer du poumon a connu des modifications rapides avec plusieurs avancées majeures au cours du début du XXI<sup>ème</sup> siècle. Le type de traitement que l'on proposera au patient se base sur le type histologique de la tumeur et ses caractéristiques immunohistochimiques et moléculaires. On prendra également en compte le stade issu de la classification TNM et les facteurs pronostiques intrinsèques au patient, et en particulier son état général évalué selon le score ECOG-PS. Le but de cette évaluation initiale est de proposer une prise en charge adaptée et la plus personnalisée possible pour chaque patient.

### *a. Chirurgie*

Le traitement chirurgical demeure le traitement curatif de référence pour le cancer bronchique de stade I de petite taille (<3cm). Des données récentes de stratégie péri-opératoire que l'on expose ci-après sont venues modifier la stratégie thérapeutique à partir du stade IB (classification TNM 8<sup>ème</sup> édition) présentant un caractère résécable.

La lobectomie, associée à un curage ganglionnaire médiastinal, reste le geste optimal lorsqu'elle est技niquement et fonctionnellement réalisable. La survie à 5 ans en cas de résection complète est de 70%. Dans un souci de réduction de la morbi-mortalité liée à la chirurgie thoracique, l'efficacité de techniques chirurgicales permettant une épargne du parenchyme pulmonaire ont été évaluées dans les stades précoces [Altorki et al. 2013]. La segmentectomie montre des résultats similaires à la lobectomie sous réserve que la tumeur soit de petite taille et périphérique (inférieure à 2cm et distance de la paroi inférieure à 2cm). Il est encore légitime de proposer une chimiothérapie adjuvante chez les patients présentant une tumeur de stade pII ou pIII, et en état physiologique de la recevoir. Il faut néanmoins noter que le bénéfice de ce traitement reste modeste avec un gain de survie globale (SG) et de survie sans maladie (SSM) à 5 ans de 5% [Arriagada et al. 2004, Arriagada et al. 2009].

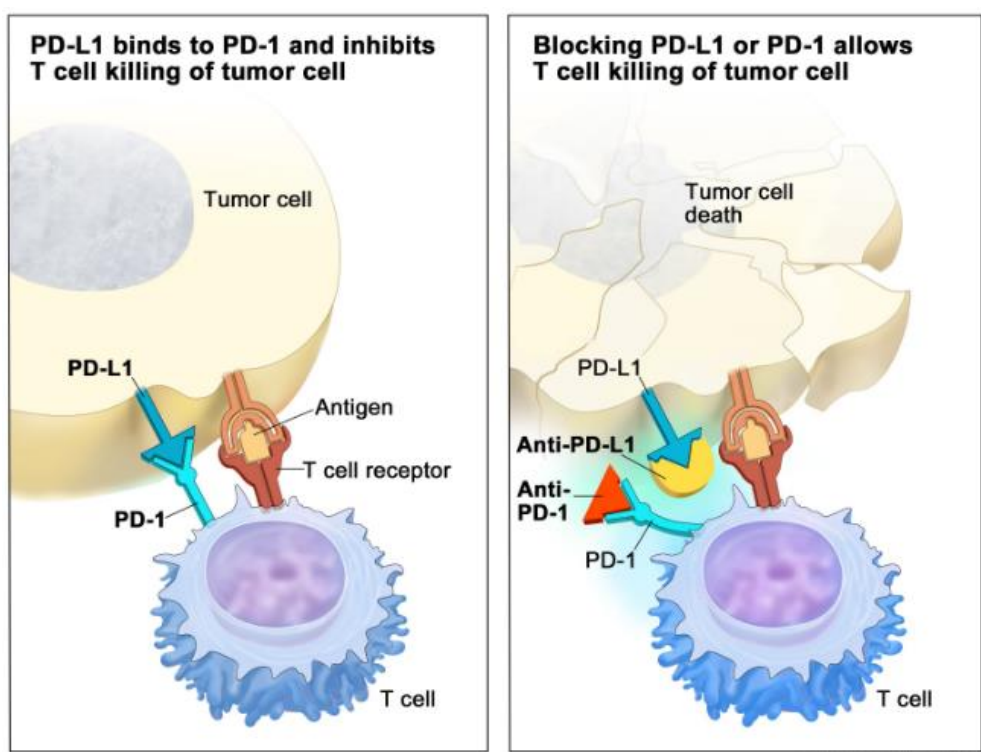
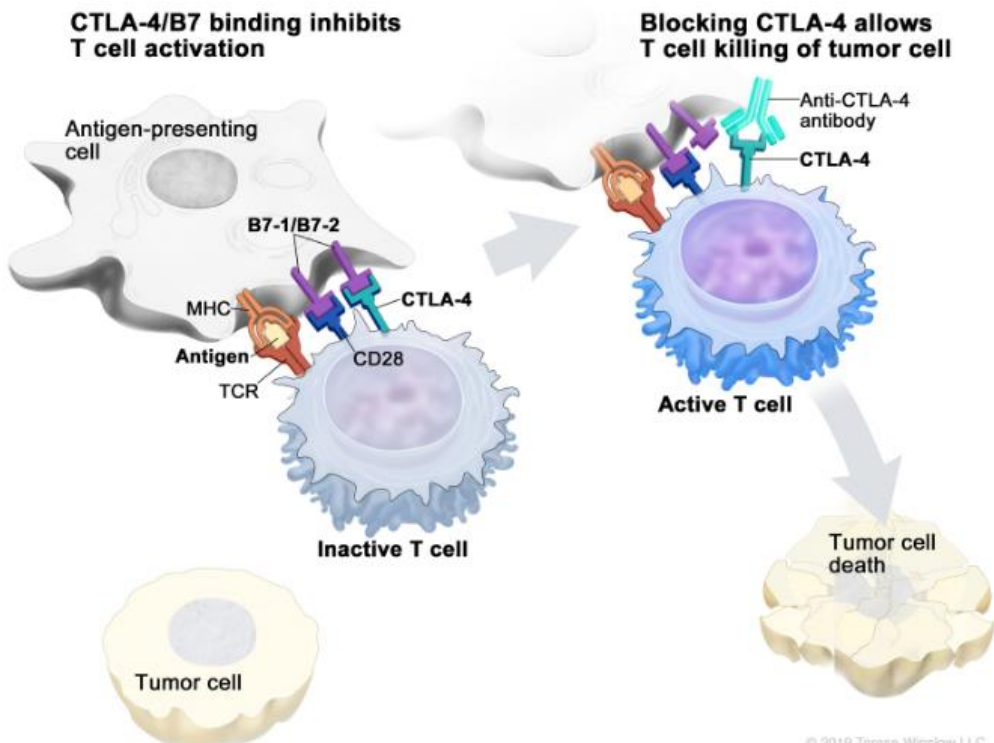
*b. Radiothérapie stéréotaxique*

La radiothérapie stéréotaxique est une option alternative à la chirurgie dans certaines conditions, en particulier en cas d'impossibilité de réaliser un traitement chirurgical du fait de comorbidités importantes, notamment respiratoires ou cardiaques. En effet, un VEMS post-opératoire prédit inférieur à 30% ou 1 000mL, une cardiopathie ischémique non équilibrée, une insuffisance cardiaque avec une FEVG < 40% ou un état général altéré avec un PS supérieur à 2 sont autant de contre-indications à une prise en charge chirurgicale. La radiothérapie stéréotaxique permet de délivrer une dose allant jusqu'à 60 Grays (Gy) dans un petit volume et a un objectif curatif avec des effets secondaires minimes. Plusieurs essais ont comparé la radiothérapie stéréotaxique à la chirurgie dans le CBNPC de stade I résécable [Chang et al. 2015, Ball et al. 2019, Chang et al. 2021] et ont montré que la radiothérapie est une option efficace et sûre dans cette situation clinique.

*c. Immunothérapie*

L'immunothérapie est un terme générique qui englobe plusieurs modalités thérapeutiques dont font partie les inhibiteurs de point de contrôle immunitaires (ICIs). Il existe actuellement deux classes d'ICIs, les inhibiteurs de programmed death 1 (PD-1)/programmed death-ligand 1 (PD-L1) et les inhibiteurs de cytotoxic T lymphocyte-associated antigen-4 (CTLA-4). Les lymphocytes T activés expriment à leur surface PD-1 dont les ligands sont PD-L1 et PD-L2. Lorsque le PD-1 exprimé par les lymphocytes T se lie à PD-L1 exprimé par les cellules tumorales, cela entraîne une inhibition des lymphocytes et empêche leur action cytotoxique. Cette liaison a un effet négatif sur l'immunité anti-tumorale en empêchant la prolifération, la production de cytokines et la capacité cytotoxique des lymphocytes T activés. Les ICIs sont des anticorps monoclonaux humanisés qui vont interagir avec PD-1, PD-L1 ou CTLA-4. Cette liaison va empêcher la liaison PD-1-PD-L1/PD-L2 et CTLA4-CD80/CD86. Ainsi, l'effet inhibiteur créé par PD-L1 est levé et les lymphocytes TCD8+ vont retrouver leurs caractéristiques prolifératives, cytotoxiques et de sécrétion de cytokines permettant d'obtenir une réponse anti-cancéreuse efficace (Figure 2.).

**Figure 2. Illustration des points de contrôle immunitaires CTLA-4/B7 et PD-L1/PD-1 et leur inhibition par des inhibiteurs de points de contrôle immunitaires [cancer.gov].**



### c. Traitement péri-opératoire

De nouvelles modalités thérapeutiques dites péri-opératoires et associant immunothérapie +/- chimiothérapie et chirurgie ont récemment été évaluées dans le CBNPC.

Des stratégies d'immunothérapie adjuvante ont d'abord été testées. On pourra citer l'essai IMpower010 [Felip et al. 2021, Felip et al. 2023] qui a évalué l'efficacité de l'atezolizumab après chimiothérapie adjuvante chez des patients présentant un CBNPC de stade IB-IIIA (classification TNM, 7<sup>ème</sup> édition) opéré. Il a été montré un bénéfice en termes de SSM en faveur de l'atezolizumab comparativement aux meilleurs soins de support dans les tumeurs de stade II-IIIA (critères de jugement principal) : HR =0.79, p=0.020. Les données de SG matures n'ont pas été rapportées. L'essai KEYNOTE-091 [O'Brien et al. 2022] a évalué l'efficacité du pembrolizumab comparativement au placebo chez des patients présentant un CBNPC de stade IB-IIIA (classification TNM, 7<sup>ème</sup> édition) opéré. Le pembrolizumab a également montré sa supériorité par rapport au placebo après chimiothérapie adjuvante en termes de SSM : HR = 0.76, p=0.014. On notera que la chimiothérapie adjuvante n'était pas obligatoire dans cette étude. Enfin, l'essai BR31 évaluant le durvalumab en adjuvant comparativement au placebo chez des patients présentant un CBNPC de stade IB-IIIA (classification TNM, 7<sup>ème</sup> édition) opéré, était négatif pour son critère de jugement principal, à savoir, la SSM [Goss et al. 2024]. L'essai Checkmate 816 [Forde et al. 2022] a évalué l'association d'un doublet à base de sels de platine au nivolumab en néoadjuvant chez des patients présentant un CBNPC résécable de stade IB à IIIA (TNM 7<sup>ème</sup> édition). Dans cet essai international randomisé de phase III les patients étaient randomisés en 1 :1 :1 et recevaient soit une chimio-immunothérapie soit une chimiothérapie seule soit une double immunothérapie. Ce dernier bras a été fermé précocement et ne fait pas partie de l'analyse définitive. Les patients recevaient trois cures de traitement à 3 semaines d'intervalle puis étaient opérés. Deux critères de jugements ont été établis : la survie sans événement et la réponse histologique complète. Les résultats, après une durée de suivi de 21 mois, ont montré une médiane de survie sans événement de 31,6 mois (intervalle de confiance [IC] 95%, 30,2 - non atteinte (NA)) avec l'association nivolumab-chimiothérapie et 20,8 mois (IC 95%, 14,0 – 26,7) avec la chimiothérapie seule (hazard ratio pour la progression, la rechute ou le décès, 0,63 ; IC 97,38%, 0,43 – 0,91, P=0,005). Concernant la réponse histologique complète, celle-ci était de 24,0% dans le groupe nivolumab-chimiothérapie (IC 95%, 18,0 – 31,0) et de 2,2% (IC 95% 0,6 – 5,6) dans le groupe

chimiothérapie seule (odds ratio, 13,94 ; IC 95%, 3,49 – 55,75 ; P<0,001).

L'essai Checkmate 77T [Cascone et al. 2024] était une étude de phase III randomisée en double aveugle internationale évaluant une association nivolumab chimiothérapie (doublet à base de sels de platine) suivie par une chirurgie et un traitement adjuvant par nivolumab comparé à une association placebo chimiothérapie (doublet à base de sels de platine) suivie par une chirurgie et un traitement adjuvant par placebo chez des patients présentant un CBNPC résécable de stade IIa à IIIb selon la 8ème classification TNM. Durant la période néoadjuvante, les patients recevaient une association nivolumab chimiothérapie ou placebo chimiothérapie toutes les 3 semaines pour 4 cycles au total. Les patients étaient par la suite opérés et recevaient dans les 90 jours suivants la chirurgie un traitement adjuvant par nivolumab à la dose de 480 mg ou placebo toutes les 4 semaines pendant 1 an. Le critère de jugement principal était la survie sans événement. Après un suivi médian de 25,4 mois, le pourcentage de patients présentant une survie sans événement de 18 mois était de 70,2 % dans le groupe nivolumab et 50 % dans le groupe de chimiothérapie, hazard ratio 0,58; IC 97,36%, 0,42 – 0,81; P<0,001).

D'autres essais de phase III ont évalué l'efficacité de molécules comme le pembrolizumab et le durvalumab dans des contextes similaires. L'essai Keynote 671 [Wakelee et al. 2023, Spicer et al. 2024] a montré un bénéfice en termes de survie sans événement et de manière notable, en termes de SG en faveur du pembrolizumab par rapport au placebo : HR 0,72, p=0,0052 pour la SG. L'essai AEGEAN [Heymach et al. 2023] a montré un bénéfice en termes de survie sans événement en faveur du durvalumab selon une stratégie péri-opératoire (HR = 0,68, p=0,004). L'ensemble de ces résultats ont conduit l'HAS à donner un avis favorable au remboursement du nivolumab :

« en association à une chimiothérapie à base de sels de platine, dans le traitement néoadjuvant des patients adultes, atteints d'un cancer bronchique non à petites cellules résécable à haut risque de récidive, dont les tumeurs expriment PD-L1 au seuil ≥ 1 % et dont les tumeurs ne présentent pas de mutation sensibilisante de l'EGFR connue, ni de translocation ALK connue » [HAS-santé.fr].

Néanmoins, la demande d'accès précoce d'utilisation du nivolumab selon les modalités de l'essai Checkmate 77t n'a pas été retenu par l'ANSM [HAS-santé.fr]

*d. Radio-chimiothérapie concomitante*

La question de l’opérabilité des patients est maintenant devenue une question essentielle de la prise en charge des patients présentant des stades localement avancés. En effet, les essais de stratégies péri-opératoires ont inclus les patients présentant des pathologies potentiellement accessibles à une radio-chimiothérapie concomitante. La question de l’opérabilité à priori du patient avant de débuter toute stratégie thérapeutique est donc centrale. Le but de la chimio-immunothérapie n’est pas de rendre le patient opérable. Un traitement par radio-chimiothérapie concomitante est recommandé chez les patients présentant une tumeur non résécable de stade IIIA, IIIB ou IIIC ou chez les patients non médicalement opérables. Il est recommandé de réaliser une association de chimiothérapie et de radiothérapie suivie d’une immunothérapie de consolidation par durvalumab, si l’état du patient le permet. La chimiothérapie doit comporter 2 à 4 cures à base de sels de platine, associée à une radiothérapie à une dose comprise entre 60 et 66Gy en fractions de 2 Gy par fraction, 5 fractions par semaine. Un traitement de consolidation par durvalumab toutes les 4 semaines pendant 12 mois est recommandé selon les données de l’assai PACIFIC [Spigel et al. 2022]. Il est également possible de proposer un traitement par chimio-radiothérapie séquentielle chez les patients présentant PS > 1 et/ou âgés et/ou fragiles.

*e. Traitement de première ligne des CBNPC de stade avancé sans addiction oncogénique*

Plusieurs essais randomisés internationaux multicentrique de phase III ont montré l’efficacité de l’immunothérapie seule ou en association avec la chimiothérapie en première ligne thérapeutique dans différents sous types histologiques. L’essai KEYNOTE-024 [Ref. Reck et al. 2016] réalisé chez les patients présentant un CBNPC avec une expression de PD-L1 ≥ 50% a montré un bénéfice en termes de SSP et de SG en faveur du pembrolizumab en comparaison à la chimiothérapie à base de sel de platine. Les essais KEYNOTE-189 et KEYNOTE-407 [Gandhi et al. 2018, Paz-Ares et al. 2018] ont évalué l’association pembrolizumab-chimiothérapie comparé à la chimiothérapie seule chez des patients présentant un CBNPC avancé avec une histologie non épidermoïde et épidermoïde, respectivement. Ces essais ont également montré un bénéfice en termes de SSP et de SG en faveur de l’association pembrolizumab-

chimiothérapie. Le cemiplimab, un autre anticorps monoclonal anti-PD-1 a lui aussi montré son efficacité en termes de SSP et SG. Il a été comparé, en première ligne thérapeutique, en monothérapie à la chimiothérapie chez les patients présentant un PD-L1 ≥ 50 % [Sezer et al. 2021], et en association à la chimiothérapie versus chimiothérapie [Gogishvili et al. 2022] quel que soit l'expression de PD-L1 et le sous-type histologique. Enfin, l'atezolizumab a lui aussi montré un bénéfice en termes de SG et de SSP par rapport à la chimiothérapie seule, en particulier chez les patients présentant un PD-L1 ≥ 50% [Herbst et al. 2020].

En prenant en compte l'ensemble de ces éléments, il est possible de résumer la prise en charge du CBNPC éligible à un traitement systémique de la manière suivante.

Chez les patients présentant un CBNPC non épidermoïde métastatique PS 0 – 1 sans addiction oncogénique, deux stratégies thérapeutiques peuvent être proposées. Chez les patients présentant un PD-L1 supérieur à 50 %, un traitement par immunothérapie en monothérapie peut être proposé. Les immunothérapies suivantes sont actuellement disponibles en France : atezolizumab 1200mg J1/J22 (ou 840mg J1/J14 ou 1680mg J1/J28), cemiplimab 350 mg J1/J22, pembrolizumab 200mg IV J1/J22 (ou 400mg/6 semaines).

Une association chimio-immunothérapie par sels de platine (cisplatine 75 mg/m<sup>2</sup> ou carboplatine AUC 5) associé au pemetrexed (500 mg/m<sup>2</sup>) et au pembrolizumab 200mg par voie IV tous les 21 jours pour 4 cycles suivis d'une maintenance par pemetrexed + pembrolizumab pour une durée totale de 2 ans ou jusqu'à progression ou de toxicité inacceptable peut être proposée quel que soit le niveau de PD-L1.

Chez les patients présentant un CBNPC de type épidermoïde, la stratégie thérapeutique est également guidée par le taux de PD-L1 évalué par IHC. En cas de PD-L1 supérieur à 50 %, un traitement par immunothérapie en monothérapie peut être proposé avec la possibilité de choisir parmi les molécules suivantes : atezolizumab 1200mg J1/J22 (ou 840mg J1/J14 ou 1680mg J1/J28), cemiplimab 350 mg J1/J22, pembrolizumab 200mg IV J1/J22 (ou 400mg/6 semaines). Une association chimio-immunothérapie par sels de platine (carboplatine AUC 6), paclitaxel (200mg/m<sup>2</sup>), et pembrolizumab (200mg IV) J1/J22 pour 4 cycles suivi d'une poursuite du pembrolizumab 200mg/3 semaines ou 400mg/6 semaines pour un total de 2 ans, ou jusqu'à progression, ou toxicité inacceptable peut être proposée quel que soit le niveau de PD-L1.

Il est nécessaire de prendre en compte les contre-indications ou les non-indications à l'utilisation de l'immunothérapie. En effet, certains éléments doivent mener à une discussion multidisciplinaire et avec le patient afin de juger de la balance bénéfice-risque de tout traitement. Par exemple, la présence d'une pathologie auto-immune préexistante, traitée ou non qui pourrait se développer ou s'exacerber lors de l'initiation d'un traitement par immunothérapie. D'autres éléments à prendre en compte sont la présence d'une pathologie virale chronique active non contrôlée (VIH, VHB, VHC) ou la prise de traitements immunomodulateurs ou immunosuppresseurs comme la corticothérapie systémique à fortes doses.

Dans ces situations, il est possible de proposer un traitement par chimiothérapie seule. Chez les patients présentant un carcinome non épidermoïde, un doublet à base de sels de platine associé à une molécule de troisième génération et au bevacizumab est indiqué. L'association cisplatine/carboplatine pemetrexed ( $500\text{mg}/\text{m}^2$ ) et bevacizumab toutes les 3 semaines pendant 4 cycles puis maintenance par pemetrexed bevacizumab est largement utilisé. Chez les patients présentant un carcinome épidermoïde, les associations cisplatine/carboplatine (AUC 6) paclitaxel ( $200\text{mg}/\text{m}^2$ ) toutes les 3 semaines ou cisplatine ( $75\text{ mg}/\text{m}^2$ ) docetaxel ( $75\text{ mg}/\text{m}^2$ ) toutes les 3 semaines peuvent être proposées.

Enfin, des stratégies thérapeutiques particulières s'appliquent chez les sujets âgés de plus de 70 ans. Dans cette situation, il est courant de proposer une chimiothérapie par carboplatine (AUC 6 J1/J29) paclitaxel ( $90\text{ mg}/\text{m}^2$  J1, J8, J15). D'autres thérapeutiques peuvent être proposées, à savoir une immunothérapie en monothérapie en cas de PD-L1  $\geq 50\%$  et un PS à 0 - 1. Les molécules suivantes sont alors disponibles : atezolizumab 1200mg J1/J22 (ou 840mg J1/J14 ou 1680mg J1/J28), cemiplimab 350 mg J1/J22 jusqu'à 2 ans, pembrolizumab 200mg IV J1/J22 jusqu'à 2 ans (ou 400mg/6 semaines). Dans de rares situations, chez des patients ne présentant que peu ou pas de comorbidités avec un état général parfaitement conservé, on peut proposer chez les non-épidermoïdes : carboplatine (AUC 5) - pemetrexed ( $500\text{ mg}/\text{m}^2$ ) – pembrolizumab 200mg IV J1/J22 ; suivi d'une maintenance par pemetrexed et pembrolizumab aux même doses jusqu'à 35 cycles, ou progression, ou toxicité inacceptable et chez les épidermoïdes : pembrolizumab 200mg IV carboplatine (AUC 6) paclitaxel ( $200\text{mg}/\text{m}^2$ ) J1/J22 suivi d'une poursuite du pembrolizumab à la même dose jusqu'à 2 ans, ou progression, ou

toxicité inacceptable. La Figure 3. résume les options thérapeutiques de première ligne du CBNPC de stade avancé sans addiction oncogénique.

**Figure 3. Algorithme de prise en charge de première ligne des patients présentant un CBNPC métastatique sans addiction oncogénique [Couraud et al. 2024].**

**A. CBNPC non épidermoïde**

**B. CBNPC épidermoïde**



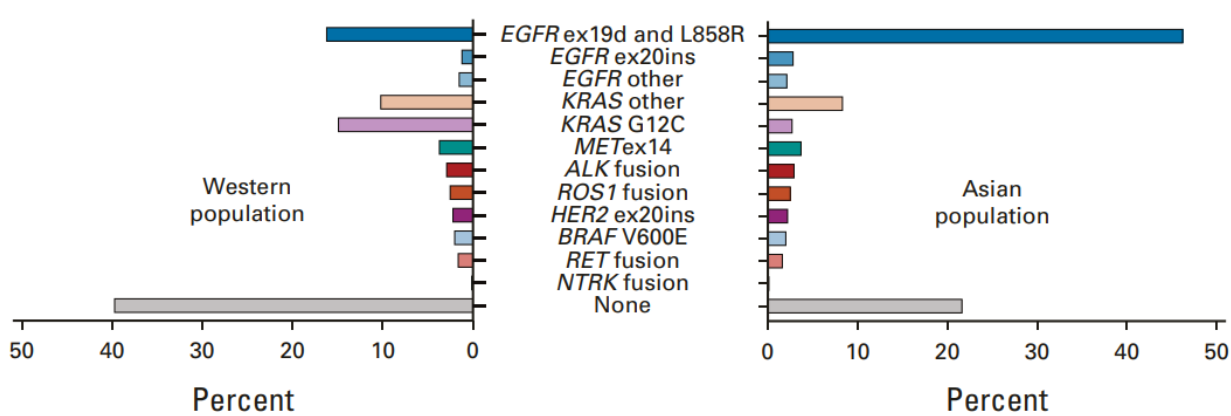
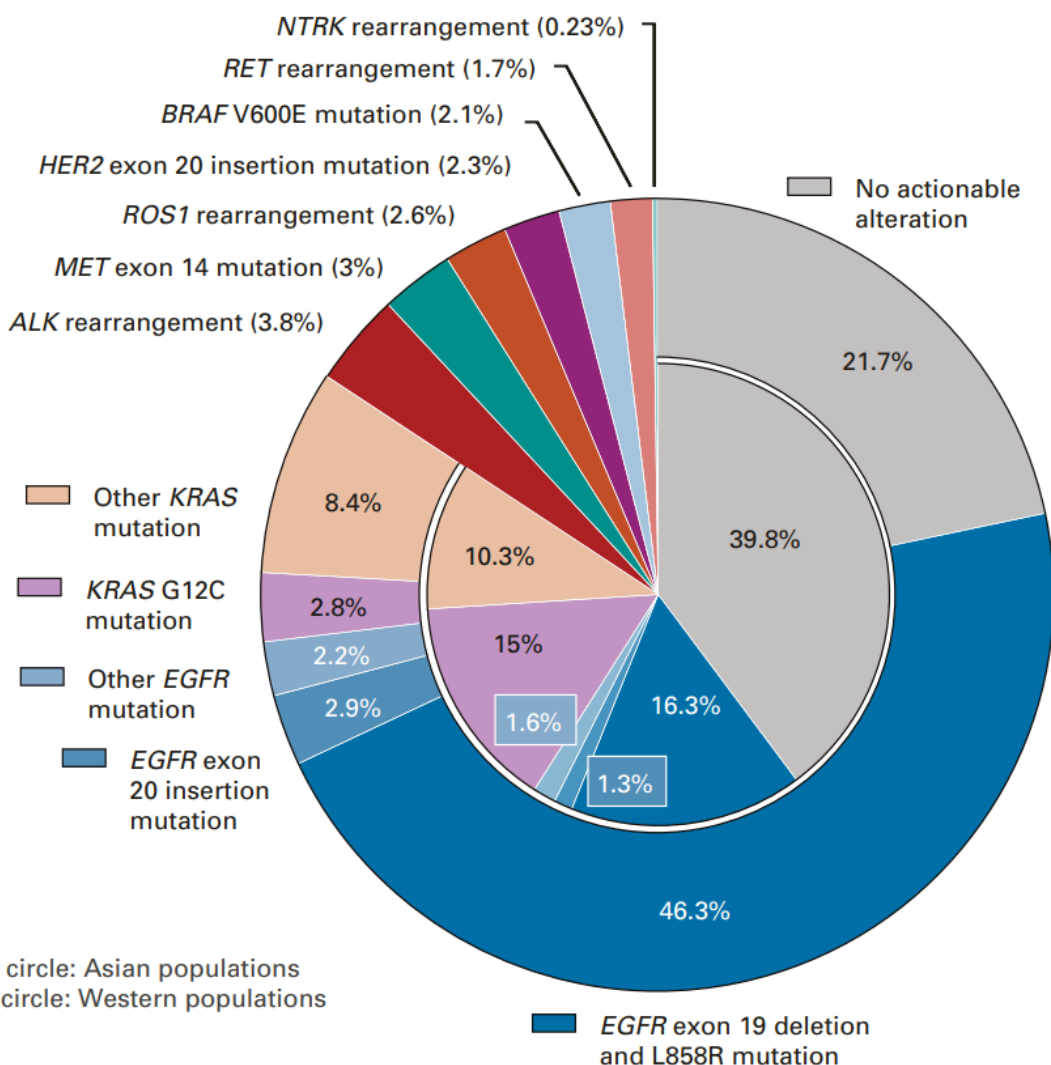
#### e. Traitement des CBNPC avec addiction oncogénique

Bien que l'immunothérapie ait constitué une évolution indéniable et a contribué à améliorer la prise en charge des patients, la découverte d'altérations moléculaires et de la possibilité de les cibler constitue elle aussi une réelle révolution en oncologie thoracique. En effet, de nombreuses altérations moléculaires pré- et post-transcriptionnelles sont actuellement connues et de nombreuses molécules les ciblant sont disponibles. Il est à noter que ces altérations concernent essentiellement les CBNPC de type non-épidermoïde chez les patients non ou petits fumeurs mais elles peuvent être mises en évidence, pour certaines d'entre elles, chez des patients fumeurs.

On notera que les mutations d'*EGFR* surviennent de manière préférentielle chez les femmes et dans les populations asiatiques alors qu'il n'est pas observé de préférence ethnique pour les fusions *ALK* et *ROS1*. Les mutations *KRAS* et *MET* surviennent dans les populations plus âgées, tabagiques et présentant un adénocarcinome. En ce qui concerne les mutations *KRAS*, on note une préférence pour les populations caucasiennes, et une association avec le tabagisme pour certaines (G12C). Les mutations *BRAF* peuvent survenir chez les fumeurs sans prédominance ethnique. La mutation *BRAF V600E* survient de manière préférentielle chez les femmes alors que les autres mutations *BRAF* surviennent de préférence chez les hommes. Les mutations *HER2* surviennent de préférence chez les femmes non fumeuses. [Gálffy et al. 2024, Fois et al. 2021]

La Figure 4. résume la fréquence des altérations moléculaires et leur répartition dans les populations asiatiques et non asiatiques.

**Figure 4. Fréquence des altérations moléculaires dans le CBNPC de type adénocarcinome**  
[Ref . Tan et al. 2022].



## *EGFR*

Epidermal growth factor receptor (EGFR), encore appelé HER1 (*Human EGFR Related*) est encodé par le gène *ErbB1* (*erythroblastic leukemia viral oncogene*). Il s'agit d'un récepteur de tyrosine kinase, membre de la famille de quatre récepteurs à tyrosine kinase ErbB/HER. Il s'agit d'une glycoprotéine transmembranaire monomérique de 170 kD composé d'un domaine N-terminal extracellulaire où se fixent les ligands, une région transmembranaire et un domaine intracellulaire C-terminal qui comprend un domaine kinase et de multiples sites de phosphorylation. Les ligands d'EGFR sont EGF et le TGF qui sont les deux ligands extracellulaires endogènes majeurs l'activant, mais aussi l'amphiréguline, et l'épigène (EPG), ces quatre molécules étant spécifiques de l'EGFR tandis que la bétacelluline, l/heparin binding EGF (HBEGF) et l'épiréguline sont des ligands de EGFR et de HER4. La fixation des ligands sur le récepteur entraîne un changement de conformation conduisant à l'homo-dimérisation ou à l'hétéro-dimérisation avec d'autres membres de la famille HER, phénomène permettant l'activation du domaine intrinsèque tyrosine kinase. Cette activation entraîne une cascade de phosphorylation activant les voies de signalisation de la phospholipase C, Ras/MAP-kinase, PI3K/PTEN/Akt, Jak/Stat, et STATs. Ces voies de signalisation sont des régulateurs potentiels de l'oncogenèse et de la croissance tumorale, de l'invasion, de l'angiogenèse et de la formation de métastases.

Les possibilités thérapeutiques en cas de présence de mutation d'*EGFR* se sont récemment élargies. Chez les patients présentant une maladie avancée, il est possible de proposer en première ligne thérapeutique un traitement par osimertinib, ITK de troisième génération. L'essai FLAURA [Soria et al. 2018] comparant l'osimertinib à un traitement par ITK de première génération de type erlotinib ou afatinib en première ligne chez les patients présentant une délétion de l'exon 19 ou une mutation L858R de l'exon 21 a montré une prolongation significative de la SSP et de la SG en faveur de l'osimertinib. La tolérance du traitement est également bonne avec une meilleure sélectivité sur le récepteur muté que sur les récepteurs sauvages.

Plus récemment, l'essai FLAURA 2 [Planchard et al. 2023] a comparé l'association osimertinib-chimiothérapie (pemetrexed associé à une molécule à base de sels de platine) à l'osimertinib seul chez les patients présentant une délétion de l'exon 19 ou une mutation L858R de l'exon 21 d'*EGFR*. Cet essai a montré un bénéfice en termes de SSP en faveur de l'association chimio-osimertinib, les données de SG étant immatures. La SSP médiane était de 25,5 mois dans le

groupe chimio-osimertinib vs 16,7 mois dans le groupe osimertinib (hazard ratio 0,62 ; IC 95%, 0,49 – 0,79; P<0,001).

L'essai MARIPOSA [Cho et al. 2024] a comparé l'association amivantamab-lazertnib à l'osimertinib chez des patients présentant un adénocarcinome bronchique avec mutation *EGFR* de type délétion de l'exon 19 ou mutation L858R de l'exon 21. Le critère de jugement principal était la SSP. L'essai a montré un bénéfice en termes de SSP en faveur de l'association amivantamab-lazertnib : 23,7 mois vs 16,6 mois (hazard ratio, 0,70 ; IC 95%, 0,58 – 0,85; P<0,001).

On notera l'existence d'autres mutations d'*EGFR*, plus rares, avec notamment des mutations de type insertion de l'exon 20 pour lesquelles les ITK sont habituellement peu efficaces. Dans ce contexte, l'association amivantamab-chimiothérapie a monté un bénéfice en termes de SSP comparativement à la chimiothérapie seule [Zhou et al. 2023].

Des essais ont également montré l'intérêt de l'utilisation des ITKs dans des stades plus précoces. L'essai ADAURA [Wu et al. 2020, Herbst et al. 2023] a évalué l'osimertinib en adjuvant chez des patients opérés d'un adénocarcinome bronchique muté *EGFR* (délétion de l'exon 19, mutation L858R de l'exon 21) de stade IB-IIIA. Les résultats finaux ont été rapportés chez les patients présentant un stade II-IIIA. Les patients avaient la possibilité de recevoir une chimiothérapie adjuvante. Après un suivi médian de 44,2 mois, la SSM était significativement plus longue dans le groupe osimertinib que dans le groupe placebo : 65,8 mois (IC 95%, 54,4 - NA) vs 21,9 mois (IC 95%, 16,6 – 27,5), HR 0,23 (IC 95% , 0,18 – 0,30). On notera enfin les résultats de l'essai LAURA [Lu et al. 2024] qui a évalué l'osimertinib en consolidation chez les patients présentant un adénocarcinome bronchique de stade III muté *EGFR* et traité par radio-chimiothérapie concomitante. Cet essai a montré des résultats positifs en termes de SSP en faveur de l'osimertinib : 39,1 mois vs 5,6 mois (hazard ratio 0,16 (IC 95%, 0,10 – 0,24); P<0,001.

## ALK

Le réarrangement NPM1-ALK a initialement été décrit chez des patients atteints de lymphome anaplasique à grandes cellules. Dans un second temps, le réarrangement EML4-ALK a été décrit chez des patients présentant un CBNPC. Depuis cette description initiale, plus de 90 partenaires de fusion ALK ont été identifiés. Le CBNPC présentant ce réarrangement

reste une tumeur relativement rare car elle représente 3 à 7 % de tous les CBNPC. Les réarrangements ALK entraînent une activation constitutive de la kinase ALK et des voies de signalisation cellulaire en aval associées, telles que RAS-MAPK, PI3K-AKT et JAK-STAT, conduisant à une prolifération et une survie cellulaire dysrégulées. De nombreux ITK de première, deuxième, troisième et de nouvelle génération ont été développés pour le traitement des CBNPC de stade avancé présentant un réarrangement ALK. Les données récentes ont permis de montrer une supériorité de l'alectinib (600 mg x 2/j) par rapport au crizotinib (250 mg x 2/j) en première ligne en termes de SSP et un bénéfice numérique en termes de SG mais les données de survies étaient non matures lors de la publication [Mok et al. 2020]. Le brigatinib (90 mg x1/j pendant 7 jours puis 180 mg x1/j) a également été comparé au crizotinib (250 mg x2/j) [Camidge et al. 2021] et a monté sa supériorité en termes de SSP et de SG avec de nouveau des données non matures rendant l'interprétation de la SG incomplète. Enfin, le lorlatinib, ITK d'ALK de troisième génération a lui également été comparé au crizotinib avec des données mises à jour de manière récente [Solomon et al. 2024] qui montrent, à 5 ans, un bénéfice en termes de SSP avec une SSP non atteinte dans le groupe lorlatinib. On notera également que le temps jusqu'à progression intra-crânienne était également non atteint dans le groupe lorlatinib. Ces résultats positionnent le lorlatinib comme ITK de choix de première ligne chez les patients présentant un CBNPC de stade IV avec une translocation ALK. Des ITK de nouvelle génération sont en cours de développement et les résultats des essais de phase précoce sont déjà encourageants [Lin et al. 2024].

De la même manière que pour les mutations *EGFR* avec l'osimertinib, l'alectinib a été évalué chez des patients présentant un CBNPC avec réarrangement ALK de stade IB-IIIA opéré. L'alectinib en adjuvant a monté un bénéfice en termes de SSM comparé à la chimiothérapie adjuvante [Wu et al. 2024]. Cette situation clinique demeure néanmoins rare voire exceptionnelle avec l'immense majorité des patients présentant une maladie avancée lors du diagnostic.

## *ROS1*

En première ligne métastatique, le crizotinib dispose d'une AMM sans remboursement et est actuellement le traitement de choix. De nombreuses autres molécules ont été évaluées et ont montré une efficacité en première ligne ou après progression sous crizotinib. Toute la

difficulté réside dans le caractère rare de cette anomalie moléculaire (1% des CBNPC environ), rendant les essais thérapeutiques de grande ampleur difficiles à réaliser. On pourra citer l'efficacité en première ligne thérapeutique de plusieurs molécules comme l'entrectinib [Drilon et al. 2019, Peters et al. 2024], le ceritinib [Lim et al. 2017], le lorlatinib [Baldacci et al. 2022, Shaw et al. 2019] ou encore le repotrectinib [Drilon et al. 2024]. Ce dernier est un pan-ITK de nouvelle génération qui cible ROS1, TRK et ALK et qui a donné des résultats prometteurs en première ligne thérapeutique. Actuellement, la prise en charge thérapeutique repose sur un traitement par crizotinib (250mg x 2/j) avec une possibilité de proposer un traitement par repotrectinib en accès compassionnel chez les patients prétraités par crizotinib. Il est également souhaitable d'inclure ces patients autant que possible dans les essais thérapeutiques.

#### *BRAF*

Chez les patients présentant un CBNPC métastatique présentant une mutation BRAF V600E, un traitement associant dabrafenib (ciblant BRAF, 150 mg x2/j) et trametinib (ciblant MEK, 2 mg x 1/j) est disponible et a montré son efficacité en première et en deuxième ligne dans des essais de phase II non contrôlés [Planchard et al. 2016, Planchard et al. 2017]. L'association encorafenib + binimetinib [Riely et al. 2023] montre également des résultats encourageants et dispose d'une AMM européenne et se présente comme une option thérapeutique supplémentaire dans cette situation.

#### *Mutations dans l'exon 14 de MET*

Plusieurs molécules ont également été évaluées dans la prise en charge des mutations de l'exon 14 de *MET*. Actuellement en France, seul le crizotinib dispose de la possibilité d'une prescription compassionnelle suite aux résultats de l'essai ACSé crizotinib [Moro-Sibilot et al. 2019]. Des inhibiteurs spécifiques ont également été développés avec des résultats encourageants comme le tepotinib [Paik et al. 2020] ou le capmatinib [Wolf et al. 2020] Ces deux molécules disposent d'une AMM européenne en deuxième ligne thérapeutique chez ces patients mais ne sont actuellement pas accessibles en France. Le seul recours thérapeutique repose sur le crizotinib en deuxième ligne et l'inclusion dans les essais thérapeutiques.

#### *Mutation HER2 (mutation ou insertion dans l'exon 20)*

L'anticorps conjugué trastuzumab-deruxtecan a montré son intérêt dans cette indication [Li et al. 2022] En outre, le zongertinib, un ITK qui lie HER2 de manière irréversible a montré des résultats préliminaires intéressants [Heymach et al. 2023, Wilding et al. 2024].

#### *KRAS G12C*

La mutation G12C est une mutation fréquente qui est habituellement retrouvée chez les patients fumeurs présentant un CBNPC. Plusieurs inhibiteurs spécifiques pour les mutations KRAS G12C ont récemment été développés, comme le sotorasib [de Langen et al. 2023] ou l'adagrasib [Jänne et al. 2022]. Actuellement, le sotorasib n'est plus accessible en France et l'adagrasib est en cours d'évaluation dans des essais de phase III. Il est néanmoins accessible en accès compassionnel chez les patients ayant échappé à une seconde ligne par docetaxel ou inéligibles à un traitement par docetaxel en seconde ligne.

## **II- Les mécanismes de résistance à l'immunothérapie**

Comme évoqué ci-dessus, l'immunothérapie constitue une modalité thérapeutique utilisée dans de nombreuses situations cliniques, aussi bien au stade localisé, localement avancé que métastatique chez les patients présentant un CBNPC.

Définir, organiser et classer les différents mécanismes de résistance constitue un réel défi, et plusieurs classifications ont été proposées. Sharma et al. [Sharma et al. 2017] ont proposé de distinguer la résistance primaire, adaptative et acquise. Actuellement, une classification simplifiée distinguant la résistance primaire et acquise est largement employée [Schoenfeld et al.2020].

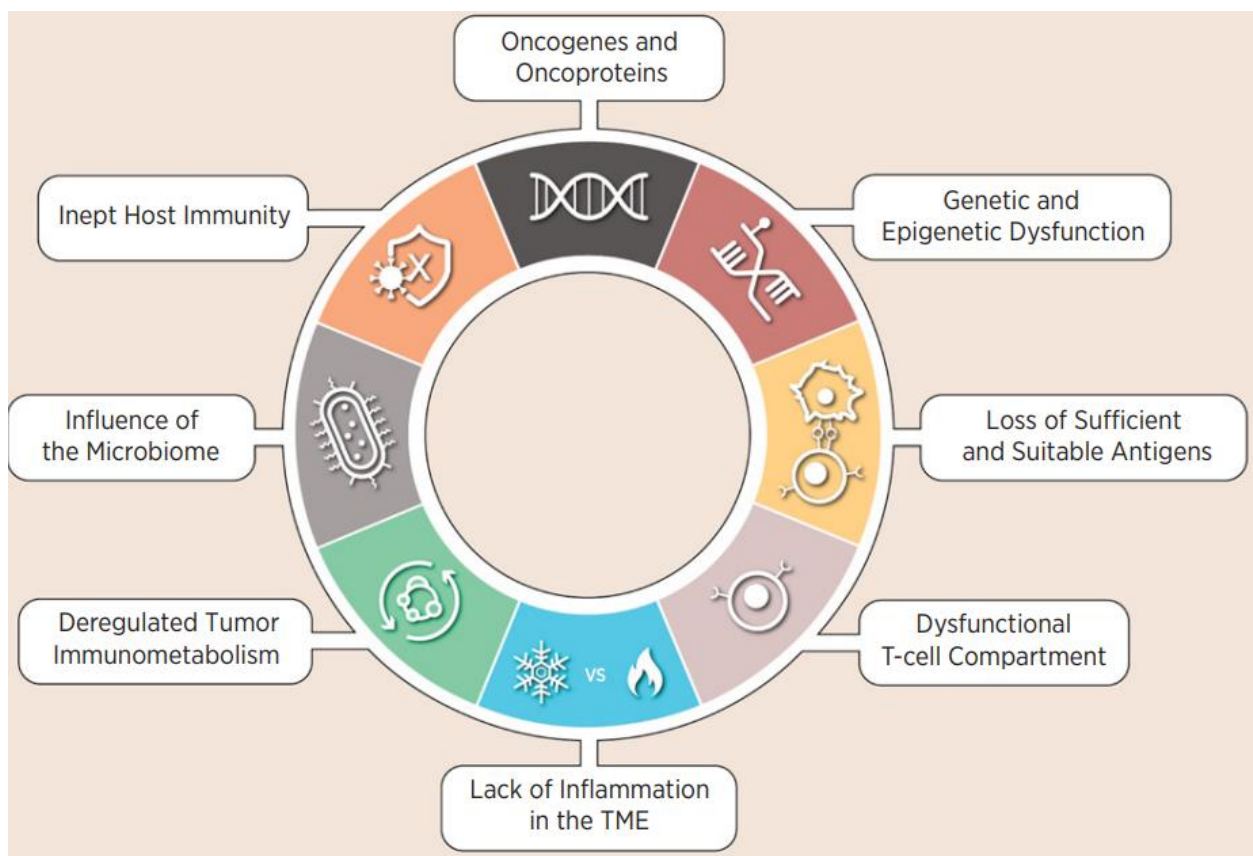
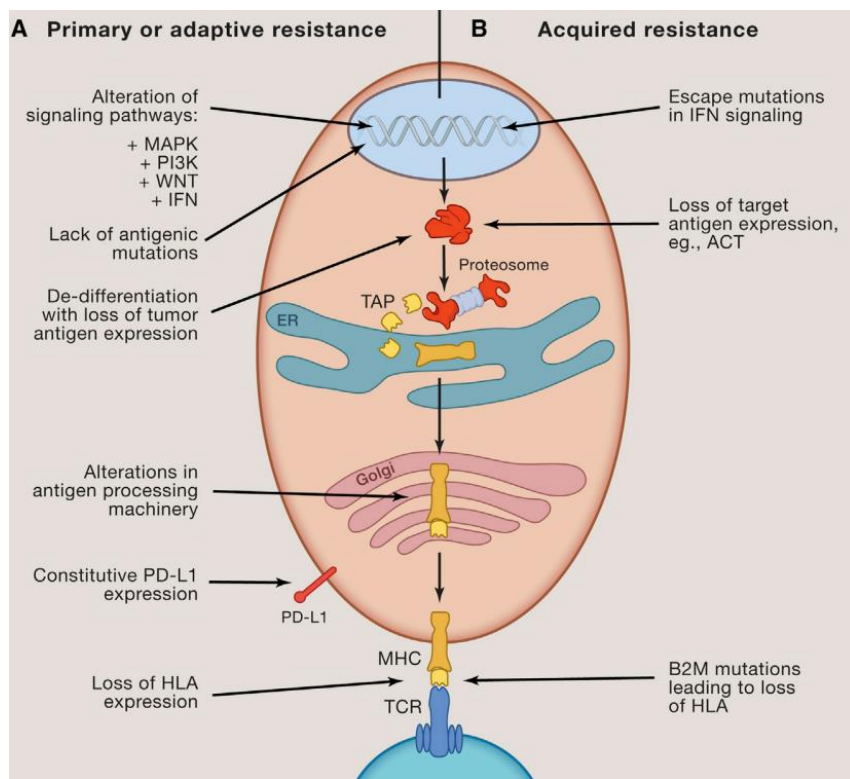
### **1. Définition des mécanismes de résistance à l'immunothérapie**

La Society for Immunotherapy of Cancer (SITC) a récemment publié un consensus de la définition de résistance à l'immunothérapie ou à la combinaison d'immunothérapie [Kluger et al. 2023]. La résistance primaire concerne les patients ayant reçu au moins deux cycles complets de traitement et qui présentent une progression tumorale ou une stabilité tumorale durant moins de 6 mois. La résistance acquise y est définie comme une progression survenant après 6 mois d'exposition au traitement et une réponse partielle, une réponse complète ou une stabilité durant au moins 6 mois. Il est noté que, pour les cancers agressifs comme le CBNPC, cette définition peut être raccourcie à 3 mois. Les mécanismes de résistance à l'immunothérapie sont résumés dans la figure 5.

**Figure 5. Mécanisme de résistance primaire et acquise à l'immunothérapie.**

**A. Mécanismes de résistance primaires et acquis [Sharma et al. 2017]**

**B. Classification biologique des mécanismes de résistance [Karasarides et al. 2022]**



Dans le CBNPC de stade avancé traité par immunothérapie seule ou en association avec la chimiothérapie, le taux de résistance primaire reste approximatif. Dans l'essai Keynote-189 [Gandhi et al. 2018], le TRO était de 47,6% dans le groupe expérimental, suggérant que plus de la moitié des patients ont présenté une résistance primaire à l'immunothérapie. Ce taux correspond à une estimation car il ne prend pas en compte les patients non-répondeurs mais qui présentent une stabilité radiologique et un bénéfice clinique qui peut durer parfois plusieurs mois. D'autres auteurs rapportent des taux de résistance primaire plus bas, allant de 7 à 44% selon les modalités thérapeutiques (deuxième ligne et plus, première ligne seule, première ligne en association avec la chimiothérapie).

Il existe un mécanisme de progression particulier que l'on a nommé hyperprogression (HP) [Champiat et al. 2016]. Dans cette situation clinique, la tumeur connaît une accélération brutale et rapide de sa croissance suite à l'exposition à une immunothérapie. Ce contexte clinique présente un pronostic très sombre et peut toucher jusqu'à 10-15% des patients présentant un CBNPC de stade avancé traités par immunothérapie seule. Les mécanismes biologiques menant à l'HP peuvent nous renseigner sur les mécanismes de résistance primaire et acquise à l'immunothérapie. Li et al. [Li et al. 2022] ont montré que les patients qui présentent une HP ont une augmentation de l'expression tumorale de fibroblast growth factor 2 (FGF2) et une dérégulation de la voie de signalisation  $\beta$ -caténine. La dérégulation de cette voie de signalisation serait secondaire à la sécrétion d'interféron-gamma (IFNG) par les lymphocytes T (modèle animal) qui pourrait promouvoir la signalisation médiée par FGF2. D'autres auteurs ont montré le rôle délétère des cellules T régulatrices effectrices exprimant PD-1 [Kamada et al. 2019]. En effet, les cellules T régulatrices effectrices exprimant PD-1 sont fortement activées et proliférantes dans le contexte d'HP et jouent un rôle inhibiteur sur l'immunité anti-tumorale. Les macrophages associés aux tumeurs (macrophages M2-like CD163 $^{+}$ CD33 $^{+}$ PD-L1 $^{+}$ ) [Lo Russo et al. 2019] jouent également un rôle dans l'HP et semblent pouvoir être reprogrammés suite à l'interaction avec le fragment Fc de l'anticorps monoclonal. Enfin, Du et al. [Du et al. 2018] ont souligné le rôle délétère d'une forte expression du PD-1 par les cellules tumorales. Les mécanismes biologiques restent néanmoins encore mal connus, et sont certainement multiples et intriqués.

La résistance acquise correspond à la situation clinique où les patients présentent une réponse initiale à l'immunothérapie suivie d'une progression dans un deuxième temps. De la même manière que pour la résistance primaire, les taux de résistance acquise ne sont pas connus de

manière précise. Ils ont été estimés par Schoenfeld et al. [Schoenfeld et al. 2020] entre 32% et 64%. D'autres auteurs [Zhou et al. 2023] ont estimé le taux de résistance acquise entre 32% et 78%.

Les principaux mécanismes biologiques de résistance acquise aux ICIs sont : les défauts de présentation antigénique, les perturbations de la signalisation liée à l'IFNG, la déplétion en néo-antigènes, l'immunosuppression/immunoexclusion médiée par la tumeur et l'action d'autres points de contrôle immunitaires [Schoenfeld et al. 2020].

Les défauts de présentation antigénique seront détaillés ci-après. La perturbation de la signalisation liée à IFNG peut survenir suite à l'acquisition de mutations au niveau des gènes encodant *Janus kinase (JAK) 1* ou *JAK2*, ce qui entraîne une perte de sensibilité des cellules cancéreuses à la signalisation IFNG [Zaretsky et al. 2016, Sucker et al. 2017]. La déplétion en néo-antigènes peut survenir suite à la perte de mutations somatiques qui encodent pour des néo-antigènes anti-tumoraux potentiels. Cette perte peut être la conséquence d'une sélection clonale, d'une répression épigénétique ou d'une perte du nombre de copies. L'ensemble de ces mécanismes menant à une évasion des cellules tumorales [Anagnostou et al. 2016]. La perte de *PTEN* est un autre mécanisme de résistance acquise qui entraîne l'augmentation de l'expression de cytokines immunosuppressives et diminue la sécrétion d'IFNG par les lymphocytes T effecteurs. Ainsi, l'infiltration immunitaire médiée par les lymphocytes T est inhibée ce qui conduit à l'échappement tumoral [Trujillo et al. 2019]. L'activation de la voie Wingless-integration stie (WNT)- $\beta$ -catenin a été liée à la production de cytokines immunosuppressives, à l'altération du priming des cellules dendritiques, à la promotion de cellules T régulatrices et à une faible infiltration lymphocytaire T, et est également un mécanisme de résistance aux ICIs [Yaguchi et al. 2012, Zhao et al. 2017]. Enfin, l'augmentation de l'activité d'autres inhibiteurs de point de contrôle immunitaires comme LAG3 ou TIM3 peuvent également contribuer à la résistance acquise [Gettinger et al. 2017].

## 2. Altérations de la présentation antigénique

Les cellules cancéreuses ont la capacité de réduire l'expression des protéines HLA à leur surface et donc d'échapper à l'immunité adaptative. Il s'agit d'un mécanisme majeur de résistance primaire et acquise à l'immunothérapie [Garrido et al. 2019, Jhunjhunwala et al.

2021]. Plusieurs mécanismes peuvent induire un défaut d'expression d'HLA :

- mutations au niveau des gènes codant pour beta-2-microglobuline ( $\beta$ 2M) telle qu'une perte bi-allélique, une perte d'hétérozygotie ou mutations par décalage du cadre de lecture.
- mécanismes de régulation épigénétique. Par exemple l'hyperméthylation de promoteurs des gènes de complexe majeur d'histocompatibilité (CMH) de classe I survient fréquemment et cela entraîne une inactivation des loci HLA-A, -B ou -C. De manière indirecte, des méthyltransférases des histones au sein de la machinerie de remodelage de la chromatine peut impacter l'infiltration lymphocytaire TCD8+, la réponse à TNF alpha, l'expression de PD-L1 et l'expression du CMH-I [Zingg et al. 2017].
- En outre, les facteurs de transcription DUX4 contrôle en partie l'expression des gènes HLA-A/B/C et  $\beta$ 2M. Une dérégulation de l'expression de DUX4 entraîne une réduction de la réponse à IFNG et une expression CMH-I réduite [Chew et al. 2019].

L'ensemble de ces mécanismes sont mal connus et mal documentés, notamment dans le CBNPC.

Une partie de nos travaux s'est donc focalisée sur la machinerie de présentation antigénique et plus particulièrement sur les composants du complexe de chargement des peptides (CCP).

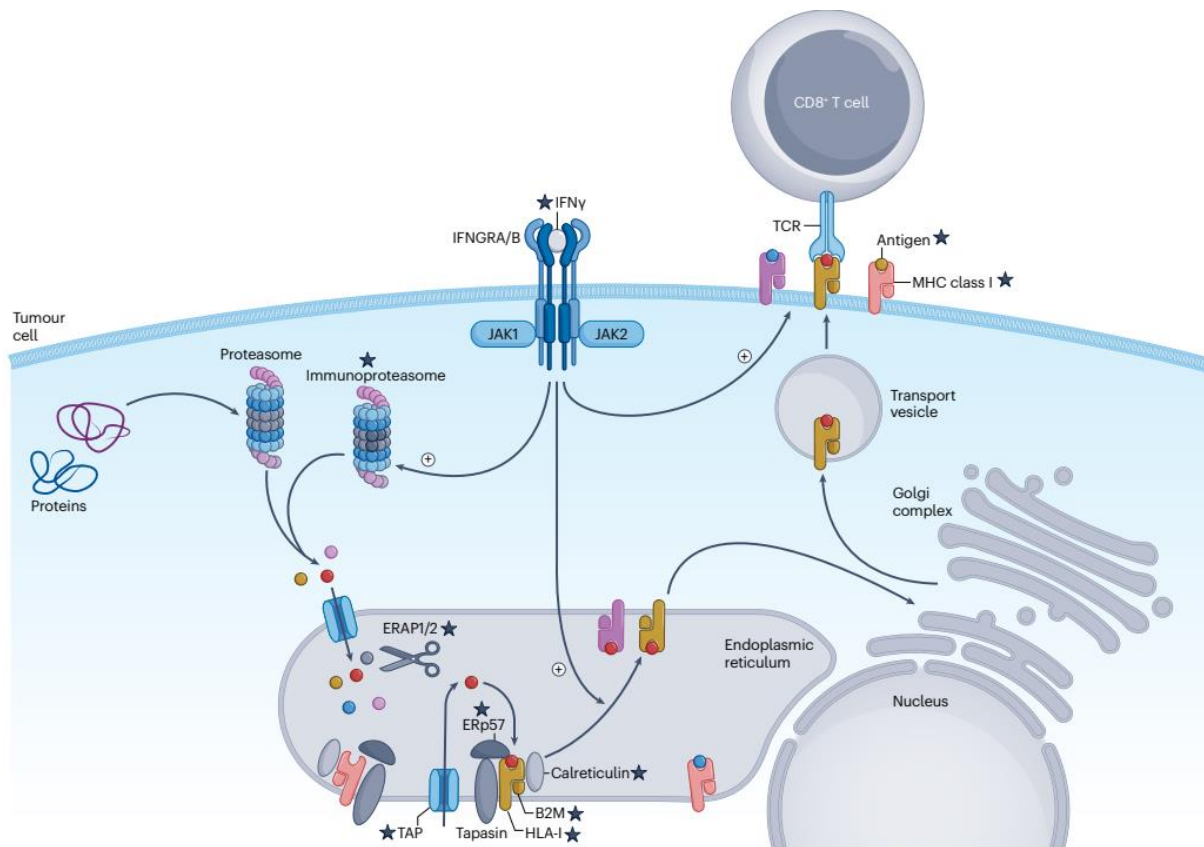
### **III- La présentation antigénique liée au complexe majeur d'histocompatibilité (CMH) de classe I**

#### **1. La formation des peptides**

La présentation antigénique liée au CMH de classe I permet aux lymphocytes T CD8+ d'identifier les cellules qui produisent des protéines du non-soi. Les peptides présentés à la surface cellulaire sont générés dans le cadre du catabolisme habituel des protéines cellulaires. De manière physiologique, l'ensemble des protéines synthétisées de manière endogène sont dégradées en oligopeptides par la voie ubiquitine-protéasome [Rock et al. 1999]. Celle-ci permet les clivages initiaux, en particulier la coupure C-terminale qui est nécessaire pour la génération de la majorité des peptides présentés par le système CMH de classe I [Rock et al. 1994, Michalek et al. 1993, Shen et al. 2004, Wei et al. 2017].

Le protéasome est un complexe enzymatique multiprotéiques qui est localisé, dans les cellules eucaryotes, au niveau du cytosol et est associé au réticulum endoplasmique (RE) [Peters et al. 1994]. Sa fonction principale consiste en la dégradation ciblée de protéines mal repliées, dénaturées ou devenues obsolètes. La dégradation se fait par protéolyse et permet d'obtenir des peptides longs de 7 à 9 acides aminés. Il existe plusieurs formes de protéasomes, connues sous les noms de protéasomes, immunoprotéasomes et thymoprotéasomes [Murata et al. 2018]. Les immunoprotéasomes sont composés de trois versions alternatives de sous-unités du site actif des protéasomes. Ces versions alternatives présentent des propriétés catalytiques différentes ce qui donne aux immunoprotéasomes la possibilité de générer une grande variété de peptides différents, souvent mieux adaptés pour la présentation antigénique de type CMH de classe I [Ref. Rock et al. 1999, Kincaid et al. 2011]. Une fois les peptides produits par l'immunoprotéasome, une partie est transférée dans la lumière du RE par le transporteur Transporter associated with Antigen Processing (TAP). La machinerie de présentation des antigènes est représentée dans la Figure 6.

**Figure 6. Représentation schématique de la machinerie de présentation antigénique dans les cellules tumorales [Yang et al. 2023]**



## 2. Le complexe de chargement des peptides

Le complexe de chargement des peptides (CCP) est un complexe multi-protéique composé de plusieurs protéines chaperones. Son rôle est la stabilisation de l'ensemble chaîne lourde de CMH-I, chaîne légère CMH-I ou  $\beta$ 2M et peptide. Les protéines chaperones qui le constituent sont tapasin, calreticulin (un homologue soluble de calnexin), ERp57 (une thiol oxydo-réductase). Le CCP complet est donc formé des protéines tapasin, calreticulin, ERp57, du complexe chaîne lourde de CMH-I/ $\beta$ 2M sans peptide et des deux transporteurs TAP (TAP 1 et 2). La Figure 7. montre la composition et l'architecture d'un CCP humain.

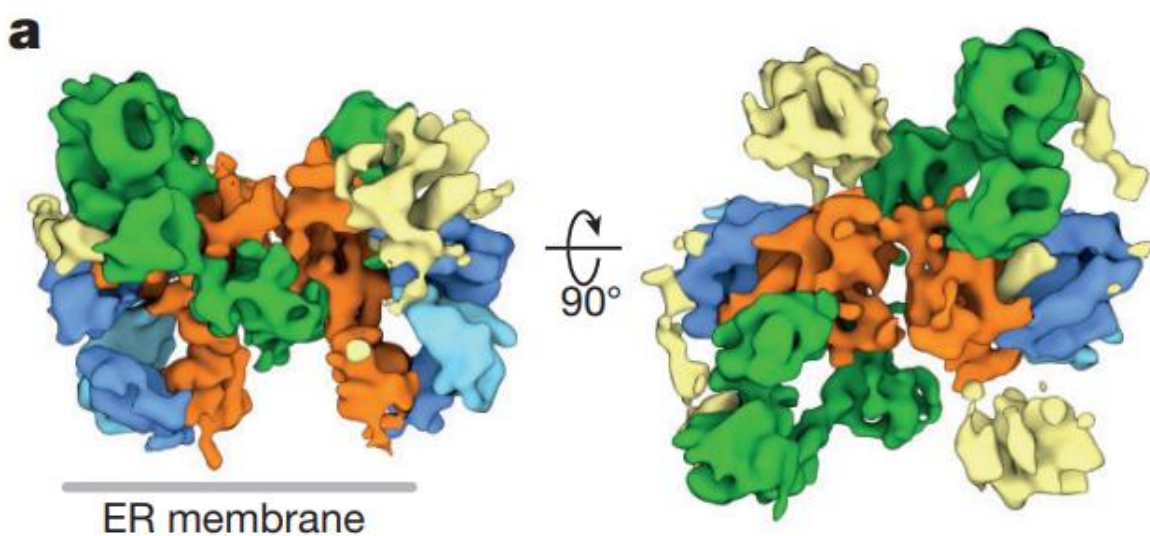
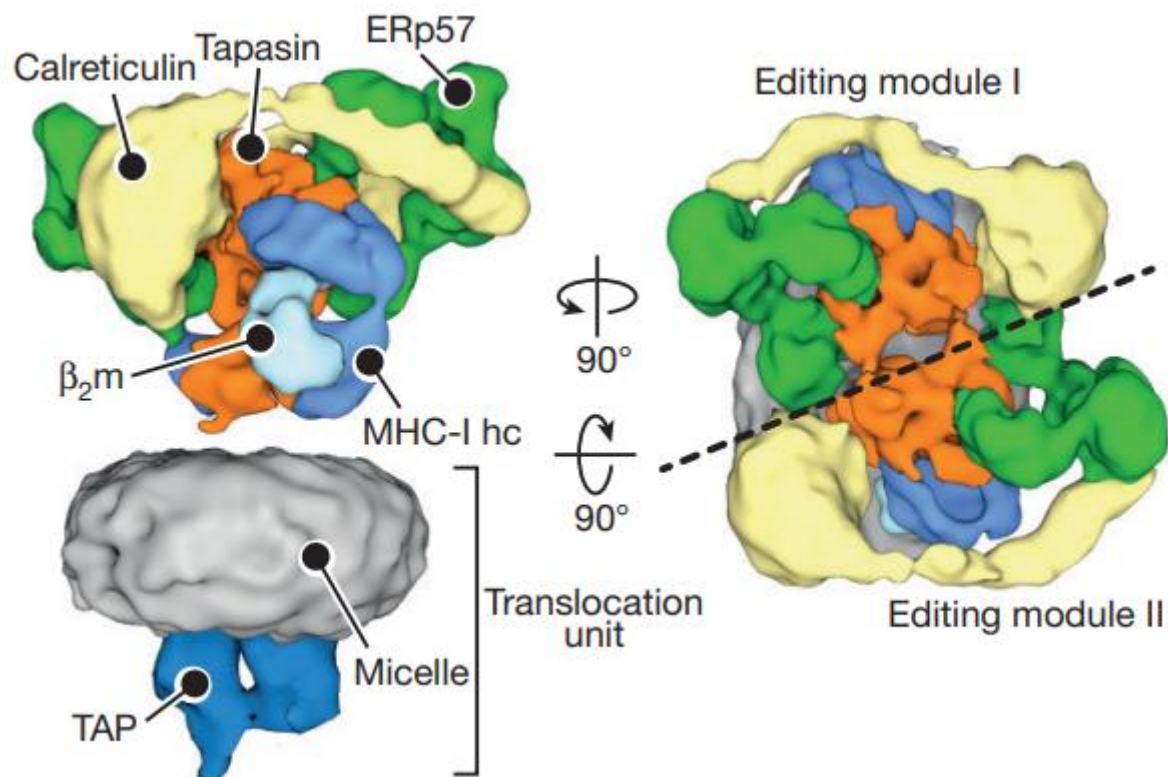
La séquence de chargement des peptides commence par le pliage de la chaîne lourde de CMH-I. Ce pliage est facilité par la protéine chaperone calnexin. La chaîne lourde s'associe ensuite avec  $\beta$ 2M pour générer un hétérodimère apte à accueillir un peptide. Cet ensemble est ensuite intégré au CCP. Afin de permettre un chargement optimal des peptides sur le complexe chaîne lourde de CMH-I/ $\beta$ 2M, un CCP intact et fonctionnel et nécessaire. Une fois le peptide chargé de manière stable, le CCP libère le complexe chaîne lourde de CMH-I/ $\beta$ 2M/peptide qui sort du RE, traverse l'appareil de Golgi et rejoint la surface cellulaire afin de présenter le peptide au lymphocytes TCD8+ et aux cellules NK.

La structure précise du CCP a été déterminée par cryo-microscopie électronique (cryo-ME) et décrite par Blees et al. [Blees et al. 2017]. D'après leur description, le CCP se compose de deux modules d'édition étroitement liés. Deux molécules de tapasin opposées, inclinées de 30° l'une vers l'autre, forment un échafaudage central. Erp57 se présente avec une conformation en forme de U et est complexé à tapasin via les domaines a et a' 12 catalytiquement actifs. En outre, il existe une disposition croisée des deux modules tapasin-ERp57 permettant de stabiliser le CCP. Tapasin se lie également à la chaîne lourde de CMH de classe I par des résidus présents dans la boucle entre les brins  $\beta$  17 et 18 du domaine immunoglobulinique de type C-terminal qui s'accrochent à la boucle de reconnaissance CD8 du domaine  $\alpha$ 3 des chaînes lourdes. Au second site de liaison, les brins  $\beta$  6 et 7 et l'hélice  $\alpha$ 2-1 des chaînes lourdes de CMH-I sont agrippés par des résidus dans les boucles reliant les brins  $\beta$  1-2 et 9-10 de tapasin, positionnant les résidus critiques R187 de tapasin et T134 de la chaîne lourde de CMH-I proches l'un de l'autre. Calreticulin possède un domaine lectine globulaire qui contient un site de liaison au glycane. Ce site de liaison détecte les motifs monoglucose des glycanes N-core

de la chaîne lourde CMH-I avant qu'il ne s'associe avec tapasin. La branche monoglucosylée du glycane N-core, issue de N86 de la chaîne lourde de CMH-I, est fixée à la surface de liaison au glycane de la calreticulin, tandis qu'une autre branche mannose s'insère probablement parmi les résidus situés au bord du sandwich  $\beta$  de la lectine. La queue C-terminale de calreticulin pointe vers la membrane lumineuse du RE, où elle est située près du domaine immunoglobulinique de type C-terminal de tapasin. Le domaine bras de calreticulin forme une ceinture elliptique discontinue autour du module d'édition et connecte la chaîne lourde de CMH-I à ERp57. La région centrale du domaine bras surplombe la fente de liaison au peptide de la chaîne lourde CMH-I. La pointe du domaine bras repose sur l'hélice H12 du domaine b' d'ERp57. Cette proposition de structure, met en évidence le rôle central du domaine immunoglobulinique de type C-terminal de tapasin, qui agit comme un centre d'interaction multivalent essentiel pour les autres sous-unités du CCP. Les auteurs précisent enfin que la présence d'une cavité centrale reliant la sortie du chemin de translocation des peptides de TAP avec la lumière du RE via deux fenêtres latérales pourrait servir de panier moléculaire pour les peptides transportés avant qu'ils ne soient modifiés par les aminopeptidases résidentes du RE.

**Figure 7. Composition et architecture du CCP humain [Blees et al. 2017]**

- A. Structure générale du PLC totalement assemblé
- B. Densité cryo-ME des deux modules d'édition pseudo-symétrique



*a. Transporter associated with antigen processing (TAP)*

TAP est un membre de la super-famille des transporteurs ABC. Les membres de cette famille transportent de nombreuses molécules (ions, grandes protéines) à travers les membranes cellulaires de manière ATP-dépendante. Les transporteurs ABC partagent deux domaines cytoplasmiques capables de lier l'ATP et deux domaines hydrophobes composés de 5-10 segments transmembranaires. TAP est composé de deux sous-unités, TAP1 (748 acides aminés) et TAP2 (686 acides aminés et 653 pour TAP2 iso). Les gènes pour TAP1 et TAP2 sont localisés dans le locus du CMH-II du chromosome 6 et sont formés de 8-12 kb chacun. Les sous-unités TAP1 et TAP2 se dimérisent afin de former le transporteur TAP. Il a été montré que TAP1 a la capacité de former des homodimères mais il n'a pas été mis en évidence d'homodimères composés exclusivement de sous-unités TAP2 [Antoniou et al. 2002]. Le transporteur TAP permet le transport des peptides du cytosol vers la lumière du RE.

*b. Tapasin*

Tapasin est une glycoprotéine transmembranaire de 48 kDa encodé par le gène *TAPBP*. Elle joue un rôle essentiel dans la sélection des peptides et dans la stabilisation du complexe chaîne lourde de CMH-I/ $\beta$ 2M/peptide.

Il s'agit d'une protéine chaperone spécifique qui joue un rôle essentiel dans la stabilisation et le chargement de peptides sur des molécules chaîne lourde CMH-I vides. Tapasin se trouve au sein du RE, dans une conformation stable, liée avec un site cystéine actif de la thiol oxydo-réductase ERp57 [Dick et al. 2002, Peaper et al. 2005]. L'hétérodimère tapasin/ERp57 recrute les molécules du CMH-I ainsi que la chaperone calereticlulin au sein du CCP [Wearsch et al. 2007]. Tapasin se lie également à TAP en s'y associant via son domaine transmembranaire ce qui permet aux chaînes lourdes CMH-I de se rapprocher des peptides qui entrent dans le RE. Ainsi, l'expression de TAP est augmentée et la quantité de peptide présente dans la lumière du RE augmente [Bangia et al. 1999, Garbi et al. 2003]. Tapasin permet également de retenir les molécules CMH-I vides dans le RE et favorise leur chargement avec des peptides de haute affinité. Enfin, tapasin permet de stabiliser les complexes chaîne lourde de CMH-I/ $\beta$ 2M vides. Tapasin permettrait également de catalyser la liaison entre chaîne lourde de CMH-I/ $\beta$ 2M et le

peptide. Parmi les autres rôles de tapasin, il a été suggéré qu'il a la possibilité d'éditer la longueur des peptides mais il semblerait qu'il ne soit plus un facilitateur [Zarling et al. 2003].

#### c. *ERp57*

ERp57, également nommé protéine disulfide isomérase 3 (PDIA3), est une thiol oxydo-réductase de 58 kDa, membre de la famille des protéines disulfides isomérase (PDI). Les PDIs sont un ensemble d'enzymes caractérisées par la présence de domaines thiredoxines. Erp57 se situe essentiellement au niveau du RE, mais il a été montré qu'il peut se trouver au niveau du noyau ou encore au niveau de la membrane cellulaire. En lien avec la présentation antigénique liée au CMH-I, ERp57 joue un rôle central. Tout d'abord, la chaîne lourde CMH-I glycosylée se lie à calnexin et ERp57. La formation de ce complexe permet de catalyser la formation de liens disuflides au sein de la chaîne lourde ce qui permet son assemblage avec  $\beta$ 2M. Dans un second temps, les deux domaines catalytiques d'ERp57 forment un hétérodimère stable avec tapasin, essentiel pour le chargement des peptides [Dong et al. 2009, Coe et al. 2010].

La présence d'ERp57 en dehors du RE a également été mise en évidence avec sa présence retrouvée au niveau du noyau, du cytosol et de la membrane cellulaire. ERp57 semble jouer un rôle de régulation génique en interagissant directement avec l'ADN, sur la signalisation de réparation de l'ADN et sur la voie de signalisation STAT3. Par ailleurs, ERp57 joue un rôle dans la mort cellulaire immunogénique. L'exposition de calreticulin à la surface des cellules déclenche la réponse immunitaire et facilite la reconnaissance et la destruction des cellules apoptotiques. ERp57 joue un rôle essentiel afin de permettre la translocation de calreticulin à la surface cellulaire [Panaretakis et al. 2009]. De manière intéressante et contradictoire, il a également été montré qu'ERp57 joue un rôle dans la dégradation de la matrice extra-cellulaire [Ros et al. 2020] soulignant le caractère ambivalent de cette chaperone.

#### d. *Calreticulin*

Calreticulin est une protéine chaperone de 46 kDa composée de 417 acides aminés. Sa

localisation principale se situe dans lumière du RE. Elle se compose d'un domaine lectine N-terminal qui permet son interaction avec intégrines  $\alpha$ , et qui contient un site de liaison à l'ADN de type récepteur stéroïdien impliqué dans les fonctions de chaperonnage, un domaine central riche en proline avec une affinité élevée et une faible capacité de liaison au  $\text{Ca}^{2+}$ , qui participe à l'activité de chaperonnage et enfin une région C-terminale hautement acide avec une faible affinité et une grande capacité de liaison au  $\text{Ca}^{2+}$ , impliquée dans les fonctions de tamponnement du  $\text{Ca}^{2+}$  suivie d'un domaine KDEL C-terminal qui assure le retour de calreticulin de l'appareil de Golgi vers le RE. Calreticulin joue plusieurs rôles, d'une part, elle participe, au sein du cycle calnexin/calreticulin, au contrôle de qualité pour les protéines et glycoprotéines nouvellement synthétisées. Ce système empêche l'exportation prématurée hors du RE de protéines mal repliées. Calreticulin, du fait de sa capacité de liaison au  $\text{Ca}^{2+}$ , joue également un rôle central dans la signalisation liée au  $\text{Ca}^{2+}$  et au maintien de l'homéostasie calcique [Milner et al. 1991]. Cela permet aussi d'optimiser la signalisation liée aux intégrines et donc des processus d'adhésion cellulaire [Coppolino et al. 1995, Coppolino et al. 1997]. Comme détaillé plus haut, calreticulin joue un rôle central au sein du CCP. Il interagit d'une part avec ERp57 de manière glycane-dépendante ce qui permet de conserver des niveaux adéquats de tapasin et de chaîne lourde CMH-I à un état de stabilité. D'autre part, elle peut récupérer dans des compartiments post-RE, des molécules CMH-I mal assemblées. Enfin, calreticulin joue un rôle dans la mort cellulaire immunogénique [Fucikova et al. 2021].

### 3. Présentation antigénique de type CMH-I et cancer

De nombreux types histologiques différents de cancer présentent des altérations de l'expression de molécules du CMH-I, y compris dans le cancer pulmonaire.

Le Tableau 3 résume les résultats des principales études ayant étudié l'expression du complexe HLA dans les CBNPC, par des techniques d'IHC. Il ressort de ces travaux qu'une majorité de patients présentant un CBNPC présentent des déficits de l'expression de HLA de classe-I. En effet, les auteurs ont tous trouvé des déficits plus ou moins marqués en HLA-A/B/C,  $\beta$ 2M, TAP1 ou encore tapasin dans les CBNPC. Le nombre de patients présentant un déficit en chaîne lourde de HLA de classe-I va ainsi de 33% à presque 100% des échantillons analysés. Il est rapporté 24% de déficit en TAP1 et jusqu'à 78,2% de déficit en  $\beta$ 2M et proche de 100% de

déficit en tapasin (sur un échantillon de très petite taille).

**Tableau 3. Résumé des études évaluant les composants de la machinerie de présentation des antigènes dans le cancer pulmonaire.**

Etude, année	N patients	Contexte clinique	Cible (anticorps)	Proportion de cas considérés comme négatifs
Passlick et al. 1994	91	CBNPC opéré	Complexe HLA-A/B/C- β2M (W6/32)	33%
Korkolopoulou et al. 1996	93	CBNPC opéré (I-II)	Complexe HLA-A/B/C- β2M (W6/32) β2M (BBM-1) HLA-A2/B17 (MA2.1) Chaîne lourde HLA-A libre (HCA2) TAP1 (AKI-7)	40%  24%
Lou et al. 2005	9 10	CBPC CBNPC (Stade I-III)	HLA-I (HC-10) β2M (Dako) TAP1 (148.3) Tapasin (TO-3)	100% 100% 95% 89%
Ramnath et al. 2005	190	CBNPC opéré (Stade I- IV)	HLA-I (HC-10)	93%
Kikuchi et al. 2007	161	CBNPC opéré	Chaîne lourde HLA-I (EMR8-5) β2M (EMR-B6)	68.9% 78.2%
Hanagiri et al. 2013	136	CBNPC opéré (Stade I)	Chaîne lourde HLA-I (EMR8-5)	64%
Shionoya et al. 2017	85	CBNPC opéré (Stade I-III)	Tapasin (TO-3)	72.9%
Datar et al. 2021	186 273 342	CBNPC (Stade I-IV)	HLA-I (HC-10) HLA-A/G libre (HC-A2) β2M (clone D8P1H, Cell Signaling Technology)	12.1% 9.0% 9.0%

Concernant l'expression spécifique de tapasin, il a été montré une perte d'expression fréquente de cette protéine dans de nombreuses histologies de cancers, comme le mélanome, le carcinome épidermoïde ORL, le carcinome rénal, le carcinome colo-rectal, le glioblastome, le neuroblastome et le cancer bronchique [Dissemond et al. 2003, Krishnakumar et al. 2033, Ogino et al. 2003, Ogino et al. 2006, Seliger et al. 2003, Atkins et al. 2004, Facoetti et al. 2005, Raffaghello et al. 2005]. Dans le CBNPC, Shionoya et al. [Shionoya et al. 2017.] ont évalué

l'expression de tapasin chez 85 patients présentant un CBNPC opéré. L'expression de tapasin était évaluée en fonction du pourcentage de cellules tumorales positives, à savoir, supérieur à 75%, de 25% à 75% et inférieur à 25% donnant un score de 2, 1 et 0, respectivement. Les patients présentant un score de 0 ou 1 étaient considérés comme ayant une expression réduite de tapasin. Seuls 27,1% des échantillons présentaient une expression normale de tapasin alors que 72,9% des cas présentaient une perte d'expression de celle-ci.

La grande majorité de ces études ont utilisé l'IHC classique pour analyser l'expression des différentes protéines analysées. Datar et al. [Datar et al. 2021.] ont analysé l'expression de HLA-A et de la chaîne lourde de HLA-A/B/C ainsi que de  $\beta$ 2M, par immunohistochimie multiplex quantitative (mQIF). Cette technique présente l'avantage de permettre une analyse quantitative objective de chaque marqueur étudié, et de permettre une analyse spatiale en créant des secteurs tumoraux et stromaux (micro-environnement tumoral). L'utilisation de logiciel de « machine learning » permet en outre des analyses spatiales fines sur le rapport des cellules entre elles ou la distance entre les cellules. Trois cohortes de patients (n=186, 273 et 342) présentant des CBNPC et dont les prélèvements étaient représentés dans des *tissue microarrays* (TMAs) ont été analysées. Les auteurs ont évalué l'expression des chaînes lourdes libres (non liées à  $\beta$ 2M) de HLA-A/B/C et de  $\beta$ 2M en utilisant les anticorps HC-A2, HC-10 et D8P1H. A travers l'ensemble des cohortes, 30,4% des tumeurs présentaient une régulation négative au niveau des cellules cancéreuses d'un ou de plusieurs marqueurs. Plus spécifiquement, 9,8% des prélèvements présentaient une régulation négative de  $\beta$ 2M, 9,0% de HLA-A et 12,1% de HLA-B/C.

L'ensemble de ces résultats montrent que les cancers, et en particulier le cancer bronchique, régule de manière négative l'expression des protéines de la machinerie de présentation antigénique. Cette régulation négative a un impact sur l'infiltration lymphocytaire, en particulier TCD8+ et sur la survie des patients [Datar et al. 2021, Shionoya et al. 2017]. Cette observation est cruciale car aujourd'hui, la majorité des patients présentant un CBNPC, quel que soit le stade, sera exposée à une molécule d'immunothérapie. Or, en l'absence de présentation antigénique adaptée, l'efficacité de ces traitements reste limitée. Il est donc pertinent d'analyser de manière précise l'expression de l'ensemble des composants de la

machinerie de présentation antigénique, et en particulier les membres du CCP afin d'évaluer leur impact sur l'infiltration lymphocytaire TCD8+ et sur la survie des patients. Il est également nécessaire de découvrir des voies de signalisation méconnues potentiellement cibles afin de proposer de nouvelles stratégies thérapeutiques chez les patients présentant un CBNPC.

#### **IV- Biomarqueurs solubles**

Dans le cadre du traitement des cancers bronchiques par anticorps anti-PD-1/PD-L1, l'évaluation de l'expression de PD-L1 à la surface des cellules tumorales par immunohistochimie reste le seul biomarqueur largement employé pour sélectionner les patients qui vont présenter une réponse prolongée aux ICI. Cette technique permet aussi de proposer des modalités thérapeutiques particulières chez certains patients, notamment ceux qui présentent un TPS  $\geq 50\%$  et qui peuvent bénéficier d'un traitement par immunothérapie seule en première ligne thérapeutique (voir partie Modalités thérapeutiques du CBNPC). Par ailleurs, il a été montré de manière régulière à travers les essais cliniques que les patients avec une expression de PD-L1  $\geq 50\%$  sur les cellules tumorales présentent un meilleur pronostic. Néanmoins, ce biomarqueur demeure imparfait car des patients qui présentent une expression de PD-L1 basse peuvent présenter un bénéfice clinique et certains patients présentant une expression de PD-L1 élevée vont présenter une survie courte. Par ailleurs, il est connu qu'il existe une hétérogénéité spatiale de l'expression de PD-L1 au sein d'un même prélèvement et entre deux sites tumoraux distincts [Kim et al. 2015, Ilie et al. 2016, Li et al. 2017, Casadevall et al. 2017, Uruga et al. 2017, Pinato et al. 2016, Mansfield et al. 2016], ainsi qu'une variation temporelle de PD-L1, en particulier au cours de traitements à base de chimiothérapie [Sheng et al. 2016, Lim et al. 2015]. Il est donc nécessaire de développer de nouveaux biomarqueurs qui pourront venir enrichir et compléter l'utilisation du PD-L1 déterminé par IHC. Dans ce contexte, des biomarqueurs solubles se sont développés. Ils présentent l'avantage d'être facilement accessibles sans procédure invasive, contrairement aux prélèvements tissulaires qui nécessitent une biopsie. Il est également possible de répéter ces prélèvements au cours de la prise en charge du patient et d'évaluer leur évolutivité au cours du traitement.

Le laboratoire Biomarqueurs et Essais Cliniques en Cancérologie et Onco-Hématologie (BECCOH) de l'hôpital Ambroise Paré (APHP), en collaboration avec le service de Pneumologie et Oncologie Thoracique (Pr. Giroux-Leprieur) dispose d'une large plasmathèque de prélèvements de patients présentant un cancer pulmonaire suivis dans le service. Ainsi, une des thématiques de recherche principale est celle des biomarqueurs solubles dans le CBNPC

de stade avancé traité par immunothérapie. L'approche est double, la consolidation et l'approfondissement des connaissances autour de certains biomarqueurs déjà étudiés au sein du laboratoire comme le PD-L1 soluble (sPD-L1) [Costantini et al. 2018, Annexe #2], d'une part ; et d'autre part, la découverte de nouveaux biomarqueurs pertinents par des techniques de screening agnostique de biomarqueurs. Cette deuxième approche a permis de mettre en évidence le potentiel de HGF comme biomarqueur et comme cible thérapeutique potentielle (Article #1. Partie Résultats).

Cette thématique m'a également permis de publier une revue de la littérature sur le sujet (1<sup>e</sup> auteur) dans *Cancers* en 2019 [Costantini et al. 2019, Annexe #3], et de co-signer plusieurs articles originaux sur les biomarqueurs plasmatiques et résistance à l'immunothérapie durant ma thèse [Giroux-Leprieur et al. 2020, Mehlman et al. 2021, Takam Kamga et al. 2024 ].

## 1. Le PD-L1 soluble (sPD-L1)

La famille d'immunoglobulines B7 est une super famille d'immunoglobulines dont les principaux membres sont B7-1, B7-2 et B7-H1 aussi connu sous le nom de programmed death ligand-1 (PD-L1). Il s'agit d'une famille de protéines transmembranaires impliquées dans la régulation de la réponse immunitaire.

### a. *B7-H1 (PD-L1)*

B7-H1, renommé PD-L1 dans un second temps du fait de l'identification de PD-1 comme son récepteur, a été identifié en 1999 par Dong et al. [Dong et al. 1999]. Il a été identifié suite à la recherche dans la base de données du National Center for Biotechnology Information de molécules partageant une homologie avec les domaines d'immunoglobulines V et C de B7-1 et B7-2. Ainsi, B7-H1 (B7-Homolog 1) a été identifié. Cette recherche a été réalisée en utilisant les données publiées des séquences d'acides aminés de B7-1 et B7-2. Le gène a par la suite pu être séquencé en totalité et cloné. Le domaine extra-cellulaire de B7-H1 partage 20% d'homologie d'acides aminés avec B7-1 et 15% d'homologie avec B7-2. Le domaine cytoplasmique est quant à lui très varié. Ainsi, le gène *B7-H1* code pour une protéine

transmembranaire de type I longue de 290 acides aminés avec des domaines d'immunoglobulines de type V et C, un domaine transmembranaire hydrophobe et une queue cytoplasmique de 30 acides aminés.

### *b. Origine du sPD-L1*

Le sPD-L1 a été identifié par Frigola et al. et rapporté en 2011 [Frigola et al. 2011].

Il a été montré que le surnageant collecté après culture de lignées de cellules tumorales présentait du sPD-L1 lorsque l'immunohistochimie PD-L1 était positive sur les cellules tumorales suggérant que celles-ci avaient la capacité de la sécréter.

Teramoto et al. [Teramoto et al. 2023.] ont montré, chez des patients atteints de CBNPC (n=63), qu'il n'existe pas de corrélation entre le taux de sPD-L1 pré-opératoire avec l'intensité de PD-L1 sur les cellules tumorales (tcPD-L1) ni avec PD-L1 tumor proportion score (TPS). Ces données suggèrent que l'intensité d'expression de PD-L1 par les cellules tumorales n'intervient pas sur le niveau de sPD-L1, mais ce qui ne remet pas en cause le fait que les cellules tumorales puissent le sécréter. De manière intéressante le sPD-L1 n'était pas corrélé avec la taille de la tumeur, ni avec le stade. Par la suite, une corrélation positive a été mise en évidence entre le sPD-L1 pré-opératoire et un score combiné associant les cellules PD-L1 positives et les macrophages associés aux tumeurs (TAMs) positifs (combined positive score) avec un R=0,240 et un P=0,030.

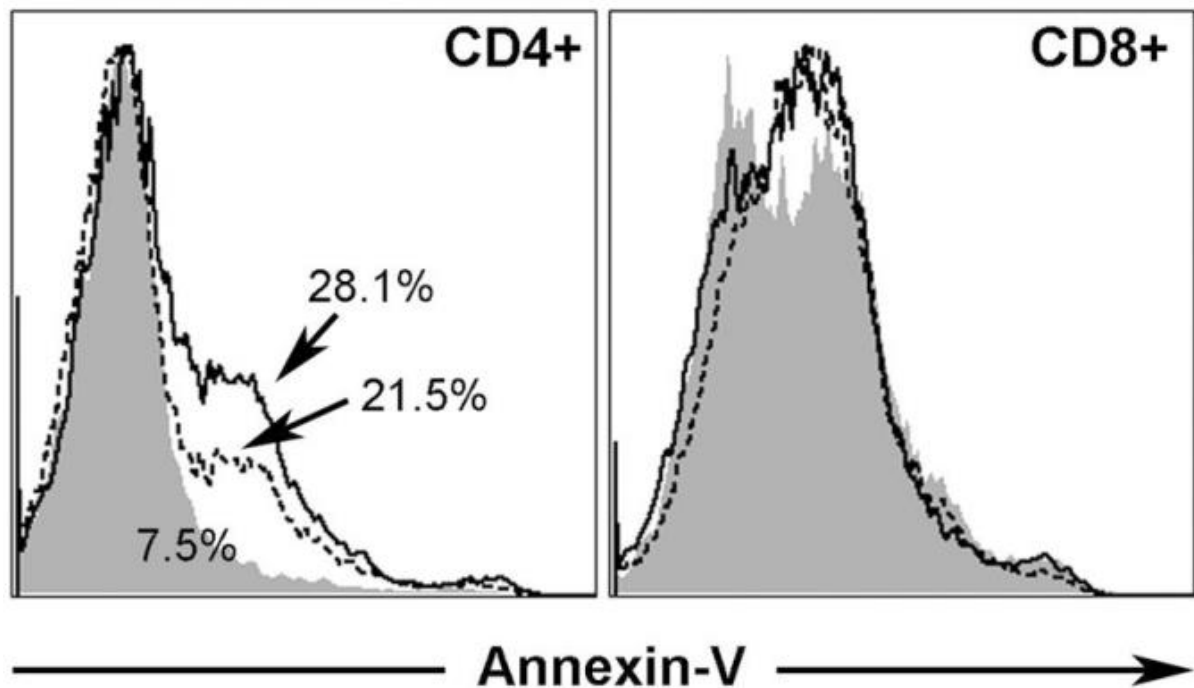
Frigola et al. [Frigola et al. 2011.] ont par la suite évalué la capacité des cellules immunitaires à sécréter sPD-L1. Ils ont montré que suite à une stimulation par du Phytohemagglutinin (PHA), les PBMCs de sujets sains sécrètent du sPD-L1 alors que les PBMCs non stimulés ne présentent pas de sécrétion détectable, suggérant qu'une stimulation préalable est nécessaire. Afin d'affiner ces résultats et déterminer quelles sont les cellules qui sécrètent du sPD-L1, les cellules ont été divisées en cellules adhérentes et non adhérentes au plastique. Les cellules adhérentes sont les seules à produire du sPD-L1 après stimulation par du PHA, suggérant que ce sont les cellules d'origine myéloïde (monocytes, macrophages et cellules dendritiques) qui sécrètent le sPD-L1. Par la suite, il a été montré que les cellules dendritiques matures sécrètent du sPD-L1 et que celui-ci conservait une activité biologique en provoquant l'apoptose de lymphocytes TCD4+ et TCD8+, contrairement à ce qui avait été

montré précédemment avec le sPD-L1 d'origine tumorale qui semblait présenter une spécificité d'activité anti-apoptotique vis-à-vis des TCD4+. Enfin, il a été montré que les cellules CD3+, activées ou non, ne sécrétaient pas sPD-L1.

### c. Fonction du sPD-L1

Firgola et al. [Firgola et al. 2011.] ont isolé des CD4 et CD8 en utilisant des billes électromagnétiques (*beads*) et les ont par la suite stimulés pendant 72 heures avec un anticorps anti-CD3. L'activation des CD4 et CD8 a été confirmée par la présence de PD-1 à la surface des cellules. Les cellules ont ensuite été mise en présence de sPD-L1, IgG contrôle avec un bloqueur de PD-L1 ou une IgG contrôle. Les cellules ont été analysées après 16 heures et l'activité apoptotique évaluée. Il a été montré que l'expression de PD-1 était maximale à 72 heures. Le panneau ci-dessous montre l'activité apoptotique évaluée dans les cellules CD4+ et CD8+ en fonction des différentes conditions. La zone grisée représente les cellules non traitées, le trait plein les cellules avec sPD-L1 et le pointillé les cellules avec bloqueurs de PD-L1. Ces résultats montrent d'une part que le sPD-L1 semble spécifiquement augmenter l'apoptose des CD4+ sans avoir d'effet sur les CD8+, et d'autre part qu'un inhibiteur de PD-L1 semble inhiber partiellement l'effet du sPD-L1.

**Figure 8. Le sPD-L1 d'origine tumorale induit l'apoptose des CD4+ et non des CD8+ [Ref. Frigola et al. 2011]**



Une autre étude de Liang et al. [Liang et al. 2023] a analysé par cytométrie de flux chez 26 patients atteints de cancer (carcinome hépatocellulaire, cholangiocarcinome, carcinome pancréatique), la corrélation entre le taux de sPD-L1 et l'apoptose des lymphocytes T périphériques (Annexin V). Il a été montré que le taux sPD-L1 avait une corrélation positive avec l'apoptose des cellules PD1+ CD4+ mais pas avec les cellules PD1+ CD8+ suggérant que le sPD-L1 joue un rôle de déplétion spécifique sur les cellules CD4+. Les auteurs ont ensuite exposé des PBMCs à du soluble monomeric human PD-L1 (smhPD-L1) ou à du soluble human PD-L1 (shPD-L1). Les PBMCs étaient stimulés par des anticorps anti-CD3 et anti-CD28 en présence ou en l'absence de smhPD-L1 et de shPD-L1. Il a été montré que le smhPD-L1 et le shPD-L1 avaient la possibilité d'inhiber la prolifération des PBMCs.

Il a également été montré dans ce travail que le smhPD-L1 et le shPD-L1 avaient la capacité d'inhiber la sécrétion de cytokines de la part des lymphocytes activés, en particulier IFNG, IL-2, TNF- $\alpha$  et IL-10.

En outre, il a été montré que l'activité anti-tumorale des PBMCs était inhibée par le smhPD-

L1. Enfin, des PBMCs étaient isolés et stimulés par un anticorps anti-CD3 et un anticorps anti-CD28 et TGFB, avec ou sans smhPD-L1 ou shPD-L1 pendant 5 jours. Il a été montré que le smhPD-L1 avait la capacité de promouvoir l'expression de FOXP3 au niveau des CD4+ de manière dose-dépendante. Cette observation suggère que le smhPD-L1 a la capacité de promouvoir la conversion des lymphocytes T CD4+ en lymphocytes T régulateurs, réduisant ainsi la réponse immunitaire de l'hôte.

En résumé, il a été montré que le sPD-L1 peut être sécrété par les cellules cancéreuses et par certaines cellules immunitaires, en particulier d'origine myéloïde. Sa sécrétion semble être indépendante de l'expression de PD-L1 par les cellules tumorales, de la taille tumorale et du stade, bien que des résultats contradictoires aient été rapportés. Le sPD-L1 joue un rôle immunomodulateur et a la capacité d'inhiber spécifiquement les lymphocytes T CD4+ en promouvant leur transformation en lymphocytes TCD4+ FOXP3+, T régulateurs.

#### *d. Le sPD-L1 comme biomarqueur*

Le sPD-L1 a montré son potentiel de biomarqueurs à travers de nombreux types de tumeurs solides différentes comme le mélanome [Mahoney et al. 2022, Machiraju et al. 2021, Oh et al. 2021], le carcinome rénal à cellules claires [Mahoney et al. 2022, Incorvaia et al. 2020, Larrinaga et al. 2021], le mésothéliome [Chiarucci et al. 2020], le cancer gastrique [Ref. Chivu-Economescu et al. 2023, Shigemori et al. 2019, Takahashi et al. 2016], le carcinome épidermoïde ORL [Alrehaili et al. 2023, Molga-Magusiak et al. 2023], le cancer du sein [Han et al. 2021, Li et al. 2022], le gliome [Ding et al. 2020] mais également à travers plusieurs hémopathies malignes comme le lymphome B diffus à grandes cellules [Fei et al. 2020, Rossille et al. 2014], le myélome multiple [Wang et al. 2015] et le lymphome de Hodgkin [Guo et al. 2018].

Le rôle de biomarqueur potentiel de sPD-L1 a également été évalué chez des patients présentant un CBNPC [Zhang et al. 2015 à Ando et al. 2019]. D'autres études ont évalué la concentration de sPD-L1 à travers différents sous-types histologiques. Enfin, plusieurs méta-analyses ont évalué le rôle du sPD-L1 dans le cancer ou spécifiquement dans le cancer du poumon. De manière générale, ces études ont montré que des niveaux de sPD-L1 plus élevés

sont délétères vis-à-vis de la réponse, la SSP, la SG et le bénéfice clinique, à travers de nombreux sous-types histologiques de néoplasies solides et hématologiques recevant des modalités thérapeutiques variées (chimiothérapie, immunothérapie, chimio-immunothérapie). Les principales études évaluant le rôle du sPD-L1 sont résumées dans le Tableau 4. En effet, le rôle du sPD-L1 a été évalué au cours de mon année de Master 2 et a fait l'objet d'une publication [Ref. Costantini et al.] (Annexe 2). Ainsi, la partie portant sur le sPD-L1 de ce travail de thèse s'inscrit dans la continuité des premiers résultats obtenus sur le sujet.

**Tableau 4. Principales études évaluant le rôle du PD-L1 soluble (sPD-L1) dans le CBNPC de stade avancé**

Etude, année	N patients	Contexte clinique	Concentration de sPD-L1	Principaux résultats
Okuma et al. 2016	96	Cancer bronchique de stade avancé traité par chimiothérapie en L1 ou L2 ou plus	Moyenne: 6950 pg/mL Cut-off: 7320 pg/mL	SG plus longue chez les patients présentant un taux de sPD-L1 plus bas ( $p=0.037$ )
Zhao et al. 2017	126	CBNPC non opérables traités par radiothérapie thoracique	Moyenne: 107,2 pg/mL Cut-off: 96,5pg/mL	SG plus longue chez les patients présentant un taux de sPD-L1 plus bas ( $p=0.005$ )
Okuma et al. 2018	39	CBNPC de stade avancé traité par nivolumab L2 en ou plus	Moyenne: 2240 pg/mL Cut-off: 3357 pg/mL	SG plus longue chez les patients présentant un taux de sPD-L1 plus bas ( $p=0.040$ )
Costantini et al. 2018	43	CBNPC de stade avancé traité par nivolumab L2 ou plus	Médiane: 39.81pg/ml Cut-off: 33.97pg/ml	SSP plus longue chez les patients présentant un taux de sPD-L1 plus bas au premier bilan d'évaluation tumoral ( $p=0.041$ )
Bonomi et al. 2019	20	CBNPC de stade avancé traité par pembrolizumab ou pembrolizumab + carboplatin/paclitaxel hebdomadaire	NR	Absence de différence de sPD-L1 entre progresseurs et répondeurs
Tiako Meyo et al. 2020	51	CBNPC de stade avancé traité par nivolumab	NR	Critère composite (sPD-1/PD-L1 positif) : SSP et SG plus longue chez les patients présentant un sCombo bas
Mazzaschi et al. 2020	109	CBNC de stade avancé traité par immunothérapie L1 ou plus	Moyenne: 87.04pg/ml Cut-off: 11.3pg/ml	SSP et SG plus longues chez les patients présentant un taux de sPD-L1 plus bas ( $p<0.001$ et $p=0.001$ )
Chmielewska et al. 2023	120	CBNPC de III ou IV traité par chimio-immunothérapie ou immunothérapie en L1 ou L2	NR	SG plus longue et taux de contrôle tumoral plus important chez les patients présentant un taux de sPD-L1 plus bas ( $p=0.0006$ et $p=0.0142$ )
Brun et al. 2024	80	CBNPC de stade avancé traité par immunothérapie L1 ou plus	Médiane: 52pg/mL Cut-off: NR	SG plus longue chez les patients présentant un taux de sPD-L1 plus bas ( $p=0.034$ )

NR : non rapporté, L1 : première ligne, L2 : deuxième ligne, CBNPC : cancer bronchique non à pektites cellules

## 2. Hepatocyte growth factor (HGF)

### *a. La protéine HGF*

HGF, aussi connu sous le nom de scatter factor, a initialement été isolée en 1984 dans du sérum de rats ayant présenté une hépatectomie partielle [Nakamura et al. 1984]. HGF est le ligand endogène naturel du récepteur mesenchymal-epithelial transition (MET, c-MET). Il est principalement sécrété par les cellules mésenchymateuses sous forme d'un précurseur inactif (pro-HGF). Pour que HGF soit activé, le pro-HGF est clivé de manière protéolytique au niveau de la liaison Arg494-Val495 par des enzymes telles que l'activateur sérique de HGF et les protéinases à sérine transmembranaires de type II [Fukushima et al. 2018]. La forme active de HGF correspond à un hétérodimère lié par des ponts disulfures. Il est composé d'une chaîne  $\alpha$  de 69 kDa et d'un chaîne  $\beta$  de 34 kDa [Organ et al. 2011]. HGF provient soit des cellules tumorales soit des cellules stromales associées à la tumeur. Dans le cancer bronchique, il est essentiellement produit par les cellules stromales et agit donc comme un facteur de signalisation paracrine. Néanmoins, les cellules tumorales peuvent également produire HGF dans certaines conditions, comme l'hypoxie par exemple [Tokunou et al. 2001].

### *b. Le récepteur mesenchymal-epithelial transition (MET/c-MET)*

Le récepteur MET fait partie de la famille des récepteurs tyrosine kinase. Il est encodé par le proto-oncogène *MET* qui est situé sur le chromosome 7 humain. MET est synthétisé sous forme d'une protéine précurseur à chaîne unique de 170 kDa (pro-MET), qui subit un clivage protéolytique générant une sous-unité extracellulaire  $\alpha$  de 50 kDa et une sous-unité transmembranaire  $\beta$  de 145 kDa. La sous-unité  $\alpha$  (peptide N-terminal) est liée à la sous-unité  $\beta$  par un pont disulfure [Bottaro et al. 1991]. La sous-unité  $\beta$  se compose d'un domaine

extracellulaire de liaison au ligand, d'un domaine transmembranaire à passage unique, et d'un segment intracellulaire. Le domaine cytoplasmique comprend un domaine juxtamembranaire impliqué dans la régulation post-traductionnelle de MET, ainsi qu'un domaine catalytique, responsable de l'activité tyrosine kinase.

Lors de la liaison HGF/MET, le récepteur se dimérisé et phosphoryle ses deux résidus tyrosine, Tyr1234 et Tyr1235, dans le domaine catalytique de la kinase [Duplaquet et al. 2018, Comoglio et al. 2018]. Dans un second temps, les résidus du site d'ancrage, Tyr1349 et Tyr1356, sont également phosphorylés ce qui conduit au recrutement de protéines intracellulaires adaptatrices et effectrices telles que la phosphoinositide 3-kinase (PI3K), la phospholipase Cc 1 (PLCc1), la protéine liée au récepteur du facteur de croissance 2 (GrB2), la protéine associée à GrB2 1 (GaB1), et le transducteur de signal et activateur de la transcription 3 (STAT3). Plusieurs voies de signalisation sont par conséquent activées dont les voies PI3K/Akt, STAT3, SRC/FAK (FAK, kinase d'adhésion focale) et mitogène-activée (MAPK)/ERK [Weidner et al. 1996, Ponzetto et al. 1994]. Ces différentes voies de signalisation sont impliquées dans des processus pro-tumoraux tels que la prolifération cellulaire, la survie, l'inhibition de l'apoptose, la migration, l'invasion et la métastase.

La signalisation HGF/MET est étroitement régulée. L'un des mécanismes de régulation est l'internalisation et la dégradation du récepteur MET via le recrutement de la proto-oncogène casitas B lineage lymphoma (CBL), une ligase ubiquitine-protéine. L'ubiquitination du MET phosphorylé peut se produire par interaction directe de CBL avec Tyr1003 dans le domaine juxta-membranaire ou indirectement par sa liaison à Tyr1356 via la protéine adaptatrice Grb2 [Mohapatra et al. 2013]. Un autre mécanisme de régulation négative de MET est fourni par l'activité des phosphatases spécifiques de la tyrosine, y compris PP2A, DEP-1, SHP2 et PTP1B [Zhang et al. 2016].

### *c. La dérégulation de la voie HGF/MET*

La voie HGF/Met est une voie intrinsèquement pro-oncogène. En effet, son activation entraîne des phénomènes pro-tumoraux tels que la prolifération, la migration, l'invasion et la survie cellulaire, l'inhibition de l'apoptose et la métastase. Les cellules cancéreuses emploient plusieurs stratégies afin d'entraîner une activation permanente de MET comme la

surexpression de *MET*, l'amplification du gène *MET*, les mutations par saut de l'exon 14 de *MET* ou la présence d'autres mutations ponctuelles somatiques ou germinales de *MET*.

La surexpression de MET peut être la conséquence d'une régulation transcriptionnelle positive causée par l'activation de hypoxia-inducible factor (HIF) [Pennacchietti et al. 2003] ou d'altérations survenant au niveau d'autres facteurs de transcription comme Ets ou Sp1 [Gambarotta et al. 1996]. Un autre mécanisme entraînant la surexpression de MET est la régulation négative de mRNAs répresseurs tels que miR-1, miR-34 et miR-449a [Gambarotta et al. 1996]. Ainsi, la présence d'un grand nombre de récepteurs MET à la surface cellulaire entraîne des dimérisations spontanées et donc des phosphorylations entraînant l'activation du récepteur, indépendamment de son ligand (HGF).

L'amplification du gène *MET* par gain du nombre de copies entraîne lui aussi la production d'un nombre excessif de protéines MET. Les mécanismes sous-tendant l'amplification de *MET* sont peu connus. Il semble que cette situation soit délétère dans divers néoplasies solides dont le CBNPC [Kim et al. 2018].

Les mutations par saut de l'exon 14 de *MET* entraîne la perte d'une région régulatrice du récepteur MET qui contient un résidu kinase (Tyr1003) qui est le site de liaison de CBL. Ainsi, l'ubiquitinisation de MET est diminuée ce qui entraîne l'absence de dégradation et donc une signalisation de MET prolongée [Trusolino et al. 2010]. Cette dérégulation post-transcriptionnelle entraîne une signalisation de MET aberrante dans les cellules tumorales et contribue au phénomène d'oncogenèse. On notera que cette mutation survient dans entre 3-5% des cas de cancer pulmonaire avec une large préférence pour le sous-type histologique des carcinomes sarcomatoïdes [Vuong et al. 2018].

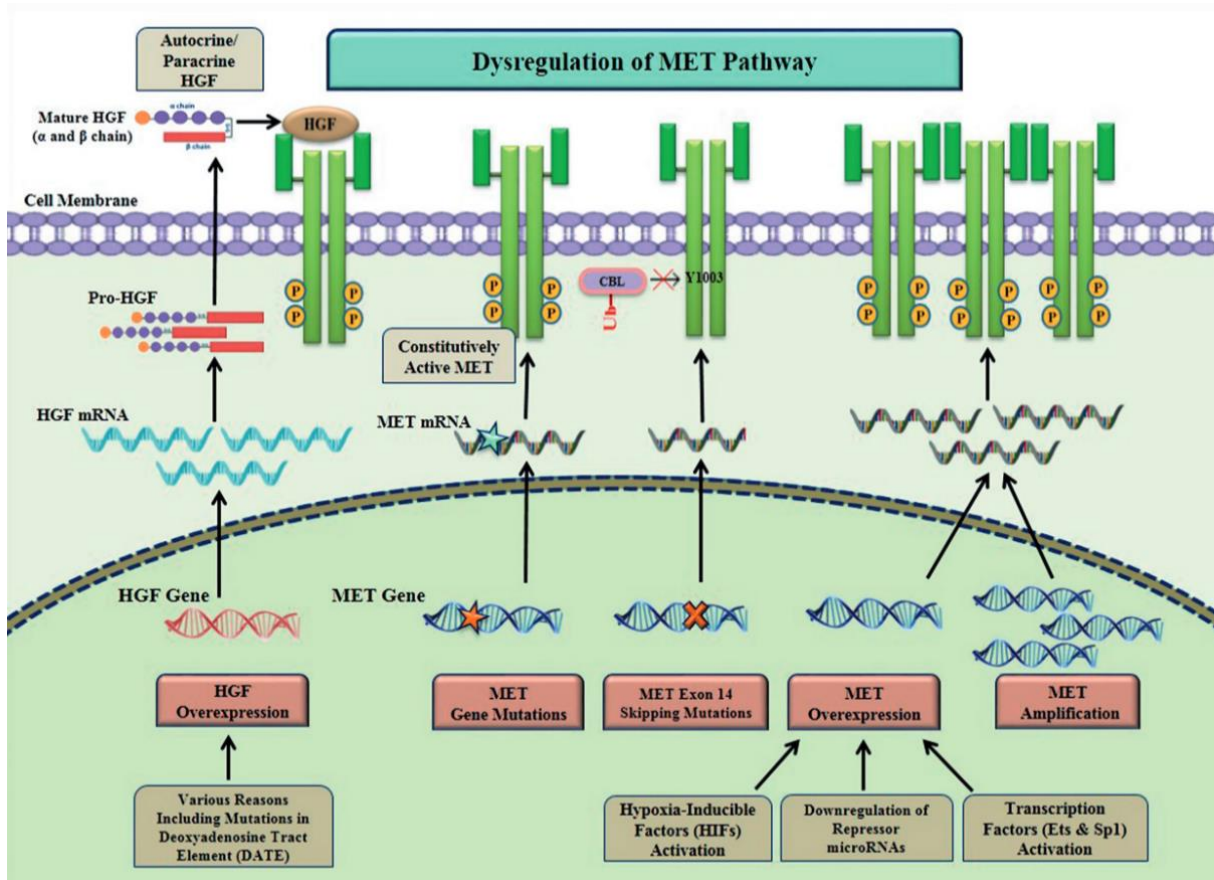
Les mutations germinales et somatiques de *MET* ont également été décrites à travers plusieurs sous-types histologiques différents. Ces mutations peuvent toucher plusieurs domaines dont les domaines kinases, juxta-membranaire ou extra-cellulaire. Les mutations du domaine kinase (Thr1191Ile, Tyr1248Cys/Asp/His, Tyr1230Cys/Tyr1235Asp, Asp1228Val, Ala1108Ser) entraînent une activation constitutive de MET qui peut être ligand-dépendante ou indépendante [Tovar et al. 2017]. Dans le domaine juxta-membranaire, on note la présence de mutations non-sens comme Tyr1010Ile, Arg988Cys ou Pro1009Ser [Tovar et al. 2017]. Les mutations du domaine extra-cellulaire (Glu168Asp, Leu299Phe, Ser323Gly, Asn375Ser) n'ont été que peu étudiées mais il semblerait qu'elles peuvent affecter le site de liaison avec HGF et la dimérisation de MET [Kong-Beltran et al. 2004].

De manière plus rare (0,5% des cas), on notera la présence de fusion de *MET*, qui peuvent présenter des partenaires de fusion multiples et qui semblent présenter un bénéfice de l'utilisation de TKI de *MET* [Riedel et al. 2024].

Enfin, des anomalies au niveau de HGF peuvent aussi entraîner une signalisation de la voie HGF/MET augmentée. En effet, il a été montré que des cytokines pro-inflammatoire et des facteurs de croissance (TNF- $\alpha$ , EGF, fibroblast growth factor, platelet derived growth factor) peuvent réguler de manière positive l'expression du gène *HGF*. Par ailleurs, l'interaction avec d'autres récepteurs tyrosine kinase peut avoir des effets similaires [Weng et al. 1997, Garnett et al. 2013]. Enfin, il a été montré que le promoteur du gène *HGF* contient une répétition de 30 desoxyadenosines, appellée DATE (deoxyadenosine tract element) qui agit comme un régulateur négatif de la transcription. En cas de mutation au sein de DATE, cela peut entraîner une activation constitutionnelle de HGF.

Les mécanismes de dérégulation de la voie HGF/MET sont illustrés dans la Figure 9.

**Figure 9. Illustration des différentes voies de dérégulation de la voie de signalisation HGF/MET [Moosavi et al. 2019]**



#### *d. HGF comme biomarqueur*

L'utilisation d'HGF comme biomarqueur a déjà été étudié dans le CBNPC. Fang et al. [Fang et al. 2014] ont évalué le niveau d'HGF pré- et post-chirurgie chez 45 patients présentant un CBNPC opéré. Ils n'ont pas mis en évidence de différence en termes de survie en fonction du niveau de HGF préopératoire évalué par ELISA.

Hosoda et al. [Hosoda et al. 2011] ont évalué le taux de HGF pré-opératoire chez 25 patients opérés pour un CBNPC. Ils ont trouvé que les patients présentant des niveaux pré-opératoires élevés de HGF (supérieur à 7,2ng/mL) avaient une SSP et une SG plus courtes que les patients avec un bas niveau de HGF.

Dans le contexte de CBNPC au stade avancé, Tsuji et al. [Tsuji et al. 2017] ont évalué le niveau de HGF chez 81 patients avec un CBNPC de stade avancé traités par chimiothérapie en première ou en deuxième ligne thérapeutique. Quatre points temporels étaient choisis : avant initiation du traitement, lors du premier bilan d'évaluation tumorale, à la meilleure réponse tumorale et lors de la progression. Ils ont montré qu'un dosage d'HGF positif lors du bilan d'évaluation prédisait une SSP plus courte aussi bien dans le contexte de la première ligne que la deuxième ligne thérapeutique.

De manière similaire, Naumnik et al. [Naumnik et al. 2016] ont évalué HGF chez 46 patients avec un CBNPC traité par chimiothérapie et 15 sujets sains. Ils ont trouvé que les patients présentant un CBNPC avaient un niveau de HGF plus élevé que les sujets sains. D'autre part, en accord avec les résultats précédents, il existait une corrélation négative entre les niveaux de HGF et la SG.

Dans un contexte clinique différent, HGF a été évalué chez des patients présentant un CBNPC avec mutation EGFR sous TKI [Umeguchi et al. 2014, Tanaka et al. 2011]. Cette situation est différente car la dérégulation de la voie HGF/MET apparaît sur à une pression thérapeutique extérieure et correspond donc à une sélection clonale de clones résistants aux ITKs

De manière intéressante, l'utilisation de HGF semble également jouer un rôle prédictif de réponse à l'immunothérapie. Bien que les données restent préliminaires, des études pilotes menées chez des patients présentant un mélanome et traités par immunothérapie ont montré qu'un taux élevé de HGF avant initiation de traitement prédisait une SSP et une SG plus courtes [Kubo et al. 2019].

#### *e. Ciblage thérapeutique de la voie HGF/MET*

La voie de signalisation HGF/MET, du fait de son caractère pro-oncogène correspond à une cible thérapeutique de choix. Cette voie de signalisation peut être ciblée de différentes manières et les molécules actuellement disponibles peuvent être classées comme suit :

- les inhibiteurs sélectifs de type I qui se lient à la conformation active (phosphorylée) du récepteur
- les inhibiteurs non sélectifs de la kinase MET, tels que les inhibiteurs de type II et III, qui se lient respectivement à la conformation inactive non phosphorylée et au site allostérique du récepteur
- les anticorps monoclonaux anti-MET
- les anticorps dirigés contre HGF

La stratégie thérapeutique dépend fortement du mécanisme qui entraîne la dérégulation de la voie HGF/MET.

En cas de mutation de type saut de l'exon 14 de MET plusieurs molécules ont été évaluées comme le crizotinib [Drilon et al. 2020, Moro-Sibilot et al. 2019], ou des inhibiteurs spécifiques de MET comme le capmatinib [Wolf et al. 2024], le tepotinib [Paik et al. 2020], le savolitinib [Lu et al. 2021] ou le glumetinib [Ai et al. 2018]. L'ensemble de ces molécules ont montré une efficacité dans ce contexte clinique avec des arguments indirects suggérant leur intérêt de manière précoce dans la prise en charge des patients avec mutation de type saut de l'exon 14 de MET. Enfin, d'autres molécules comme les anticorps bispécifiques ont également montré une activité dans ce contexte. L'amivantamab est une anticorps monoclonal bispécifique qui cible EGFR et MET avec une affinité accrue pour MET. Il a également montré une efficacité dans ce contexte clinique particulier [Krebs et al. 2022]. L'ensemble des données ne sont pas encore publiées ni matures et la stratégie thérapeutique optimale chez ces patients n'est pas encore connue.

La surexpression de MET n'est pas classiquement considérée comme une addiction oncogénique. Dans cette situation clinique, on pourra citer le développement du Teliso-V, un anticorps conjugué, médicament qui est composé de l'anticorps monoclonal humanisé anti-MET ABT-700 avec un anti-microtubule (le monomethyl auristatin E). Cette molécule a été évaluée dans le contexte de CBNPC présentant une surexpression de MET dans plusieurs essais

de phase I et II [Camidge et al. 2024, Waqar et al. 2021]. Les premiers résultats sont encourageants, mais parfois discordants justifiant la poursuite du développement de la molécule dans des essais de phase III qui sont en cours [clinicaltrials.gov].

Il est également possible de cibler HGF et d'empêcher ainsi la liaison entre MET et HGF. Des anticorps monoclonaux anti-HGF ont été développés et testés à travers plusieurs essais. On pourra citer par exemple le rilotumumab [Iveson et al. 2014], un anticorps monoclonal humanisé anti-HGF. Cette molécule a été évaluée dans un essai de phase I-II dans le cancer du poumon [Ref. Tarhini et al. 2017] associée à l'erlotinib chez des patients qui pouvaient présenter ou non une mutation d'EGFR.

Au total, les possibilités de cibler le voie HGF/MET sont multiples [Remon et al. 2023]. En fonction du mécanisme entraînant la dérégulation de la voie de signalisation, la stratégie thérapeutique devra être adaptée. Jusqu'à présent, les anomalies au niveau de MET ont été exploitées avec des nécessités d'affiner la stratégie thérapeutique à employer. En revanche, l'exploitation d'anomalies au niveau de HGF en vue d'une thérapeutique personnalisée n'ont été que très peu étudiées dans le cancer du poumon.

## **OBJECTIFS**

Ce travail de thèse s'est structuré autour de trois objectifs touchant d'une part la thématique des biomarqueurs solubles et d'autre part la thématique de biomarqueurs tissulaires.

### **1. Découverte de nouveaux biomarqueurs solubles (*Article #1*)**

Le premier objectif de ce travail était de réaliser un travail de screening agnostique selon une technique d'ELISA multiplex afin de découvrir de nouveaux biomarqueurs plasmatiques potentiels utilisables dans le CBNPC de stade avancé traité par immunothérapie.

### **2. Poursuite de l'étude du sPD-L1 (*Article #2*)**

Le deuxième objectif était de poursuivre l'étude du sPD-L1 dans le cadre du CBNPC de stade avancé traité par immunothérapie, seule ou en association avec la chimiothérapie afin d'évaluer son potentiel de biomarqueur dans ce contexte clinique.

### **3. Analyse des composants du complexe de chargement des peptides (*Articles #3 et #4*)**

Des défauts des composants de la machinerie de présentation antigénique constitue un mécanisme de résistance à l'immunothérapie. Nous avons cherché à cartographier de manière précise les éléments constitutifs du CCP chez des patients présentant un CBNPC traité par chimiothérapie ou par immunothérapie.

## **RESULTATS**

**Article #1: Plasma biomarkers screening by multiplex ELISA assay in patients with advanced non-small cell lung cancer treated with immune checkpoint inhibitors.** Publié dans *Cancers*.

Costantini A, Takam Kamga P, Julie C, Corjon A, Dumenil C, Dumoulin J, Ouaknine J, Giraud V, Chinet T, Rottman M, Emile JF, Giroux Leprieur E. Plasma Biomarkers Screening by Multiplex ELISA Assay in Patients with Advanced Non-Small Cell Lung Cancer Treated with Immune Checkpoint Inhibitors. *Cancers (Basel)*. 2020 Dec 31;13(1):97. doi: 10.3390/cancers13010097. PMID: 33396187

L'object du travail présenté dans cet article était de découvrir, par une méthode de screening agnostique d'ELISA multiplex, de nouveaux biomarqueurs pronostique ou prédictifs de réponse à l'immunothérapie dans le CBNPC de stade avancé traité par ICIs.

Dans cette étude pilote, 35 patients atteints de CBNPC de stade avancé et traités par immunothérapie seule en première ligne (pembrolizumab) ou nivolumab en deuxième ligne ou plus (nivolumab) ont été inclus. Un échantillon de plasma prélevé avant l'initiation du traitement par immunothérapie a été analysé selon une technique d'ELISA multiplex comprenant 48 cytokines.

La cytokine ayant montré les résultats les plus intéressant était HGF. En effet, les patients présentant une progression précoce avaient des taux significativement plus élevés à l'état basal que les patients présentant une progression tardive. Par ailleurs, les patients avec un bénéfice clinique de l'immunothérapie avaient des taux de HGF significativement plus bas que ceux ne présentant pas de bénéfice clinique ( $p=0.010$ ). En outre, les patients avec une concentration basse de HGF avaient une SSP et une SG significativement plus longue que les patients avec une concentration haute de HGF ( $p=0.002$  et  $p=0.001$ , respectivement).

Ces résultats soulignent l'importance de la voie proto-oncogène HGF/MET dans le cancer bronchique et présente HGF comme un biomarqueur potentiel permettant de prédire la réponse à l'immunothérapie dans le CBNPC de stade avancé. Ces résultats ont permis de débuter des travaux de recherche précliniques spécifiques sur le rôle de la voie HGF/MET au sein d'un laboratoire, confirmant ces résultats préliminaires (manuscrit en cours de révisions pour *Cancer Immunology, Immunotherapy*, présenté en Annexe 1, dont je suis co-auteur).

## Article

# Plasma Biomarkers Screening by Multiplex ELISA Assay in Patients with Advanced Non-Small Cell Lung Cancer Treated with Immune Checkpoint Inhibitors

Adrien Costantini <sup>1,2</sup>, Paul Takam Kamga <sup>2,3</sup>, Catherine Julie <sup>2,3</sup>, Alexandre Corjon <sup>3</sup>, Coraline Dumenil <sup>1</sup>, Jennifer Dumoulin <sup>1</sup>, Julia Ouaknine <sup>1</sup>, Violaine Giraud <sup>1</sup>, Thierry Chinet <sup>1,2</sup>, Martin Rottman <sup>4,5</sup>, Jean-François Emile <sup>2,3</sup> and Etienne Giroux Leprieur <sup>1,2,\*</sup>

<sup>1</sup> Department of Respiratory Diseases and Thoracic Oncology, APHP—Hôpital Ambroise Paré, 92100 Boulogne-Billancourt, France; adrien.costantini@aphp.fr (A.C.); coraline.dumenil@aphp.fr (C.D.); jennifer.dumoulin@aphp.fr (J.D.); julia.ouaknine@aphp.fr (J.O.); violaine.giraud@aphp.fr (V.G.); thierry.chinet@aphp.fr (T.C.)

<sup>2</sup> EA 4340 BECCOH, UVSQ, Université Paris-Saclay, 92100 Boulogne-Billancourt, France; takam.paul@gmail.com (P.T.K.); catherine.julie@aphp.fr (C.J.); jean-francois.emile@uvsq.fr (J.F.E.)

<sup>3</sup> Department of Pathology, APHP—Hôpital Ambroise Paré, 92100 Boulogne-Billancourt, France; alexandre.corjon@aphp.fr

<sup>4</sup> Department of Microbiology, APHP—Hôpital Raymond Poincaré, 92380 Garches, France; martin.rottman@aphp.fr

<sup>5</sup> UMR 1173, UVSQ, Université Paris-Saclay, 78180 Montigny-le-Bretonneux, France

\* Correspondence: etienne.giroux-leprieur@aphp.fr; Tel: +33-1-49-09-58-02



Citation: Costantini, A.; Kamga, P.; Julie, C.; Corjon, A.; Dumenil, C.; Dumoulin, J.; Ouaknine, J.; Giraud, V.; Chinet, T.; Rottman, M.; et al. Plasma Biomarkers Screening by Multiplex ELISA Assay in Patients with Advanced Non-Small Cell Lung Cancer Treated with Immune Checkpoint Inhibitors. *Cancers* **2021**, *13*, 97. <https://doi.org/10.3390/cancers13010097>

Received: 9 November 2020

Accepted: 23 December 2020

Published: 31 December 2020

**Publisher's Note:** MDPI stays neutral with regard to jurisdictional claims in published maps and institutional affiliations.



Copyright: © 2020 by the authors. Licensee MDPI, Basel, Switzerland. This article is an open access article distributed under the terms and conditions of the Creative Commons Attribution (CC BY) license (<https://creativecommons.org/licenses/by/4.0/>).

**Keywords:** non-small cell lung cancer; immune checkpoint inhibitor; biomarker; plasma; resistance; toxicity; hepatocyte growth factor; Fibroblast Growth Factor; interleukine-12

## 1. Introduction

Lung cancer is the leading cause of cancer related death worldwide [1]. At the advanced stage, its prognosis is bleak with limited efficacy of cytotoxic chemotherapy (CT). Immune checkpoint inhibitors (ICIs), humanised monoclonal antibodies targeting notably programmed death 1 (PD-1) or programmed death ligand 1 (PD-L1), have recently been developed. PD-L1 and programmed death-ligand 2 (PD-L2) are membranous proteins expressed by malignant cells that interact with PD-1 expressed by T-cells. When PD-L1/PD-L2 and PD-1 bind, the T-cells' cytotoxic anti-tumour activity is down-regulated. By blocking the interaction between PD-L1 and PD-1, ICIs restore cytotoxic immune response. ICIs have shown their efficacy in advanced non-small cell lung cancer (NSCLC). Nivolumab, an anti-PD-1 antibody, is currently used for second-line treatment in Anaplastic Lymphoma Kinase (ALK) and Epidermal Growth Factor Receptor (EGFR) wild-type advanced NSCLC [2,3]. Pembrolizumab, (anti-PD-1 antibody) is used for first-line treatment in ALK and EGFR wild-type advanced NSCLC that have a high ( $\geq 50\%$ ) PD-L1 expression on tumour cells as determined by immunohistochemistry (IHC) [4]. Pembrolizumab can also be used in the first-line setting in association with platinum-pemetrexed doublet CT independent of PD-L1 expression determined by IHC [5,6]. Other drugs such as atezolizumab or durvalumab (anti-PD-L1 monoclonal antibodies) have also shown their efficacy in different settings [7–9]. However, the use of PD-L1 expression as a predictive biomarker remains challenging, as some patients experience tumour response with low/negative PD-L1 expression [2,3,7,9]. Furthermore, PD-L1 expression as determined by IHC can vary within one tumour sample, between two different locations of the same tumour [10–16] as well as over time, notably after CT [17,18]. There is currently an unmet need for biomarkers to better select patients who will benefit from ICIs. Other than tissue-based biomarkers, plasma-based biomarkers are being investigated [19,20] as plasma has the advantage of being easily accessible, allows sequential analysis during follow-up and reflects the different tumour clones present throughout the body.

In this study, we aimed to perform baseline plasma biomarker screening using a multiplex ELISA assay in patients with advanced NSCLC receiving anti-PD-1 monoclonal antibodies nivolumab or pembrolizumab. The aim was to perform exploratory analyses of the potential association between baseline biomarker levels and clinical outcomes and toxicity. Due to the exploratory nature of the study, no primary endpoint was chosen.

## 2. Results

### 2.1. Patients

Between March 2014 and February 2018, 86 patients received nivolumab or pembrolizumab for treatment of NSCLC. Thirty-five patients (41%) signed the consent form and had plasma available for analyses. Their characteristics are presented in Table 1. Gender was evenly distributed among the patients (51% male), they were mainly current or former smokers (83%) and with adenocarcinoma histology (77%). All patients were negative for Epidermal Growth Factor Receptor (EGFR) sensitising mutations and Anaplastic Lymphoma Kinase (ALK) translocation. ICIs were given as first-line treatment (pembrolizumab,  $n = 8$ ) because of high PD-L1 NSCLC, in the second-line setting (nivolumab,  $n = 21$ ) or beyond (nivolumab,  $n = 6$ ). At the time of cut-off, median follow-up was 47.0 months (IQR 36.0–70.0), twenty-four patients (69%) were deceased due to tumour progression, seven (20%) had controlled disease under ICIs and four (11%) were receiving further treatment after ICI failure. Objective Response Rate (ORR) under immunotherapy was 49% with 17 patients presenting with partial response under ICIs as best response, 5 (14%) presenting with stable disease and 13 (37%) presenting with progressive disease as best tumour response. Median Progression Free Survival (PFS) under ICIs was 4.0 months (IQR 2.0–7.0) and median Overall Survival (OS) was 21.0 months (IQR 10.0–35.0). Twenty-two patients (63%) did not present with clinical benefit whilst receiving immunotherapy, twelve (34%) presented with clinical benefit and one patient (3%) could not be evaluated.

Twenty-three patients (66%) presented with early progression and twelve patients (34%) presented with late progression while receiving ICIs.

**Table 1.** Patients' characteristics.

Characteristics	All Patients ( <i>n</i> = 35)
Sex	
Male <i>n</i> (%)	18 (51%)
Female <i>n</i> (%)	17 (49%)
Age at diagnosis, median (range)	67 (37–84)
Smoking history	
Non-smoker, <i>n</i> (%)	6 (17%)
Smoker, <i>n</i> (%)	29 (83%)
Histology	
Non squamous	27 (77%)
Squamous	5 (14%)
Other	3 (9%)
Stage at diagnosis	
I-II, <i>n</i> (%)	2 (6%)
III-IV, <i>n</i> (%)	33 (94%)
PS at ICIs initiation	
0–1, <i>n</i> (%)	26 (74%)
2, <i>n</i> (%)	9 (26%)
Type of ICIs	
Pembrolizumab (1st line)	8 (26%)
Median number of infusions (range)	9 (2–37)
Nivolumab (≥2nd line)	27 (77%)
Median number of infusions	8 (1–76)

PS: performance status; ICIs: immune checkpoint inhibitors.

## 2.2. Plasma Biomarkers

Amongst the tested cytokines, three seemed to be associated with outcome in our cohort: soluble HGF (sHGF), soluble FGF (sFGF) and IL-12 (Figure 1). Table S1 shows the raw data for the measured biomarkers in pg/mL.

At ICI initiation, median sHGF was 171.35 pg/mL (IQR 144.05–210.5). A stepwise approach was used: first, all biomarkers were tested with regards to progression pattern (early vs. late progression). Patients who presented with early progression (*n* = 23) had higher sHGF levels at ICIs initiation than patients with late progression (*n* = 12): 206.2 pg/mL vs. 155.8 pg/mL, *p* = 0.025 (Figure S1). When Benjamini–Hochberg correction for multiple testing was applied, this did not translate into significant results. Secondly, only biomarkers with promising results with regards to progression pattern were selected. Patients who did not present with clinical benefit (*n* = 22) had higher sHGF levels at immunotherapy initiation than patients who presented with clinical benefit (*n* = 12): 210.9 pg/mL versus (vs.) 155.8 pg/mL, *p* = 0.010 (Figure 2). When Benjamini–Hochberg correction for multiple testing was applied using a false discovery rate (Q) of 5%, results remained significant.

This did not translate into ORR with no statistically significant difference in sHGF levels in patients presenting with stable or progressive disease (*n* = 18) as compared to those presenting with response (*n* = 17): 207.1 pg/mL vs. 137.3 pg/mL, *p* = 0.145.

To further determine the effect of sHGF on survival, we used ROC curves to determine the optimal sHGF cut-off in order to separate our patients into two groups: high and low baseline sHGF concentrations. Table 2 shows the characteristics of the patients with high (*n* = 16) and low (*n* = 19) pre-ICI sHGF levels. Of note, patients with low pre-ICI sHGF levels had better PS than patients with high sHGF levels (PS 0–1.89% vs. 59%, *p* = 0.049). We found that an sHGF level of 171.35 pg/mL offered a sensitivity of 70% and a specificity of 83% to determine PFS. The area under the curve (AUC) was 0.73 (Figure S2). Using

this cut-off, we constructed Kaplan–Meier survival curves and compared PFS and OS between patients with high ( $n = 16$ ) and low ( $n = 19$ ) baseline sHGF levels. PFS was significantly shorter in the high baseline sHGF group: median PFS under immunotherapy was 2.5 months [95% CI (1.0–3.0)] vs. 8.0 months [95% CI (4.0—not reached (NR))],  $p = 0.002$  (Figure 3A). In the same way, OS was significantly shorter in the high sHGF group: median OS under immunotherapy was 5.5 months [95% CI (2.0–15.0)] vs. 35.0 months [95% CI (22.0–NR)],  $p = 0.001$  (Figure 3B).

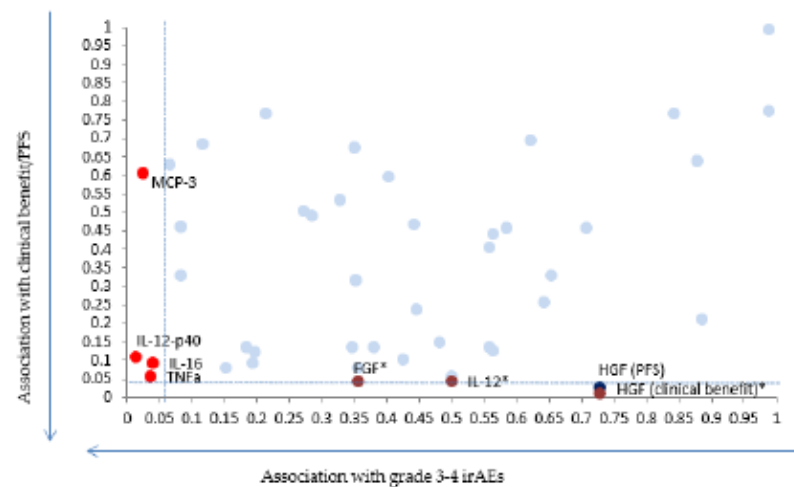


**Figure 1.** Scatter plot showing  $p$ -values for the 48 chemokines and cytokines with regards to grade 3–4 immune adverse events (irAEs) (x axis) and Progression Free Survival (PFS) or clinical benefit (y axis). \* Indicates biomarkers for which results remain significant after applying correction for multiple testing.

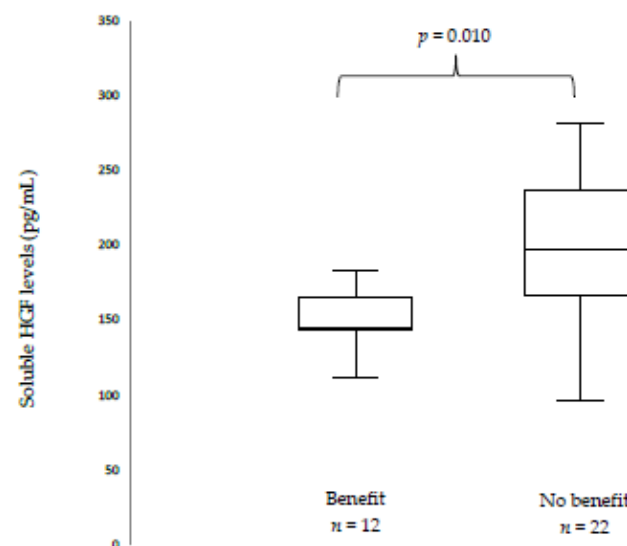


**Figure 2.** Box plots showing baseline soluble Hepatocyte Growth Factor (sHGF) levels in patients with and without clinical benefit. The median is indicated by the line within the box, the boundaries of the box indicate the 25th and 75th percentile and the whiskers the 10th and 90th percentile.

**Table 2.** Characteristics of patients with high and low pre-ICI sHGF levels.

Characteristics	Patients with Low sHGF ( <i>n</i> = 18)	Patients with High sHGF ( <i>n</i> = 17)	<i>p</i> -Value
Sex			
Male <i>n</i> (%)	11 (61%)	7 (41%)	<i>p</i> = 0.238
Female <i>n</i> (%)	7 (39%)	10 (59%)	
Age at diagnosis, median (range)	66.5 (48–84)	70 (37–82)	<i>p</i> = 0.457
Smoking history			
Non-smoker, <i>n</i> (%)	1 (6%)	5 (29%)	<i>p</i> = 0.061
Smoker, <i>n</i> (%)	17 (94%)	12 (71%)	
Histology			
Non squamous	15 (83%)	12 (70%)	<i>p</i> = 0.657
Squamous	2 (11%)	3 (18%)	
Other	1 (6%)	2 (12%)	
Stage at diagnosis			
I-II, <i>n</i> (%)	2 (11%)	0 (0%)	<i>p</i> = 0.157
III-IV, <i>n</i> (%)	16 (89%)	17 (100%)	
PS at ICI initiation			
0–1, <i>n</i> (%)	16 (89%)	10 (59%)	<i>p</i> = 0.042
≥2, <i>n</i> (%)	2 (11%)	7 (41%)	
Type of ICI			
Pembrolizumab (1st line)	4 (22%)	4 (24%)	<i>p</i> = 0.110
Nivolumab (≥2nd line)	11 (61%)	10 (59%)	

PS: performance status, ICIs: immune checkpoint inhibitors.

### 2.3. Fibroblast Growth Factor (FGF)

Patients who did not present with clinical benefit had lower sFGF levels at immunotherapy initiation than patients who presented with clinical benefit: 4.0 pg/mL vs. 4.8 pg/mL (*p* = 0.043) and this result remained significant after applying correction for multiple testing. This did not translate into significant results with regards to ORR (4.2 pg/mL for non-responders vs. 4.4 pg/mL for responders, *p* = 0.380) or progression pattern (4.0 pg/mL for early progression vs. 4.8 pg/mL for late progression, *p* = 0.056).

### 2.4. Interleukine-12 (IL-12)

Patients who did not present with clinical benefit had lower IL-12 levels at immunotherapy initiation than patients who presented with clinical benefit: 1.3 pg/mL vs. 2.2 pg/mL (*p* = 0.043) and this result remained significant after applying correction for multiple testing. This did not translate into significant results with regards to ORR (1.9 pg/mL for non-responders vs. 1.9 pg/mL for responders, *p* = 0.572) or progression pattern (1.4 pg/mL for early progression vs. 2.2 pg/mL for late progression, *p* = 0.080).

### 2.5. Immune-Related Adverse Events (irAEs)

Six patients (17%) presented with grade III–IV toxicity whilst receiving immunotherapy: auto-immune kidney failure/nephritis (*n* = 1), auto-immune cholangitis (*n* = 1), interstitial pneumonia/pneumonitis (*n* = 2), one patient with multiple toxicities (encephalitis, skin, arthro-myalgia), arthro-myalgia (*n* = 1). Of the tested biomarkers, higher levels of TNF- $\alpha$  (*p* = 0.036), IL-16 (*p* = 0.040), IL-12p40 (*p* = 0.015) and MCP3 (*p* = 0.025) were significantly associated with grade 3–4 irAEs under immunotherapy. When correction for multiple testing was applied, results did not remain significant.

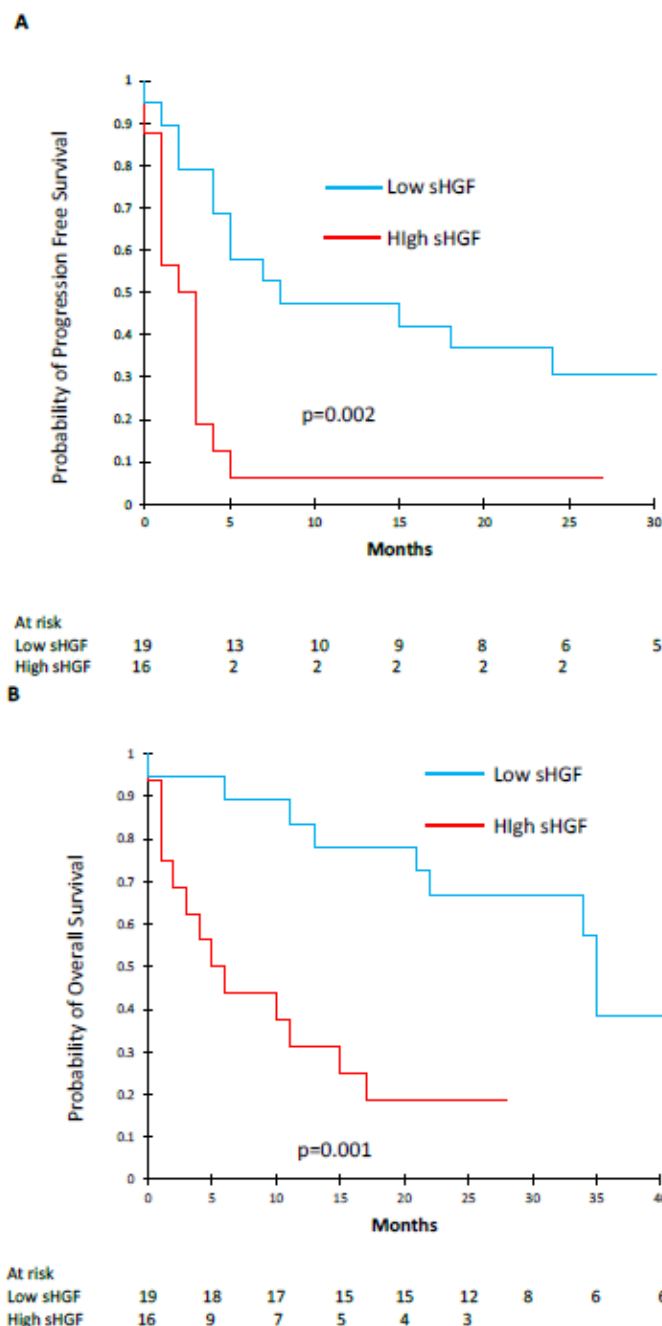


**Figure 3.** Kaplan–Meier curves showing progression free survival (PPS) (A) and overall survival (B) according to baseline sHGF levels.

### 3. Discussion

Although ICIs have transformed patient care across numerous cancer types, their efficacy remains sub-optimal and the need for biomarkers in order to better select patients who will benefit from them is essential. In this pilot study, we performed large baseline

plasma biomarker screening using a multiplex ELISA assay in patients with advanced NSCLC treated with nivolumab or pembrolizumab. We were able to show a significant association between clinical benefit under ICIs and levels of sHGF, sFGF and IL-12. Results with regards to the progression pattern were promising but significance was lost when correction for multiple testing was applied. Similarly, we found a potential association high immune toxicities and levels of IL-16, TNF- $\alpha$ , IL-12p40 and MCP3.

HGF is a polypeptide growth factor that belongs to the plasminogen family. It is a disulfide-linked  $\alpha$ - $\beta$  heterodimer consisting of a 69 kDa  $\alpha$ -chain and a 34 kDa  $\beta$ -chain. HGF is produced by mesenchymal cells (stromal cells and fibroblasts) in an inactive single-chain precursor of 728 amino acids (pro-HGF), which is then activated by posttranslational conversion by a serine protease in areas of tissue injury. The MET gene encodes for c-MET, a high-affinity receptor of HGF [21,22] that is, in a physiological setting, expressed on epithelial cells. HGF specifically activates c-MET receptor tyrosine kinase activity. The HGF/c-MET pathway can induce epithelial-to-mesenchymal transition (EMT), motility, proliferation and is involved in regeneration and tissue repair [23,24].

In cancer, c-MET activation promotes communication between mesenchymal cells and epithelial cells, tissue infiltration, cancer cell proliferation, and the induction of angiogenesis [25].

This is the first study to report results regarding pre-ICI sHGF levels and outcomes in patients with advanced NSCLC treated with ICIs. We found that patients who presented with clinical benefit and late progression had lower pre-ICI sHGF levels than patients who did not. Furthermore, patients with low pre-ICI sHGF levels as determined by ROC curves presented with significantly longer PFS and OS than patients with high pre-ICI sHGF levels.

This result is in line with what has been shown in previous studies investigating sHGF. In resectable NSCLC, sHGF levels were associated with survival [26,27]. In patients with advanced NSCLC receiving cytotoxic CT, sHGF levels were evaluated at different time-points during follow-up (pre-treatment, response-evaluation 1–2 months after treatment initiation, best tumour response and disease progression) in 55 patients [28]. Positive-sHGF at response-evaluation predicted poor PFS compared with negative-sHGF in first-line (median, 153.5 vs. 288.0;  $p < 0.05$ ) and second-line treatment (87.0 vs. 219.5;  $p = 0.01$ ). Multiple Cox proportional hazards models showed significant independent associations between poor PFS and positive-sHGF at response-evaluation (hazard ratio, 4.24; 95% CI, 2.05 to 9.46;  $p < 0.01$ ) and positive-sHGF at pre-treatment or at response-evaluation predicted poor PFS (35.0 vs. 132.0;  $p < 0.01$ , 50.0 vs. 215.0;  $p < 0.01$ , respectively).

Soluble HGF has also been extensively investigated in patients with EGFR mutant advanced NSCLC treated with EGFR tyrosine kinase inhibitors (TKIs). Preclinical and clinical studies have shown that sHGF is associated with poor outcome with EGFR TKIs, notably through the activation of the MET pathway [29–32]. Some recent reports have evaluated sHGF levels in patients receiving ICIs. Kubo et al. [33] published a retrospective study on 29 patients with metastatic melanoma treated with pembrolizumab or nivolumab. Patients without tumour response had higher baseline sHGF levels than patients with tumour response ( $p = 0.00124$ ). Furthermore, patients with low sHGF levels showed longer OS ( $p = 0.039$ ; HR 0.3125, 95% CI 0.1036–0.9427) and PFS ( $p = 0.0068$ ; HR 0.2087, 95% CI 0.06525–0.6676) than those with high sHGF levels.

The interaction between the HGF/c-MET pathway and anti-tumour immune-response is complex and yet to be fully understood. It has been shown [34,35] that PD-L1 expression occurs more frequently with MET activation. In fact, PD-L1 expression was positively associated with MET gene amplification in 389 NSCLC samples and, in a separate study of 155 resected NSCLC tumour samples. There is evidence that the HGF/c-MET axis interacts with immuno-modulation: HGF treated monocytes have immuno-suppressive phenotypes, HGF promotes immuno-tolerant CD4+ response, C-MET+ CD 8 + T cells produce more inflammatory cytokines and HGF treated antigen presenting cells attenuate cytokine production and memory T cell formation. Also, it is established that HGF induces macrophage

transition to the M2 phenotype, which is pro-generative. However, several studies have suggested that HGF could also have a pro-immune role [36,37] and further research is needed to better understand the exact role of HGF in anti-tumour immune response.

Amongst the other tested biomarkers, statistically significant results were found with sFGF and IL-12 with regards to clinical benefit. Patients with higher baseline sFGF levels presented with clinical benefit as compared to those with lower baseline sFGF levels. Although FGF signalling is associated with cellular proliferation, survival, migration and differentiation, there is also evidence that the FGF pathway can act in a tumour suppressive manner in some circumstances [38].

Finally, we found that patients who did not present with clinical benefit had lower IL-12 levels at immunotherapy initiation than patients who presented with clinical benefit. This finding can be explained by the fact that IL-12 has a clear anti-tumour activity through the activation of T and natural killer (NK) lymphocytes leading to the production of interferon gamma (IFN $\gamma$ ) [39].

The onset of irAEs is difficult to predict, and although grade 3–4 adverse events remain relatively infrequent, they can be severe, impacting quality of life, sometimes life-threatening, and can lead to treatment interruption. Predicting the onset of the irAEs is a major challenge and the use of soluble biomarkers has already been partly explored in a previous study [20] finding that low sPD-L2, low IL-2 and high IFN- $\gamma$  levels in patients with advanced NSCLC treated with nivolumab were associated with grade 3–4 toxicities. In this study, we found several candidate biomarkers to predict irAEs. Higher levels of TNF- $\alpha$  ( $p = 0.036$ ), IL-16 ( $p = 0.040$ ), IL-12p40 ( $p = 0.015$ ) and MCP3 ( $p = 0.025$ ) were all seemingly associated with grade 3–4 irAEs under immunotherapy. If confirmed, these results could help predict which patients are at risk for high-grade toxicity as early as the beginning of treatment, leading to closer follow-up of such patients.

Our work has several limitations. This was a small exploratory monocentric pilot study, with a possibility of lack of power for some statistical analyses. However, when correction for multiple testing was applied some relevant results remained significant. Finally, it is difficult to differentiate the prognostic and the predictive role of these biomarkers, as no validation cohort with a control group was used and further studies are needed to confirm these preliminary results.

#### 4. Materials and Methods

##### 4.1. Experimental Design

This study was an exploratory study, based on the analysis of consecutive patients in the Department of Respiratory Medicine and Thoracic Oncology (APHP—Ambroise Paré Hospital) treated by nivolumab or pembrolizumab for stage III (non-irradiable) or IV NSCLC between 2014 and 2018, and for whom plasma samples at diagnosis were available. Exploratory endpoints were ORR, PFS, OS, clinical benefit, early or late progression and grade 3–4 toxicity, according to plasmatic concentrations of a panel of potential biomarkers.

##### 4.2. Patients and Plasma

Tumour response was evaluated every eight (nivolumab) or nine (pembrolizumab) weeks using iRECIST criteria [40]. Medical records were reviewed and data retrospectively extracted on clinical and pathological features as well as treatment history. Plasma samples were drawn before initiating immunotherapy (C1). Briefly, two 10 mL-EDTA tubes of peripheral blood were taken, plasma was isolated after centrifugation within one hour and immediately stored at  $-80^{\circ}\text{C}$ .

##### 4.3. Ethical Considerations

All included patients signed an informed consent allowing blood to be drawn and stored within the Centre de Ressources Biologiques (CRB) of the Ambroise Paré University Hospital during their follow-up and treatment. The protocol was approved by the Institutional Review Board CPP IDF n\_8 (ID CRB 2014-A00187-40).

#### 4.4. Outcomes

ORR was defined as the proportion of patients who presented with partial or complete response whilst receiving ICIs. Clinical benefit was defined as complete response, partial response or stability, according to iRECIST [40], lasting 6 months or more after initiation of immunotherapy. PFS was defined as the time between ICI initiation and tumour progression or death. OS was defined as the time between ICI initiation and death. Patients were defined as presenting with early progression as opposed to late progression if disease progression occurred within six months of initiating ICIs.

Immune related adverse events (irAEs) were assessed using Common Terminology Criteria for Adverse Events (CTCAE v4.0).

#### 4.5. Multiplex ELISA Technique

Multiplex ELISA was performed on the patients' plasma samples using a commercial kit and according to the manufacturer's guidelines (Bio-Plex-Pro™ Human Cytokines Assay, Bio-Rad). This assay allows testing of 48 chemokines, cytokines and growth factors in plasma samples. The assay principle is that of a sandwich ELISA: capture antibodies directed against the desired biomarker are covalently coupled to fluorescently dyed magnetic microspheres (beads) each with a distinct colour code or spectral address. After several wash series, the final detection complex is formed with the addition of streptavidin-phycerythrin (SA-PE) conjugate with phycerythrin serving as a fluorescent indicator. Data are drawn using an automated reader, a red and green laser illuminates the fluorescent dyes within each bead allowing to provide bead classification and PE excitation, which is detected by a photomultiplier tube (PMT). Data are presented as median fluorescence intensity (MFI) as well as concentration in pg/mL. The concentration of analyte bound to each bead is proportional to the MFI of the reporter signal. All samples, standards and negative controls were tested in duplicate. For all the 48 tested cytokines, the related mean intra-assay CV (coefficient of variation) ranged from 1.7 to 5.0%, and inter-assay CV from 1.2 to 7.9%.

The following proteins were tested in this assay: Interleukin-1a (IL-1a), IL-1b, IL-1ra, IL-2ra, IL-2, IL-3, IL-4, IL-5, IL-6, IL-7, IL-8, IL-9, IL-10, IL-12, IL-12p40, IL-13, IL-15, IL-17, IL-16, IL-18, Eotaxin, Fibroblast Growth Factor (FGF), Granulocyte-Colony Stimulating Factor (G-CSF), Granulocyte Macrophage-Colony Stimulating Factor (GM-CSF), Interferon gamma (IFN-g), IP-10, Monocyte chemoattractant protein 1 (MCP-1), MCP-3, Macrophage Inflammatory Protein 1 alpha (MIP-1a), MIP-1b, Platelet Derived Growth Factor-bb (PDGF-bb), Regulated upon Activation, Normal T Cell Expressed and Presumably Secreted (RANTES), Tumour Necrosis Factor-alpha (TNF-a), Vascular Endothelial Growth Factor (VEGF), Cutaneous T-cell-Attracting Chemokine (CTACK), Growth Regulated Oncogene-alpha (GRO-a), Hepatocyte Growth Factor (HGF), Interferon-alpha 2 (IFN-a2), Leukemia inhibitory factor (LIF), Monocyte-Colony Stimulating Factor (M-CSF), Macrophage migration Inhibitory Factor (MIF), Monokine Induced by Gamma interferon (MIG), beta-Nerve Growth Factor (b-NGF), Stem Cell Factor (SCF), Stem Cell Growth Factor-beta (SCGF-b), Stromal Cell-Derived Factor-1 (SDF-1a), Tumour Necrosis Factor-beta (TNF-b), TNF-related apoptosis-inducing ligand (TRAIL).

#### 4.6. Statistical Analysis

Median soluble concentrations of all the tested biomarkers were analysed according to ORR, PFS, OS, clinical benefit, early or late progression response profile and grade 3–4 toxicity.

The comparison of median biomarker levels between groups was performed using the Mann-Whitney test and interquartile range (IQR) is given for each value.

A stepwise approach was adopted. First, all biomarkers were tested with regards to PFS. Biomarkers who presented with significant or closely significant *p*-values were then tested in a second step with regards to clinical benefit. In both cases, correction for multiple

testing was applied using the Benjamini–Hochberg [41] method correction for multiple testing and setting a false discovery rate ( $Q$ ) at 5%.

The Receiving Operating Curve (ROC) method was used to determine a cut-off level for each biomarker with a significant difference for endpoints with the Mann–Whitney test. The Kaplan–Meier method was used to determine OS and PFS. Comparison between survival curves was performed using a log-rank method. Data analysis was computed using XLStat v 19.4 (Addinsoft).  $p$ -values were considered significant if  $<0.05$ .

## 5. Conclusions

This is the first study to show the prognostic value of sHGF in patients with advanced NSCLC treated with ICIs. This finding is in line with previous data reported in localised NSCLC, EGFR mutated NSCLC and advanced NSCLC treated with CT. Furthermore, this study brings original data with regards to the use of FGF or IL-12 as potential biomarkers of ICI efficacy, and IL-16, TNF- $\alpha$ , IL-12p40 and MCP3 as biomarkers of irAEs.

These preliminary results need to be validated in a large prospective population, including patients treated with ICI-CT combo treatment.

**Supplementary Materials:** The following are available online at <https://www.mdpi.com/2072-694/13/1/97/s1>, Figure S1: Box plots showing baseline soluble HGF levels in patients with early and late progression. The median is indicated by the line within the box, the boundaries of the box indicate the 25th and 75th percentile and the whiskers the 10th and 90th percentile, Figure S2: ROC curve used to determine the sHGF cut-off level, Table S1: Raw values of the different measured biomarkers.

**Author Contributions:** Conceptualization, E.G.L.; methodology, E.G.L.; data curation, E.G.L.; A.C. (Adrien Costantini); M.R.; writing—original draft preparation, E.G.L. and A.C. (Adrien Costantini); writing—review and editing, E.G.L.; A.C. (Alexandre Corjon); P.T.K.; C.D.; J.D.; J.O.; V.G.; T.C.; C.J.; J.-F.E.; supervision, E.G.L. All authors have read and agreed to the published version of the manuscript.

**Funding:** This research received no external funding.

**Institutional Review Board Statement:** The study was conducted according to the guidelines of the Declaration of Helsinki, and approved by the Institutional Review Board CPP IDF n\_8 (ID CRB 2014-A00187-40).

**Informed Consent Statement:** Informed consent was obtained from all subjects involved in the study.

**Data Availability Statement:** Data are available upon reasonable request.

**Conflicts of Interest:** EGL: Bristol Myers Squibb (honoraria, advisory board, research funding), MSD (honoraria, advisory board). JFE: Bristol Myers Squibb (advisory board). The other authors declare no conflict of interest.

## References

1. Siegel, R.L.; Miller, K.D.; Jemal, A. Cancer statistics, 2016. *CA Cancer J. Clin.* **2016**, *66*, 7–30. [[CrossRef](#)] [[PubMed](#)]
2. Brahmer, J.; Reckamp, K.L.; Baas, P.; Crino, L.; Eberhardt, W.E.E.; Poddubskaya, E.; Antonia, S.; Pluzanski, A.; Vokes, E.E.; Holgado, E.; et al. Nivolumab versus Docetaxel in Advanced Squamous-Cell Non-Small-Cell Lung Cancer. *N. Engl. J. Med.* **2015**, *373*, 123–135. [[CrossRef](#)] [[PubMed](#)]
3. Borghaei, H.; Paz-Ares, L.; Horn, L.; Spigel, D.R.; Steins, M.; Ready, N.E.; Chow, L.Q.; Vokes, E.E.; Felip, E.; Holgado, E.; et al. Nivolumab versus Docetaxel in Advanced Nonsquamous Non-Small-Cell Lung Cancer. *N. Engl. J. Med.* **2015**, *373*, 1627–1639. [[CrossRef](#)] [[PubMed](#)]
4. Reck, M.; Rodriguez-Abreu, D.; Robinson, A.G.; Hui, R.; Csőszsi, T.; Fülöp, A.; Gottfried, M.; Peled, N.; Tafreshi, A.; Cuffe, S.; et al. Pembrolizumab versus Chemotherapy for PD-L1-Positive Non-Small-Cell Lung Cancer. *N. Engl. J. Med.* **2016**, *375*, 1823–1833. [[CrossRef](#)] [[PubMed](#)]
5. Gandhi, L.; Rodriguez-Abreu, D.; Gadgeel, S.; Esteban, E.; Felip, E.; Angelis, F.D.; Domine, M.; Clingan, P.; Hochmair, M.J.; Powell, S.F.; et al. Pembrolizumab plus Chemotherapy in Metastatic Non-Small-Cell Lung Cancer. *N. Engl. J. Med.* **2018**. [[CrossRef](#)]
6. Paz-Ares, L.; Luft, A.; Vicente, D.; Tafreshi, A.; Gümus, M.; Mazières, J.; Hermes, B.; Çay Şenler, E.; Csőszsi, T.; Fülöp, A.; et al. Pembrolizumab plus Chemotherapy for Squamous Non-Small-Cell Lung Cancer. *N. Engl. J. Med.* **2018**, *379*, 2040–2051. [[CrossRef](#)]

7. Rittmeyer, A.; Barlesi, F.; Waterkamp, D.; Park, K.; Ciardiello, F.; von Pawel, J.; Gadgeel, S.M.; Hida, T.; Kowalski, D.M.; Dols, M.C.; et al. Atezolizumab versus docetaxel in patients with previously treated non-small-cell lung cancer (OAK): A phase 3, open-label, multicentre randomised controlled trial. *Lancet* **2017**, *389*, 255–265. [CrossRef]
8. Socinski, M.A.; Jotte, R.M.; Cappuzzo, F.; Orlandi, F.; Stroyakovskiy, D.; Nogami, N.; Rodriguez-Abreu, D.; Moro-Sibilot, D.; Thomas, C.A.; Barlesi, F.; et al. Atezolizumab for First-Line Treatment of Metastatic Nonsquamous NSCLC. *N. Engl. J. Med.* **2018**, *378*, 2288–2301. [CrossRef]
9. Antonia, S.J.; Villegas, A.; Daniel, D.; Vicente, D.; Murakami, S.; Hui, R.; Yokoi, T.; Chiappori, A.; Lee, K.H.; de Wit, M.; et al. Durvalumab after Chemoradiotherapy in Stage III Non-Small-Cell Lung Cancer. *N. Engl. J. Med.* **2017**, *377*, 1919–1929. [CrossRef]
10. Kim, S.; Kim, M.-Y.; Koh, J.; Go, H.; Lee, D.S.; Jeon, Y.K.; Chung, D.H. Programmed death-1 ligand 1 and 2 are highly expressed in pleomorphic carcinomas of the lung: Comparison of sarcomatous and carcinomatous areas. *Eur. J. Cancer* **2015**, *51*, 2698–2707. [CrossRef]
11. Ilie, M.; Long-Mira, E.; Bence, C.; Butori, C.; Lassalle, S.; Bouhlel, L.; Fazzalari, I.; Zahaf, K.; Lalvée, S.; Washetine, K.; et al. Comparative study of the PD-L1 status between surgically resected specimens and matched biopsies of NSCLC patients reveal major discordances: A potential issue for anti-PD-L1 therapeutic strategies. *Ann. Oncol.* **2016**, *27*, 147–153. [CrossRef] [PubMed]
12. Li, C.; Huang, C.; Mok, T.S.; Zhuang, W.; Xu, H.; Miao, Q.; Fan, X.; Zhu, W.; Huang, Y.; Lin, X.; et al. Comparison of 22C3 PD-L1 Expression between Surgically Resected Specimens and Paired Tissue Microarrays in Non-Small Cell Lung Cancer. *J. Thorac. Oncol.* **2017**, *12*, 1536–1543. [CrossRef] [PubMed]
13. Casadevall, D.; Clavé, S.; Taus, Á.; Hardy-Werbin, M.; Rocha, P.; Lorenzo, M.; Menéndez, S.; Salido, M.; Albanell, J.; Pijuan, L.; et al. Heterogeneity of Tumor and Immune Cell PD-L1 Expression and Lymphocyte Counts in Surgical NSCLC Samples. *Clin. Lung. Cancer* **2017**, *18*, 682–691.e5. [CrossRef] [PubMed]
14. Uruga, H.; Bozkurtlar, E.; Huynh, T.G.; Muzikansky, A.; Goto, Y.; Gomez-Caraballo, M.; Hata, A.N.; Gainor, J.F.; Mark, E.J.; Engelman, J.A.; et al. Programmed Cell Death Ligand (PD-L1) Expression in Stage II and III Lung Adenocarcinomas and Nodal Metastases. *J. Thorac. Oncol.* **2017**, *12*, 458–466. [CrossRef]
15. Pinato, D.J.; Shiner, R.J.; White, S.D.T.; Black, J.R.M.; Trivedi, P.; Stebbing, J.; Sharma, R.; Mauri, F.A. Intra-tumoral heterogeneity in the expression of programmed-death (PD) ligands in isogenic primary and metastatic lung cancer: Implications for immunotherapy. *Oncimmunology* **2016**, *5*, e1213934. [CrossRef]
16. Mansfield, A.S.; Aubry, M.C.; Moser, J.C.; Harrington, S.M.; Dronca, R.S.; Park, S.S.; Dong, H. Temporal and spatial discordance of programmed cell death-ligand 1 expression and lymphocyte tumor infiltration between paired primary lesions and brain metastases in lung cancer. *Ann. Oncol.* **2016**, *27*, 1953–1958. [CrossRef]
17. Sheng, J.; Fang, W.; Yu, J.; Chen, N.; Zhan, J.; Ma, Y.; Yang, Y.; Huang, Y.; Zhao, H.; Zhang, L. Expression of programmed death ligand-1 on tumor cells varies pre and post chemotherapy in non-small cell lung cancer. *Sci. Rep.* **2016**, *6*, 20090. [CrossRef]
18. Lim, S.H.; Hong, M.; Ahn, S.; Choi, Y.-L.; Kim, K.-M.; Oh, D.; Ahn, Y.C.; Jung, S.-H.; Ahn, M.-J.; Park, K.; et al. Changes in tumour expression of programmed death-ligand 1 after neoadjuvant concurrent chemoradiotherapy in patients with squamous oesophageal cancer. *Eur. J. Cancer* **2016**, *52*, 1–9. [CrossRef]
19. Okuma, Y.; Wakui, H.; Utsumi, H.; Sagawa, Y.; Hosomi, Y.; Kuwano, K.; Homma, S. Soluble Programmed Cell Death Ligand 1 as a Novel Biomarker for Nivolumab Therapy for Non-Small-cell Lung Cancer. *Clin. Lung. Cancer* **2018**, *19*, 410–417.e1. [CrossRef]
20. Costantini, A.; Julie, C.; Dumenil, C.; Hélias-Rodzewicz, Z.; Tisserand, J.; Dumoulin, J.; Giraud, V.; Labrune, S.; Chinet, T.; Emile, J.-F.; et al. Predictive role of plasmatic biomarkers in advanced non-small cell lung cancer treated by nivolumab. *Oncimmunology* **2018**, *7*, e1452581. [CrossRef]
21. Bottaro, D.P.; Rubin, J.S.; Faletto, D.L.; Chan, A.M.; Kmiecik, T.E.; Vande Woude, G.F.; Aaronson, S.A. Identification of the hepatocyte growth factor receptor as the c-met proto-oncogene product. *Science* **1991**, *251*, 802–804. [CrossRef] [PubMed]
22. Naldini, L.; Vigna, E.; Narsimhan, R.P.; Gaudino, G.; Zarnegar, R.; Michalopoulos, G.K.; Comoglio, P.M. Hepatocyte growth factor (HGF) stimulates the tyrosine kinase activity of the receptor encoded by the proto-oncogene c-MET. *Oncogene* **1991**, *6*, 501–504. [PubMed]
23. Birchmeier, C.; Birchmeier, W.; Gherardi, E.; Vande Woude, G.F. Met, metastasis, motility and more. *Nat. Rev. Mol. Cell. Biol.* **2003**, *4*, 915–925. [CrossRef] [PubMed]
24. Matsumoto, K.; Nakamura, T. Hepatocyte growth factor and the Met system as a mediator of tumor-stromal interactions. *Int. J. Cancer* **2006**, *119*, 477–483. [CrossRef]
25. Bervenuti, S.; Comoglio, P.M. The MET receptor tyrosine kinase in invasion and metastasis. *J. Cell. Physiol.* **2007**, *213*, 316–325. [CrossRef]
26. Siegfried, J.M.; Weissfeld, L.A.; Singh-Kaw, P.; Weyant, R.J.; Testa, J.R.; Landreneau, R.J. Association of immunoreactive hepatocyte growth factor with poor survival in resectable non-small cell lung cancer. *Cancer Res.* **1997**, *57*, 433–439.
27. Hosoda, H.; Izumi, H.; Tukada, Y.; Takagiwa, J.; Chiaki, T.; Yano, M.; Arai, H. Plasma hepatocyte growth factor elevation may be associated with early metastatic disease in primary lung cancer patients. *Ann. Thorac. Cardiovasc. Surg.* **2012**, *18*, 1–7. [CrossRef]
28. Tsuji, T.; Sakamori, Y.; Ozasa, H.; Yagi, Y.; Ajimizu, H.; Yasuda, Y.; Funazo, T.; Nomizo, T.; Yoshida, H.; Nagai, H.; et al. Clinical impact of high serum hepatocyte growth factor in advanced non-small cell lung cancer. *Oncotarget* **2017**, *8*, 71805–71816. [CrossRef]

29. Kasahara, K.; Arao, T.; Sakai, K.; Matsumoto, K.; Sakai, A.; Kimura, H.; Sone, T.; Horiike, A.; Nishio, M.; Ohira, T.; et al. Impact of serum hepatocyte growth factor on treatment response to epidermal growth factor receptor tyrosine kinase inhibitors in patients with non-small cell lung adenocarcinoma. *Clin. Cancer Res.* **2010**, *16*, 4616–4624. [[CrossRef](#)]
30. Yano, S.; Wang, W.; Li, Q.; Matsumoto, K.; Sakurama, H.; Nakamura, T.; Ogino, H.; Kakiuchi, S.; Hanibuchi, M.; Nishioka, Y.; et al. Hepatocyte growth factor induces gefitinib resistance of lung adenocarcinoma with epidermal growth factor receptor-activating mutations. *Cancer Res.* **2008**, *68*, 9479–9487. [[CrossRef](#)]
31. Yamada, T.; Takeuchi, S.; Kita, K.; Bando, H.; Nakamura, T.; Matsumoto, K.; Yano, S. Hepatocyte growth factor induces resistance to anti-epidermal growth factor receptor antibody in lung cancer. *J. Thorac. Oncol.* **2012**, *7*, 272–280. [[CrossRef](#)] [[PubMed](#)]
32. Yamada, T.; Matsumoto, K.; Wang, W.; Li, Q.; Nishioka, Y.; Sekido, Y.; Sone, S.; Yano, S. Hepatocyte growth factor reduces susceptibility to an irreversible epidermal growth factor receptor inhibitor in EGFR-T790M mutant lung cancer. *Clin. Cancer Res.* **2010**, *16*, 174–183. [[CrossRef](#)] [[PubMed](#)]
33. Kubo, Y.; Fukushima, S.; Inamori, Y.; Tsuruta, M.; Egashira, S.; Yamada-Kanazawa, S.; Nakahara, S.; Tokuzumi, A.; Miyashita, A.; Aoi, J.; et al. Serum concentrations of HGF are correlated with response to anti-PD-1 antibody therapy in patients with metastatic melanoma. *J. Dermatol. Sci.* **2019**, *93*, 33–40. [[CrossRef](#)] [[PubMed](#)]
34. Saigi, M.; Alburquerque-Bejar, J.J.; Mc Leer-Florin, A.; Pereira, C.; Pros, E.; Romero, O.A.; Baixeras, N.; Esteve-Codina, A.; Nadal, E.; Brambilla, E.; et al. MET-Oncogenic and JAK2-Inactivating Alterations Are Independent Factors That Affect Regulation of PD-L1 Expression in Lung Cancer. *Clin. Cancer Res.* **2018**, *24*, 4579–4587. [[CrossRef](#)] [[PubMed](#)]
35. Albitar, M.; Sudarsanam, S.; Ma, W.; Jiang, S.; Chen, W.; Funari, V.; Blocker, F.; Agersborg, S. Correlation of MET gene amplification and TP53 mutation with PD-L1 expression in non-small cell lung cancer. *Oncotarget* **2018**, *9*, 13682–13693. [[CrossRef](#)] [[PubMed](#)]
36. Titmarsh, H.E.; O’Connor, R.; Dhaliwal, K.; Akram, A.R. The Emerging Role of the c-MET-HGF Axis in Non-small Cell Lung Cancer Tumor Immunology and Immunotherapy. *Front. Oncol.* **2020**, *10*, 54. [[CrossRef](#)]
37. Papaccio, E.; Della Corte, C.M.; Viscardi, G.; Di Liello, R.; Esposito, G.; Sparano, F.; Ciardiello, F.; Morgillo, F. HGF/MET and the Immune System: Relevance for Cancer Immunotherapy. *Int. J. Mol. Sci.* **2018**, *19*, 3595. [[CrossRef](#)]
38. Turner, N.; Grose, R. Fibroblast growth factor signalling: From development to cancer. *Nat. Rev. Cancer* **2010**, *10*, 116–129. [[CrossRef](#)]
39. Berraondo, P.; Etcheberria, I.; Ponz-Sarvise, M.; Melero, I. Revisiting Interleukin-12 as a Cancer Immunotherapy Agent. *Clin. Cancer Res.* **2018**, *24*, 2716–2718. [[CrossRef](#)]
40. Seymour, L.; Bogaerts, J.; Perrone, A.; Ford, R.; Schwartz, L.H.; Mandrekar, S.; Lin, N.U.; Littré, S.; Dancey, J.; Chen, A.; et al. iRECIST: Guidelines for response criteria for use in trials testing immunotherapeutics. *Lancet Oncol.* **2017**, *18*, e143–e152. [[CrossRef](#)]
41. Benjamini, Y.; Hochberg, Y. Controlling the false discovery rate: A practical and powerful approach to multiple testing. *J. R. Stat. Soc. Ser. B Methodol.* **1995**, *57*, 289–300. [[CrossRef](#)]

**Article #2: Soluble PD-L1 (sPD-L1) as a biomarker of durable response and survival for first-line immune checkpoint inhibitor (ICI) treatment in advanced non-small cell lung cancer (NSCLC).** En cours de revue dans *ERJ Open Research*.

Costantini A, Takam Kamga P , Elvire Pons-Tostivint E, Delphine Fradin D, Jean-François Emile JF, Etienne Giroux-Leprieur E. Soluble PD-L1 (sPD-L1) as a biomarker of durable response and survival for first-line immune checkpoint inhibitor (ICI) treatment in advanced non-small cell lung cancer (NSCLC). *ERJ Open Res.* 2024. *Under Review*.

Des premiers résultats évaluant le rôle de sPD-L1 dans le CBNPC de stade avancé traité par nivolumab en deuxième ligne ou plus ont été obtenus au cours de mon année de Master 2 et ont été publiés dans *Oncoimmunology* (Annexe #2, premier auteur). Au cours de mes travaux de Thèse, nous avons cherché à poursuivre et à mieux caractériser le rôle de biomarqueur potentiel de sPD-L1 dans le contexte de patients présentant un CBNPC de stade avancé et traités par immunothérapie seule ou en association avec la chimiothérapie en première ligne thérapeutique.

En ce sens, nous avons réalisé une étude multicentrique composée de plusieurs cohortes de patients (n=110) : une cohorte de patients traités par chimiothérapie et deux cohortes de patients traités par immunothérapie seule ou associée à la chimiothérapie. Malgré des résultats non complètement homogènes à travers les cohortes, nous avons confirmé le rôle délétère du sPD-L1 chez les patients présentant une concentration élevée de sPD-L1 avant initiatoin du traitement. Nous avons également souligné le rôle prédictif de réponse à l'immunothérapie du sPD-L1 mesuré avant l'initiation du traitement et mis en évidence l'importance de la variation du sPD-L1 lors des premières semaines de traitement en vue d'anticiper la SG.

Enfin, par des analyses in vitro, nous avons montré que les cellules tumorales et immunitaires peuvent sécréter le sPD-L1 et que le plasma de patient peut inhiber la prolifération lymphocytaire.

**Soluble PD-L1 (sPD-L1) as a biomarker of durable response and survival for first-line immune checkpoint inhibitor (ICI) treatment in advanced non-small cell lung cancer (NSCLC).**

Adrien Costantini<sup>a, b</sup>, Paul Takam Kamga<sup>b</sup>, Elvire Pons-Tostivint<sup>c</sup>, Delphine Fradin<sup>c</sup>, Jean-François Emile<sup>b, d</sup>, Etienne Giroux-Leprieur<sup>a, b</sup>

<sup>a</sup>APHP-Ambroise Paré Hospital, Department of Respiratory Diseases and Thoracic Oncology, Boulogne-Billancourt, France.

<sup>b</sup>Université Paris-Saclay, UVSQ, EA 4340 BECCOH, Boulogne-Billancourt, France

<sup>c</sup> Nantes Université, Centre Hospitalier Universitaire Nantes, Medical oncology, F-44000 Nantes, France

<sup>d</sup>APHP-Ambroise Paré Hospital, Department of Pathology, Boulogne-Billancourt, France

**Corresponding author**

Etienne Giroux-Leprieur

APHP-Ambroise Paré Hospital, Department of Respiratory Diseases and Thoracic Oncology

9 avenue Charles de Gaulle

92 100, Boulogne-Billancourt

France

e-mail address : etienne.giroux-leprieur@aphp.fr

Conflict of interest declaration

Adrien Costantini has no conflict of interest with relation to the present work

Paul Takam Kamga has no conflict of interest with relation to the present work

Elvire Pons-Tostivint has no conflict of interest with relation to the present work

Delphine Fradin has no conflict of interest with relation to the present work

Jean-François Emile has no conflict of interest with relation to the present work

Etienne Giroux-Leprieur has no conflict of interest with relation to the present work

## Abstract

### Introduction

There is a need for biomarkers to predict response and survival to ICIs in patients with advanced non-small cell lung cancer (NSCLC). Soluble PD-L1 (sPD-L1) has shown biomarker potential. The objective of this study was to evaluate sPD-L1 in patients with advanced NSCLC treated with first-line ICIs.

### Methods

We constructed three prospective cohorts of patients with advanced NSCLC treated with first-line chemotherapy (CT), (Cohort #1), ICIs, or CT-ICIs (Cohort #2 and #3). Plasma was collected at baseline and at first tumour evaluation. sPD-L1 levels were measured by ELISA and compared to response and survival metrics.

### Results

Patients were mostly male smokers with adenocarcinomas. Baseline sPD-L1 was lower in responders vs non-responders in Cohort #2 ( $p=0.0233$ ). Patients with low baseline sPD-L1 had longer OS in Cohorts #2 and #3: median OS 18.0 months vs 4.0 months, ( $p=0.0277$ ) and not reached (NR) vs 13.0 months ( $p=0.0360$ ). First tumour evaluation sPD-L1 was lower in responders in Cohorts #1 ( $p=0.0138$ ) and #2 ( $p=0.0009$ ). Patients with low sPD-L1 at first tumour evaluation had longer OS in Cohort #2: 45.0 months vs 12.5 ( $p=0.0041$ ). Patients with stable/decreasing sPD-L1 had longer OS throughout the Cohorts: median OS of 15.5 vs 6.0 months, 45.0 vs 14.0 months and not reached (NR) vs 17.0 months in Cohorts #1, #2 and #3. In vitro studies confirmed that cancer and immune cells secreted sPD-L1 and that NSCLC patient plasma has the capacity to inhibit lymphocyte proliferation.

### Conclusion

sPD-L1 has prominent biomarker potential in advanced NSCLC treated with first-line ICIs.

## **Introduction**

Lung cancer is the leading cause of cancer-related death worldwide [1]. The use of immune checkpoint inhibitors (ICIs), humanised monoclonal antibodies that target immune checkpoints such as the programmed death-1 (PD-1)/programmed death ligand 1 (PD-L1) pathway have changed the treatment landscape of lung cancer. In the advanced stage, first-line strategies including ICIs alone or in association with chemotherapy have become the standard of care [2-9].

However, robust biomarkers to predict response to ICIs are lacking. Tissue based markers such as the expression of PD-L1 on the surface of cancer cells (tumour proportion score, TPS) as determined by immunohistochemistry (IHC) is imperfect. PD-L1 can be expressed by cancer cells as well as by immune cells [10]. Furthermore, PD-L1 expression is heterogeneous within one sample, between primary and metastatic sites and over time [11-13]. Finally, inter- and intra-observer discrepancies have also been reported [14, 15].

There is currently an unmet need to develop new reliable biomarkers in order to predict response to ICIs in solid tumours and especially in advanced NSCLC.

Plasma-based soluble biomarkers have several advantages. They are easy to access, as they only require a blood sample whereas tissue sample can be difficult to obtain and cause discomfort, pain and anxiety due to the procedures needed to obtain them. Blood-based biomarkers can be monitored during anti-cancer treatment, which is not the case with tissue-based markers as repeat biopsies are only rarely performed outside of clinical research settings. Finally, blood based-biomarkers have the capacity to encompass the entirety of the tumour burden and its clonality.

Plasma-based soluble PD-L1 (sPD-L1) is actively being explored as a potential prognostic and predictive biomarker in the context of advanced non-small cell lung cancer (NSCLC). The aim of this study was to evaluate the potential role of sPD-L1 as a prognostic and predictive biomarker in different cohorts of patients with advanced NSCLC, treated in the first-line setting with chemotherapy (CT) alone, ICIs alone or ICIs in association with CT.

## **Methods**

### **Patients and samples**

We performed a multi-centric non-interventional study that enrolled consecutive patients with advanced NSCLC, prospectively included in the Department of Respiratory Medicine and Thoracic Oncology (APHP–Ambroise Pare Hospital) and in the Department of Medical Oncology (CHU Nantes). Several cohorts were constructed; Cohort #1 (APHP–Ambroise Pare Hospital) was comprised of patients who received CT alone as first-line treatment between May 2015 and August 2020 with a data lock performed on the 14<sup>th</sup> of June 2021. Cohort #2 (APHP–Ambroise Pare Hospital) was comprised of patients who received ICIs alone or in association with CT as first-line treatment between October 2017 and April 2021, with a data lock performed on the 30<sup>th</sup> of September 2021. Cohort #3 (CHU Nantes), was comprised of patients with advanced NSCLC treated with ICIs alone or in association with CT as first-line treatment between May 2021 and December 2022 with a data lock was performed on the 28<sup>th</sup> of May 2024.

All patients continued treatment until disease progression evaluated by RECIST 1.1 criteria, unacceptable toxicity or death.

Plasma samples were collected at diagnosis (baseline sample), and at first tumour evaluation (on treatment sample). Two 10ml-EDTA tubes of peripheral blood were taken, and plasma was isolated within one hour after and immediately stored at -80°C

### **Enzyme-linked immunosorbent assay (ELISA) technique**

sPD-L1 concentrations were calculated by ELISA. ELISA tests were performed using a commercially available kit (ab214565 Human SimpleStep PD-L1 [28-8] ELISA Kit, Abcam) according to manufacturer's instructions. Corresponding recombinant proteins were used for each test at pre-specified concentrations to build standard curves. The results were obtained using a spectrophotometer (reading at 450nm), and concentrations were calculated according to the standard curves. All samples, standards and negative controls were tested in duplicate. We defined sPD-L1 variation as a 5% increase or decrease of sPD-L1 levels compared to baseline. In case of a change of less than 5%, sPD-L1 was considered as stable. sPD-L1 levels are expressed in pg/ml [16].

### Cell culture

The cell lines used were A545 and NCI-H596 (H596). A549 is a lung adenocarcinoma cell line presenting with KRAS G12S mutation. H596 is a lung adenosquamous carcinoma presenting with PIK3CA, Rb1 and TP53 mutations. Cells were cultured in DMEM culture medium supplemented with 10% fetal bovine serum (FBS) and penicillin-streptomycin antibiotic cocktails. Cells were incubated in a humidified incubator supplied with 5% CO<sub>2</sub>.

### PBMCs

PBMC were isolated from human blood by density gradient centrifugation using Lymphoprep (Stemcells Technologies). Isolated PBMC, stained or not with Carboxyfluorescein succinimidyl ester (CFSE, for proliferation assays), were maintained in complete RPMI or IMDM media for monoculture or coculture assays respectively. PBMC were activated with 10 µg/mL phytohemagglutinin. Lymphocyte activation/proliferation was assessed either through MTS colorimetric assay or CFSE staining assay.

### MTS proliferation assay

Lymphocyte proliferation was assessed using MTS proliferation assays as previously described. Briefly, at the end of cell culture, 10 µL of MTS reagent (Abcam, ab197010) was added into each well and kept in incubator for 2 hours. Metabolically active, viable cells convert MTS into a colored formazan. The product was then measured at 490 nm in a spectrophotometric microplate reader (Bio rad PR 3100 EIA PhD software). The viability was expressed as the percentage of optical density of treated cells compared to optical density of cells treated with the specific vehicle.

### Outcomes

We evaluated the following endpoints in this exploratory analysis. Progression free survival (PFS) defined as the time between treatment initiation and disease progression as evaluated by RECIST 1.1 criteria. Overall survival (OS) defined as the time between treatment initiation and death. Overall response rate (ORR) defined as the proportion of patients presenting with partial (PR) or complete response (CR). Durable clinical benefit (DCB) defined as patients presenting with stable disease (SD) or PR lasting 6 months or more. Patients with progressive disease (PD), and SD or PR lasting less than 6 months were considered as not presenting with

durable clinical benefit (NDB).

#### Statistical analysis

Median soluble concentrations of sPD-L1 was analysed according to ORR, clinical benefit. The comparison of median biomarker levels between groups was performed using Mann-Whitney test and the standard error of the mean (SEM) is given for each value. Kaplan-Meier method was used to determine OS and PFS. Comparison between survival curves was performed using log-rank method. High and low sPD-L1 levels was determined using quartiles. In a consistent manner for all cohorts, the highest quartile was defined as high sPD-L1 and the three lowest quartiles as low sPD-L1. Data analysis was computed using GraphPad Prism (Version 10.0). P-values were considered as significant if <0.05.

#### Ethical considerations

All patients signed an informed consent allowing blood to be drawn and stored within the Centre de Ressources Biologiques (CRB) of the Ambroise Paré University Hospital during their follow-up and treatment. The protocol was approved by the following Institutional Review Boards: CPP IDF n 8 (ID CRB 2014-A00187-40) and CHU de Nantes (DC-2011-1399, DC-2017-2987).

## **Results**

### **Patient characteristics and outcomes**

Cohort #1 was comprised of 32 patients who received CT alone as first-line treatment for advanced NSCLC. Cohort #2 and Cohort #3 were comprised of respectively 45 and 33 patients who received ICIs alone or in association with CT as first-line treatment for advanced NSCLC. Across the cohorts, the patients were mostly male (72%, 60%, 58%), with a median age at diagnosis of 68.5, 65 and 63 years, current or former smokers (94%, 93%, 100%) and presented with lung adenocarcinoma histology (69%, 71%, 64%), respectively in Cohorts #1, #2 and #3. The patients' characteristics are summarised in Tables 1-3.

The ORR to first-line treatment was 34% in Cohort #1, 52% in Cohort #2 and 67% in cohort #3. After respectively 29.0, 30.0 and 23.0 months of median follow-up in Cohorts #1, #2 and #3, median OS was 11.0 months, 16.0 months and 31.0 months and median PFS was 4.0 months, 7.0 months and 13.0 months.

Patients in the high and low sPD-L1 groups had similar baseline characteristics.

### **Baseline sPD-L1 predicts durable response and survival to ICIs**

In Cohort #1, median baseline sPD-L1 levels were 15.16 pg/ml in non-responders versus (vs) 15.87 pg/ml ( $p=0.4487$ ) in responders (Figure 1.A). Patients with NDB had median baseline sPD-L1 levels of 15.16 pg/ml vs 16.25 pg/ml ( $p=0.8883$ ) for patients who presented with DCB (Figure 1.B). Survival analysis found that patients with low baseline sPD-L1 levels had a median OS of 8.0 months vs 19.0 months, hazard ratio (HR) 1.79 95% CI [0.71 – 4.47],  $p=0.2623$  in the high baseline sPD-L1 group (Figure 2.A).

In Cohort #2, median baseline sPD-L1 levels were 59.65 pg/ml vs 30.40 pg/ml ( $p=0.0233$ ) in non-responders and responders, respectively (Figure 1.A). Patients with NDB had median baseline sPD-L1 levels of 53.65 pg/ml vs 31.17 pg/ml ( $p=0.4813$ ) for patients who presented with DCB (Figure 1.B). Survival analysis showed that patients with low baseline sPD-L1 levels had a median OS of 18.0 months vs 4.0 months, HR 0.42 95% CI [0.15 – 1.14],  $p=0.0277$  in patients with high baseline sPD-L1 (Figure 2.B).

In Cohort #3, median baseline sPD-L1 levels were 79.88 pg/ml vs 79.88 pg/ml ( $p=0.5098$ ) in non-responders and responders, respectively (Figure 1.A). Patients with NDB had a median baseline sPD-L1 value of 72.11 pg/ml vs 81.34 pg/ml for patients who presented with DCB ( $p=0.9850$ ) (Figure 1.B). Patients with low baseline sPD-L1 levels had a median OS of 31.0 vs

not reached (NR), HR 1.71 95% CI [0.46 - 6.27], p=0.4781 in patients with high baseline sPD-L1 levels. (Figure 2.C.)

**sPD-L1 measured at first tumour evaluation maintains its predictive value of response and survival to ICIs**

In Cohort #1, median sPD-L1 measured at first tumour evaluation was 14.74 pg/ml vs 4.45 pg/ml (p=0.0138) in non-responders and responders, respectively (Figure 1.A). Furthermore, patients with NDB had a median sPD-L1 value of 13.91 pg/ml vs 10.16 pg/ml (p=0.0531) for patients with DCB. (Figure 1.B.). Patients with low sPD-L1 evaluated at first tumour evaluation had a median OS of 13.0 months vs 11.0 HR 0.91 95% CI [0.34 – 2.44], p=0.8439 for patients with high sPD-L1 levels measured at the same time-point. (Figure 2.A.)

In Cohort #2, median sPD-L1 measured at first tumour evaluation was 79.65 pg/ml vs 29.40 pg/ml (p=0.0009) in non-responders and responders, respectively (Figure 1.A). Similarly, patients with NDB had a median sPD-L1 value of 65.59 pg/ml vs 31.97 pg/ml (p=0.0477) for patients with DCB. (Figure 1.B.). Patients with low sPD-L1 evaluated at first tumour evaluation had a median OS of 45.0 months vs 12.5 HR 0.28 95% CI [0.08 – 0.91], p=0.0041 for patients with high sPD-L1 levels measured at the same time-point. (Figure 2.B.).

In Cohort #3, median sPD-L1 measured at first tumour evaluation was 79.22 pg/ml vs 68.39 pg/ml (p=0.8143) in non-responders and responders, respectively (Figure 1.A). Patients with NDB had a median sPD-L1 value of 79.22 pg/ml vs 68.39 pg/ml (p=0.3307) in patients with DCB. (Figure 1.B.). Patients with low sPD-L1 evaluated at first tumour evaluation had a median OS of 31.0 months vs NR HR 1.71 95% CI [0.47 – 6.27], p=0.6031 for patients with high sPD-L1 levels measured at the same time-point (Figure 2.C).

**The decrease of sPD-L1 between baseline and first tumour evaluation is prognostic in advanced NSCLC**

In Cohort #1, responders had significantly higher sPD-L1 levels at baseline than at first tumour evaluation: 15.87pg/ml vs 4.45pg/ml (p=0.0284) whereas non-responders had similar levels of sPD-L1 at baseline and at first tumour evaluation: 13.36pg/ml vs 16.37 pg/ml (p=0.4116). Responders had a decrease of sPD-L1 levels between baseline and first tumour evaluation in 87.5% of cases and non-responders in 47% of cases (p=0.0858). Patients with increasing sPD-L1 levels between baseline and first tumour evaluation were non-responders in 89% of cases

whilst patients with stable/decreasing sPD-L1 levels were responders in 50% of cases (Figure 3.A).

In Cohort #2, responders and non-responders had similar baseline and on-treatment sPD-L1 levels: 30.40pg/ml vs 29.40pg/ml ( $p=0.7331$ ) and 59.65pg/ml vs 79.65pg/ml ( $p=0.2014$ ). Only 17% of non-responders had stable/decreasing sPD-L1 levels between baseline and first tumour evaluation compared to 59% of responders ( $p=0.0535$ ). Patients with stable/decreasing sPD-L1 levels between baseline and first tumour evaluation were responders in 83% of cases whilst 59% of patients with increasing sPD-L1 levels were non-responders (Figure 3.B).

In Cohort #3, responders and non-responders had similar baseline and on-treatment sPD-L1 levels: 159.1 pg/mL and 179.9 pg/ml ( $p=0.3190$ ) and 217.7pg/ml vs 174.4pg/ml ( $p=0.5737$ ). Responders had stable/decreasing sPD-L1 levels between baseline and first tumour evaluation in 64% of cases whilst non-responders did so in 54% of cases ( $p=0.7136$ ). Patients with stable/decreasing sPD-L1 levels between baseline and first tumour evaluation were responders in 74% of cases

#### sPD-L1 variation between baseline and first tumour evaluation is associated with survival

In Cohort #1, median OS was 15.5 months vs 6.0 months in the stable/decreasing and increasing groups, respectively, HR 0.34 95% CI [0.12 – 0.98],  $p=0.0082$ . Median progression free survival (PFS) was 5.5 months vs 3.0 months in the stable/decreasing and increasing groups, respectively, HR= 0.55 95% CI [0.22 - 1.40],  $p=0.0941$ .

In Cohort #2, patients with stable/decreasing sPD-L1 levels between baseline and first tumour evaluation had a median OS of 45.0 months vs 14.0 months in the increasing group, HR 0.38 95% CI [0.13 -1.07],  $p=0.1158$ . Median PFS was 15.0 months vs 6.0 months in the stable/decreasing and increasing groups, respectively, HR 0.77 95% CI [0.32 -1.89],  $p=0.560$ .

In Cohort #3 median OS was NR vs 31.0 months in the stable/decreasing and increasing groups, respectively, , HR= 0.55 95% CI (0.18 -1.73),  $p=0.2980$ . Median PFS was 13.0 vs 13.5 in the stable/decreasing and increasing groups, respectively,  $p=0.4694$ , HR= 1.244 95% CI (0.57 -2.70),  $p=0.5777$ .

We performed an exploratory analysis by combining Cohort #2 and Cohort #3 in order to increase the power of our analysis. We found that patient with stable/decreasing sPD-L1 between baseline and first tumour evaluation had significantly longer OS: median OS 45.0 vs

16.0 months HR 0.38 95% CI [0.1714 – 0.8386], p=0.0166 (Figure 4).. Results for PFS did not show a significant difference with a median PFS of 13.0 vs 11.0 months HR 0.92 95% CI[0.5175 – 1.646], p=0.7749 for the stable/decreasing and increasing groups, respectively

These results are summarised in Figure 4.

#### sPD-L1 produced by cancer and immune cells inhibits lymphocyte proliferation

We aimed to evaluate whether PBMCs obtained from a healthy donor had the capacity to secrete sPD-L1. Untreated PBMCs and PBMCs stimulated with PHA for 24 hours were cultured. The supernatant was collected and we found that stimulated PBMCs produced significantly more sPD-L1 than un treated PBMCs at the same time point: 46.59 pg/ml vs 115.7pg/ml , p=0.0040 (Figure 5. A.).

Cancer cell lines also consistently produced sPD-L1 regardless of their histological sub-type. We collected the supernatant of A549 (lung adenocarcinoma) and H596 (lung adenosquamous) cancer cell line and observed consistent sPD-L1 levels suggesting that cancer cells, regardless of their histology, have the ability to secrete sPD-L1 (Figure 5.B)..

To evaluate the functional role of sPD-L1 on lymphocyte proliferation, we exposed PBMCs stimulated with PHA to control plasma and to plasma from NSCLC patients. We found that NSCLC plasma inhibited lymphocyte proliferation to a greater degree than control plasma (Figure 5.C). Interestingly, we found that plasma containing high and low levels of sPD-L1 inhibited lymphocytes proliferation to the same extent. These results suggest complex and multi-molecular interactions between the cancer cells and immune cells within the tumour micro-environment (Figure 5.D).

## **Discussion**

In this study, we further examined the potential of sPD-L1 as a prognostic and predictive biomarker in patients with advanced NSCLC.

We examined baseline and on treatment sPD-L1 levels in three cohorts of patients with advanced NSCLC exposed to different treatment modalities that were received in the first-line setting (CT alone, ICIs alone or ICIs in association with CT). We found that baseline sPD-L1 levels were significantly lower in responders than in non-responders in Cohort #2, with a similar trend in Cohort #3 but not in Cohort #1. We also found that lower baseline sPD-L1 levels were associated with OS and PFS in the ICI cohorts but not the CT cohort suggesting a predictive role of sPD-L1.

sPD-L1 evaluated at first tumour evaluation was significantly lower in responders than in non-responders in two of our cohorts (Cohort #1, patients treated with CT and Cohort #2, patients treated with ICIs alone or in association with CT). Furthermore, patients with DCB had lower on treatment levels of sPD-L1, consistently throughout our Cohorts and significantly so in Cohort #2. Lower sPD-L1 levels measured at first tumour evaluation were also associated with OS and PFS in the ICI cohorts.

Next, we evaluated the dynamic change of sPD-L1. Throughout the Cohorts, the majority of responders had stable/decreasing sPD-L1 levels between baseline and first tumour evaluation whilst a majority of non-responders had increasing sPD-L1 levels (Cohort #1 and #2).

In terms of survival, patients with stable/decreasing sPD-L1 levels between baseline and first tumour evaluation had longer OS throughout the cohorts and significantly so in Cohort #1. The trend was similar in Cohorts #2 and #3 but our analysis lacked power to uncover any statistically significant differences. When combining Cohorts #2 and #3 in an exploratory analysis, we found that patients with stable/decreasing sPD-L1 had significantly longer OS.

We have previously shown that sPD-L1 levels measured at first tumour evaluation in patients with advanced NSCLC treated with nivolumab in the second-line setting or more was significantly higher in non-responders and in patients with NDB compared to responders and patients with DCB. Furthermore, we found that patients with stable/decreasing sPD-L1 levels between baseline and first tumour evaluation had significantly longer PFS and OS than patients with increasing sPD-L1 levels [16].

Here, we confirm the predictive role of baseline sPD-L1 with regards to response to ICIs.

Interestingly, sPD-L1 variation seems to predict response, benefit and survival regardless of the treatment modality with however a strong indicator of benefit in case of stable/decreasing sPD-L1 in patients receiving ICIs.

The use of sPD-L1 as a potential prognostic and predictive biomarker is actively being explored in solid tumours such as melanoma [17-19], clear cell renal cell carcinoma [17, 20-21], mesothelioma [22], gastric cancer [23-25] head and neck squamous cell carcinoma [26, 27], breast cancer [28, 29], glioma [30] as well as in haematological malignancies such as diffuse large B-cell lymphoma [31, 32], multiple myeloma [33] and hodgkin lymphoma [34]. The role of sPD-L1 has also been extensively evaluated in patients with NSCLC [16, 35-59]. Other authors have analysed sPD-L1 concentrations simultaneously in different cancer types [60, 61]. Finally, several meta-analyses have evaluated the role of sPD-L1 in cancer [62, 63], or specifically in lung cancer [64-67]. Some authors have reported contradictory results. Geiger et al. [68] evaluated soluble PD-1 (sPD-1) and sPD-L1 in a cohort of 243 patients with advanced NSCLC treated with platinum (carboplatin or cisplatin) in association with paclitaxel. Baseline levels of the analysed biomarkers as well as the change in concentration under treatment overlapped in responders and non-responders. Furthermore, none of the analysed biomarkers showed prognostic value with regards to OS. Kuroaki et al. [69] evaluated the use of sPD-1 and sPD-L1 in a cohort of 171 patients with solid tumours (head and neck cancer, urothelial cancer, renal cell cancer, gastric cancer, oesophageal cancer, malignant pleural mesothelioma, or microsatellite instability-high tumors) treated with nivolumab or pembrolizumab at any time during their treatment. They did not find a relation between OS/PFS and sPD-L1 levels but found that patients with low sPD-1 and high sPD-L1 concentrations had a significantly shorter PFS (HR of 1.79 [95% CI, 1.13–2.83], p= 0.01) and a tendency toward shorter OS (HR of 1.70 [95% CI, 0.99–2.91], p= 0.05) compared with all other patients.

Shimizu et al. [70] performed a meta-analysis in order to evaluate the impact of sPD-L1 variation in patients with advanced NSCLC receiving ICIs. They did not find that changes in sPD-L1 levels during PD-1 inhibitor treatment significantly influenced the prognosis of advanced NSCLC patients; however, the two studies included in the meta-analysis were of small size [42, 71] (total n=26) and patients did not all receive ICIs in the first-line setting. Due to the small size of this analysis, these results seem difficult to extrapolate and need further validation.

The general common finding from these numerous studies is that higher sPD-L1 levels is

deleterious with regards to outcome (response, PFS, OS, clinical benefit) across different solid and haematological malignancies and across different treatment modalities (chemotherapy, ICIs). Although some opposing results have been reported and refinement is still needed, the bulk of the data supports the use of sPD-L1 as a biomarker in solid tumours and specifically in advanced NSCLC.

Our findings are original as we used the dynamic change of sPD-L1 between baseline and first tumour evaluation to evaluate the use of sPD-L1 as a biomarker in advanced NSCLC treated in the first-line setting with and without ICIs. Only few studies have evaluated the dynamics of sPD-L1 and the results have been heterogeneous. We bring a further degree of originality as all our patients had sPD-L1 measured before any treatment was received and at first tumour evaluation. Finally, we evaluated three cohorts in a multi-centric fashion with cohorts constructed depending on treatment modalities.

There is currently a host of data supporting the use of sPD-L1 as a prognostic marker in solid tumours and its use as a predictive marker in response to ICIs in NSCLC and other solid tumours. We further confirm this role and especially the potential for using sPD-L1 variation as a marker for anticipating prognosis and have uncovered a predictive role of sPD-L1 for response to ICIs.

We propose using sPD-L1 as a marker in combination with radiological response criteria. In patients presenting with PR or SD but with increasing sPD-L1 levels compared to baseline, an early switch to second-line therapy or an intensification of the first line treatment could be beneficial rather than pursuing first line ICIs. We propose to craft a clinical trial wherein patients with increasing sPD-L1 levels between baseline and first tumour evaluation and P or SD on imaging would be randomized to receive either early second-line treatment or continue first-line treatment until disease progression. The hypothesis being that sPD-L1 is a surrogate marker of anti-cancer treatment efficacy with an increased detection capability when compared to imaging. Thus, combining imaging modalities and sPD-L1 would lead to earlier treatment modifications and potentially clinical benefit and prolonged survival.

To understand the functional role of sPD-L1, we performed several in vitro experiments. We confirmed that sPD-L1 can be secreted by cancer as well as immune cells [72, 73] and found

that lung cancer patient plasma has the ability to inhibit T-cell proliferation to a greater extent than control plasma. The knowledge surrounding the origin and function of sPD-L1 has greatly increased. sPD-L1 seems to originate from alternate splicing creating an mRNA coding for sPD-L1 [74, 75]. It also seems that sPD-L1 can be shed from cancer cells upon apoptosis. Furthermore, sPD-L1 seems to play an immunosuppressive role in the tumour micro-environment by interacting with T-cells expressing PD-1 and could also serve as a decoy for ICIs [76]. Finally, CDK12 seems to regulate the alternate splicing of PD-L1 mRNA with the potential for using CDK12 inhibitors in order to inhibit sPD-L1 production [77]. Despite these advances, challenges remain to uncover the underlying biological mechanisms leading to differing sPD-L1 secretion levels and to fully harness the biomarker potential of sPD-L1 in the clinical setting.

### Limitations

Our study is not without limitations. Although we were able to construct three cohorts of patients to perform our analysis the total number of patients was relatively small leading to a lack of power for some analyses. Furthermore, sPD-L1 levels were heterogeneous between our cohorts leading to difficulties in determining an optimal cut-off for sPD-L1. These differences could be explained by the fact that two different centers with potentially differing pre-analytical treatment of the samples participated in the study. Furthermore, some older samples that could have gone through several freeze-thaw cycles were included which could have an impact on sPD-L1 levels. However, to limit these variations and render the results interpretable, all samples were tested in duplicate. Furthermore, the analysis of decreasing/stable versus increasing sPD-L1 levels was performed by pooling two Cohorts as the absolute level of sPD-L1 would not impact this analysis.

### Strengths

Our study also displays several strengths. The cohorts were prospectively constructed, well characterized and allow to compare baseline and samples taken at first tumour evaluation of patients treated with CT alone or an association with ICIs for advanced NSCLC. In our cohort, all patients who received ICIs did so in the first line setting which is original with regards to other trials published evaluating sPD-L1 levels.

We also bring original in vitro analysis data showing that plasma of patients presenting with

cancer interferes with lymphocytes but that the level of sPD-L1 measured in the plasma does not impact this. This suggests that other more complex mechanisms are at work causing lymphocytes dysfunction.

## **Conclusion**

There is currently a wealth of data suggesting the biomarker potential of sPD-L1 across different cancer types including NSCLC. We bring further evidence of its potential use as a predictive biomarker in patients with advanced NSCLC treated with ICIs with an emphasis on the utility of the variation of sPD-L1 under treatment. As we have shown, the variation of sPD-L1 under treatment with ICIs has the ability to predict response and OS.

Strategy-based clinical trials with original designs are needed in order to harness the potential use of sPD-L1 variation as a biomarker in advanced NSCLC.

## **Tables**

Table 1. Baseline patient characteristics for Cohort #1

<b>Cohort #1</b>	Total (n=32)	Low baseline sPD-L1 (n=23)	High baseline sPD-L1 (n=7)
Gender			
Female	9 (28%)	6 (26%)	2 (29%)
Male	23 (72%)	17 (74%)	5 (71%)
Smoker			
Yes	30 (94%)	22 (96%)	6 (86%)
No	2 (6%)	1 (4%)	1 (14%)
Age at diagnosis (median)	68.5	69	65
Histology			
Adenocarcinoma	22 (69%)	16 (70%)	5 (71%)
Squamous cell carcinoma	6 (19%)	5 (22%)	0 (0%)
Other	4 (12%)	2 (9%)	2 (29%)
PS at treatment initiation			
0-1	27 (84%)	18 (78%)	7 (100%)
2-4	5 (16%)	5 (22%)	0 (0%)
Metastatic sites at diagnosis			
Liver	3 (9%)	3 (13%)	0 (0%)
Central nervous system (CNS)	9 (28%)	7 (30%)	2 (29%)
Bone	12 (38%)	10 (43%)	2 (29%)
Treatment			
Platinum pemetrexed	20 (63%)	15 (65%)	5 (71%)
Platinum weekly paclitaxel	5 (16%)	2 (9%)	1 (14%)
Platinum pemetrexed bevacizumab	2 (6%)	1 (4%)	1 (14%)
Platinum paclitaxel	2 (6%)	2 (9%)	0 (0%)
Platinum gemcitabine	2 (6%)	1 (4%)	0 (0%)
Gemcitabine	1 (3%)		

Table 2. Baseline patient characteristics for Cohort #2

Cohort #2	Total (n=45)	Low baseline sPD-L1 (n=31)	High baseline sPD-L1 (n=10)
Gender			
Female	18 (40%)	11 (35%)	4 (40%)
Male	27 (60%)	20 (65%)	6 (60%)
Smoker			
Yes	42 (93%)	29 (94%)	9 (90%)
No	3 (7%)	2 (6%)	1 (10%)
Age at diagnosis (median)	65	64	79
Histology			
Adenocarcinoma	32 (71%)	23 (74%)	6 (60%)
Squamous cell carcinoma	8 (18%)	4 (13%)	3 (30%)
Other	5 (11%)	4 (13%)	1 (10%)
PS at treatment initiation			
0-1	35 (78%)	27 (87%)	5 (50%)
2-4	10 (22%)	4 (13%)	5 (50%)
Metastatic sites at diagnosis			
Liver	5 (11%)	2 (6%)	3 (30%)
Central nervous system (CNS)	10 (22%)	8 (26%)	2 (20%)
Bone	19 (42%)	12 (39%)	5 (50%)
Treatment			
Pembrolizumab	28 (62%)	16 (52%)	9 (90%)
Chemo-immunotherapy	17 (28%)	15 (48%)	1 (10%)

Table 3. Baseline patient characteristics for Cohort #3

<b>Cohort #3</b>	Total (n=33)	Low baseline sPD-L1 (n=25)	High baseline sPD-L1
Gender			
Female	14 (42%)	11 (56%)	5 (63%)
Male	19 (58%)	14 (44%)	3 (38%)
Smoker			
Yes	33 (100%)	25 (100%)	8 (100%)
No	0 (0%)	0 (0%)	0 (0%)
Age at diagnosis (median)	63	64	61.5
Histology			
Adenocarcinoma	21 (64%)	16 (64%)	5 (63%)
Squamous cell carcinoma	5 (15%)	4 (16%)	1 (13%)
Other	7 (21%)	5 (20%)	2 (25%)
PS at treatment initiation			
0-1	27 (82%)	19 (76%)	8 (100%)
2-4	6 (18%)	6 (24%)	0 (0%)
Metastatic sites at diagnosis			
Liver	3 (9%)	3 (12%)	0 (0%)
Central nervous system (CNS)	9 (27%)	7 (28%)	2 (25%)
Bone	9 (27%)	5 (20%)	4 (50%)
First line treatment			
Pembrolizumab	13 (39%)	10 (40%)	3 (38%)
Chemo-immunotherapy	20 (61%)	15 (60%)	5 (63%)

## Figures

Figure 1. Baseline and on treatment sPD-L1 levels across the cohorts in responders and non-responders (NR) (A), and in patients with durable clinical benefit (DCB) and non durable benefit (NDB) (B). Results are expressed as median with standard error of the mean (SEM).

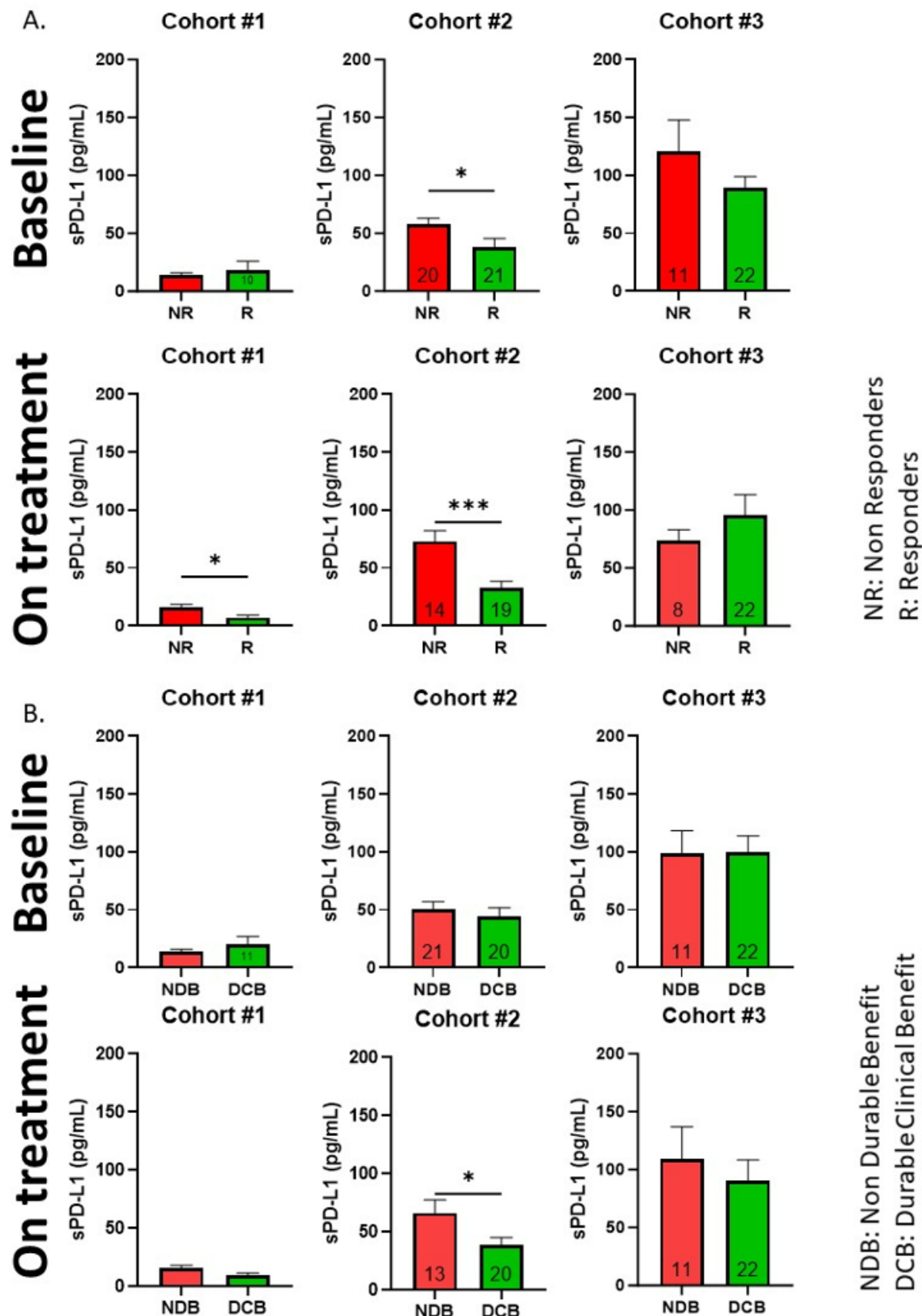


Figure 2. Overall survival (OS) depending on high/low sPD-L1 levels at baseline and first tumour evaluation in Cohort #1 (A), #2 (B) and #3 (C).

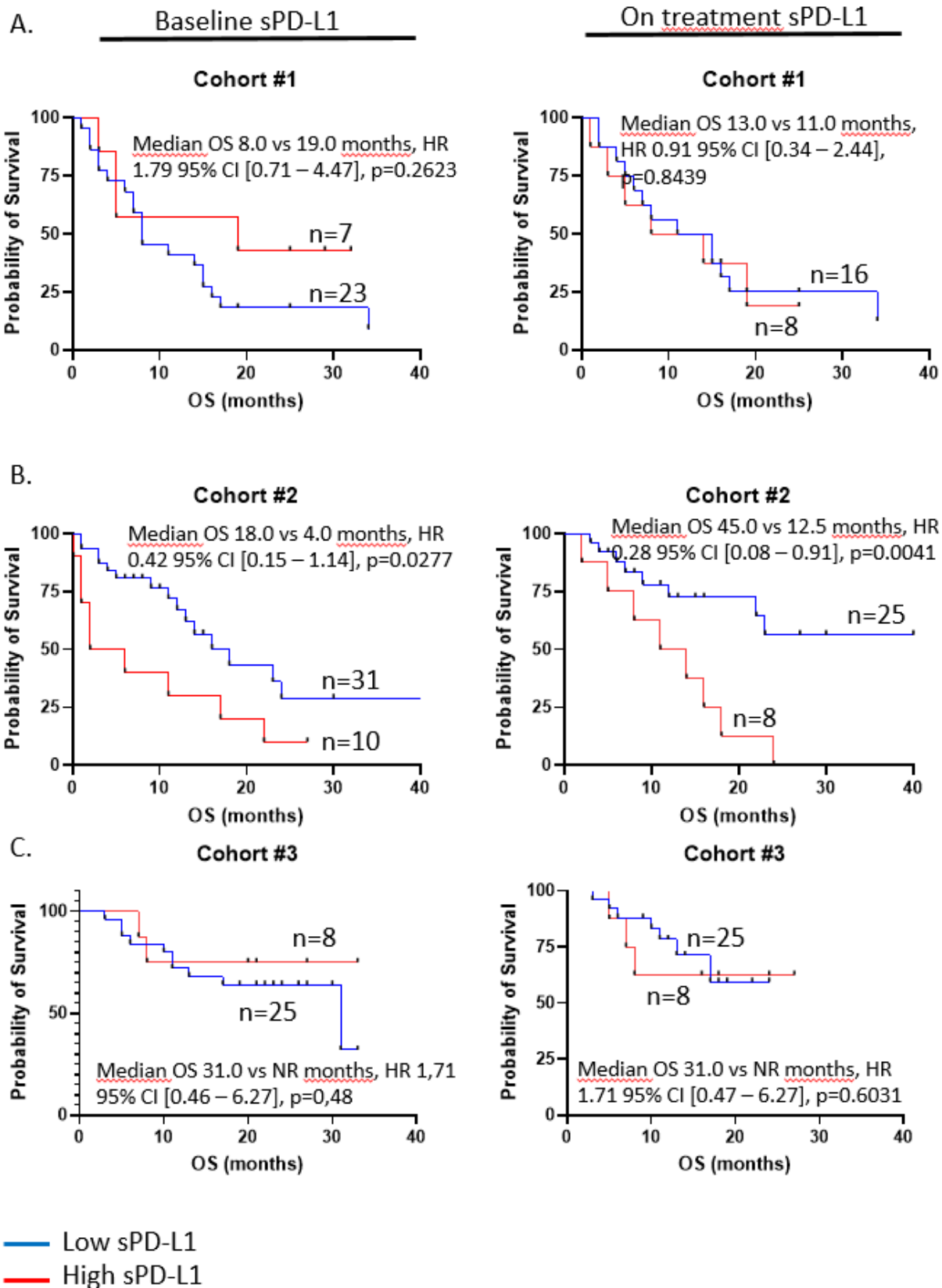
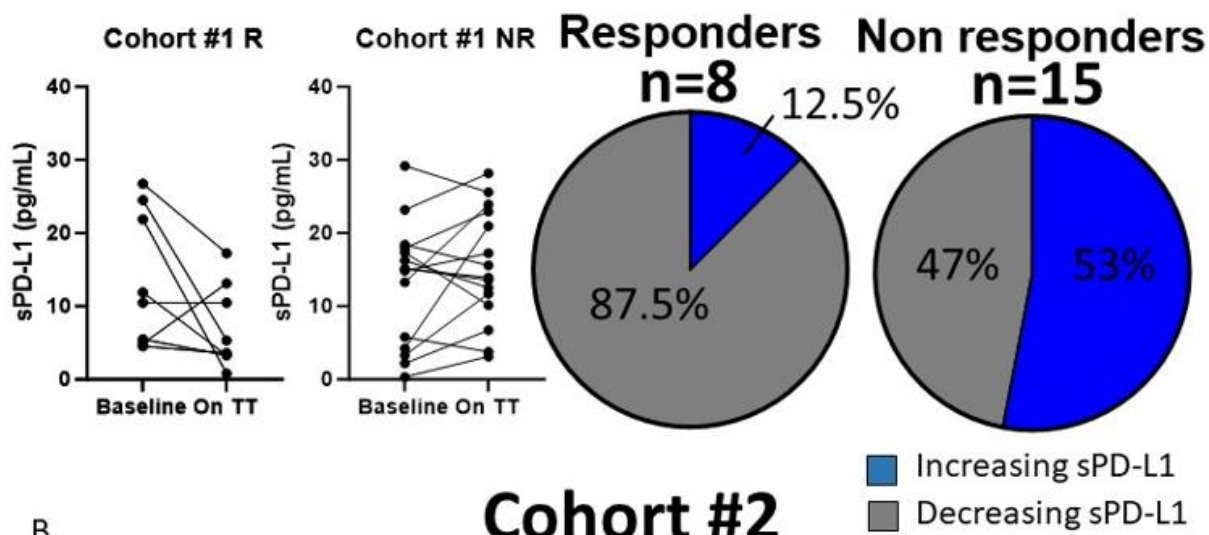


Figure 3. The variation of sPD-L1 in paired patient samples and the proportion of responders and non-responders presenting with increasing or stable/decreasing sPD-L1 levels between baseline and first tumour evaluation in Cohorts #1 (A), #2 (B) and #3 (C).

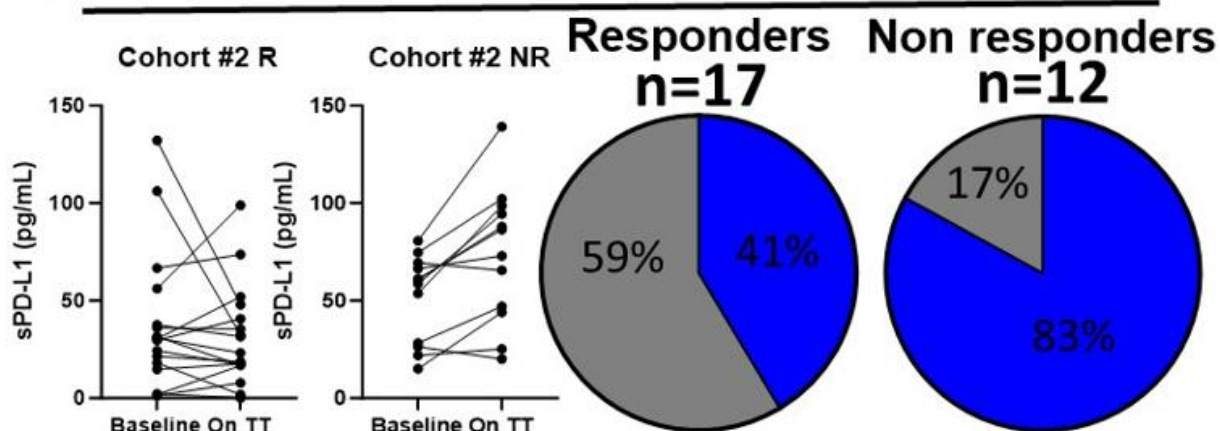
A.

## Cohort #1



B.

## Cohort #2



C.

## Cohort #3

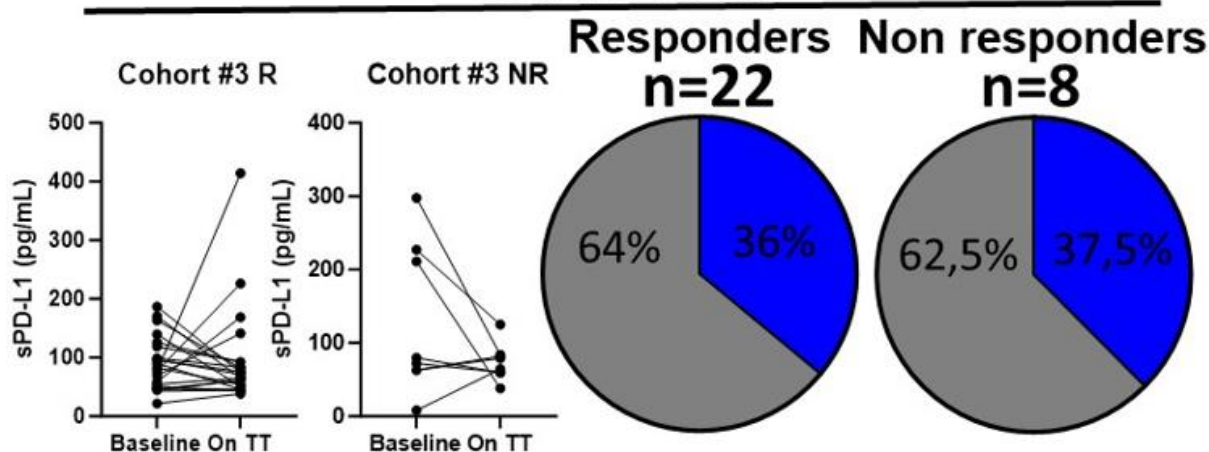


Figure 4. Overall survival (OS) in patients presenting with increasing versus stable/decreasing sPD-L1 levels between baseline and first tumour evaluation in Cohorts #1 (A), #2 (B), #3 (C) and #2 and #3 combined (D).

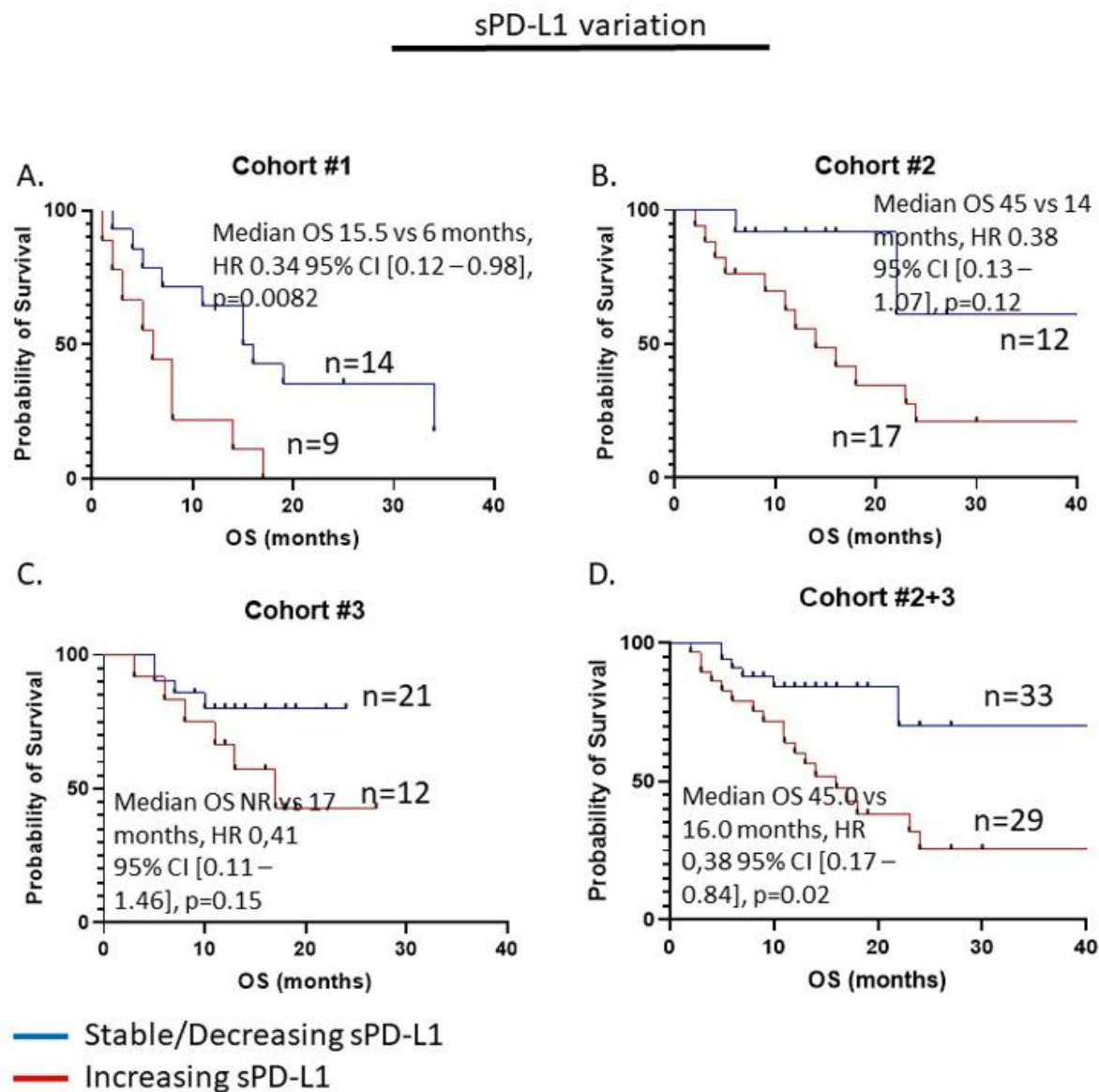
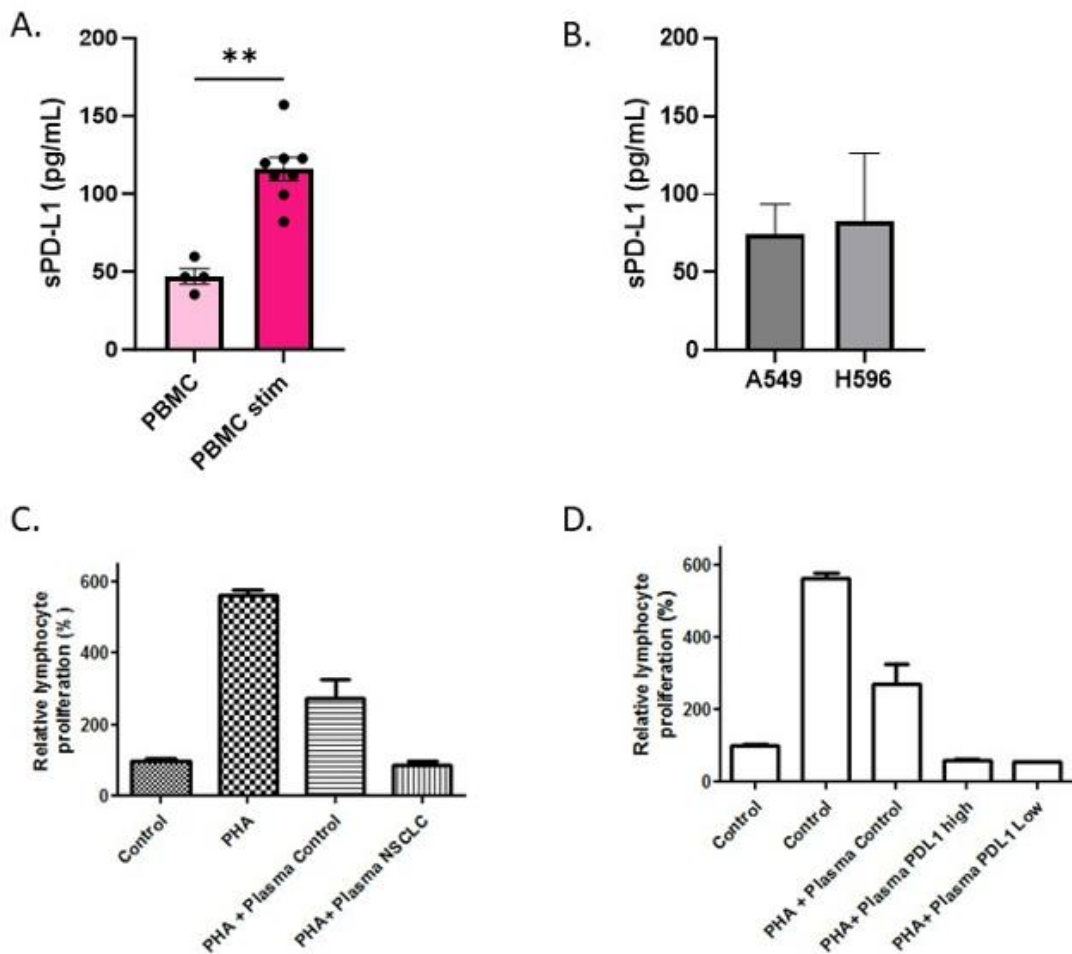


Figure 5. sPD-L1 secretion evaluated by ELISA in PBMCs (A) and lung cancer cell lines (B). Lymphocyte proliferation evaluated after exposure to control and lung cancer patient plasma (C) and lung cancer patient plasma with high and low sPD-L1 evaluated by ELISA (D).



## **References**

1. World Health Organization. Cancer. 2018. Available at: <http://www.who.int/news-room/fact-sheets/detail/cancer>. Accessed 11<sup>th</sup> of July, 2024.
2. Pembrolizumab versus Chemotherapy for PD-L1-Positive Non-Small-Cell Lung Cancer. Reck M, Rodríguez-Abreu D, Robinson AG, Hui R, Csőzsi T, Fülöp A, Gottfried M, Peled N, Tafreshi A, Cuffe S, O'Brien M, Rao S, Hotta K, Leiby MA, Lubiniecki GM, Shentu Y, Rangwala R, Brahmer JR; KEYNOTE-024 Investigators.N Engl J Med. 2016 Nov 10;375(19):1823-1833. doi: 10.1056/NEJMoa1606774. Epub 2016 Oct 8.PMID: 27718847
3. Pembrolizumab plus Chemotherapy in Metastatic Non-Small-Cell Lung Cancer. Gandhi L, Rodríguez-Abreu D, Gadgeel S, Esteban E, Felip E, De Angelis F, Domine M, Clingan P, Hochmair MJ, Powell SF, Cheng SY, Bischoff HG, Peled N, Grossi F, Jennens RR, Reck M, Hui R, Garon EB, Boyer M, Rubio-Viqueira B, Novello S, Kurata T, Gray JE, Vida J, Wei Z, Yang J, Raftopoulos H, Pietanza MC, Garassino MC; KEYNOTE-189 Investigators.N Engl J Med. 2018 May 31;378(22):2078-2092. doi: 10.1056/NEJMoa1801005. Epub 2018 Apr 16.PMID: 29658856
4. Atezolizumab for First-Line Treatment of Metastatic Nonsquamous NSCLC. Socinski MA, Jotte RM, Cappuzzo F, Orlandi F, Stroyakovskiy D, Nogami N, Rodríguez-Abreu D, Moro-Sibilot D, Thomas CA, Barlesi F, Finley G, Kelsch C, Lee A, Coleman S, Deng Y, Shen Y, Kowanetz M, Lopez-Chavez A, Sandler A, Reck M; IMpower150 Study Group.N Engl J Med. 2018 Jun 14;378(24):2288-2301. doi: 10.1056/NEJMoa1716948. Epub 2018 Jun 4.PMID: 29863955
5. Pembrolizumab plus Chemotherapy for Squamous Non-Small-Cell Lung Cancer. Paz-Ares L, Luft A, Vicente D, Tafreshi A, Gümrük M, Mazières J, Hermes B, Çay Şenler F, Csőzsi T, Fülöp A, Rodríguez-Cid J, Wilson J, Sugawara S, Kato T, Lee KH, Cheng Y, Novello S, Halmos B, Li X, Lubiniecki GM, Piperdi B, Kowalski DM; KEYNOTE-407 Investigators.N Engl J Med. 2018 Nov 22;379(21):2040-2051. doi: 10.1056/NEJMoa1810865. Epub 2018 Sep 25.PMID: 30280635
6. Nivolumab plus Ipilimumab in Advanced Non-Small-Cell Lung Cancer. Hellmann MD, Paz-Ares L, Bernabe Caro R, Zurawski B, Kim SW, Carcereny Costa E, Park K, Alexandru A, Lupinacci L, de la Mora Jimenez E, Sakai H, Albert I, Vergnenegre A, Peters S, Syrigos K, Barlesi F, Reck M, Borghaei H, Brahmer JR, O'Byrne KJ, Geese WJ, Bhagavatheeswaran P, Rabindran SK, Kasinathan RS, Nathan FE, Ramalingam SS.N Engl J Med. 2019 Nov 21;381(21):2020-2031. doi: 10.1056/NEJMoa1910231. Epub 2019 Sep 28.PMID: 31562796
7. Atezolizumab for First-Line Treatment of PD-L1-Selected Patients with NSCLC. Herbst RS, Giaccone G, de Marinis F, Reinmuth N, Vergnenegre A, Barrios CH, Morise M, Felip E, Andric Z, Geater S, Özgüroğlu M, Zou W, Sandler A, Enquist I, Komatsubara K, Deng Y, Kuriki H, Wen X, McClelland M, Moccia S, Jassem J, Spigel DR.N Engl J Med. 2020 Oct 1;383(14):1328-1339. doi: 10.1056/NEJMoa1917346.PMID: 32997907
8. Nivolumab versus Docetaxel in Advanced Squamous-Cell Non-Small-Cell Lung Cancer. Brahmer J, Reckamp KL, Baas P, Crino L, Eberhardt WE, Poddubskaya E, Antonia S, Pluzanski A, Vokes EE, Holgado E, Waterhouse D, Ready N, Gainor J, Arén Frontera O, Havel L, Steins M, Garassino MC, Aerts JG, Domine M, Paz-Ares L, Reck M, Baudelet C, Harbison CT, Lestini B, Spigel DR.N Engl J Med. 2015 Jul 9;373(2):123-35. doi: 10.1056/NEJMoa1504627. Epub 2015 May 31.PMID: 26028407

9. Nivolumab versus Docetaxel in Advanced Nonsquamous Non-Small-Cell Lung Cancer. Borghaei H, Paz-Ares L, Horn L, Spigel DR, Steins M, Ready NE, Chow LQ, Vokes EE, Felip E, Holgado E, Barlesi F, Kohlhäufl M, Arrieta O, Burgio MA, Fayette J, Lena H, Poddubskaya E, Gerber DE, Gettinger SN, Rudin CM, Rizvi N, Crinò L, Blumenschein GR Jr, Antonia SJ, Dorange C, Harbison CT, Graf Finckenstein F, Brahmer JR.N Engl J Med. 2015 Oct 22;373(17):1627-39. doi: 10.1056/NEJMoa1507643. Epub 2015 Sep 27.PMID: 26412456
10. PD-L1 as a biomarker of response to immune-checkpoint inhibitors. Doroshow DB, Bhalla S, Beasley MB, Sholl LM, Kerr KM, Gnjatic S, Wistuba II, Rimm DL, Tsao MS, Hirsch FR.Nat Rev Clin Oncol. 2021 Jun;18(6):345-362. doi: 10.1038/s41571-021-00473-5. Epub 2021 Feb 12.PMID: 33580222
11. Temporal and spatial discordance of programmed cell death-ligand 1 expression and lymphocyte tumor infiltration between paired primary lesions and brain metastases in lung cancer. A S Mansfield, M C Aubry, J C Moser, S M Harrington, R S Dronca, S S Park, H Dong. Ann Oncol. 2016 Oct;27(10):1953-8. doi: 10.1093/annonc/mdw289. Epub 2016 Aug 8.
12. Programmed Death-Ligand 1 Heterogeneity and Its Impact on Benefit From Immune Checkpoint Inhibitors in NSCLC. Hong L, Negrao MV, Dibaj SS, Chen R, Reuben A, Bohac JM, Liu X, Skoulidis F, Gay CM, Cascone T, Mitchell KG, Tran HT, Le X, Byers LA, Sepesi B, Altan M, Elamin YY, Fossella FV, Kurie JM, Lu C, Mott FE, Tsao AS, Rinsurongkawong W, Lewis J, Gibbons DL, Glisson BS, Blumenschein GR Jr, Roarty EB, Futreal PA, Wistuba II, Roth JA, Swisher SG, Papadimitrakopoulou VA, Heymach JV, Lee JJ, Simon GR, Zhang J.J Thorac Oncol. 2020 Sep;15(9):1449-1459. doi: 10.1016/j.jtho.2020.04.026. Epub 2020 May 8.PMID: 32389639
13. Heterogeneity of programmed death-ligand 1 expression and infiltrating lymphocytes in paired resected primary and metastatic non-small cell lung cancer. Wu J, Sun W, Yang X, Wang H, Liu X, Chi K, Zhou L, Huang X, Mao L, Zhao S, Ding T, Meng B, Lin D.Mod Pathol. 2022 Feb;35(2):218-227. doi: 10.1038/s41379-021-00903-w. Epub 2021 Sep 7.PMID: 34493824
14. Intra- and Interobserver Reproducibility Assessment of PD-L1 Biomarker in Non-Small Cell Lung Cancer. Cooper WA, Russell PA, Cherian M, Duhig EE, Godbolt D, Jessup PJ, Khoo C, Leslie C, Mahar A, Moffat DF, Sivasubramaniam V, Faure C, Reznichenko A, Grattan A, Fox SB.Clin Cancer Res. 2017 Aug 15;23(16):4569-4577. doi: 10.1158/1078-0432.CCR-17-0151. Epub 2017 Apr 18.PMID: 28420726
15. PD-L1 immunohistochemistry in clinical diagnostics of lung cancer: inter-pathologist variability is higher than assay variability. Brunnström H, Johansson A, Westbom-Fremer S, Backman M, Djureinovic D, Patthey A, Isaksson-Mettävainio M, Gulyas M, Micke P.Mod Pathol. 2017 Oct;30(10):1411-1421. doi: 10.1038/modpathol.2017.59. Epub 2017 Jun 30.PMID: 28664936
16. Predictive role of plasmatic biomarkers in advanced non-small cell lung cancer treated by nivolumab. Costantini A, Julie C, Dumenil C, Hélias-Rodzewicz Z, Tisserand J, Dumoulin J, Giraud V, Labrune S, Chinet T, Emile JF, Giroux Leprieur E. Oncoimmunology. 2018 Apr 20;7(8):e1452581. doi: 10.1080/2162402X.2018.1452581. eCollection 2018.PMID: 30221046
17. Soluble PD-L1 as an early marker of progressive disease on nivolumab. Mahoney KM, Ross-Macdonald P, Yuan L, Song L, Veras E, Wind-Rotolo M, McDermott DF, Stephen Hodi F, Choueiri TK, Freeman GJ.J Immunother Cancer. 2022 Feb;10(2):e003527. doi: 10.1136/jitc-2021-003527.PMID: 35131863
18. Soluble immune checkpoints and T-cell subsets in blood as biomarkers for resistance to immunotherapy in melanoma patients. Machiraju D, Wiecken M, Lang N, Hülsmeyer I, Roth J, Schank TE, Eurich R, Halama N, Enk A, Hassel JC. Oncoimmunology. 2021 May 25;10(1):1926762. doi: 10.1080/2162402X.2021.1926762.PMID: 34104542

19. Soluble PD-L1 is a predictive and prognostic biomarker in advanced cancer patients who receive immune checkpoint blockade treatment. Oh SY, Kim S, Keam B, Kim TM, Kim DW, Heo DS. *Sci Rep.* 2021 Oct 5;11(1):19712. doi: 10.1038/s41598-021-99311-y. PMID: 34611279
20. Baseline plasma levels of soluble PD-1, PD-L1, and BTN3A1 predict response to nivolumab treatment in patients with metastatic renal cell carcinoma: a step toward a biomarker for therapeutic decisions. Incorvaia L, Fanale D, Badalamenti G, Porta C, Olive D, De Luca I, Brando C, Rizzo M, Messina C, Rediti M, Russo A, Bazan V, Iovanna JL. *Oncimmunology.* 2020 Oct 27;9(1):1832348. doi: 10.1080/2162402X.2020.1832348. PMID: 33178494
21. Sccoluble PD-L1 Is an Independent Prognostic Factor in Clear Cell Renal Cell Carcinoma. Larrinaga G, Solano-Iturri JD, Errarte P, Unda M, Loizaga-Iriarte A, Pérez-Fernández A, Echevarría E, Asumendi A, Manini C, Angulo JC, López JL. *S Cancers (Basel).* 2021 Feb 7;13(4):667. doi: 10.3390/cancers13040667. PMID: 33562338
22. Circulating Levels of PD-L1 in Mesothelioma Patients from the NIBIT-MESO-1 Study: Correlation with Survival. Chiarucci C, Cannito S, Daffinà MG, Amato G, Giacobini G, Cutaia O, Lofiego MF, Fazio C, Giannarelli D, Danielli R, Di Giacomo AM, Coral S, Calabò L, Maio M, Covre A. *Cancers (Basel).* 2020 Feb 5;12(2):361. doi: 10.3390/cancers12020361. PMID: 32033266
23. Soluble PD-L1 as a diagnostic and prognostic biomarker in resectable gastric cancer patients. Chivu-Economescu M, Herlea V, Dima S, Sorop A, Pechianu C, Procop A, Kitahara S, Necula L, Matei L, Dragu D, Neagu AI, Bleotu C, Diaconu CC, Popescu I, Duda DG. *Gastric Cancer.* 2023 Nov;26(6):934-946. doi: 10.1007/s10120-023-01429-7. Epub 2023 Sep 5. PMID: 37668884
24. Soluble PD-L1 Expression in Circulation as a Predictive Marker for Recurrence and Prognosis in Gastric Cancer: Direct Comparison of the Clinical Burden Between Tissue and Serum PD-L1 Expression. Shigemori T, Toiyama Y, Okugawa Y, Yamamoto A, Yin C, Narumi A, Ichikawa T, Ide S, Shimura T, Fujikawa H, Yasuda H, Hiro J, Yoshiyama S, Ohi M, Araki T, Kusunoki M. *Ann Surg Oncol.* 2019 Mar;26(3):876-883. doi: 10.1245/s10434-018-07112-x. Epub 2018 Dec 18. PMID: 30565045
25. Serum levels of soluble programmed cell death ligand 1 as a prognostic factor on the first-line treatment of metastatic or recurrent gastric cancer. Takahashi N, Iwasa S, Sasaki Y, Shoji H, Honma Y, Takashima A, Okita NT, Kato K, Hamaguchi T, Yamada Y. *J Cancer Res Clin Oncol.* 2016 Aug;142(8):1727-38. doi: 10.1007/s00432-016-2184-6. Epub 2016 Jun 2. PMID: 27256004
26. Soluble Programmed Death-Ligand 1 (sPD-L1) as a Promising Marker for Head and Neck Squamous Cell Carcinoma: Correlations With Clinical and Demographic Characteristics. Alrehaili AA, Gharib AF, Almalki A, Alghamdi A, Hawsawi NM, Bakhuraysah MM, Alhuthali HM, Etewa RL, Elsawy WH. *Cureus.* 2023 Aug 29;15(8):e44338. doi: 10.7759/cureus.44338. eCollection 2023 Aug. PMID: 37779773
27. Prognostic and predictive role of soluble programmed death ligand-1 in head and neck cancer . Molga-Magusiak M, Rzepakowska A, Żurek M, Kotuła I, Demkow U, Niemczyk K. *Braz J Otorhinolaryngol.* 2023 May-Jun;89(3):417-424. doi: 10.1016/j.bjorl.2023.02.005. Epub 2023 Feb 21. PMID: 36868994
28. The clinical implication of soluble PD-L1 (sPD-L1) in patients with breast cancer and its biological function in regulating the function of T lymphocyte. Han B, Dong L, Zhou J, Yang Y, Guo J, Xuan Q, Gao K, Xu Z, Lei W, Wang J, Zhang Q.. *Cancer Immunol Immunother.* 2021 Oct;70(10):2893-2909. doi: 10.1007/s00262-021-02898-4. Epub 2021 Mar 10. PMID: 33688997

29. The interaction between the soluble programmed death ligand-1 (sPD-L1) and PD-1<sup>+</sup> regulator B cells mediates immunosuppression in triple-negative breast cancer. Li X, Du H, Zhan S, Liu W, Wang Z, Lan J, PuYang L, Wan Y, Qu Q, Wang S, Yang Y, Wang Q, Xie F. *Front Immunol*. 2022 Jul 22;13:830606. doi: 10.3389/fimmu.2022.830606. eCollection 2022. PMID: 35935985
30. The Change of Soluble Programmed Cell Death-Ligand 1 in Glioma Patients Receiving Radiotherapy and Its Impact on Clinical Outcomes. Ding XC, Wang LL, Zhu YF, Li YD, Nie SL, Yang J, Liang H, Weichselbaum RR, Yu JM, Hu M. *Front Immunol*. 2020 Oct 30;11:580335. doi: 10.3389/fimmu.2020.580335. eCollection 2020. PMID: 33224142
31. Plasma soluble PD-L1 and STAT3 predict the prognosis in diffuse large B cell lymphoma patients. Fei Y, Yu J, Li Y, Li L, Zhou S, Zhang T, Li L, Qiu L, Meng B, Pan Y, Ren X, Qian Z, Wang X, Zhang H. *J Cancer*. 2020 Oct 17;11(23):7001-7008. doi: 10.7150/jca.47816. eCollection 2020. PMID: 33123290
32. High level of soluble programmed cell death ligand 1 in blood impacts overall survival in aggressive diffuse large B-Cell lymphoma: results from a French multicenter clinical trial. Rossille D, Gressier M, Damotte D, Maucort-Boulch D, Pangault C, Semana G, Le Gouill S, Haioun C, Tarte K, Lamy T, Milpied N, Fest T; Groupe Ouest-Est des Leucémies et Autres Maladies du Sang; Groupe Ouest-Est des Leucémies et Autres Maladies du Sang. *Leukemia*. 2014 Dec;28(12):2367-75. doi: 10.1038/leu.2014.137. Epub 2014 Apr 15. PMID: 24732592
33. Serum levels of soluble programmed death ligand 1 predict treatment response and progression free survival in multiple myeloma. Wang L, Wang H, Chen H, Wang WD, Chen XQ, Geng QR, Xia ZJ, Lu Y. *Oncotarget*. 2015 Dec 1;6(38):41228-36. doi: 10.18632/oncotarget.5682. PMID: 26515600
34. High Serum Level of Soluble Programmed Death Ligand 1 is Associated With a Poor Prognosis in Hodgkin Lymphoma. Guo X, Wang J, Jin J, Chen H, Zhen Z, Jiang W, Lin T, Huang H, Xia Z, Sun X. *Transl Oncol*. 2018 Jun;11(3):779-785. doi: 10.1016/j.tranon.2018.03.012. Epub 2018 Apr 24. PMID: 29698935
35. Plasma levels of soluble programmed death ligand-1 may be associated with overall survival in nonsmall cell lung cancer patients receiving thoracic radiotherapy. Zhao J, Zhang P, Wang J, Xi Q, Zhao X, Ji M, Hu G. *Medicine (Baltimore)*. 2017 Feb;96(7):e6102. doi: 10.1097/MD.0000000000006102. PMID: 28207525
36. High plasma levels of soluble programmed cell death ligand 1 are prognostic for reduced survival in advanced lung cancer. Okuma Y, Hosomi Y, Nakahara Y, Watanabe K, Sagawa Y, Homma S. *Lung Cancer*. 2017 Feb;104:1-6. doi: 10.1016/j.lungcan.2016.11.023. Epub 2016 Dec 5. PMID: 28212990
37. Soluble Programmed Cell Death Ligand 1 as a Novel Biomarker for Nivolumab Therapy for Non-Small-cell Lung Cancer. Okuma Y, Wakui H, Utsumi H, Sagawa Y, Hosomi Y, Kuwano K, Homma S. *Clin Lung Cancer*. 2018 Sep;19(5):410-417.e1. doi: 10.1016/j.cllc.2018.04.014. Epub 2018 May 5. PMID: 29859759
38. Circulating immune biomarkers as predictors of the response to pembrolizumab and weekly low dose carboplatin and paclitaxel in NSCLC and poor PS: An interim analysis. Bonomi M, Ahmed T, Addo S, Kooshki M, Palmieri D, Levine BJ, Ruiz J, Grant S, Petty WJ, Triozi PL. *Oncol Lett*. 2019 Jan;17(1):1349-1356. doi: 10.3892/ol.2018.9724. Epub 2018 Nov 19. PMID: 30655905
39. Soluble sPD-L1 and Serum Amyloid A1 as Potential Biomarkers for Lung Cancer. Jovanović D, Roksandić-Milenković M, Kotur-Stevuljević J, Ćeriman V, Vukanić I, Samardžić N, Popević S, Ilić B, Gajić M, Simon M, Simon I, Spasojević-Kalimanovska V, Belić M, Mirkov D, Šumarac Z, Milenković V. *J Med Biochem*. 2019 May 11;38(3):332-341. doi: 10.2478/jomb-2018-0036. eCollection 2019 Jul. PMID: 31156344
40. Predictive Value of Soluble PD-1, PD-L1, VEGFA, CD40 Ligand and CD44 for Nivolumab Therapy in Advanced Non-Small Cell Lung Cancer: A Case-Control Study. Tiako Meyo M, Jouinot A, Giroux-Leprieur E, Fabre E, Wislez M, Alifano M, Leroy K, Boudou-Rouquette P, Tlemsani C, Khoudour N, Arrondeau J,

Thomas-Schoemann A, Blons H, Mansuet-Lupo A, Damotte D, Vidal M, Goldwasser F, Alexandre J, Blanchet B. *Cancers (Basel)*. 2020 Feb 18;12(2):473. doi: 10.3390/cancers12020473. PMID: 32085544

41. Study on the Expression Levels and Clinical Significance of PD-1 and PD-L1 in Plasma of NSCLC Patients. He J, Pan Y, Guo Y, Li B, Tang Y. *J Immunother.* 2020 Jun;43(5):156-164. doi: 10.1097/CJI.0000000000000315. PMID: 32168233
42. Soluble PD-L1 in NSCLC Patients Treated with Checkpoint Inhibitors and Its Correlation with Metabolic Parameters. Castello A, Rossi S, Toschi L, Mansi L, Lopci E. *Cancers (Basel)*. 2020 May 27;12(6):1373. doi: 10.3390/cancers12061373. PMID: 32471030
43. Soluble PD-L1 and Circulating CD8+PD-1+ and NK Cells Enclose a Prognostic and Predictive Immune Effector Score in Immunotherapy Treated NSCLC patients. Mazzaschi G, Minari R, Zecca A, Cavazzoni A, Ferri V, Mori C, Squadrilli A, Bordi P, Buti S, Bersanelli M, Leonetti A, Cosenza A, Ferri L, Rapacchi E, Missale G, Petronini PG, Quaini F, Tiseo M. *Lung Cancer*. 2020 Oct;148:1-11. doi: 10.1016/j.lungcan.2020.07.028. Epub 2020 Aug 2. PMID: 32768804
44. Soluble PD-L1 as a Predictor of the Response to EGFR-TKIs in Non-small Cell Lung Cancer Patients With EGFR Mutations. Jia Y, Li X, Zhao C, Ren S, Su C, Gao G, Li W, Zhou F, Li J, Zhou C.. *Front Oncol.* 2020 Aug 25;10:1455. doi: 10.3389/fonc.2020.01455. eCollection 2020. PMID: 32983977
45. Association between serum level soluble programmed cell death ligand 1 and prognosis in patients with non-small cell lung cancer treated with anti-PD-1 antibody. Murakami S, Shibaki R, Matsumoto Y, Yoshida T, Goto Y, Kanda S, Horinouchi H, Fujiwara Y, Yamamoto N, Ohe Y. *Thorac Cancer*. 2020 Dec;11(12):3585-3595. doi: 10.1111/1759-7714.13721. Epub 2020 Oct 27. PMID: 33108686
46. Prediction of Clinical Outcome in Locally Advanced Non-Small Cell Lung Cancer Patients Treated With Chemoradiotherapy by Plasma Markers. Sui X, Jiang L, Teng H, Mi L, Li B, Shi A, Yu R, Li D, Dong X, Yang D, Yu H, Wang. *Front Oncol.* 2021 Feb 17;10:625911. doi: 10.3389/fonc.2020.625911. eCollection 2020. PMID: 33680949
47. Novel Biomarkers of Dynamic Blood PD-L1 Expression for Immune Checkpoint Inhibitors in Advanced Non-Small-Cell Lung Cancer Patients. Yang Q, Chen M, Gu J, Niu K, Zhao X, Zheng L, Xu Z, Yu Y, Li F, Meng L, Chen Z, Zhuo W, Zhang L, Sun J. *Front Immunol.* 2021 Apr 16;12:665133. doi: 10.3389/fimmu.2021.665133. eCollection 2021. PMID: 33936103
48. The integration of systemic and tumor PD-L1 as a predictive biomarker of clinical outcomes in patients with advanced NSCLC treated with PD-(L)1blockade agents. Zamora Atenza C, Anguera G, Riudavets Melià M, Alserawan De Lambo L, Sullivan I, Barba Joaquin A, Serra Lopez J, Ortiz MA, Mulet M, Vidal S, Majem M. *Cancer Immunol Immunother.* 2022 Aug;71(8):1823-1835. doi: 10.1007/s00262-021-03107-y. Epub 2022 Jan 5. PMID: 34984538
49. The correlation of serum sPD-1 and sPD-L1 levels with clinical, pathological characteristics and lymph node metastasis in nonsmall cell lung cancer patients. Ancın B, Özercan MM, Yılmaz YM, Uysal S, Kumbasar U, Sarıbaş Z, Dikmen E, Doğan R, Demircin M. *Turk J Med Sci*. 2022 Aug;52(4):1050-1057. doi: 10.55730/1300-0144.5407. Epub 2022 Aug 10. PMID: 36326416
50. Prognostic Role of Soluble and Extracellular Vesicle-Associated PD-L1, B7-H3 and B7-H4 in Non-Small Cell Lung Cancer Patients Treated with Immune Checkpoint Inhibitors. Genova C, Tasso R, Rosa A, Rossi G, Reverberi D, Fontana V, Marconi S, Croce M, Dal Bello MG, Dellepiane C, Tagliamento M, Ciferri MC, Zullo L, Fedeli A, Alama A, Cortese K, Gentili C, Cellia E, Anselmi G, Mora M, Barletta G, Rijavec E, Grossi F, Pronzato P, Coco S. *Cells*. 2023 Mar 8;12(6):832. doi: 10.3390/cells12060832. PMID: 36980174
51. Association between response to anti-PD-1 treatment and blood soluble PD-L1 and IL-8 changes in patients with NSCLC. Yi L, Wang X, Fu S, Yan Z, Ma T, Li S, Wei P, Zhang H, Wang J. *Discov Oncol.* 2023 Mar 29;14(1):35. doi: 10.1007/s12672-023-00641-2. PMID: 36991160

52. Clinical roles of soluble PD-1 and PD-L1 in plasma of NSCLC patients treated with immune checkpoint inhibitors. Himuro H, Nakahara Y, Igarashi Y, Kouro T, Higashijima N, Matsuo N, Murakami S, Wei F, Horaguchi S, Tsuji K, Mano Y, Saito H, Azuma K, Sasada T. *Cancer Immunol Immunother.* 2023 Aug;72(8):2829-2840. doi: 10.1007/s00262-023-03464-w. Epub 2023 May 16. PMID: 37188764
53. Prognostic impact of soluble PD-L1 derived from tumor-associated macrophages in non-small-cell lung cancer. Teramoto K, Igarashi T, Kataoka Y, Ishida M, Hanaoka J, Sumimoto H, Daigo Y. *Cancer Immunol Immunother.* 2023 Nov;72(11):3755-3764. doi: 10.1007/s00262-023-03527-y. Epub 2023 Aug 30. PMID: 37646826
54. Analysis of soluble programmed death-1 ligand-1 of lung cancer patients with different characteristics. Zhu HB, Song X. *Eur Rev Med Pharmacol Sci.* 2023 Sep;27(18):8690-8696. doi: 10.26355/eurrev\_202309\_33792. PMID: 37782182
55. The influence of plasma sPD-L1 concentration on the effectiveness of immunotherapy in advanced NSCLC patients. Chmielewska I, Grenda A, Krawczyk P, Frąk M, Kuźnar Kamińska B, Mitura W, Milanowsk. *J.Cancer Immunol Immunother.* 2023 Dec;72(12):4169-4177. doi: 10.1007/s00262-023-03552-x. Epub 2023 Oct 10. PMID: 37816808
56. Plasma sPD-L1 and VEGF levels are associated with the prognosis of NSCLC patients treated with combination immunotherapy. Dong C, Hui K, Gu J, Wang M, Hu C, Jiang X. *Anticancer Drugs.* 2024 Jun 1;35(5):418-425. doi: 10.1097/CAD.0000000000001576. Epub 2024 Feb 23. PMID: 38386011
57. Soluble immune checkpoint factors reflect exhaustion of antitumor immunity and response to PD-1 blockade. Hayashi H, Chamoto K, Hatae R, Kurosaki T, Togashi Y, Fukuoka K, Goto M, Chiba Y, Tomida S, Ota T, Haratani K, Takahama T, Tanizaki J, Yoshida T, Iwasa T, Tanaka K, Takeda M, Hirano T, Yoshida H, Ozasa H, Sakamori Y, Sakai K, Higuchi K, Uga H, Suminaka C, Hirai T, Nishio K, Nakagawa K, Honjo T. *J Clin Invest.* 2024 Apr 1;134(7):e168318. doi: 10.1172/JCI168318. PMID: 38557498
58. Soluble programmed death ligand 1 as prognostic biomarker in non-small cell lung cancer patients receiving nivolumab, pembrolizumab or atezolizumab therapy. Brun SS, Hansen TF, Wen SWC, Nyhus CH, Bertelsen L, Jakobsen A, Hansen TS, Nederby L. *Sci Rep.* 2024 Apr 18;14(1):8993. doi: 10.1038/s41598-024-59791-0. PMID: 38637655
59. Soluble Immune Checkpoints, Gut Metabolites and Performance Status as Parameters of Response to Nivolumab Treatment in NSCLC Patients. Zizzari IG, Di Filippo A, Scirocchi F, Di Pietro FR, Rahimi H, Ugolini A, Scagnoli S, Vernocchi P, Del Chierico F, Putignani L, Rughetti A, Marchetti P, Nuti M, Botticelli A, Napoletano C. *J Pers Med.* 2020 Nov 4;10(4):208. doi: 10.3390/jpm10040208. PMID: 33158018
60. Soluble PD-L1 is a predictive and prognostic biomarker in advanced cancer patients who receive immune checkpoint blockade treatment. Oh, S.Y.; Kim, S.; Keam, B.; Kim, T.M.; Kim, D.-W.; Heo, D.S. *Sci. Rep.* 2021, 11, 19712.
61. Sex-related differences in serum biomarker levels predict the activity and efficacy of immune checkpoint inhibitors in advanced melanoma and non-small cell lung cancer patients. Pasello G, Fabricio ASC, Del Bianco P, Salizzato V, Favaretto A, Piccin L, Zustovich F, Fabozzi A, De Rossi C, Pigozzo J, De Nuzzo M, Cappelletto E, Bonanno L, Palleschi D, De Salvo GL, Guarneri V, Gion M, Chiarion-Silini V. *S J Transl Med.* 2024 Mar 5;22(1):242. doi: 10.1186/s12967-024-04920-6. PMID: 38443899
62. Pre-treatment soluble PD-L1 as a predictor of overall survival for immune checkpoint inhibitor therapy: a systematic review and meta-analysis. Széles Á, Fazekas T, Váncsa S, Váradi M, Kovács PT, Krafft U, Grünwald V, Hadaschik B, Csizmarik A, Hegyi P, Váradi A, Nyirády P, Szarvas T. *Cancer Immunol*

Immunother. 2023 May;72(5):1061-1073. doi: 10.1007/s00262-022-03328-9. Epub 2022 Nov 16. PMID: 36385210

63. Soluble PD-L1 as a Prognostic Factor for Immunotherapy Treatment in Solid Tumors: Systematic Review and Meta-Analysis. Scirocchi F, Strigari L, Di Filippo A, Napoletano C, Pace A, Rahimi H, Botticelli A, Ruggeri A, Nuti M, Zizzari IG. *Int J Mol Sci.* 2022 Nov 21;23(22):14496. doi: 10.3390/ijms232214496.
64. Soluble PD-L1 as a predictive biomarker in lung cancer: a systematic review and meta-analysis. Cheng Y, Wang C, Wang Y, Dai L. *Future Oncol.* 2022 Jan;18(2):261-273. doi: 10.2217/fon-2021-0641. Epub 2021 Dec 7. PMID: 34874185
65. Prognostic Role of Soluble Programmed Death Ligand 1 in Non-Small Cell Lung Cancer: A Systematic Review and Meta-Analysis. Liao G, Zhao Z, Qian Y, Ling X, Chen S, Li X, Kong F. *Front Oncol.* 2021 Dec 23;11:774131. doi: 10.3389/fonc.2021.774131. eCollection 2021. PMID: 35004295
66. Prognostic value of soluble programmed cell death ligand-1 in patients with non-small-cell lung cancer: a meta-analysis. Wang Y, He H.. *Immunotherapy.* 2022 Aug;14(12):945-956. doi: 10.2217/imt-2021-0238. Epub 2022 Jul 13. PMID: 35822688
67. Prognostic significance of blood-based PD-L1 analysis in patients with non-small cell lung cancer undergoing immune checkpoint inhibitor therapy: a systematic review and meta-analysis. Cui Q, Li W, Wang D, Wang S, Yu J. *World J Surg Oncol.* 2023 Oct 11;21(1):318. doi: 10.1186/s12957-023-03215-2. PMID: 37821941
68. Missing prognostic value of soluble PD-1, PD-L1 and PD-L2 in lung cancer patients undergoing chemotherapy - A CEPAC-TDM biomarker substudy. Geiger K, Joerger M, Roessler M, Hettwer K, Ritter C, Simon K, Uhlig S, Holdenrieder S. *Tumour Biol.* 2024;46(s1):S355-S367. doi: 10.3233/TUB-230015. PMID: 38277316
69. The combination of soluble forms of PD-1 and PD-L1 as a predictive marker of PD-1 blockade in patients with advanced cancers: a multicenter retrospective study. Kuroasaki T, Chamoto K, Suzuki S, Kanemura H, Mitani S, Tanaka K, Kawakami H, Kishimoto Y, Haku Y, Ito K, Sato T, Suminaka C, Yamaki M, Chiba Y, Yaguchi T, Omori K, Kobayashi T, Nakagawa K, Honjo T, Hayashi H. *Front Immunol.* 2023 Dec 11;14:1325462. doi: 10.3389/fimmu.2023.1325462. eCollection 2023. PMID: 38149256
70. Soluble PD-L1 changes in advanced non-small cell lung cancer patients treated with PD-1 inhibitors: an individual patient data meta-analysis. Shimizu T, Inoue E, Ohkuma R, Kobayashi S, Tsunoda T, Wada S. *Front Immunol.* 2023 Nov 23;14:1308381. doi: 10.3389/fimmu.2023.1308381. eCollection 2023. PMID: 38115995
71. Plasma Levels of Soluble PD-L1 Correlate With Tumor Regression in Patients With Lung and Gastric Cancer Treated With Immune Checkpoint Inhibitors. Ando K, Hamada K, Watanabe M, Ohkuma R, Shida M, Onoue R, Kubota Y, Matsui H, Ishiguro T, Hirasawa Y, Ariizumi H, Tsurutani J, Yoshimura K, Tsunoda T, Kobayashi S, Wada S. *Anticancer Res.* 2019 Sep;39(9):5195-5201. doi: 10.21873/anticanres.13716. PMID: 31519633
72. Identification of a soluble form of B7-H1 that retains immunosuppressive activity and is associated with aggressive renal cell carcinoma. Frigola X, Inman BA, Lohse CM, Krco CJ, Cheville JC, Thompson RH, Leibovich B, Blute ML, Dong H, Kwon ED. *Clin Cancer Res.* 2011 Apr 1;17(7):1915-23. doi: 10.1158/1078-0432.CCR-10-0250. Epub 2011 Feb 25. PMID: 21355078
73. Soluble B7-H1: differences in production between dendritic cells and T cells. Frigola X, Inman BA, Krco CJ, Liu X, Harrington SM, Bulur PA, Dietz AB, Dong H, Kwon ED. *Immunol Lett.* 2012 Feb 29;142(1-2):78-82. doi: 10.1016/j.imlet.2011.11.001. Epub 2011 Nov 25. PMID: 22138406

74. Identification and characterization of an alternative cancer-derived PD-L1 splice variant. Hassounah NB, Malladi VS, Huang Y, Freeman SS, Beauchamp EM, Koyama S, Souders N, Martin S, Dranoff G, Wong KK, Pedamallu CS, Hamerman PS, Akbay EA. *Cancer Immunol Immunother.* 2019 Mar;68(3):407-420. doi: 10.1007/s00262-018-2284-z. Epub 2018 Dec 18.
75. Soluble PD-L1 generated by endogenous retroelement exaptation is a receptor antagonist. Ng KW, Attig J, Young GR, Ottina E, Papamichos SI, Kotsianidis I, Kassiotis G. *eLife.* 2019 Nov 15;8:e50256. doi: 10.7554/eLife.50256. PMID: 31729316
76. Soluble PD-L1 works as a decoy in lung cancer immunotherapy via alternative polyadenylation. Sagawa R, Sakata S, Gong B, Seto Y, Takemoto A, Takagi S, Ninomiya H, Yanagitani N, Nakao M, Mun M, Uchibori K, Nishio M, Miyazaki Y, Shiraishi Y, Ogawa S, Kataoka K, Fujita N, Takeuchi K, Katayama R. *JCI Insight.* 2022 Jan 11;7(1):e153323. doi: 10.1172/jci.insight.153323. PMID: 34874919
77. Trans-Regulation of Alternative PD-L1 mRNA Processing by CDK12 in Non-Small-Cell Lung Cancer Cells. Larsen TV, Maansson CT, Daugaard TF, Andresen BS, Sorensen BS, Nielsen AL. *Cells.* 2023 Dec 15;12(24):2844. doi: 10.3390/cells12242844. PMID: 38132164

**Article #3: Role of HLA class-I antigen peptide loading complex (PLC) components in immune evasion and treatment sensitivity in human lung cancer.** Manuscrit en cours de soumission à *Clinical Cancer Research*.

**Article #4: A brief report evaluating the role of IL-8 on MHC class-I molecule expression.**

Manuscrit en cours de préparation.

Dans un premier temps, nous avons évalué les composants du complexe de chargement des peptides (CCP) dans le CBNPC. Cette analyse a été effectuée par mQIF à travers plusieurs cohortes de patients bien caractérisées et dont les échantillons étaient représentés dans des TMAs. Cette première analyse a permis de montrer que la présence de défauts d'expression des composants du CCP était une occurrence fréquente, ainsi que la régulation négative de tapasin au sein des cellules cancéreuses. Nous avons ensuite cherché à comprendre la cause de cette régulation négative de tapasin et avons d'abord montré une association négative entre le taux de mRNA d'IL-8 et de tapasin selon des données disponibles publiquement. Dans un second temps, nous avons montré par Western Blot et par mQIF qu'IL-8 a la capacité de réduire l'expression de tapasin au niveau de lignées de cellules cancéreuses de cancer bronchique. Ces travaux ont été réalisés au sein du Schalper Lab (Yale University, USA) au cours de ma deuxième et troisième année de thèse, et sont présentés dans l'Article #3.

En se basant sur ces résultats, nous avons ensuite poursuivi notre étude du rôle d'IL-8 au sein de l'EA 4340 (quatrième année de thèse), et avons cherché à évaluer son impact sur l'expression de HLA-A/B/C au niveau de la surface cellulaire. Nous avons d'abord confirmé qu'IL-8 a la capacité de diminuer l'expression d'HLA A/B/C au niveau de la surface cellulaire. Ensuite, nous avons montré qu'IL-8 inhibe en partie l'effet stimulateur d'IFNG. Enfin, nous avons montré qu'IL-8 a la capacité de réduire l'activité anti-tumorale de lymphocytes T dirigés de manière spécifique contre les cellules cancéreuses. Ces résultats préliminaires, qui sont en attente de données complémentaires, sont présentés dans l'Article #4.

**Role of the HLA class-I antigen peptide loading complex (PLC) components in immune evasion and treatment sensitivity in human lung cancer**

Adrien Costantini<sup>1</sup>, Kishu Ranjan<sup>1</sup>, Soldano Ferrone<sup>2</sup>, Kurt A. Schalper<sup>1\*</sup>

<sup>1</sup>Department of Pathology, School of Medicine, Yale University, New Haven, 06520, CT, USA

<sup>2</sup>Department of Surgery, Massachusetts General Hospital and Harvard Medical School, Boston, 02114, MA, USA

\*Correspondence to: Kurt A. Schalper; Brady Memorial Laboratory, Room BML 113, New Haven, CT, USA. Email: kurt.schalper@yale.edu, Phone: (203) 737-4205, Fax: 203-737-5089

## **Introduction**

Immune checkpoint inhibitors (ICIs) targeting the Programmed Death-1 (PD-1)/Programmed Death Ligand-1 (PD-L1) axis and Cytotoxic T-Lymphocyte Antigen-4 (CTLA-4) have transformed lung cancer care, benefiting patients across stages and histological subtypes [Ref Zhou et al]. However, the clinical efficacy of ICIs in patients with non-small cell lung cancer (NSCLC) varies considerably with only a subset of patients presenting with prolonged benefit and a majority experiencing primary or acquired resistance to ICIs [Passaro et al. JCO].

For CD8+ T-cells to effectively recognize and eliminate cancer cells, an intact Human Leukocyte Antigen (HLA) Class-I/Major Histocompatibility Complex (MHC) Class-I antigen processing and presentation machinery (APM) is necessary [[Jhunjhunwala et al.](#)]. Cell-surface expression of HLA-A, -B and -C has been shown to be downregulated in a subset of patients with NSCLC [Ref Datar et al.]. Beta-2-microglobulin ( $\beta$ 2M), an essential component of peptide trafficking to the cell surface has also been found to be downregulated in NSCLC but also across other tumor types [Ref Datar et al.]. However, the mechanisms leading to HLA-A/B/C and  $\beta$ 2M downregulation are unclear as DNA sequencing data revealed that deleterious mutations leading to  $\beta$ 2M loss of function are exceptional affecting between 1.4% and 3.4% of patients [Ref Datar et al.]. The peptide loading complex (PLC) is an intricate multi-chaperone system located within the endoplasmic reticulum (ER). It is comprised of Transporter Associated with Antigen Processing (TAP) which has two sub-units (1 and 2), Tapasin (Tpn), Calreticulin (CRT) as well as Endoplasmic Reticulum Protein 57 (ERp57). The PLC allows for optimal peptide selection and stable loading onto MHC Class-I heavy chain/ $\beta$ 2M complexes [Ref Thomas et al.]. Tpn is an ER-resident protein chaperone that plays an essential role in MHC class-I antigen presentation. Tpn allows for optimal peptide selection and loading onto MHC Class-I heavy chain/ $\beta$ 2M complexes and MHC stabilization by binding with TAP and ERp57. It has been shown that several cancer types such as maxillary sinus squamous cell carcinoma [Ogino et al.], laryngeal squamous cell carcinoma [Ogino et al.], renal cell carcinoma [Seliger et al.], high grade intraepithelial neoplasia and colorectal carcinoma [Atkins et al.], oral squamous cell carcinoma [Koike et al.] as well as melanoma [Dissemont et al.] present with alterations to Tpn levels and that lower Tpn levels correlate with shorter survival. In lung cancer, it has been shown that up to 72.9% of cases (n=85) present with heterogeneous lack of Tpn expression [Ref Shionoya et al.].

CRT is an ER-resident protein chaperone and  $\text{Ca}^{2+}$ -buffer that helps with correct protein folding, adhesion and integrin signaling. It also plays a role in immunogenic cell death (ICD) by promoting the uptake of cells to whose surface it has migrated [Ref Fucikova et al.]. Furthermore, in cohorts of patients treated with radiation therapy, surgery and chemotherapy or chemotherapy alone, higher CRT correlated with improved overall survival (OS) and advanced stage [Ref Liu et al. Fucikova et al Cancer Res, Garg et al.]

ERp57, also known as PDIA3, is part of the Protein Disulfide Isomerase (PDI) family that are cellular oxidoreductase enzymes. ERp57 is an ER resident but can also be found in several sub-cellular or even extra-cellular locations. ERp57 plays a role in optimal protein folding by facilitating disulfide bond isomerization and forms a disulfide bridge with Tpn allowing the stabilization of the PLC. Other roles of ERp57 include redox activation of protein kinase RNA-like ER kinase (PERK) in response to protein unfolding, participating in the signal transduction processes of STAT3 pathways (nucleus localization), ICD in complex with CRT (cell surface localization) as well as matrix degradation by tumor cells [Ref Ros et al, Chichiarelli et al].

These observations raise several questions and challenges. First, if deleterious mutations to APM components are uncommon, what are the epigenetic or post-translational alterations commanding these alterations? Second, effectively predicting response and efficacy of ICIs remains a challenge and the discovery of novel predictive biomarkers is an unmet need. Third, and most challengingly, there is a need to develop novel targetable immunological pathways and the APM appears as an excellent target as its potential has not been exploited therapeutically.

To address these queries, we performed multiplexed quantitative immunofluorescence (mQIF) to simultaneously, spatially and quantitatively analyze the components of the PLC Tpn, CRT and ERp57 in baseline biopsy samples of human NSCLC from patients who received chemotherapy or ICIs. This allowed us to uncover cancer-cell specific Tpn downregulation as a frequent event leading to decreased CD8+ T-cell infiltration, immune evasion, and resistance to ICIs. We further uncovered an unknown interleukin-8 (IL-8) driven mechanism leading to epigenetic downregulation of Tpn in human NSCLC.

## **Results**

### **Cancer-cell selective downregulation of Tpn in human NSCLC**

We established an mQIF panel for simultaneous detection of the markers 40 ,6-diamidino-2-phenylindole (DAPI) for all cells, cytokeratin (CK) for tumor epithelial cells, and members of the PLC Tpn, CRT and ERp57 to analyze formalin-fixed paraffin embedded (FFPE) tumor specimens.

Using this assay, we analyzed baseline/pre-treatment tumor samples from five independent retrospective cohorts of patients treated for NSCLC all of which were represented in tissue microarrays (TMAs). Cohorts #1-3 were comprised of patients treated with chemotherapy, patients in Cohort #4 had received ICIs and Cohort #5 was comprised of patients presenting with EGFR and KRAS mutations or wild-type tumors for KRAS and EGFR. Table 1. summarizes the baseline patient characteristics from Cohorts #1-4. It is relevant to underline that Cohorts #1 and #2 present with similar baseline characteristics: mostly female smokers with early-stage adenocarcinoma. Cohort #3 is comprised essentially of male smokers presenting with early-stage squamous cell carcinoma and Cohort #4 has an equal amount of male and female smokers presenting with advanced stage adenocarcinoma all of whom received ICIs during treatment.

Figure 1A. shows the staining pattern obtained, with the proteins of interest having a peri-nuclear cytoplasmic staining pattern. Both CK-negative stromal cells and CK-positive cancer cells had this similar staining pattern. In Figure 1A. we show two extreme phenotypes that could be observed after staining: unaltered expression of the PLC components with equal expression within the tumor and the stroma (left) and cancer cell-specific downregulation of all the components of the PLC (right). We observed all other combinations with a large proportion of patients presenting with cancer cell specific Tpn downregulation alone or in association with other members of the PLC in 57-65% of cases (Figure 2B.). More specifically, Tpn cancer-cell specific downregulation alone was observed in 28-36% of cases, Tpn-CRT associated cancer-cell specific downregulation in 20-29% of cases and CRT cancer-cell specific downregulation alone in 9-13% of cases. Cancer cell specific downregulation of ERp57 alone or in association with other components was a rare occurrence and only 19-32% of patients presented with unaltered expression of all PLC components. The specific proportion of each phenotype is detailed in Supplementary Figure XX.

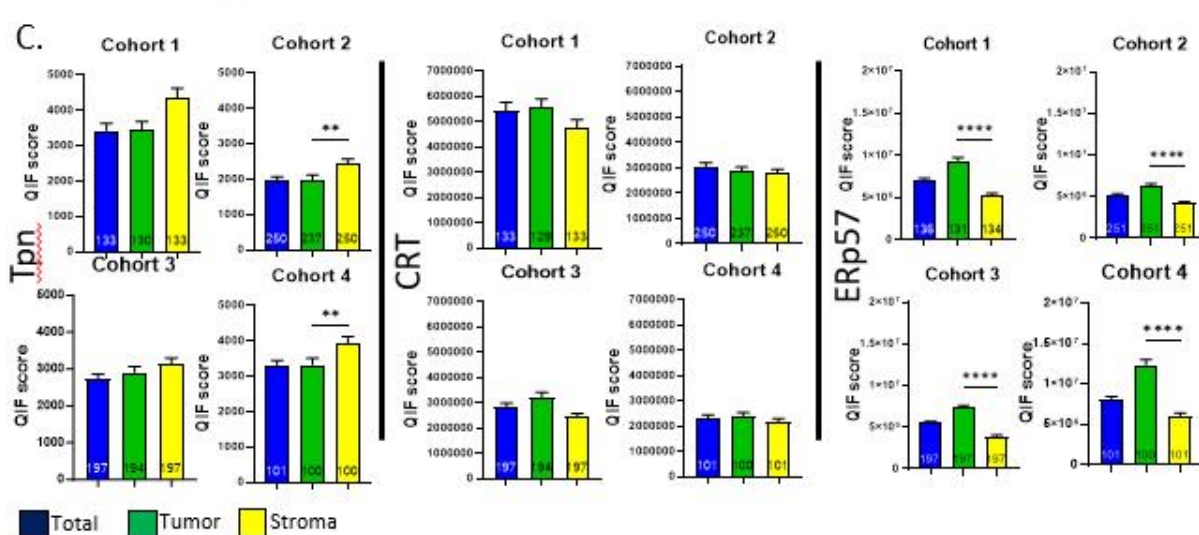
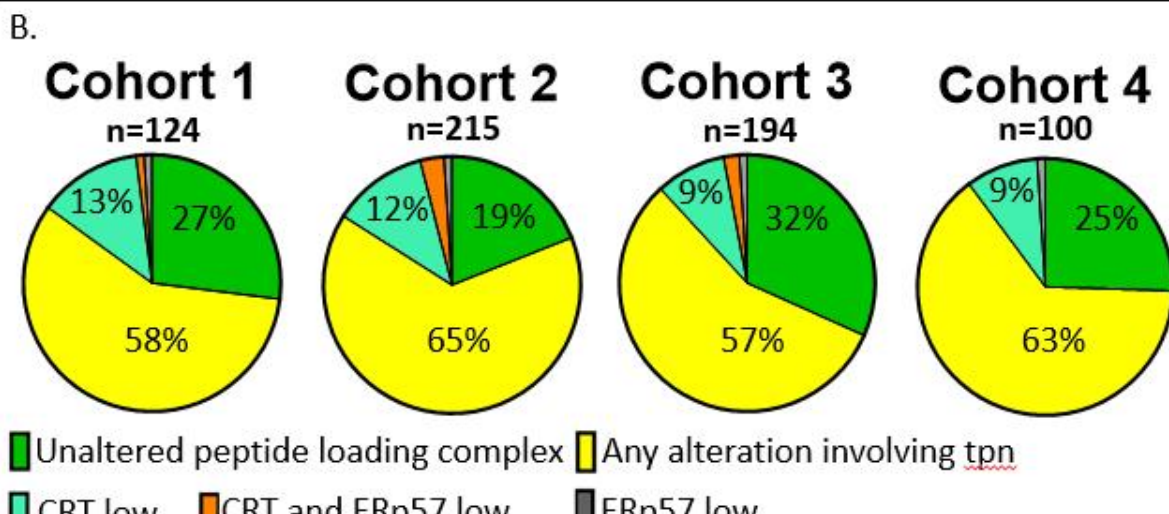
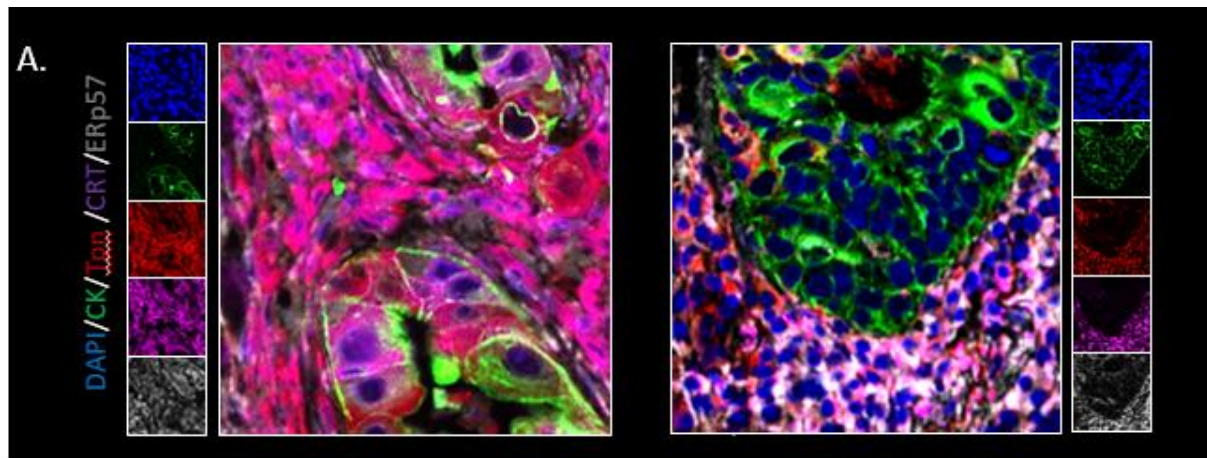
Next, we evaluated the QIF score of each protein within the total, tumor and stromal compartments across the cohorts. Consistent with our previous findings, we found that Tpn levels were numerically higher in the stroma compared to the tumor compartment across all cohorts and significantly so in Cohorts #2 and #4. CRT levels were consistently numerically higher in the tumor compartment across all cohorts, but the difference was not significant. ERp57 was consistently and significantly higher in the tumor compartment than in the stromal compartment across all cohorts.

We hypothesized that PLC component levels would decrease with advancing disease stage as more advanced tumors would have an increased probability of presenting with APM deficiencies due to increased mutational load. As shown in **Supplementary Figure XX**. We found that Tpn levels in the total tissue area were significantly higher in stage IV tumors compared to stage I, II and III. Results were similar when analysis was performed in tumor compartment and in the stromal compartment. CRT levels were not influenced by stage and ERp57 was also significantly higher in stage IV compared to stages I, II or III in the total compartment with similar results when analyzing only tumor or stromal compartments.

These results show that cancer-cell specific Tpn downregulation alone or in association with other members of the PLC is a frequent occurrence in baseline samples of human NSCLC. Second, a wide variety of phenotypes exist with one or several PLC members having the potential for being downregulated specifically in cancer-cells. Finally, the analysis by compartment confirms these findings showing higher stromal Tpn QIF scores across all cohorts. ERp57 also presents a pattern of consistently higher scores in the tumor compartment.

**Figure 1. Cancer-cell selective downregulation of Tpn in human NSCLC**

A. mQIF image showing the simultaneous detection of DAPI (blue), CK (green), Tpn (red), CRT (magenta) and ERp57 (gray) in NSCLC tissues. The left panel shows unaltered expression of the PLC components with equal staining in the tumor (CK+) and stromal (CK-) compartments. The right panel shows cancer-cell specific downregulation of all the components of the PLC. B. Pie charts showing the proportion of patients presenting with each specific observed phenotype across 4 NSCLC cohorts. Cohorts #1-3 were comprised of patients not treated with ICIs and patients in Cohort #4 had received ICIs.C. Bar graphs showing the mean + SEM mQIF score for Tpn, CRT and ERp57 in each cohort and in each compartment. Total score (mQIF of marker of interest in all nucleated cell) in blue, tumor compartment (mQIF score of marker of interest in CK+ cells) in green and stromal compartment (mQIF score of marker of interest in CK- cells) in yellow.



### Cancer-cell specific Tpn downregulation is associated with lower tumor infiltrating lymphocytes (TILs) and worse outcome

We aimed to evaluate the consequence of cancer-cell specific Tpn downregulation on CD8+ TILs levels. As shown in Figure 2A. patients presenting with high (left) Tpn levels present with a higher CD8+ T-cell infiltration than patients presenting with low (right) Tpn levels.

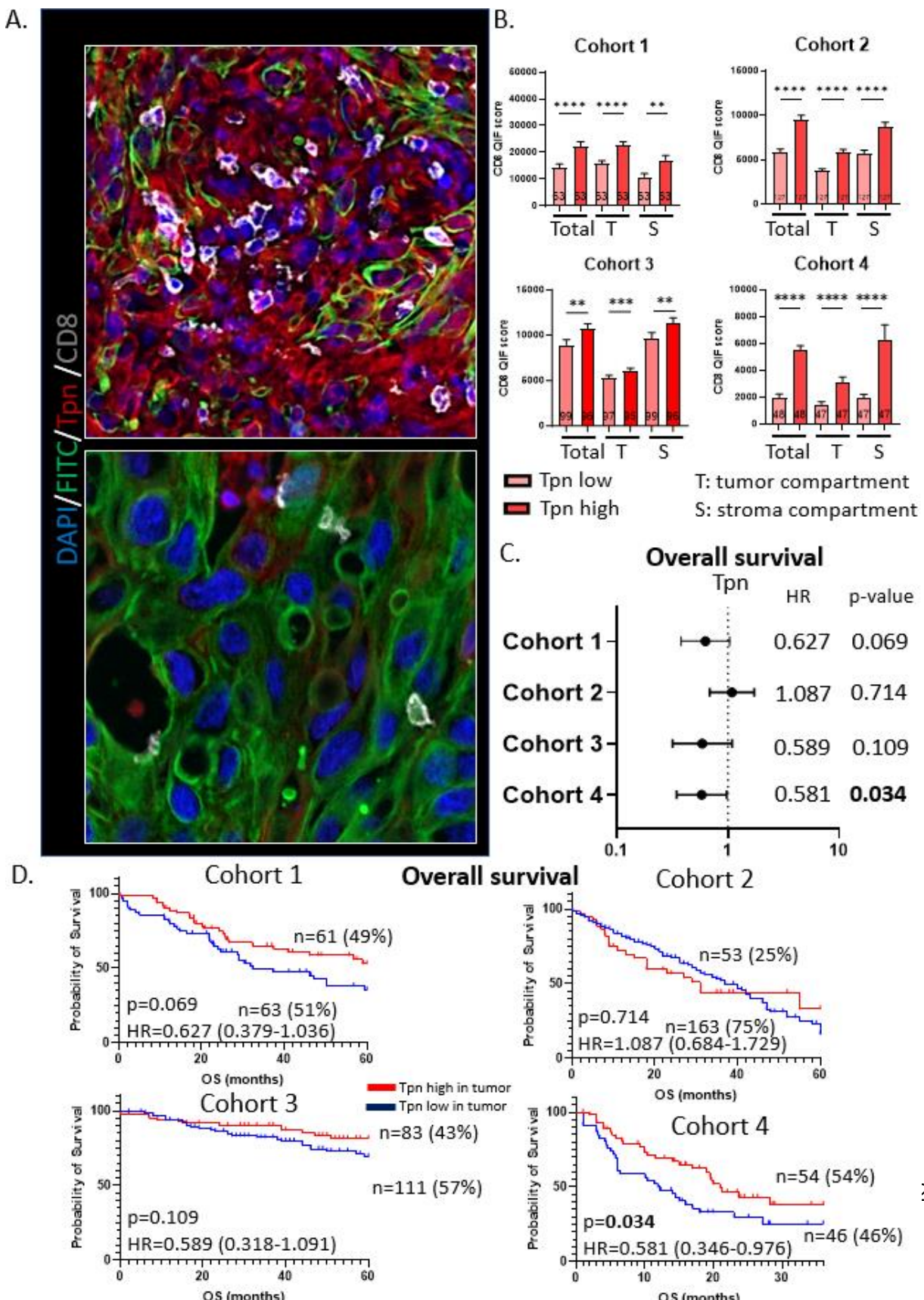
Patients were then stratified as Tpn high/low based on the median Tpn mQIF score in each cohort. As shown in Figure 2B. CD8 QIF scores were significantly and consistently higher across all compartments and all cohorts in the Tpn high group, showing a strong and consistent link between Tpn and CD8+ infiltration.

Survival analysis showed that patients presenting with lower baseline Tpn levels presented with shorter overall survival (OS). Figure 2C. summarizes the hazard ratios (HR) and p-values with regards to Tpn levels and OS. Lower Tpn levels were detrimental in Cohorts #1, #3 and #4 but not in cohort #2. Figure 2D. shows the Kaplan Meier survival curves with regards to OS depending on low or high Tpn levels in the tumor compartment. Tpn cut-off was determined using the optimal cut-off method and the same cut-off was then applied to all cohorts allowing for a homogeneous and consistent analysis.

In Cohort #4, survival was significantly longer in patients presenting with higher Tpn levels than in patients with lower Tpn levels: median OS 21.00 months vs 12.08 months, respectively, HR 0.581, 95% CI [0.346-0.976], p=0.034. The trend was similar in Cohort #1 with median OS of not reached (NR) vs 32.35 months, HR 0.626, 95% CI [0.379-1.036], p=0.069 and Cohort #3 with median OS of NR vs NR, HR 0.589, 95% CI [0.318-1.091], p=0.109. In Cohort #2, Tpn did not seem to correlate with survival. We performed the same analysis for CRT and ERp57 (**Supplementary Figure XX.**) and did not find any significant correlation with survival. Of note, higher CRT levels seemed to be beneficial in the chemotherapy treated cohorts (Cohorts #1 and #2) whereas lower CRT levels seemed to be beneficial in the ICI treated cohort (Cohort #4). There was no clear association between ERp57 and OS.

**Figure 2. Cancer-cell specific Tpn downregulation is associated with lower tumor infiltrating lymphocytes (TILs) and worse outcome**

A. mQIF image showing the simultaneous detection of DAPI (blue), CK (green), Tpn (red), CD8 (gray) in NSCLC tissues. The top panel shows high Tpn levels and high CD8 infiltration. The bottom panel low Tpn levels and low CD8 infiltration. B. Bar graphs showing the mean + SEM mQIF score for CD8 depending on Tpn levels across the cohorts and compartments. C. Forest plot summarizing the HR and p-values for OS depending on Tpn levels in each cohort. The dotted line indicates the limit of 1 for HR. HR lower than one are in favor of higher Tpn levels whereas HR higher than 1 or in favor of lower Tpn levels. The circle indicates the HR and the whiskers the 95% CI for each cohort. D. Kaplan-Meier survival curves showing OS depending on Tpn levels.



### Cancer-cell specific Tpn downregulation is epigenetically modulated by IL-8

We aimed to assess the mechanisms leading to cancer-cell specific Tpn downregulation and accessed the publicly available datasets at cbiportal.org. We included the following cohorts in our analysis: Lung adenocarcinoma (Tumor Cancer Genome Atlas (TCGA), Firehose Legacy, n=582) Lung Squamous Cell carcinoma (TCGA, Firehose Legacy, n=481). We observed that mutations (missense, splice, truncating, deep deletion) to the *TAPBP*, *CalR* or *PDIA3* genes were an extremely rare occurrence observed in less than 2% of cases throughout these two cohorts and suggesting epigenetic or post-translational modifications could result in decreased protein levels and especially of Tpn (Figure 3A.). To explore these hypotheses, we accessed the bulk RNA sequencing data openly available at cbiportal.org for the two previous cohorts (Lung adenocarcinoma and lung squamous cell carcinoma, TCGA, Firehose Legacy) and plotted Tpn, CRT and ERp57 mRNA expression depending on cytokine levels with the hypothesis of a cytokine mediated effect on these proteins. The cut-off used to determine high and low cytokine levels was the median. Figure 3B. shows the association between *TAPBP* mRNA and *IFNG* mRNA and *TAPBP* mRNA and *CXCL8* mRNA. Interferon-gamma (IFN- $\gamma$ ) mediated Tpn upregulation is a known and demonstrated mechanism and this was confirmed on the RNA sequencing data serving as a positive control. Out of all the evaluated cytokines, *CXCL8* mRNA was the only one to show a significantly negative correlation with *TAPBP* mRNA levels. The other cytokines (Supplementary Figure XX.) showed either no (*IL4*, *IL6*) or positive correlations (*IL10*, *IL17A*).

To functionally assess this observation obtained from bulk RNA sequencing, we performed immunoblotting to evaluate Tpn levels after IL-8 treatment in human A549, PC9 and H1703 cancer cell lines. Cells were treated with 20ng/mL of IL-8 for 6, 12, 24, 48 hours or left untreated for 48 hours. As illustrated and quantified in Figure 3C. IL-8 caused early and significant decrease in Tpn levels in A549 and H1703 human lung cancer cell lines with a peak effect observed between 6 and 12 hours of IL-8 treatment. Effect of IL-8 on Tpn on PC9 is reported in Supplementary Figure XX.

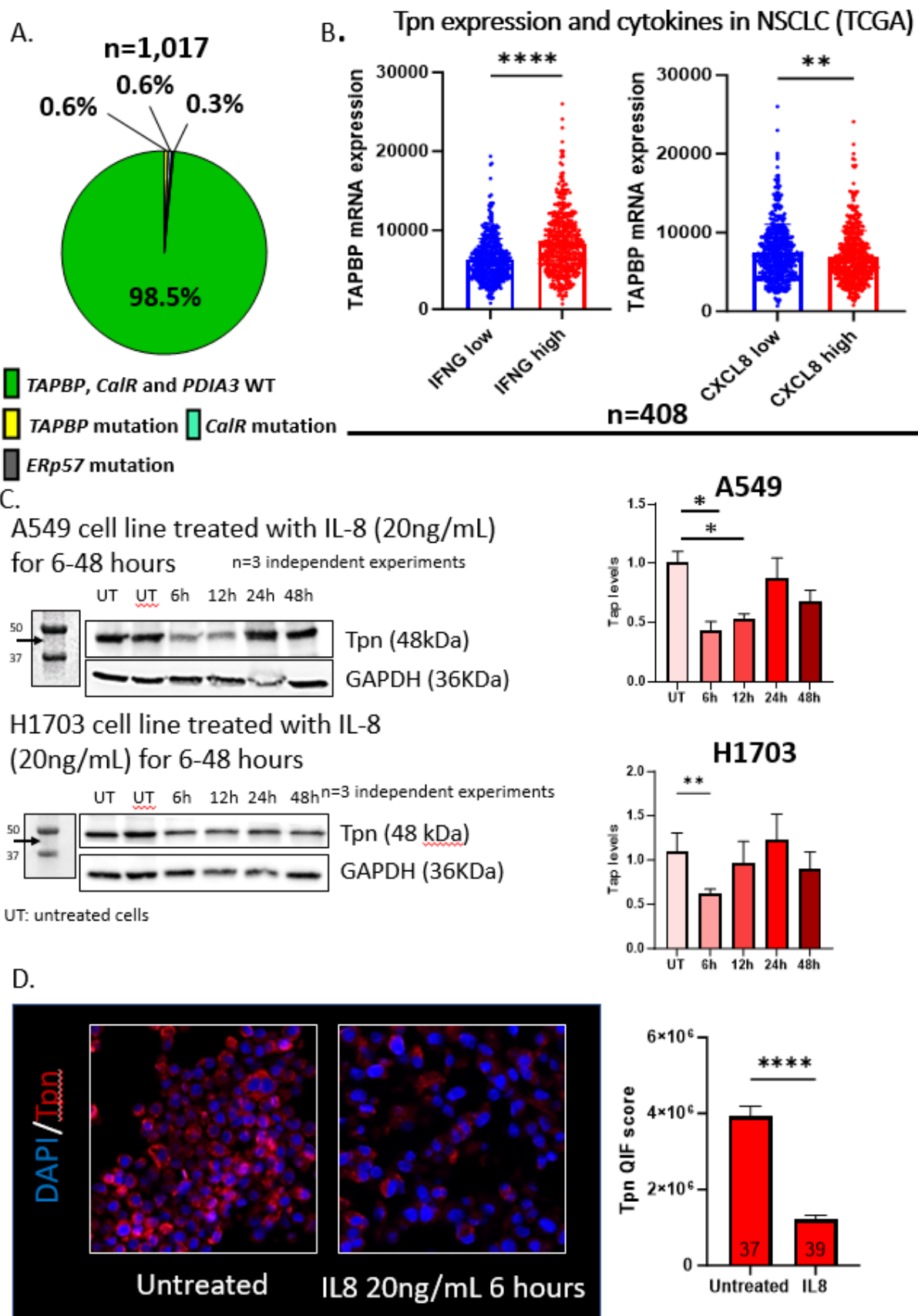
To further evaluate this phenomenon, we performed mQIF for Tpn on A549 cells treated with IL-8 20ng/mL for 6 hours or left untreated. We confirmed that IL-8 treatment caused a significant decrease in Tpn protein levels compared to untreated cells (Figure 3C.)

These results show that mutations to *TAPBP* are uncommon and do not account for the prominent Tpn cancer-cell specific downregulation observed in NSCLC cohorts. Tpn

downregulation might be post-translational or epigenetic. We then showed through two independent methods (immunoblotting and mQIF) that IL-8 has a prominent and negative effect on Tpn protein levels in human NSCLC cell lines. This effect is most prominent between 6 and 12 hours after IL-8 treatment.

**Figure 3.** Cancer-cell specific Tpn downregulation is epigenetically mediated by IL-8

A. Pie charts showing the proportion of patients presenting with no (green) or deleterious mutation to *TAPBP* (yellow), *CalR* (cyan) or *ERP57* (purple). B. Graphs obtained from bulk RNA sequencing from two cohorts of human NSCLC (Lung adenocarcinoma and lung squamous cell carcinoma, TCGA, Firehose Legacy), cbioportal.org, showing *TAPBP* mRNA expression depending on *IFNG* mRNA and *CXCL8* mRNA expression. C. Representative immunoblotting image and quantification of Tpn protein in human A549 (top) and H1703 (bottom) cell lines left untreated or treated with 20ng/mL of IL-8 for up to 48 hours. D. Representative mQIF images (left) of A549 cells left untreated or treated with IL-8 20ng/mL for 6 hours. Bar graphs (right) show mean + SEM Tpn QIF score in untreated and treated cells.



### IL-8 impacts cell-surface HLA expression

To further evaluate the impact of IL-8 on the antigen presenting machinery, we exposed cancer cell lines to IL-8 and evaluated the cell surface expression of HLA-A/B/C by flow cytometry.

First, we performed a time course to evaluate the optimal impact of IL-8 on HLA-A/B/C cell-surface expression. We found that the effect of 20ng/mL of IL-8 was strongest after 48 hours of exposure as compared to untreated cells. The level of HLA-A/B/C in untreated cells was considered as the baseline expression of HLA-A/B/C. The results are shown in Figure XX.

HLA-A/B/C cell surface expression is known to be increased after exposure to IFNG. Next, we aimed to evaluate whether IL-8 had the capacity to inhibit IFNG mediated signalling. A549 and H596 cells were left untreated, treated with IFNG alone for 48 hours, or treated with IL-8 followed by IFNG for 48 hours. We found that IL-8 has the ability to inhibit IFNG-mediated HLA-A/B/C cell surface expression.

## **Discussion**

Using spatially resolved mQIF analysis of human NSCLC samples represented in independent cohorts as well as in vitro functional studies we identified cancer-cell selective Tpn downregulation as a dominant mechanism of adaptive immune evasion and immunotherapy resistance in NSCLC. Our results show that cancer-cell specific Tpn downregulation results in lower CD8+ T-cell infiltration in affected tumors as well as shorter survival specifically in patients treated with ICIs suggesting a predictive biomarker potential for Tpn. Our study also reveals a yet unknown regulatory pathway in which IL-8 epigenetically modulates the *TAPBP* gene resulting in reduced Tpn protein levels. These results are significant and have potential implications for the development of biomarkers as well as for developing novel therapeutic strategies such as direct IL-8 blockade using monoclonal antibodies or pharmacological inhibition of the IL-8 receptors CXCR-1 and CXCR-2. This approach could be combined with PD-L1/PD-1 axis blockers to further improve treatment efficacy.

Our approach to map out the PLC using mQIF is, to our knowledge, the first to be reported. Our technique allows for highly detailed spatially resolved analysis of the cancer cells and their micro-environment. The objective quantification of scores allows for robust and consistent analysis across samples.

The evaluation of Tpn levels by IHC has been performed in several cancer types including NSCLC showing that patients can present between 72.9% (n=85) [Ref Lou et al.] and up to 89.5% (n=19) [Ref Shionoya et al.] of low Tpn levels in tumor samples. These studies did not use mQIF and Tpn levels were scored by eye by evaluating the percentage of positive cells. This approach can be error prone due to difficulties linked with tumor/stroma differentiation and identification, subjective evaluation by a pathologist and cell counting. Patients were then classified as follows: score 2 (> 75% positive cells), score 1 (25–75% positive cells), and score 0 (< 25% positive cells), with score 0 and 1 usually combined to produce the Tpn low group thus loosing the resolution a continuous score could bring. Furthermore, the number of patients in these studies was relatively small and the study by Lou et al. grouped different histological subtypes (NSCLC, SCLC) rendering the interpretation difficult. Using mQIF, we found that baseline cancer-cell specific Tpn downregulation affected between 57% and 65% of patients in four independent cohorts. Taken together, these results seem consistent and underline the fact that alterations to Tpn within cancer cells are frequent.

Tpn levels were associated with CD8+ T-cell infiltration and survival and we confirmed this by showing consistently higher CD8+ levels throughout the compartments in case of higher Tpn levels. We also found longer OS in 3 out 4 cohorts in case of higher Tpn levels, but interestingly the most prominent effect seemed to be in the ICI treated cohort offering a potential role to Tpn as a predictive biomarker to ICI response.

In the updated 5-year outcomes in the Keynote-189 study [Ref. Garassino et al.], evaluating the association of platinum-pemetrexed doublet chemotherapy associated with pembrolizumab, the five-year OS rate in the study arm was 19.4% (11.3% in the control arm) and the five-year PFS rate was 7.5% vs 0.6% in the intervention and control arms respectively. These results underline the fact that although the addition of anti-PD-1 therapy does improve outcome, primary and acquired resistance to ICIs affects a vast majority of patients. Interestingly, we found that patients had unaltered expression of PLC components within cancer cells in 19-32% of cases, remarkably close in some cohorts to the five-year OS rate of the Keynote-189 study.

Tpn plays a role as an ER-retaining signal for empty MHC-class I proteins. In absence of Tpn, empty MHC-class I peptides are trafficked to the cell surface but are unstable and rapidly degraded. These previous findings are in line with our results that show that cases presenting with cancer-cell specific Tpn downregulation have lower CD8+ T-cell infiltration and shorter survival due to impaired cell-surface antigen presentation. Further complexifying our understanding, it has been shown that some HLA class-I peptides such as HLA-B2705 have the ability of stably loading peptides and trafficking to the cell surface in the absence of Tpn, whereas others do not. It is also relevant to note that peptide selection could occur as only more abundant and/or more stable peptides would be presented in the case of Tpn absence. These results further support the fact that although Tpn is not always indispensable for appropriate peptide loading, it plays a key role in this process and restoring it is a major challenge of modern precision immuno-oncology. [Ref. Peh et al.].

CRT is a  $\text{Ca}^{2+}$ -binding ER resident chaperon protein that is involved in several cell processes. Other than assisting in peptide loading along with Tpn and ERp57, CRT participates in  $\text{Ca}^{2+}$ -dependent processes, such as adhesion and integrin signalling. During immunogenic cell death (ICD), a type of cell death that results in an antigen specific immune response, CRT is exposed to the cell-surface of cancer cells and facilitates the uptake of the dying cells or their corpses by antigen presenting cells (APCs) leading to more effective anti-cancer antigen-specific

adaptive immunity. CRT's multiple and complex roles are underlined by the sometimes-conflicting results found across several studies. In NSCLC, it seems that higher CRT correlate with longer OS as well as a higher density of mature DCs but not for CD8+ T-cells, B-cells or macrophage. This was in fact the trend we observed in our chemotherapy treated cohorts. Interestingly, although the result was not statistically significant, the role of CRT seemed to be different in the ICI treated cohort. These results remain preliminary and would need to be further validated in an independent cohort of ICI treated patients.

To our knowledge, no study of ERp57 by IHC has been performed in lung or other histologies. ERp57 has several roles apart from its role in peptide folding in the PLC. The most interesting of these seems to be extra-cellular matrix-degradation [Ref. Ros et al.], in line with our observation that cancer cells all highly express ERp57 suggesting that extra-cellular matrix-degradation, allowing cells to metastasize, is functionally more important than the role played in peptide folding. Once again, more studies are necessary to explore this in depth.

The mechanism leading to cancer-cell specific Tpn downregulation is unknown. Using publicly available datasets accessed at cbiportal.org, we confirmed that mutations to the *TAPBP* gene are extremely uncommon, hinting that Tpn modulation is regulated by epigenetic or post-translational mechanisms. We observed a negative correlation between *IL-8* and *TAPBP* mRNA levels that led us to further investigate the possibility of a novel cytokine-mediated epigenetic regulation of Tpn by IL-8 in cancer cells. We show, using two independent methods (immunoblotting and mQIF) that IL-8 can downregulate Tpn protein levels in human NSCLC cell lines with a prominent affect appearing between 6 and 12 hours after IL-8 treatment.

Although our proposed model is original, fast-acting cytokine modification of protein levels is a known phenomenon. IFNG has the potential of increasing *TAPBP* mRNA and Tpn protein levels in mouse primary embryonic fibroblasts in as little as 3 hours [Ref Abarca-Heifeman et al. Seliger et al.]. It has also been shown that cytokines such as IL-4 have the possibility of increasing *TAPBP* mRNA expression after 24 hours of treatment [Ref Seliger et al.].

To further evaluate the impact of IL-8 on the antigen processing machinery, we exposed cancer cell lines to IL-8 and evaluated the cell-surface expression of HLA-A/B/C using flow cytometry. First, we found that IL-8 negatively affects HLA-A/B/C cell surface expression with an optimal effect after 48 hours. Furthermore, we found that IL-8 has the ability to inhibit IFNG-mediated HLA-A/B/C upregulation.

IL-8, a member of the CXC chemokine family was originally identified as a chemotactic factor

for neutrophils [Ref Walz et al.]. IL-8 has a pro-tumoral role through the action of angiogenesis, inflammation and tumor-cell migration and invasion thus promoting metastases. It has been shown [Ref Schalper et al. Sanmamed et al.] that serum IL-8 levels are inversely correlated with response to ICIs and that cancer cells can produce IL-8. In a mouse model of glioma [Ref Liu et al.], IL-8 blockade using monoclonal antibodies (mAbs) or a pharmacological inhibitor of CXCR1/CXCR2 increased the efficacy of immune checkpoint blockade. Furthermore, several cells seem to produce IL-8 such as CD4+ T-cells, myeloid as well as tumor cells. Clinical trials are ongoing using IL-8 blockade [Ref Rossi et al.]. An anti-IL-8 mAb has been tested in a Phase I study [Ref Bilusic et al.] in unselected patients affected by solid tumors. Fifteen patients with metastatic heavily pre-treated tumors were enrolled. The treatment was considered as safe and 73% of patients had stable disease with median treatment duration of 24 weeks. Treatment also seemed effective as it caused IL-8 serum levels to decrease at day 3. Trials are still ongoing but our findings seem to effectively explain the potential anti-cancer activity of this IL-8 mAb.

Several other trials are ongoing testing IL-8 blockade in different settings across different tumor types such as myelodysplastic syndrome, hormone sensitive prostate cancer, NSCLC, HCC, colon cancer, adenocarcinoma of the pancreas [NCT05148234, NCT03689699, NCT04123379, NCT04572451, NCT03400332, NCT03026140, NCT02451982]. Published data shows that IL-8 blockade led to stable disease in 73% of heavily pre-treated, unselected patients across different tumor types, with no dose-limiting toxicities and in general positive safety signals.

We hypothesize that optimal efficacy of IL-8 blockade would be observed in patients presenting with high serum IL-8 levels as well as low cancer-cell levels of Tpn protein. Combining double IL-8 and PD-1/PD-L1 axis blockade in this population could lead to enhanced and prolonged anti-tumor response.

Our study is not without limitations. Although we analysed a large number of patient samples, this was performed using TMAs exposing us to tumor heterogeneity with the risk of certain markers being over or under-represented in the analyzed samples. We did address this question by performing an independent staining experiment on another block from the same cohort and showing correlation between the marker scores suggesting our results are reproducible in different biopsy samples. Furthermore, our in vitro studies were performed using cell lines and we do not have in vivo work to support our findings. However, murine

work involving IL-8 is complex as mice do not express IL-8. Finally, we acknowledge that we have not functionally shown that Tpn levels affect antigen presentation, although this has been shown previously, nor that differing Tpn levels impact CD8+ T-cell mediated cancer cell killing. These experiments are currently ongoing. Finally, although we have shown that IL-8 impacts Tpn and HLA-A/B/C cell-surface expression, we can only speculate as to the direct link between these two observations. We plan to perform further studies with direct Tpn inhibition using shRNA to create Tpn KD cell lines. These cell lines will then be used in order to evaluate HLA-A/B/C expression and perform co-culture experiments with tumor killing experiments.

To conclude, we have shown that cancer-cell specific Tpn downregulation occurs frequently in NSCLC, it affects CD8+ T-cell infiltration and impacts survival. Mutations to the *TAPBP* gene are rare and an epigenetic IL-8 driven autocrine signaling pathway leads to early-onset Tpn downregulation that could be effectively inhibited using IL-8 mAbs or CXCR1/2 blockade in combination with ICIs. Further studies are ongoing to better understand this novel potential therapeutic target.

## **Materials and methods**

### **Patients and samples**

Formalin-fixed paraffin-embedded (FFPE) tumor tissue samples from retrospective collections of human NSCLCs represented in tissue microarrays (TMA) were analyzed. TMAs were constructed including 2–4 individual 0.6 mm (diameter) cores from each tumor sample.

Five Cohorts were analyzed in this study, Cohort #1 included 191 patients (225 samples) with primary NSCLC treated at Yale New Haven Hospital (New Haven, CT) between 1988 and 2003. Cohort #2 included 373 patients (374 samples) with primary NSCLC from Greece collected between 1990 to 2007. Cohort #3 included 220 patients (287 samples) with primary NSCLC treated at Yale New Haven Hospital (New Haven, CT) between 2011 and 2016. Cohort #4 included 191 patients (195 samples) with primary NSCLC treated at Yale New Haven Hospital (New Haven, CT), between 2014 and 2019. Cohort #5 included 129 patients (139 samples) with primary lung adenocarcinoma from Yale New Haven Hospital (New Haven, CT) clinically tested for activating mutations in EGFR and KRAS.

Patients in Cohorts #1-3 had not received immune checkpoint inhibitors (ICIs) whilst patients in Cohort #4 had received ICIs. Cohort #4 initially included baseline but also biopsies performed during treatment. In order for our analysis to be homogeneous throughout the cohorts, only baseline biopsy samples obtained before any type of treatment was initiated were considered.

The actual number of samples analyzed for each cohort/study was lower, due to unavoidable loss of tissue or lack of malignant cells in some spots as is commonly seen in TMA studies. Clinicopathologic information was available for all cohorts including but not restricted to age at diagnosis, gender, stage, histology, smoking status, and survival. The baseline features are summarized in Table 1.

This study was carried out in accordance with the principles of the Declaration of Helsinki and all tissue and clinical information were used in a deidentified fashion after approval from the Yale Internal Review Board (Yale Human Investigation Committee) protocols #9505008219 and #1608018220 or local institutional protocols, which approved the patient consent forms or waiver of consent.

### Cell lines

The cell lines used included A549, PC-9 and NCI-H1703 (H1703). A549 is a lung adenocarcinoma cell line presenting with KRAS G12S mutation. PC-9 is a lung adenocarcinoma cell line presenting with a p.Glu746\_Ala750 deletion in exon 19 of the EGFR gene. H1703 is a lung squamous cell carcinoma cell line. Cells were cultured in DMEM (A549) or RPMI (PC-9, H1703) culture medium supplemented with 10% fetal bovine serum (FBS) and penicillin-streptomycin antibiotic cocktails. Cells were incubated in a humidified incubator supplied with 5% CO<sub>2</sub>.

### Multiplexed quantitative immunofluorescence

A multiplexed quantitative immunofluorescence (mQIF) panel was standardized for simultaneous and spatially resolved measurement of Tpn, CRT, ERp57, 40 ,6-diamidino-2-phenylindole (DAPI) and CK.

Multiplexed QIF was performed as reported previously [Ref. Porciuncula et al.]. TMA sections were deparaffinized, rehydrated, and processed for antigen retrieval with 1 mmol/L EDTA, pH 8.0 (Sigma-Aldrich) in a pressure-boiling module (PT module, Lab Vision) at 97°C for 20 minutes. Slides were then incubated with dual endogenous enzyme block buffer (Dako, No. S2003) at room temperature for 10 minutes and subsequently in blocking solution containing 0.3% BSA and 0.05% Tween 20 at room temperature for 30 minutes.

Primary antibodies included: anti-Tapasin Rabbit IgG mAb, clone E6P2Z (Cell Signaling Technology), concentration: 2.1ng/mL incubated at 4°C overnight; anti-Calreticulin Mouse IgG1 mAb, clone FMC75, (Abcam), concentration 100ng/mL, incubated at 4°C overnight ; anti-ERp57 Rabbit IgG mAb, clone EPR10678(B), (Abcam), concentration 146ng/mL, incubated at room temperature for 1 hour. Tumor epithelial cells were stained for cytokeratin (CK) by incubating all slides with anti-pan-cytokeratin mouse IgG1 mAb, clone AE1/AE3 (eBioscience, Invitrogen), concentration 5ng/mL, incubated at room temperature for 1 hour. Nuclei were stained with 40 ,6-diamidino-2- phenylindole (DAPI) incubated at room temperature for 10 minutes.

Secondary antibodies were incubated at room temperature for 1 hour: anti-rabbit Envision (Dako), anti-mouse Envision (Dako), goat anti-rabbit IgG conjugated with horseradish peroxidase, (Abcam), concentration 100ng/mL, incubated at room temperature for 1 hour. Fluorophore-conjugated reagents were added sequentially after each primary-secondary

antibody pair: Cy3-tyramide (Akoya Biosciences), Cy5-tyramide (Akoya Biosciences), and biotinylated tyramide (Akoya Biosciences) followed by streptavidin conjugated with Alexa Fluor 750 (Thermo Fisher Scientific).

Residual HRP activity was quenched between incubations with secondary antibodies/fluorophores by treating the slides twice at room temperature for 7 minutes with a solution of DPBS containing 0.136mg of benzoic hydrazide and 50 µL of hydrogen peroxide. Washes were performed for 30 seconds at room temperature after each reagent application with TBS followed by TBST (TBS with 0.1% Tween 20).

An index TMA used for initial antibody validation and containing positive and negative controls for each marker of interest was included during each experiment in order to control for inter-experimental variations.

#### QIF analysis and scoring

The TMA slides were scanned using an automated Vectra Polaris microscope (Akoya Biosciences) using pre-defined and fixed exposure times for each fluorophore.

Quantitative measurement and analysis of the fluorescence signal was performed using the AQUA method (Navigate Biopharma) that enables objective and sensitive measurement of targets within user-defined compartments [Ref. Porciuncula et al.]. Compartments were defined on the basis of CK positivity (tumor cells), CK negativity (stromal cells), and DAPI positivity (total, all nucleated cells). QIF scores were calculated by dividing the signal intensity of markers in a given compartment by the area of the compartment. Scores were normalized by exposure time and bit depth. A cancer-cell/stromal cell ratio of the markers <1 was considered as cancer cell-selective marker downregulation. The specific marker staining patterns and cancer cell-specific loss was confirmed by visual inspection by trained personnel.

#### Immunoblotting

Protein from flash frozen cells was extracted using RIPA buffer (50mM Tris [pH 8], 150mM NaCl, 5mM MgCl, 1% Triton X-100, 0.5% sodium deoxycholate, 0.1% SDS) supplemented with a protease and phosphatase inhibitor cocktail (Thermo Scientific #78440).

Protein quantification was performed and 20µg of protein was loaded into each well (A549 and PC-9 cell lines) and 5 µg of protein was loaded for H1703 cell line. Protein extract was subjected to SDS-PAGE and transferred onto PVDF membranes (Bio-Rad). Membranes were

blocked for one hour in 5% BSA in TBS-T followed by incubation with the following antibodies: recombinant anti-tapasin rabbit mAb, clone [EPR25083-20] (Abcam), concentration 0.501ng/mL, incubation overnight at 4°C, goat anti-rabbit IgG (HRP conjugated) (CST), incubation 1 hour at room temperature, anti-GAPDH mouse mAb, clone 6C5 (EMD Millipore), concentration 0.53ng/mL, incubation 1 hour at room temperature, goat anti-mouse IgG (HRP conjugated), incubation 1 hour at room temperature. Chemiluminescent Signal detection was performed on the ChemiDoc XRS+ system (BioRad) using SignalFire Plus ECL reagent (CST) for Tapasin revelation and SignalFire ECL reagent (CST) for GAPDH revelation.

#### Statistical analysis

QIF score comparisons were performed using Mann–Whitney test for two groups. Relationships between continuous scores were analyzed by Spearman correlation. Survival functions were compared using Kaplan–Meier estimates and statistical significance was determined using the log-rank test. Associations between the markers and statistical significance were determined using JMP Pro. v11 and GraphPad Prism v7.0a software. Significance was assessed using two-tailed Student's t-test. Differences were considered to be statistically significant when  $P < 0.05$ .

## Tables

Table 1. Patient characteristics across Cohorts #1-4

<b>Cohort #1 (n=191)</b>		<b>Cohort #2 (n=373)</b>	
<b>Gender</b>		<b>Gender</b>	
Female	101 (53%)	Female	43 (12%)
Male	88 (46%)	Male	308 (83%)
Missing	2 (1%)	Missing	22 (6%)
<b>Age at diagnosis (median)</b>	65	<b>Age at diagnosis (median)</b>	64
<b>Histology</b>		<b>Histology</b>	
Adenocarcinoma	112 (59%)	Adenocarcinoma	138 (37%)
Squamous cell carcinoma	28 (15%)	Squamous cell carcinoma	167 (45%)
Large cell carcinoma	18 (9%)	Large cell carcinoma	3 (1%)
Adenosquamous carcinoma	15 (8%)	Adenosquamous carcinoma	4 (1%)
Other*	3 (2%)	Other*	38 (10%)
Missing	15 (8%)	Missing	23 (6%)
<b>Smoking status</b>		<b>Smoking status</b>	
Smoker	169 (88%)	Smoker	281 (75%)
Non-smoker	14 (7%)	Non-smoker	29 (8%)
Missing	8 (4%)	Missing	63 (17%)
<b>Stage at diagnosis</b>		<b>Stage at diagnosis</b>	
I	95 (50%)	I	109 (29%)
II	25 (13%)	II	93 (25%)
III	35 (18%)	III	101 (27%)
IV	15 (8%)	IV	42 (11%)
Missing	21 (11%)	Missing	28 (8%)

**Cohort #3 (n=220)**

<b>Gender</b>	
Female	135 (61%)
Male	85 (39%)
Missing	0 (0%)
<b>Age at diagnosis (median)</b>	68
<b>Histology</b>	
Adenocarcinoma	153 (70%)
Squamous cell carcinoma	56 (25%)
Large cell carcinoma	5 (2%)
Adenosquamous carcinoma	1 (<1%)
Other	2 (1%)
Missing	3 (1%)
<b>Smoking status</b>	
Smoker	190 (86%)
Non-smoker	30 (14%)
Missing	0 (0%)
<b>Stage at diagnosis</b>	
I	151 (69%)
II	50 (23%)
III	16 (7%)
IV	1 (<1%)
Missing	2 (<1%)

**Cohort #4 (n=191)**

<b>Gender</b>	
Female	80 (42%)
Male	86 (45%)
Missing	25 (13%)
<b>Age at diagnosis (median)</b>	67.5
<b>Histology</b>	
Adenocarcinoma	112 (59%)
Squamous cell carcinoma	36(19%)
Large cell carcinoma	4 (2%)
Adenosquamous carcinoma	3 (2%)
Other	11 (6%)
Missing	25 (13%)
<b>Smoking status</b>	
Smoker	146 (76%)
Non-smoker	19 (10%)
Missing	26 (14%)
<b>Stage at diagnosis</b>	
I	1 (<1%)
II	6 (3%)
III	14 (7%)
IV	145 (76%)
Missing	25(13%)

\* Carcinosarcoma, Non-small cell carcinoma not otherwise specified, carinoid, sarcomatoid, Non-small cell lung cancer, neuroendocrine carcinoma, LCNEC and SCC, small cell carcinoma, giant cell carcinoma

## **References**

- Zhou F, Qiao M, Zhou C. The cutting-edge progress of immune-checkpoint blockade in lung cancer. *Cell Mol Immunol.* 2021 Feb;18(2):279-293. doi: 10.1038/s41423-020-00577-5. Epub 2020 Nov 11. PMID: 33177696
- Passaro A, Brahmer J, Antonia S, Mok T, Peters S. Managing Resistance to Immune Checkpoint Inhibitors in Lung Cancer: Treatment and Novel Strategies. *J Clin Oncol.* 2022 Feb 20;40(6):598-610. doi: 10.1200/JCO.21.01845. Epub 2022 Jan 5. PMID: 34985992
- Jhunjhunwala S, Hammer C, Delamarre L. Antigen presentation in cancer: insights into tumour immunogenicity and immune evasion. *Nat Rev Cancer.* 2021 May;21(5):298-312. doi: 10.1038/s41568-021-00339-z. Epub 2021 Mar 9. PMID: 33750922
- Datar IJ, Hauc SC, Desai S, Gianino N, Henick B, Liu Y, Syrigos K, Rimm DL, Kavathas P, Ferrone S, Schalper KA. Spatial Analysis and Clinical Significance of HLA Class-I and Class-II Subunit Expression in Non-Small Cell Lung Cancer. *Clin Cancer Res.* 2021 May 15;27(10):2837-2847. doi: 10.1158/1078-0432.CCR-20-3655. Epub 2021 Feb 18. PMID: 33602682
- Thomas C, Tampé R. MHC I assembly and peptide editing - chaperones, clients, and molecular plasticity in immunity. *Curr Opin Immunol.* 2021 Jun;70:48-56. doi: 10.1016/j.coim.2021.02.004. Epub 2021 Mar 6. PMID: 33689959
- Ogino T, Bandoh N, Hayashi T, Miyokawa N, Harabuchi Y, Ferrone S. Association of tapasin and HLA class I antigen down-regulation in primary maxillary sinus squamous cell carcinoma lesions with reduced survival of patients. *Clin Cancer Res.* 2003 Sep 15;9(11):4043-51. PMID: 14519625
- Ogino T, Shigyo H, Ishii H, Katayama A, Miyokawa N, Harabuchi Y, Ferrone S. HLA class I antigen down-regulation in primary laryngeal squamous cell carcinoma lesions as a poor prognostic marker. *Cancer Res.* 2006 Sep 15;66(18):9281-9. doi: 10.1158/0008-5472.CAN-06-0488. PMID: 16982773
- Seliger B, Atkins D, Bock M, Ritz U, Ferrone S, Huber C, Störkel S. Characterization of human lymphocyte antigen class I antigen-processing machinery defects in renal cell carcinoma lesions with special emphasis on transporter-associated with antigen-processing down-regulation. *Clin Cancer Res.* 2003 May;9(5):1721-7. PMID: 12738726
- Atkins D, Breuckmann A, Schmahl GE, Binner P, Ferrone S, Krummenauer F, Störkel S, Seliger B. MHC class I antigen processing pathway defects, ras mutations and disease stage in colorectal carcinoma. *Int J Cancer.* 2004 Mar 20;109(2):265-73. doi: 10.1002/ijc.11681. PMID: 14750179
- Koike K, Dehari H, Shimizu S, Nishiyama K, Sonoda T, Ogi K, Kobayashi J, Sasaki T, Sasaya T, Tsuchihashi K, Tsukahara T, Hasegawa T, Torigoe T, Hiratsuka H, Miyazaki A. Prognostic value of HLA class I expression in patients with oral squamous cell carcinoma. *Cancer Sci.* 2020 May;111(5):1491-1499. doi: 10.1111/cas.14388. Epub 2020 Apr 15. PMID: 32167621
- Dissemond J, Kothen T, Mörs J, Weimann TK, Lindeke A, Goos M, Wagner SN. Downregulation of tapasin expression in progressive human malignant melanoma. *Arch Dermatol Res.* 2003 Jun;295(2):43-9. doi: 10.1007/s00403-003-0393-8. Epub 2003 Mar 28. PMID: 12682852
- Shionoya Y, Kanaseki T, Miyamoto S, Tokita S, Hongo A, Kikuchi Y, Kochin V, Watanabe K, Horibe R, Saijo H, Tsukahara T, Hirohashi Y, Takahashi H, Sato N, Torigoe T. Loss of tapasin in human lung and colon cancer cells and escape from tumor-associated antigen-specific CTL recognition. *Oncoimmunology.* 2017 Jan 3;6(2):e1274476. doi: 10.1080/2162402X.2016.1274476. eCollection 2017. PMID: 28344889
- Fucikova J, Spisek R, Kroemer G, Galluzzi L. Calreticulin and cancer. *Cell Res.* 2021 Jan;31(1):5-16. doi: 10.1038/s41422-020-0383-9. Epub 2020 Jul 30. PMID: 32733014

Liu R, Gong J, Chen J, Li Q, Song C, Zhang J, Li Y, Liu Z, Dong Y, Chen L, Jin B. Calreticulin as a potential diagnostic biomarker for lung cancer. *Cancer Immunol Immunother.* 2012 Jun;61(6):855-64. doi: 10.1007/s00262-011-1146-8. Epub 2011 Nov 15. PMID: 22083347

Fucikova J, Becht E, Iribarren K, Goc J, Remark R, Damotte D, Alifano M, Devi P, Biton J, Germain C, Lupo A, Fridman WH, Dieu-Nosjean MC, Kroemer G, Sautès-Fridman C, Cremer I. Calreticulin Expression in Human Non-Small Cell Lung Cancers Correlates with Increased Accumulation of Antitumor Immune Cells and Favorable Prognosis. *Cancer Res.* 2016 Apr 1;76(7):1746-56. doi: 10.1158/0008-5472.CAN-15-1142. Epub 2016 Feb 3. PMID: 26842877

Garg AD, Elsen S, Krysko DV, Vandenabeele P, de Witte P, Agostinis P. Resistance to anticancer vaccination effect is controlled by a cancer cell-autonomous phenotype that disrupts immunogenic phagocytic removal. *Oncotarget.* 2015 Sep 29;6(29):26841-60. doi: 10.18632/oncotarget.4754. PMID: 26314964

Ros M, Nguyen AT, Chia J, Le Tran S, Le Guezennec X, McDowall R, Vakhrushev S, Clausen H, Humphries MJ, Saltel F, Bard FA. ER-resident oxidoreductases are glycosylated and trafficked to the cell surface to promote matrix degradation by tumour cells. *Nat Cell Biol.* 2020 Nov;22(11):1371-1381. doi: 10.1038/s41556-020-00590-w. Epub 2020 Oct 19. PMID: 33077910

Chichiarelli S, Altieri F, Paglia G, Rubini E, Minacori M, Eufemi M. ERp57/PDIA3: new insight. *Cell Mol Biol Lett.* 2022 Feb 2;27(1):12. doi: 10.1186/s11658-022-00315-x. PMID: 35109791

Garassino MC, Gadgeel S, Speranza G, Felip E, Esteban E, Dómíne M, Hochmair MJ, Powell SF, Bischoff HG, Peled N, Grossi F, Jennens RR, Reck M, Hui R, Garon EB, Kurata T, Gray JE, Schwarzenberger P, Jensen E, Pietanza MC, Rodríguez-Abreu D. Pembrolizumab Plus Pemetrexed and Platinum in Nonsquamous Non-Small-Cell Lung Cancer: 5-Year Outcomes From the Phase 3 KEYNOTE-189 Study. *J Clin Oncol.* 2023 Apr 10;41(11):1992-1998. doi: 10.1200/JCO.22.01989. Epub 2023 Feb 21. PMID: 36809080

Peh CA, Burrows SR, Barnden M, Khanna R, Cresswell P, Moss DJ, McCluskey J. HLA-B27-restricted antigen presentation in the absence of tapasin reveals polymorphism in mechanisms of HLA class I peptide loading. *Immunity.* 1998 May;8(5):531-42. doi: 10.1016/s1074-7613(00)80558-0. PMID: 9620674

Abarca-Heidemann K, Friederichs S, Klamp T, Boehm U, Guethlein LA, Ortmann B. Regulation of the expression of mouse TAP-associated glycoprotein (tapasin) by cytokines. *Immunol Lett.* 2002 Oct 1;83(3):197-207. doi: 10.1016/s0165-2478(02)00104-9. PMID: 12095710

Seliger B, Schreiber K, Delp K, Meissner M, Hammers S, Reichert T, Pawlischko K, Tampé R, Huber C. Downregulation of the constitutive tapasin expression in human tumor cells of distinct origin and its transcriptional upregulation by cytokines. *Tissue Antigens.* 2001 Jan;57(1):39-45. doi: 10.1034/j.1399-0039.2001.057001039.x. PMID: 11169257

Walz A, Peveri P, Aschauer H, Baggolini M. Purification and amino acid sequencing of NAF, a novel neutrophil-activating factor produced by monocytes. *Biochem Biophys Res Commun.* 1987 Dec 16;149(2):755-61. doi: 10.1016/0006-291X(87)90432-3. PMID: 3322281

Schalper KA, Carleton M, Zhou M, Chen T, Feng Y, Huang SP, Walsh AM, Baxi V, Pandya D, Baradet T, Locke D, Wu Q, Reilly TP, Phillips P, Nagineni V, Gianino N, Gu J, Zhao H, Jose Luis Perez-Gracia JL, Sanmamed MF, Melero I. Elevated serum interleukin-8 is associated with enhanced intratumor neutrophils and reduced clinical benefit of immune-checkpoint inhibitors. *Nat Med.* 2020 May;26(5):688-692. doi: 10.1038/s41591-020-0856-x. Epub 2020 May 11. PMID: 32405062

Sanmamed MF, Perez-Gracia JL, Schalper KA, Fusco JP, Gonzalez A, Rodriguez-Ruiz ME, Oñate C, Perez G, Alfaro C, Martín-Algarra S, Andueza MP, Gurpide A, Morgado M, Wang J, Bacchiocchi A, Halaban R, Kluger H, Chen L, Sznol M, Melero I.. Changes in serum interleukin-8 (IL-8) levels reflect and predict response to anti-PD-1 treatment in melanoma and non-small-cell lung cancer patients. *Ann Oncol.* 2017 Aug 1;28(8):1988-1995. doi: 10.1093/annonc/mdx190. PMID: 28595336

Liu H, Zhao Q, Tan L, Wu X, Huang R, Zuo Y, Chen L, Yang J, Zhang ZX, Ruan W, Wu J, He F, Fang Y, Mao F, Zhang P, Zhang X, Yin P, Yan Z, Xu W, Lu H, Li Q, Liang M, Jia Y, Chen C, Xu S, Shi Y, Ping YF, Duan GJ, Yao XH, Han Z, Pang T, Cui Y, Zhang X, Zhu B, Qi C, Wang Y, Lv SQ, Bian XW, Liu X. Neutralizing IL-8 potentiates immune checkpoint blockade efficacy for glioma. *Cancer Cell*. 2023 Apr 10;41(4):693-710.e8. doi: 10.1016/j.ccr.2023.03.004. Epub 2023 Mar 23. PMID: 36963400

Rossi AJ, Khan TM, Saif A, Marron TU, Hernandez JM. Treatment of Hepatocellular Carcinoma with Neoadjuvant Nivolumab Alone Versus in Combination with a CCR2/5 Inhibitor or an Anti-IL-8 Antibody. *Ann Surg Oncol*. 2022 Jan;29(1):30-32. doi: 10.1245/s10434-021-10269-7. Epub 2021 Jun 11. PMID: 34117573. DOI: 10.1245/s10434-021-10269-7

Bilusic M, Heery CR, Collins JM, Donahue RN, Palena C, Madan RA, Karzai F, Marté JL, Strauss J, Gatti-Mays ME, Schlom J, Gulley JL. Phase I trial of HuMax-IL8 (BMS-986253), an anti-IL-8 monoclonal antibody, in patients with metastatic or unresectable solid tumors. *J Immunother Cancer*. 2019 Sep 5;7(1):240. doi: 10.1186/s40425-019-0706-x. PMID: 31488216

Porciuncula A, Morgado M, Gupta R, Syrigos K, R, Zacharek SJ, Frederick JP, Schalper KA. Spatial Mapping and Immunomodulatory Role of the OX40/OX40L Pathway in Human Non-Small Cell Lung Cancer. *Clin Cancer Res*. 2021 Nov 15;27(22):6174-6183. doi: 10.1158/1078-0432.CCR-21-0987. Epub 2021 Sep 13. PMID: 34518312

**A brief report evaluating the role of IL-8 on MHC class-I molecule expression.**

Adrien Costantini<sup>a, b</sup>, Paul Takam Kamga<sup>b</sup>, Jean-François Emile<sup>b, d</sup>, Etienne Giroux-Leprieur<sup>a, b</sup>

<sup>a</sup>APHP-Ambroise Paré Hospital, Department of Respiratory Diseases and Thoracic Oncology, Boulogne-Billancourt, France.

<sup>b</sup>Université Paris-Saclay, UVSQ, EA 4340 BECCOH, Boulogne-Billancourt, France

<sup>d</sup>APHP-Ambroise Paré Hospital, Department of Pathology, Boulogne-Billancourt, France

Corresponding author: Etienne Giroux-Leprieur, APHP-Ambroise Paré Hospital, Department of Respiratory Diseases and Thoracic Oncology, 9 avenue Charles de Gaulle 92 100, Boulogne-Billancourt, France

e-mail address : etienne.giroux-leprieur@aphp.fr

## **Introduction**

Lung cancer is the leading cause of cancer-related death in the world. Despite recent therapeutical advances, the prognosis remains bleak with a majority of patients at the advanced stage experiencing either primary or acquired resistance [Passaro et al.]. Cancer cells have developed numerous strategies to resist immune checkpoint inhibitors [Schoefeld et al.] (ICIs) such as

- alterations within the interferon-gamma (IFNG) signalizing pathway
- neo-antigen depletion
- PTEN loss
- activation of the Wingless-integration site (WNT)- $\beta$ -catenin pathway
- activation of other checkpoint inhibitors
- defects in antigen processing and presentation within the major histocompatibility complex (MHC) class-I antigen processing and presentation machinery (APM)

In order to mount an effective anti-tumoral immune response, an intact APM is essential [Garrido et al. Jhunjhunwala et al.]. The peptide loading complex (PLC) is a multi-chaperone structure comprise of tapasin, calreticulin, ERp57, TAP1/2, MHC class-I heavy chain and beta-2-microglobuline ( $\beta$ 2M) [Blees et al.]. The PLC plays a central role in optimal peptide loading onto MHC- class-I heavy chain/ $\beta$ 2M peptides and has roles in editing and stable loading. In lung cancer, several studies have evaluated the impact of HLA-A/B/C cell surface loss as well as the impact of alterations to calreticulin, TAP1, tapasin or  $\beta$ 2M, showing that the loss of one or more of these components is frequent and impacts outcome [Ref. Lou, Korkolopoulou, Hanagiri, Ramnath, Passlick, Shionoya, Datar, Kikuchi].

Recently, we have shown using mQIF that patients affected with lung cancer frequently lose the expression of PLC components such as tapasin [Ref. Costantini et al.] or TAP2 [Ref. Ranjan et al.]. We also found evidence of original cytokine-mediated signalling that could lead to cancer-cell specific downregulation of PLC members. Specifically, we found that IL-8 has a negative effect on tapasin with a prominent effect observed after 6 hours. Interestingly, elevated serum levels of IL-8 have shown to be deleterious in lung cancer patients treated with ICIs [Ref. Sanmamed et al. Schalper et al.].

Here, we aimed to further evaluate the role of IL-8 in cancer-cell immune evasion by analysing the impact IL-8 has on cell-surface expression of HLA-A/B/C and subsequently evaluate the

effect on specific cancer-cell killing by HLA-matched T cells.

## **Materials and methods**

### Cell lines

Human NSCLC lines (A549 and H596) were purchased from the American Type Culture Collection (ATCC). A549 is a human lung adenocarcinoma cell line presenting with a KRAS G12S, TP53 and STK11 mutations. H596 is a human lung adenosquamous carcinoma cell-line presenting with PIK3CA, RB1 and TP53 mutations. Cells were maintained in complete DMEM/F12 medium (DMEM/F12 supplemented with 10% foetal bovine serum (FBS), 1% L-Glutamine (l-Glu) and 1% Penicillin/Streptomycin (P/S)). Cells were incubated in a humidified incubator supplied with 5% CO<sub>2</sub>. Exponentially grown cells were used in this study. Cells were also periodically tested for mycoplasma contamination. Cells were chosen based on HLA-A/B/C cell surface expression according to publicly available RNA data (Human protein Atlas). A549 cells present with relatively low HLA-A/B/C levels, whereas H596 present with higher HLA-A/B/C levels.

### Evaluation of HLA-A/B/C cell-surface expression

To evaluate the impact of IL-8 and determine its potential maximum efficacy, cells were cultured in a 6-well plate and exposed to IL-8 (20ng/mL) for incremental different durations: 6 hours, 12 hours, 24 hours, 48 hours. Post-incubation, cells were collected and stained with HLA-A/B/C and cytokeratin and analyzed by flow cytometry.

Next, cells were left untreated, stimulated with IFNG alone or with IL-8 followed by IFNG. In all cases, the total incubation time was 48 hours. Post-incubation, cells were collected and

stained with cytokeratine and HLA-A/B/C and analyzed by flow cytometry. In all cases, subsequent analysis following Flow cytometry was performed using FlowJo software (TreeStar).

#### In vitro tumor killing assay

Cells were either treated with IFNG or left untreated and were then exposed to anti-HER2/neu T cells (Cellero, Cat# ASTC-1126; specifically recognize 369-377 amino acid region of the HER2 protein) alone or in association with IL-8. Annexin V staining assay was carried out using FITC Annexin V Apoptosis Detection Kit (Biolegend, Cat# 640922) as per manufacturer instruction and analyzed by flow cytometer (). Subsequent analysis was performed by using FlowJo software (TreeStar).

#### Statistical analysis

Statistical analyses were conducted using GraphPad Prism version 5 software (La Jolla, CA, USA). Statistical comparisons were conducted using one-way Anova and Student's t-test. Differences were considered significant for p-values < 0.05.

## Results

#### Cell surface HLA-A/B/C expression is sensitive to IL-8

A549 cells were exposed to IL-8 for 6, 12, 24 and 48 hours or left untreated for 48 hours. Cell-surface HLA-A/B/C expression was evaluated by flow cytometry in order to determine:

- whether IL-8 has an impact on cell-surface HLA-A/B/C expression.
- at what time-point the effect of IL-8 on cell-surface HLA-A/B/C expression is the most important.

Compared to untreated cells that we considered as having baseline HLA-A/B/C cell-surface expression, we found that IL-8 (20ng/ml) started to cause HLA-A/B/C cell-surface expression decrease after 12 hours of exposure, with a maximal effect observed at 48 hours and, reaching statistical significance at this time-point ( $p=0.0010$ ) (Figure 1. A).

### IL-8 inhibits IFNG mediated HLA-A/B/C cell surface upregulation

After showing that IL-8 can reduce cell-surface HLA-A/B/C expression, we aimed to evaluate whether IL-8 had the capacity to inhibit IFNG-mediated stimulation and to what extent. We observed that cells treated with IFNG alone for 48 hours had a steep increase in HLA-A/B/C cell-surface expression and that IL-8 had the capacity to partially inhibit this upregulation. Cells exposed to IL-8 followed by IFNG had reduced HLA-A/B/C cell-surface expression. Statistical analysis showed statistical significance using the one-way Anova test ( $p=0.0003$ ). A t-test was then used on the most visually significant difference in order to limit the use of statistical tests. We found that HLA-A/B/C cell-surface expression was significantly lower in the IL-8-IFNG treated A549 cells compared to the IFNG treated cells ( $p=0.0055$ ). The trend was strong and similar in the H596 cell line with a positive Anova ( $p=0.0170$ ) and a t-test trending towards significance ( $p=0.0815$ ) but the analysis probably lacked power (Figure 1.B).

### IL-8 reduces CD8+ mediated cancer-cell killing

Finally, we set-up a co-culture model wherein cancer-cell lines were exposed to HLA-matched T-cells to simulate cancer-cell specific T-cell mediated apoptosis. Cancer cells were exposed to T-cells with and without prior IFNG stimulation, and to IL-8 and T-cells with or without prior IFNG stimulation. We observed that exposure to T-cells increased cancer-cell apoptosis evaluated by Annexin V staining. When IL-8 was introduced to the co-culture model, we found that apoptosis decreased. One-way Anova was significant for both A549 and H596 cells. We then proceeded with performing t-tests to compare our conditions with and without IL-8 and found that IL-8 significantly reduced Annexin V expression and thus apoptosis of cancer-cells in both A549 ( $p=0.0462$ ) and H596 ( $p=0.0406$ ) cells (Figure 1.C).

## **Discussion**

In this brief report, we have shown the IL-8 has the ability to modulate HLA-A/B/C cell-surface expression. First, we observed that IL-8 can negatively regulate HLA-A/B/C cell-surface expression with effects observed after 12 hours and maximal effect observed at 48 hours. The difference compared to untreated cells reached statistical significance at this time-point. This effect was observed on A549 cells. Several points can be discussed. First, according to RNA

data, A549 present with relative low levels of cell-surface HLA-A/B/C, thus, finding an effect of IL-8 suggests that the effect is strong and could be more significant in cells presenting with high baseline levels of cell-surface HLA-A/B/C. Second, in order for IL-8 to have an effect, the target cells would need to possess the IL-8 receptors CXCR1 and CXCR2. Although we did not evaluate this specifically, published data has already reported that this cell-line does present with the adequate receptors [Ref. Khan et al. Zhu et al.].

We have previously shown that IL-8 has a negative effect on tapasin as early as after 6 hours of exposure. Thus, we hypothesize that the negative effect of IL-8 on HLA-A/B/C cell-surface expression is the result of cancer-cell specific tapasin downregulation. Although we have not specifically shown this correlation in this report, we plan to further evaluate this role by creating stable tapasin KD cell lines using small hairpin (sh) RNAs. Using this cell line, we will be able to evaluate cell-surface HLA-A/B/C expression and immune-cell evasion.

Next, we evaluated the capacity of IL-8 to inhibit IFNG-mediated HLA-A/B/C cell-surface upregulation. IFNG is a pleiotropic cytokine that plays a role in various domains such as promoting antiviral activity, facilitating macrophage activation, controlling Th1/Th2 balance, and regulating cellular apoptosis and proliferation [Ng et al.]. IFNG is primarily produced by cells of the immune system such as natural killer (NK) cells and innate lymphoid cells (ILCs), and adaptive immune cells, such as T helper 1 ( $T_{H}1$ ) cells and CD8 $^{+}$  cytotoxic T lymphocytes (CTLs). In the context of cancer, IFNG can have anti-tumour as well as pro-tumour effects: cytotoxic effect of IFNG on tumour cells, but also the promotion of inhibitory molecules such as programmed cell ligand 1 (PDL1), PDL2, indoleamine 2,3-dioxygenase 1 (IDO1), inducible nitric oxide synthase (iNOS), FAS and FAS ligand (FASL), all of which limit antitumour immunity [Gocher et al.]. Of note, it has been shown that IFNG can induce HLA class-I expression [Yano et al.] as well as tapasin (mouse) in a time-dependant manner [Abarca-Heidemann et al.]. First, our results confirm that IFNG has the capacity to induce HLA-A/B/C cell-surface expression in A549 and H596 cells. Second, we found that IL-8 has the ability to inhibit IFNG-mediated HLA-A/B/C cell-surface expression. Finally, we aimed to evaluate the functional impact the decrease of the cell-surface expression of HLA-A/B/C could have on the effect on cancer-cell specific T-cell mediated apoptosis. We found that both A549 and H596 cells exposed to T-cells presented with increased apoptosis as compared to unexposed cells. When IL-8 was added to the media, both A49 and H596 cells presented with decreased apoptosis rates as compared to non-IL-8 treated cells. These observations suggest that cancer cells have the ability to evade

T-cell killing through IL-8 signalling. Furthermore, it is probable that this evasion results from tapasin downregulation, leading to decreased cell-surface HLA-A/B/C expression.

Taken together, these results bring more evidence on the role played by IL-8 in cancer-cell immune-evasion. We hypothesize that cancer-cells have the ability to secrete IL-8, causing autocrine and paracrine signalling pathways, induced tapasin downregulation, leading to decreased HLA-A/B/C cell-surface expression and immune escape.

### **Conclusion**

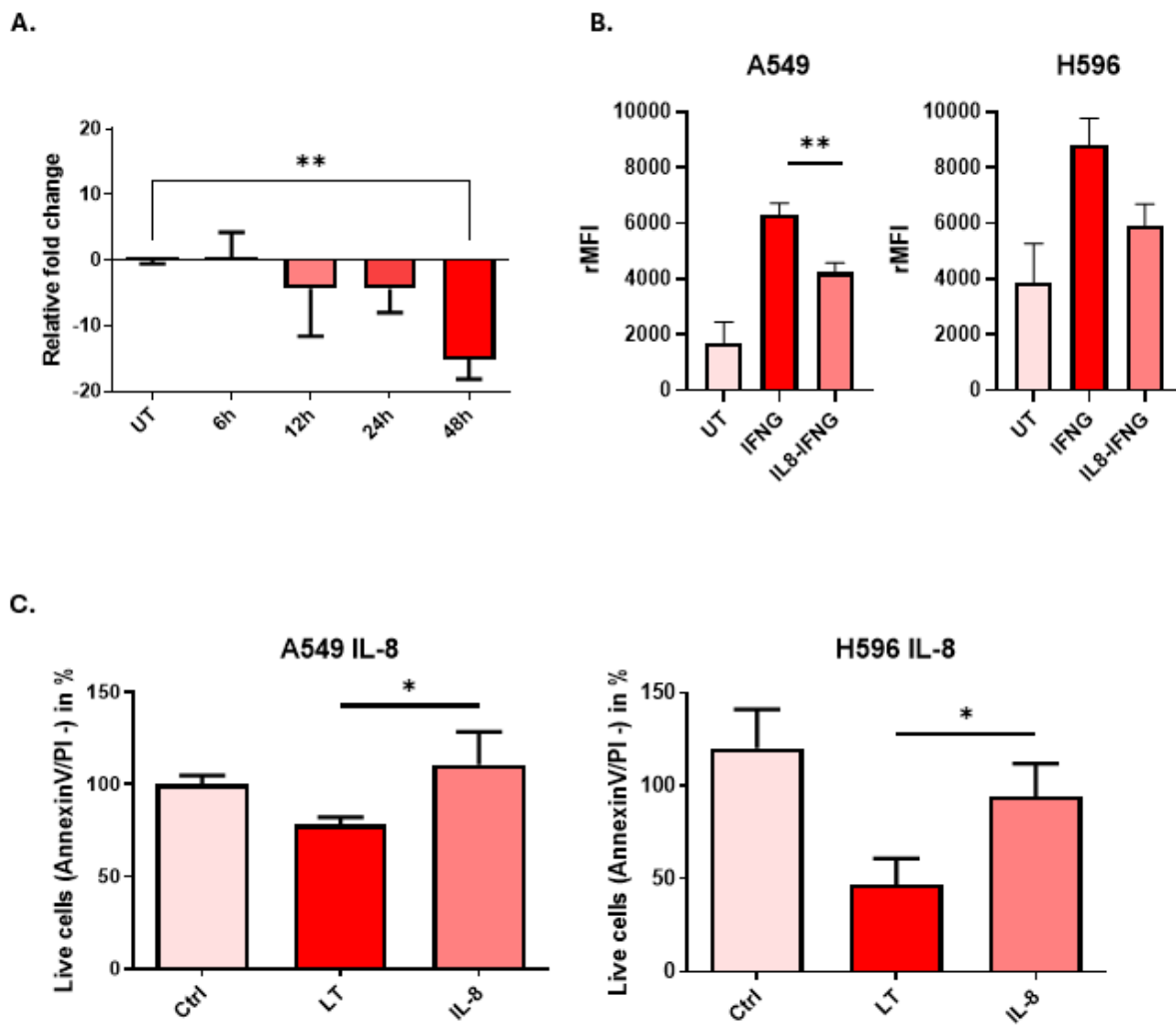
We bring further evidence that IL-8 signalling plays a role in cancer-cell immune escape by negatively impact tapasin and HLA-A/B/C cell-surface expression. These results highlight IL-8 as a reasonable therapeutic target, preferentially with patients presenting with high IL-8 plasma levels as well as low tapasin expression on cancer-cells.

Work is ongoing to further understand and better characterize the mechanisms of action of IL-8, and the best IL-8 targeted inhibition strategy.

## **Figure**

A. IL-8 reduces HLA-A/B/C cell-surface expression on A549 cancer cells in a time-dependent manner. B. IL-8 partially inhibits IFNG-mediated HLA-A/B/C cell-surface upregulation in A549 and H596 cancer-cell lines. C. IL-8 reduces the specific T-cell cancer-cell killing in A549 and H596 cancer cell lines.

2



Ctrl: control, LT: lymphocytes, IL-8: interleukin 8

## **References**

- Passaro A, Brahmer J, Antonia S, Mok T, Peters S. Managing Resistance to Immune Checkpoint Inhibitors in Lung Cancer: Treatment and Novel Strategies. *J Clin Oncol.* 2022 Feb 20;40(6):598-610. doi: 10.1200/JCO.21.01845. Epub 2022 Jan 5. PMID: 34985992
- Schoenfeld AJ, Hellmann MD. Acquired Resistance to Immune Checkpoint Inhibitors. *Cancer Cell.* 2020 Apr 13;37(4):443-455. doi: 10.1016/j.ccr.2020.03.017. PMID: 32289269
- Garrido F. MHC/HLA class I loss in cancer cells. *Adv Exp Med Biol.* 2019;1151:15–78. -
- Jhunjhunwala S, Hammer C, Delamarre L. Antigen presentation in cancer: insights into tumour immunogenicity and immune evasion. *Nat Rev Cancer.* 2021;21:298–312.
- Blees A, Januliene D, Hofmann T, Koller N, Schmidt C, Trowitzsch S, Moeller A, Tampé R. Structure of the human MHC-I peptide-loading complex. *Nature.* 2017 Nov 23;551(7681):525-528. doi: 10.1038/nature24627. Epub 2017 Nov 6. PMID: 29107940
- Antoniou AN, Ford S, Pilley ES, Blake N, Powis SJ. Interactions formed by individually expressed TAP1 and TAP2 polypeptide subunits. *Immunology.* 2002 Jun;106(2):182-9. doi: 10.1046/j.1365-2567.2002.01415.x. PMID: 12047747
- Lou Y, Vitalis TZ, Basha G, Cai B, Chen SS, Choi KB, Jeffries AP, Elliott WM, Atkins D, Seliger B, Jefferies WA. Restoration of the expression of transporters associated with antigen processing in lung carcinoma increases tumor-specific immune responses and survival. *Cancer Res.* 2005 Sep 1;65(17):7926-33. doi: 10.1158/0008-5472.CAN-04-3977. PMID: 16140964
- Korkolopoulou P, Kaklamantis L, Pezzella F, Harris AL, Gatter KC. Loss of antigen presenting molecules (MHC class I and TAP-1) in lung cancer. *Br J Cancer.* 1996 Jan;73(2):148-53. doi: 10.1038/bjc.1996.28. PMID: 8546899
- Hanagiri T, Shigematsu Y, Shinohara S, Takenaka M, Oka S, Chikaishi Y, Nagata Y, Baba T, Uramoto H, So T, Yamada S. Clinical significance of expression of cancer/testis antigen and down-regulation of HLA class-I in patients with stage I non-small cell lung cancer. *Anticancer Res.* 2013 May;33(5):2123-8. PMID: 23645764
- Ramnath N, Tan D, Li Q, Hylander BL, Bogner P, Ryes L, Ferrone S. Is downregulation of MHC class I antigen expression in human non-small cell lung cancer associated with prolonged survival? *Cancer Immunol Immunother.* 2006 Aug;55(8):891-9. doi: 10.1007/s00262-005-0085-7. Epub 2005 Sep 27.
- Kikuchi E, Yamazaki K, Torigoe T, Cho Y, Miyamoto M, Oizumi S, Hommura F, Dosaka-Akita H, Nishimura M. HLA class I antigen expression is associated with a favorable prognosis in early stage non-small cell lung cancer. *Cancer Sci.* 2007 Sep;98(9):1424-30. doi: 10.1111/j.1349-7006.2007.00558.x. Epub 2007 Jul 23. PMID: 17645781
- Passlick B, Izicki JR, Simmel S, Kubuschok B, Karg O, Habekost M, Thetter O, Schweiberer L, Pantel K. Expression of major histocompatibility class I and class II antigens and intercellular adhesion molecule-1 on operable non-small cell lung carcinomas: frequency and prognostic significance. *Eur J Cancer.* 1994;30A(3):376-81. doi: 10.1016/0959-8049(94)90259-3. PMID: 8204362

Shionoya Y, Kanaseki T, Miyamoto S, Tokita S, Hongo A, Kikuchi Y, Kochin V, Watanabe K, Horibe R, Saijo H, Tsukahara T, Hirohashi Y, Takahashi H, Sato N, Torigoe T. Loss of tapasin in human lung and colon cancer cells and escape from tumor-associated antigen-specific CTL recognition. *Oncoimmunology*. 2017 Jan; 3(2):e1274476. doi: 10.1080/2162402X.2016.1274476. eCollection 2017. PMID: 28344889

Datar IJ, Hauc SC, Desai S, Gianino N, Henick B, Liu Y, Syrigos K, Rimm DL, Kavathas P, Ferrone S, Schalper KA. Spatial Analysis and Clinical Significance of HLA Class-I and Class-II Subunit Expression in Non-Small Cell Lung Cancer. *Clin Cancer Res*. 2021 May 15;27(10):2837-2847. doi: 10.1158/1078-0432.CCR-20-3655. Epub 2021 Feb 18. PMID: 33602682

Sanmamed MF, Perez-Gracia JL, Schalper KA, Fusco JP, Gonzalez A, Rodriguez-Ruiz ME, Oñate C, Perez G, Alfaro C, Martín-Algarra S, Andueza MP, Gurpide A, Morgado M, Wang J, Bacchiocchi A, Halaban R, Kluger H, Chen L, Sznol M, Melero I. Changes in serum interleukin-8 (IL-8) levels reflect and predict response to anti-PD-1 treatment in melanoma and non-small-cell lung cancer patients. *Ann Oncol*. 2017 Aug 1;28(8):1988-1995. doi: 10.1093/annonc/mdx190. PMID: 28595336

Schalper KA, Carleton M, Zhou M, Chen T, Feng Y, Huang SP, Walsh AM, Baxi V, Pandya D, Baradet T, Locke D, Wu Q, Reilly TP, Phillips P, Nagineni V, Gianino N, Gu J, Zhao H, Perez-Gracia JL, Sanmamed MF, Melero I. Elevated serum interleukin-8 is associated with enhanced intratumor neutrophils and reduced clinical benefit of immune-checkpoint inhibitors. *Nat Med*. 2020 May;26(5):688-692. doi: 10.1038/s41591-020-0856-x. Epub 2020 May 11. PMID: 32405062

Ng CT, Fong LY, Abdullah MNH. Interferon-gamma (IFN gamma): Reviewing its mechanisms and signaling pathways on the regulation of endothelial barrier function. *Cytokine*. 2023 Jun;166:156208. doi: 10.1016/j.cyto.2023.156208. Epub 2023 Apr 21. PMID: 37088004

Gocher AM, Workman CJ, Vignali DAA. Interferon-gamma: teammate or opponent in the tumour microenvironment? *Nat Rev Immunol*. 2022 Mar;22(3):158-172. doi: 10.1038/s41577-021-00566-3. Epub 2021 Jun 21. PMID: 34155388

Yano T, Fukuyama Y, Yokoyama H, Kuninaka S, Asoh H, Katsuda Y, Ichinose Y. HLA class I and class II expression of pulmonary adenocarcinoma cells and the influence of interferon gamma. *Lung Cancer*. 1998 Jun;20(3):185-90. doi: 10.1016/s0169-5002(98)00010-5. PMID: 9733053

Abarca-Heidemann K, Friederichs S, Klamp T, Boehm U, Guethlein LA, Ortmann B. Regulation of the expression of mouse TAP-associated glycoprotein (tapasin) by cytokines. *Immunol Lett*. 2002 Oct 1;83(3):197-207. doi: 10.1016/s0165-2478(02)00104-9. PMID: 12095710

## **DISCUSSION GLOBALE**

A travers ce travail, nous avons cherché à aborder plusieurs problématiques actuelles en oncologie thoracique. Nous avons effectué une étude de screening de biomarqueurs afin de chercher à découvrir de nouveaux biomarqueurs d'intérêt dans le CBNPC traité par immunothérapie et avons mis en évidence le rôle potentiel d'HGF (Article #1.). Ce premier travail a servi de fondation à d'autres travaux au sein du laboratoire, confirmant l'importance potentielle d'HGF (Annexe 1.). En parallèle, nous avons poursuivi nos travaux sur le sPD-L1 et avons évalué son rôle de biomarqueur dans le CBNPC de stade avancé traité par immunothérapie seule ou en association avec la chimiothérapie en première ligne thérapeutique (Article #2.). Enfin, nous avons exploré par mQIF, les composants du CCP afin d'élucider les mécanismes de résistance primaire et acquise à l'immunothérapie. Cette analyse a permis de mettre en évidence une voie de signalisation cytokino-induite originale et potentiellement ciblable thérapeutiquement (Articles #3 et #4).

### **I- La voie HGF/MET dans le CBNPC de stade avancé**

Dans un premier temps, par une analyse ELISA multiplex, nous avons cherché à mettre en évidence de nouveaux biomarqueurs potentiels dans le CBNPC de stade avancé traité par immunothérapie. Nous avons identifié l'HGF comme potentiel biomarqueur prédictif de réponse à l'immunothérapie.

Nous avons montré que les patients présentant une résistance primaire à l'immunothérapie présentaient, avant l'initiation du traitement, des taux plus élevés de HGF que les patients présentant une résistance acquise. En outre, nous avons montré que le taux de HGF avant l'initiation du traitement était significativement plus élevé chez les patients ne présentant pas de bénéfice clinique par rapport à ceux présentant un bénéfice clinique : 210,9 pg/mL vs 155,8 pg/mL,  $p = 0.010$ . Nous avons par la suite montré que les patients avec un taux élevé de HGF avant initiation du traitement présentaient une SSP et une SG significativement plus courte que les patients avec un taux bas de HGF : 2,5 mois [IC 95% (1,0 – 3,0)] vs 8,0 mois [IC 95% (4,0 – NA)],  $p = 0.002$  et 5,5 mois [IC 95% (2,0 – 15,0)] vs 35,0 mois [IC 95% (22,0 - NA)],  $p =$

0,001, respectivement pour ls SSP et la SG.

Cette première étude apporte des résultats pertinents et originaux sur le potentiel rôle de biomarqueur de HGF chez les patients présentant un CBNPC de stade avancé traités par immunothérapie. Il s'agit de la première étude à montrer le rôle de biomarqueur dans ce contexte clinique. Elle vient par ailleurs confirmer des résultats similaires obtenus dans d'autres histologies comme le mélanome. Ce travail présente néanmoins des limites. Il s'agit d'une étude pilote de screening réalisée de manière mono-centrique et sur un nombre limité d'échantillons. On pourra par ailleurs noter que le groupe de patients était hétérogène car il comprenait des patients traités en première ligne par immunothérapie seule et en deuxième ligne après progression sous chimiothérapie.

D'autres points peuvent également être discutés comme la sélection du cut-off pour définir les patients présentant un taux élevé ou un taux bas de HGF. Enfin, du fait de la multitude de biomarqueurs évalués, la multiplication des tests statistiques peut mener à un résultat erroné. Nous avons néanmoins limité l'impact de cette multiplication de tests en appliquant une correction statistique pour la réalisation de tests multiples. Ces premiers résultats ont permis de développer d'autres projets de recherche et ont conduit à la réalisation de l'article présenté en Annexe 1. Ce travail a cherché à évaluer de manière plus précise le rôle de la voie HGF/MET dans la résistance à l'immunothérapie chez les patients présentant un CBNPC de stade avancé traités par ICI seuls ou en association avec la chimiothérapie en première ligne thérapeutique. Il a été montré que HGF semble jouer un rôle prédictif de réponse chez les patients traités par immunothérapie. En effet, les concentrations élevées de HGF étaient associées à un taux élevé de progression. Par ailleurs, il a été montré que le surnageant de cellules de CBNPC sécrétaien de l'HGF, que la prolifération des lymphocytes CD3+CD8+, dans un modèle de co-culture avec cellules tumorales de CBNPC, était inhibée en présence d'HGF recombinant, même en présence de pembrolizumab et qu'un inhibiteur d'HGF/MET permettait de restaurer l'activation lymphocytaire et induisait la production d'IFNG.

Ces résultats pré-cliniques pourraient servir de fondation pour développer des essais thérapeutiques à la structure originale. Le rationnel biologique semble être assez fort pour proposer une stratégie thérapeutique ciblée en fonction du taux de HGF. En effet, nos résultats ont montré que les patients avec des taux élevés de HGF présentaient une résistance accrue à l'immunothérapie. On pourrait alors sélectionner les patients en fonction du taux de HGF et proposer, aux patients avec un taux élevé, une inhibition de la voie HGF/MET soit par

anticorps monoclonal anti-HGF, soit par inhibition de MET, associé à une immunothérapie voire une chimio-immunothérapie. Cette proposition offrirait une thérapie adaptée à un sous-groupe particulier de patients. Il serait également pertinent de prendre en compte l'existence d'une altération de MET, que ce soit une amplification, une surexpression ou la présence d'une mutation ponctuelle ou d'une mutation de type saut de l'exon 14 de *MET*.

## **II- Le sPD-L1 dans le CBNC de stade avancé traité par immunothérapie**

Nous avons poursuivi notre évaluation du sPD-L1 chez les patients présentant un CBNPC de stade avancé traités par immunothérapie seule ou en association à la chimiothérapie en première ligne thérapeutique. Nous avons montré de manière multi-centrique que des niveaux élevés de sPD-L1 sont délétères. Nous avons par ailleurs montré que la variation de sPD-L1 entre l'initiation du traitement et le premier bilan d'évaluation tumoral semble jouer un rôle prépondérant pour prédire la réponse chez les patients traités par un traitement contenant de l'immunothérapie.

Ce travail a été réalisé de manière multi-centrique dans deux centres académiques ce qui constitue une de ses forces. On pourra néanmoins souligner certaines limites et discuter plusieurs éléments.

D'une part, les taux de sPD-L1 ne sont pas homogènes à travers les différentes cohortes de patients. Cela peut provenir de plusieurs causes. D'une part, le conditionnement pré-analytique peut varier d'un échantillon à l'autre mais surtout d'un centre à l'autre. Cette raison peut certainement expliquer les différences observées entre les cohortes. On remarquera également une variation intra-centre, cela peut survenir du fait que certains échantillons soient plus anciens et aient déjà subis de cycles de décongélation/recongélation ayant pu alterer en partie les protéines présentes. Néanmoins, les différentes cohortes ont été analysées de manière indépendante ce qui a permis une analyse adéquate de la valeur de sPD-L1. L'analyse de la variation de sPD-L1, étant donné qu'elle s'affranchit de la valeur absolue de sPD-L1, a pu être réalisée en combinant plusieurs cohortes afin d'augmenter la puissance de l'analyse. On pourra noter que les résultats ne sont pas parfaitement homogènes à travers toutes les cohortes de patients. Il existe probablement une réalité biologique sous-jacente avec un rôle prédictif du sPD-L1 chez les patients traités par immunothérapie. Il est

également possible qu'il existe un manque de puissance en particulier dans une des cohortes qui dispose d'un nombre limité d'échantillons. Finalement, ces résultats confirment nos résultats précédents et un grand nombre d'études publiées dans le CBNPC et dans d'autres histologies de cancers solides, soulignant le rôle du sPD-L1 comme biomarqueur. Les données initiales nous ont également montré qu'il est produit par les cellules tumorales et certaines cellules immunitaires myéliodes, et qu'il a la capacité d'inhiber les lymphocytes TCD4+ de manière préférentielle. On soulignera aussi que le sPD-L1 semble indépendant de l'expression de PD-L1 à la surface des cellules tumorales objectivé par IHC et de la taille tumorale.

La question actuelle est donc la manière d'utiliser de manière optimale ce biomarqueur. Cela pourrait s'envisager de plusieurs manières. D'une part, un taux de sPD-L1 élevé avant initiation du traitement semble prédire un mauvais pronostic sous immunothérapie, mais cette donnée est difficile à exploiter en clinique. En revanche, on pourrait se servir de la variation de sPD-L1 en cours de traitement. En effet, les patients qui présentent une augmentation du taux de sPD-L1 en début de traitement présentent une survie plus courte sous immunothérapie. Dans une situation clinique où le taux de sPD-L1 augmente précocement, avant la progression clinique ou radiologique, on pourrait proposer une intensification du traitement ou un changement de ligne précoce. Cela permettrait d'offrir une possibilité thérapeutique supplémentaire et anticipée.

Ainsi, le sPD-L1 pourrait se présenter comme un test compagnon, dynamique, dont l'utilisation pourrait rentrer dans un faisceau d'arguments associant l'état clinique et les résultats radiologiques.

### **III- Le rôle des composants du complexe de chargement des peptides (CCP) dans la résistance à l'immunothérapie chez les patients présentant un CBNPC de stade avancé**

Notre troisième axe de recherche s'est focalisé sur l'analyse des composants du CCP sur des prélèvements histologiques de patients présentant un CBNPC traité par chimiothérapie ou par immunothérapie. Cette analyse a été réalisée par mQIF qui permet une analyse spatiale et quantitative des marqueurs d'intérêt. Elle permet également de définir des compartiments spécifiques (cellules cancéreuses, stroma) et d'analyser l'expression des protéines dans ces compartiments.

Cette analyse a été réalisée sur plusieurs cohortes de patients, présentant des caractéristiques cliniques et de survie bien définies et représentées dans des TMAs.

Cette étude comprend plusieurs points positifs. Outre les avantages de la mQIF décrits ci-dessus, l'analyse a été effectuée avec des anticorps rigoureusement validés en vue de cette utilisation spécifique. En résumé, chaque anticorps a été titré en utilisant des TMAs de référence afin de déterminer la concentration optimale d'utilisation en utilisant des courbes signal/bruit permettant de déterminer un ratio signal/bruit optimal. Par ailleurs, le marquage des cohortes a été réalisé lors de la même expérience limitant les variations inter-cohortes. Enfin, lors de la réalisation du marquage des cohortes, une lame TMA utilisée pour la validation des anticorps a également été marquée afin de s'assurer de la reproductibilité de l'expérience.

L'utilisation de TMAs présente également plusieurs avantages. Elle permet de regrouper un grand nombre d'échantillons sur une lame ce qui nous a permis d'analyser un grand nombre de patients en parallèle. Néanmoins, il faut souligner que l'échantillon tumoral utilisé est de petite taille et expose donc au risque de ne pas prendre en compte parfaitement l'hétérogénéité tumorale. Afin de pallier cette limite, une autre lame de chaque cohorte a été marquée et des corrélations réalisées avec les résultats initiaux montrait une bonne corrélation entre les différents échantillons.

Nous avons pu montrer que les altérations des composants du CCP sont fréquentes dans le CBNPC et homogènes à travers les différentes cohortes analysées. Nous avons en outre montré que la régulation négative de tapasin par les cellules cancéreuses est un phénomène fréquent qui impacte la survie en particulier chez les patients traités par immunothérapie. En outre, nous avons montré que l'infiltration lymphocytaire T CD8+ est négativement impactée en cas de baisse de tapasin, ce qui pourrait en partie expliquer la moindre survie chez ces patients.

Après cette première observation, nous avons cherché à analyser le mécanisme expliquant la régulation négative de tapasin. Nous avons mis en évidence l'existence d'une potentielle voie de signalisation cytokine-médiée avec un rôle d'IL-8. En effet, la présence d'altérations du gène *TAPBP* restent rares. L'hypothèse d'une régulation épigénétique de tapasin est ainsi au premier plan. Notre approche a permis de mettre en évidence, en utilisant plusieurs méthodes (Western Blot, mQIF), qu'IL-8 a un effet de régulation négative sur tapasin. A notre connaissance, c'est la première fois que le rôle potentiel d'IL-8 sur tapasin est décrit.

Dans un second temps, nous avons cherché à évaluer par cytométrie de flux l'impact d'IL-8 sur l'expression au niveau de la surface cellulaire de HLA-A/B/C et nous avons montré que l'effet d'IL-8 est maximal après 48 heures d'exposition et qu'IL-8 peut inhibier l'action stimulatrice d'IFNG. L'ensemble de ces résultats sont originaux mais présentent encore certaines limites. Nous avons montré de manière indépendante qu'IL-8 module, d'une part tapasin et, d'autre part HLA-A/B/C, mais n'avons pas montré que cette régulation est concomittante. Des analyses complémentaires sont prévues pour étayer cela. Par ailleurs, l'expression en surface de HLA-A/B/C est une expression globale, et il a été montré que des peptides vides peuvent se rendre à la surface cellulaire sans l'intervention de tapasin. Une analyse plus fine avec des peptides chargés devra être faite. Enfin, nous prévoyons de poursuivre notre analyse en mettant en place des cellules présentant un knock-down pour tapasin en utilisant des shRNA. Cette technique permettra de mettre en place une lignée cellulaire stable de cellules tapasin knocked-down (KD) et d'évaluer l'expression de HLA-A/B/C et de réaliser des expériences de co-culture.

Ces premiers résultats sont pertinents et encourageants, mais il existe encore des éléments à affiner, en particulier le mode d'action d'IL-8 pour inhiber l'expression de tapasin. On peut néanmoins imaginer des applications cliniques de l'utilisation de l'expression d'IL-8 et de tapasin. En effet, des patients présentant une expression basse de tapasin et élevée d'IL-8 seraient potentiellement des candidats intéressants pour une stratégie thérapeutique d'inhibition d'IL-8 par un anticorps monoclonal anti-IL-8 associé à une immunothérapie anti-PD1/PD-L1.

## **PERSPECTIVES**

L'ensemble de ces résultats vont nous permettre de prévoir et développer de nouveaux projets de recherche translationnelle.

Nous allons poursuivre notre analyse de l'impact d'IL-8 sur tapasin avec plusieurs expériences prévues. D'une part, nous allons chercher à créer une lignée cellulaire stable présentant un knock down (KD) de tapasin en utilisant des small hairpins RNAs (shRNAs). Cette lignée cellulaire pourra ensuite être utilisée afin d'analyser l'expression de HLA-A/B/C et réaliser de nouvelles expériences de co-culture. En outre, nous souhaiterions développer des expériences de pulse-chase afin de suivre une protéine de tapasin marquée et de connaître sa localisation cellulaire dans un contexte physiologique et dans des conditions expérimentales différentes comme après exposition à l'IFNG ou à l'IL-8 par exemple.

Nous avons également pour projet de poursuivre l'analyse de composants du CCP dans le CBNPC et le CBPC de stade avancé. Nous avons à notre disposition dans le laboratoire des biopsies couplées prélevées avant initiation de l'immunothérapie et lors de la progression (essai REBIMMUNE, NCT04300062). Nous avons pour objectif de constituer une cohorte qui pourrait être représentée dans un TMA et qui comprendrait les échantillons pré-thérapeutiques et à progression de patients présentant une résistance primaire d'une part, et acquise d'autre part ainsi que des échantillons pré-thérapeutiques de patients très longs répondeurs et patients rapidement progresseurs. L'analyse par mQIF de composants du CCP pourra nous informer sur les mécanismes de résistance primaires et acquis à l'immunothérapie.

Afin de développer et maintenir l'expérience acquise en mQIF, nous avons pour projet d'effectuer les analyses translationnelles de plusieurs études de l'IFCT ayant testé l'immunothérapie dans les CBNPC. On pourra en particulier prévoir une analyse de l'infiltration lymphocytaire T et des composants du CCP.

En outre, dans le cadre de notre intégration au sein du laboratoire BioMaps nous avons pour projet de mettre en place des expériences de pulse-chase avec une molécule de tapasin marquée radioactive afin de la suivre en conditions physiologiques et après expositions à des cytokines telles que IFNG ou IL-8.

Enfin, on envisage à terme d'extrapoler ces résultats précliniques à la clinique, en mettant en place des essais thérapeutiques innovants (d'escalade ou désescalade thérapeutique basé sur

les biomarqueurs ; utilisant des inhibiteurs sélectifs de HGF/MET ou d'IL-8 en association avec les ICIs...) pour améliorer l'efficacité des ICIs dans les CBNPC.

## **CONCLUSION**

La prise en charge du cancer pulmonaire a connu des modifications majeures depuis le début du XXI<sup>ème</sup> siècle avec d'une part la découverte d'addictions oncogéniques donnant accès à des thérapies ciblées, et d'autre part l'utilisation d'ICIs comme les anticorps anti-PD-1/PD-L1 qui sont actuellement utilisés à tous les stades de la maladie.

Malgré ces avancées majeures, des obstacles et des limites à l'efficacité du traitement demeurent. En effet, la grande majorité des patients présentant un CBNPC de stade avancé traité par immunothérapie, va présenter une résistance primaire ou acquise à plus ou moins long terme. Nous manquons actuellement de biomarqueurs fiables pour prédire la réponse à l'immunothérapie et surtout pour anticiper celle-ci en cours de traitement. Nous manquons également de connaissance sur les mécanismes de résistance à l'immunothérapie et en particulier les altérations touchant la voie de présentation antigénique. Enfin, il est nécessaire de mettre en évidence de nouvelles voies de signalisations cliniquement pertinentes afin de proposer de nouvelles stratégies thérapeutiques basées sur des rationnels biologiques forts. En ce sens, nous avons souligné dans ce travail de thèse l'importance de la voie de signalisation potentiellement cibleable HGF/MET, confirmé le rôle du sPD-L1 comme biomarqueur prédictif de réponse à l'immunothérapie et l'importance de sa variation en cours de traitement, et enfin, apporté des données originales sur la régulation cytokino-induite des composants du CCP.

Des travaux sont encore en cours pour affiner et améliorer notre compréhension et nos connaissances de ces différents éléments. La mise en place d'essais cliniques ou translationnels novateurs sont maintenant nécessaires pour proposer des stratégies thérapeutiques innovantes et adaptées à chaque situation clinique individuelle.

## **ANNEXES**

**Annexe #1:** article “Role of the HGF/c-MET pathway in resistance to immune checkpoint inhibitors in advanced non-small cell lung cancer” (co-auteur).

**Annexe #2:** article “Predictive role of plasmatic biomarkers in advanced non-small cell lung cancer treated by nivolumab” (1e auteur), travail de Master 2 sur le sPDL1.

**Annexe #3:** article “Plasma Biomarkers and Immune Checkpoint Inhibitors in Non-Small Cell Lung Cancer: New Tools for Better Patient Selection?” (1e auteur), revue de la littérature sur les biomarqueurs plasmatiques et immunothérapie.

**Annexe #1. Role of the HGF/c-MET pathway in resistance to immune checkpoint inhibitors in advanced non-small cell lung cancer.** En cours de revue dans *Cancer Immunology, Immunotherapy*.

## **Role of the HGF/c-MET pathway in resistance to immune checkpoint inhibitors in advanced non-small cell lung cancer**

### **Authors**

Assya Akli<sup>1</sup>; Paul Takam Kamga<sup>1</sup>; Catherine Julie<sup>1,2</sup>; Claude Capron<sup>1,3</sup> ; Adrien Costantini<sup>4</sup>; Coraline Dumenil<sup>4</sup> ; Jennifer Dumoulin <sup>4</sup> ; Violaine Giraud<sup>4</sup> ; Florence Parent<sup>5</sup>; Andrei Seferian<sup>5</sup> , Catherine Guettier<sup>5</sup>, Mathieu Glorion <sup>6</sup> ; Elisabeth Longchampt<sup>7</sup> ; Jean-François Emile<sup>1,2</sup> ; Étienne Giroux-Leprieur <sup>1,4\*</sup>

1 Université Paris-Saclay, UVSQ, EA 4340 BECCOH, Boulogne-Billancourt, France ;

2 –APHP-Ambroise Paré Hospital, Department of Pathology, Boulogne-Billancourt, France ;

3 APHP-Ambroise Paré Hospital, Department of Hematology and Immunology,, Boulogne-Billancourt, France ;

4 APHP-Ambroise Paré Hospital, Department of Respiratory Diseases and Thoracic Oncology, Boulogne-Billancourt, France.

5. APHP- Kremlin Bicetre Hospital, Department of Pathology, Kremlin Bicetre, France

6.Foch Hospital, Department of Thoracic Surgery, Suresnes, France

7. Foch Hospital, Department of Pathology, Suresnes, France

\*Corresponding author: Etienne Giroux Leprieur, MD, PhD, Department of Respiratory Diseases and Thoracic Oncology, APHP – Hopital Ambroise Pare, 9 avenue Charles de Gaulle, 92100 Boulogne- Billancourt, France. Tel: +33149095802. Fax: +33149095806. Email: [etienne.giroux-leprieur@aphp.fr](mailto:etienne.giroux-leprieur@aphp.fr)

## **ABSTRACT**

Most of advanced non-small cell lung cancer (NSCLC) patients will experience tumor progression with immunotherapy (IO). Preliminary data suggested an association between high plasma HGF levels and poor response to IO in advanced NSCLC. Our study aimed to evaluate further the role of the HGF/MET pathway in resistance to IO in advanced NSCLC. We included retrospectively 82 consecutive NSCLC patients from two Academic Hospitals. Among them, 49 patients received ICIs alone or in combination with chemotherapy (CT), while 33 patients received chemotherapy alone as the control group. We analysed plasma HGF levels by ELISA and expression of PD-L1, MET/phospho-MET, and CD8+ T-Cell infiltration on lung tumour tissue by immunohistochemistry. We investigated the contribution of HGF/MET to IO response by culturing peripheral blood mononuclear cells (PBMC) with or without pembrolizumab, with recombinant HGF, or co-cultured with NSCLC patients-derived explants. Additionally, cMET inhibitors were used to evaluate the contribution of MET activation in NSCLC-mediated immunosuppression. High HGF levels were associated with high progression rate with IO ( $p = 0.0092$ ), but not with CT. ELISA analysis of supernatants collected from cultured NSCLC cells showed that HGF was produced by tumor cells. Furthermore, when activated PBMCs were cultured in the presence of recombinant HGF or on NSCLC monolayer, the proliferation of CD3+CD8+ lymphocytes was inhibited, even in the presence of pembrolizumab. The addition of HGF/MET inhibitors restored lymphocyte activation and induced IFN $\gamma$  production. In conclusion, inhibiting the HGF/MET signaling pathway could be a promising approach to enhance the efficacy of immunotherapy.

## **1. Introduction**

Lung cancer is the first cause of cancer deaths worldwide. Most of the cases are diagnosed at a metastatic stage with a survival of less than 5% at 5 years<sup>1(1)</sup>. Immune checkpoint inhibitors (ICIs) are able to restore an anti-tumor immunological response. They are the corner stone of the first-line treatment of advanced non-small cell lung cancer (NSCLC) without oncogenic addiction, either in monotherapy in case of high Programmed Death-Ligand-1 expression (PD-L1 > 50%) by tumor cells or in combination with platinum-based chemotherapy<sup>2-4</sup>. However, nearly 50% of patients do not experience tumor response with ICIs<sup>5</sup>. The identification of biomarkers related to treatment resistance remains a major challenge.

HGF (Hepatocyte growth factor) is a growth factor secreted by stromal mesenchymal cells and by neutrophils. *MET* (Mesenchymal Epithelial Transition) is a pro-oncogene encoding the epithelial MET receptor. The MET receptor is a member of the tyrosine kinase receptor family. HGF is the ligand of MET, inducing homo- or heterodimerization of MET with other receptors with tyrosine kinase activity thereby activating several downstream signaling pathways (Ras-MAP kinase, PI-3K-AKT-mTOR, JAK-STAT pathways)<sup>6</sup>. Physiologically, the HGF/MET pathway plays a key role in "invasive growth"<sup>7</sup> involving mechanisms of migration, differentiation, proliferation, and cell survival. Activation of MET by HGF promotes "epithelial-mesenchymal transition" (EMT) by disruption of intercellular contacts, detachment, and then migration of cells.

Recently, we performed a pilot study that analyzed the expression levels of 48 plasma biomarkers in 35 consecutive patients with advanced NSCLC treated with ICIs, using ELISA Multiplex assay<sup>8</sup>. We showed a significant association between circulating Hepatocyte Growth Factor (HGF) levels at the beginning of ICI therapy and treatment efficacy. Progression-free survival (PFS) and overall survival (OS) were significantly shorter in the group with high HGF

levels at baseline.

Therefore, we hypothesize that the activation of the HGF/MET pathway is associated with resistance to ICIs given in first-line treatment in advanced NSCLC. We performed translational and in vitro studies to investigate this hypothesis.

## **2. Material and Methods**

### **2.1 Patients and samples**

All consecutive patients with a treatment-naïve stage IIIb, IIIc or IV (according to 8<sup>th</sup> classification) NSCLC from the Department of Pulmonology and Thoracic Oncology of two academic centers (APHP – Ambroise Paré Hospital and APHP-Bicêtre Hospital), and receiving a first line treatment by chemotherapy, immunotherapy or a combination of chemotherapy and immunotherapy, between September 2017 and January 2022, were included. Plasma samples were prospectively collected from NSCLC patients treated at Ambroise Paré Hospital, after signature of an informed consent (CPP IDF n°VIII). Tumor biopsies were collected at diagnosis at the Ambroise Paré Hospital and Bicêtre Hospital, and stored as Formalin-fixed paraffin-embedded tissue blocks. PBMC (Peripheral Blood Mononuclear Cells) were obtained from peripheral blood samples of healthy donors. We have evaluated the overall response rate at the first tumor evaluation, PFS and OS, according to plasma concentration of the circulating biomarkers, and histologic expression of tissue biomarkers. Tumor response was evaluated every two months using RECIST 1.1 criteria.

### **2.2 Reagents and antibodies**

ELISA assay Kits for HGF (ab275901) and interferon-γ (IFN-γ, ab100537) were provided by ABCAM (Cambridge, UK). Phytohemagglutinin (00-4977-03) for PBMC activation was from

Thermofischer Scientific (Paris, France). The antibodies used for Flow cytometric analysis of lymphocytes, including mouse anti-huCD45- BV421 (HI30, 563879), mouse anti-CD3-PE-Cy7 (SK7, 557851), and anti-huCD8-APC were all from Thermofischer Scientific (Paris, France). For IHC, anti-hu-phospho-Met ((Tyr1234/1235) was provided by Thermofischer Scientific (Paris, France). CFSE for cell proliferation assays was from Thermofischer Scientific (C34554, France). MTS colorimetric (ab197010) assay was acquired from ABCAM (Cambridge, UK). Pembrolizumab was a kind gift of the Pharmacy Unit of APHP-Ambroise Paré Hospital (Boulogne-Billancourt, France). c-MET/HGF inhibitors, Crizotinib (PZ0191) and SGX-523 (S1112), were acquired from Sigma-Aldrich (Darmstadt, Germany) and Selleckchem (Munich, Germany) respectively.

### **2.3 ELISA assay**

ELISA assay to quantify soluble HGF and IFN- $\gamma$  in plasma samples and media collected from NSCLC culture, was performed according to the manufacturer's instructions (ab275901 and ab100537 respectively). Briefly, standards protein and plasma samples diluted at least at 1 / 2 ratio in sample buffers were added in ELISA well plates, then probed both with streptavidin conjugated primary antibodies and HRP conjugate secondary antibody for 90 minutes. The assays were revealed through the addition of HRP substrate. The plates were analyzed using a spectrophotometric plate reader (Bio rad PR 3100 EIA PhD software), set at a wavelength of 450 nm. Protein concentrations were calculated from their optical density using the standard curve. All samples standards and negative controls were tested in duplicate.

### **2.4 Immunohistochemistry (IHC)**

Treatment-naive tumor sections (3  $\mu$ m) were probed with anti-Pho-cMet/c-MET antibodies

through an automated technique (LEICA, BOND-III). Slides were read with optical microscope in blinded by a thoracic pathologist (CJ). Percentage of positive cells were obtained by cell counting. Tumor membrane labeling for pMET was expressed according to the number of positive tumor cells, classifying the samples in two groups: low expression (no labeling to low intensity labeling <10% of tumor cells) and high expression (moderate 10-50% of tumor cells to high intensity labeling >50% of tumor cells)<sup>9</sup>. Epithelial and alveolar macrophages cells on the same slide were considered as negative and positive controls, respectively.

## **2.5 Cell cultures and co-cultures**

### **2.5.1 NSCLC cell lines**

Human NSCLC lines (A549 and H596) were obtained from ATCC and were maintained in complete DMEM/F12 medium (DMEM/F12 supplemented with 10% foetal bovine serum (FBS), 1% L-Glutamine (l-Glu) and 1% Penicillin/Streptomycin (P/S)). Cells were grown in 96 well plates as confluent monolayer for co-culture experiments.

### **2.5.2 Primary NSCLC cultures**

Primary NSCLC cells were isolated from immunohistochemically confirmed fresh lung cancer samples obtained at the time of NSCLC surgery. The resected fresh lung cancer tissues were collected and rinsed in RPMI medium, then cut into small size and rinsed with sterile phosphate-buffered saline (PBS), then sample were digested in Trypsin-EDTA for 1h at 37°C. Digested sampled were then washed and cultured in DMEM/F12 containing 10% FBS, 1% Glutamax, 10 mM HEPES, and Primocyn. At passage 2, cells were used for culture and coculture experiments.

### **2.5.3 PBMC isolation and Culture/Co-culture**

PBMC were isolated from human blood by density gradient centrifugation using Lymphoprep (Stemcells Technologies). Isolated PBMC, stained or not with Carboxyfluorescein succinimidyl ester (CFSE, for proliferation assays), were maintained in complete RPMI or IMDM media for monoculture or coculture assays respectively. PBMC were activated with 10 µg/mL phytohemagglutinin, and cultured in the presence of HGF or on an established primary NSCLC cells monolayer. To evaluate the contribution of HGF to lymphocyte activation or ICIs-mediated activation of lymphocytes, culture media were supplemented with pembrolizumab (20 nM corresponding to 3 µg/mL) and/or c-MET/HGF inhibitors (Crizotinib (1 µM) and SGX-523 (0.5 µM). Lymphocyte activation/proliferation was assessed either through MTS colorimetric assay or CFSE staining assay.

### **2.6 MTS proliferation assay**

Lymphocyte proliferation was assessed using MTS proliferation assays as previously described<sup>10</sup>. Briefly, at the end of cell culture, 10 µL of MTS reagent (ABCAM, ab197010) was added into each well and keeping in incubator for 2 hours. Metabolically active, viable cells converted MTS into a colored formazan. The product was then measured at 490 nm in a spectrophotometric microplate reader (Bio rad PR 3100 EIA PhD software). The viability was expressed as the percentage of optical density of treated cells compared to optical density of cells treated with the specific vehicle.

### **2.7 CFSE staining and flow cytometry.**

To assess immunomodulatory properties of CSF-1, Pembrolizumab or NSCLC cells, PBMC were stained before each experiment with 1 µM carboxyfluorescein succinimidyl ester (CFSE; Life Technologies). The proliferation was assessed by flow cytometry on viable CD45pos cells CD3pos cells and/or CD3posCD8pos cells by using FlowJo software (TreeStar) as relative

CSFE dilution of treated cells compared to cell treated with specific vehicle as previously described<sup>10,11</sup>.

## **2.8 Statistical analysis**

All statistical analyses were conducted using Excel (Microsoft Office), XLSTAT (Addinsoft, 2023), and GraphPad Prism version 5 software (La Jolla, CA, USA). Statistical comparisons were conducted using Student's t-test and one-way Anova respectively, or the Mann-Whitney and the Kruskal-Wallis methods for non-parametric distribution. Associations between variables were tested using Pearson's Chi-square or Fisher's exact test. Survival curves were generated based on HGF levels using the Kaplan-Meier method, followed by the Log Rank test. Multivariate analyses were performed using logistic regression and Cox proportional hazards for drug response and patient survival, respectively. Differences were considered significant for p-values < 0.05. Subsequently, the expression values were categorized as high (above the first quartile, >Q1) or low (below the first quartile, <Q1) based on the distribution of HGF expression values.

## **3. Results**

### **3.1 Clinical characteristics of NSCLC patients**

We enrolled 82 consecutive NSCLC patients. Among them, 49 patients received ICIs alone or in combination with chemotherapy, while 33 patients received chemotherapy alone as the control group. All patients had at least one pretreatment sample available, either plasma or tissue, obtained from a pre-treatment biopsy. Table 1 provides a summary of the patients'

characteristics. Most patients were male (70%) and had a history of smoking or were former smokers (95%). Adenocarcinoma was the most prevalent histological type (68%). The median age at diagnosis was 66 years, ranging from 37 to 91 years. Finally, most patients (65%) had a performance status (PS) of 0-1 at the start of treatment. After 10.9 months of median follow-up, 25 (51%) patients treated with ICIs had died, including 37 (76%) patients who had experienced tumor progression.

**Table 1: Clinical characteristics of the patients**

	<b>Overall population=82</b>	<b>Chemotherapy n= 33</b>	<b>Immunotherapy +/- CT n=49</b>
<b>Age (years) (range)</b>	66 (37-91)	67 (42-91)	65 (37-84)
<b>Sex</b>			
<i>Man</i>	57 (70)	24 (73)	33 (67)
<i>Woman</i>	25 (30)	9 (27)	16 (33)
<b>Smoking status</b>			
<i>Active or former smoker</i>	75 (91)	30 (91)	45 (92)
<i>Never-smoker</i>	7 (9)	3 (9)	4 (8)
<b>Histology</b>			
<i>adenocarcinoma</i>	56 (68)	24 (73)	32 (66)
<i>squamous cell carcinoma</i>	14 (17)	6 (18)	8 (16)
<i>other</i>	12 (15)	3 (9)	9 (18)
<b>PS</b>			
0-1	65 (79)	26 (79)	39 (80)
≥2	17 (21)	7 (21)	10 (20)

<b>Stade / TNM</b>			
IIIB or IIIC	5 (6)	2 (6)	3 (6)
IV	77 (94)	31 (94)	46 (94)
<b>PD-L1</b>			
< 50%	26(32)	13(39)	13(27)
≥ 50%	41(50)	5 (15)	36(73)
Non available (NA)	15(18)	15 (45)	0 (0)
<b>Number of metastatic sites</b>			
1	34 (41)	16 (48)	18 (37)
2 or more	48(59)	17 (52)	31(53)

All variables are expressed as n (%), unless otherwise specified.

### 3.2. Expression of phospho-MET, HGF and correlation with demographics

To investigate the impact of HGF/MET pathway expression in NSCLC patients treated with ICIs or chemotherapy, we assessed the expression of markers of this pathway: phospho-MET (pMET, activated form of the MET receptor) and HGF. pMET was assessed through IHC of tumor biopsies collected before treatment initiation in both groups (ICIs treated patients n=22 patients; CT treated patients n=8 patients). (**Figure 1A-B**). In patients treated with ICIs, p-MET was highly expressed in 19 out of 21 patients (90%) and weakly expressed in 2 patients (10%). Besides, all 8 patients in the CT-treated group exhibited high pMET expression (100%) (n=8/8; 100%) (**Figure 1B**).

We next analyzed the expression of HGF in plasma samples collected from patients at the diagnostic, first evaluation and progression. The median HGF expression level in the total

population was 1153 pg/ml (IQR 545 - 2300) at diagnosis. In the ICIs-treated population (ICIs alone or in combination with chemotherapy), the median HGF level before treatment was 892 pg/ml (IQR 376.8 - 1580). For patients treated with ICIs alone, the median HGF level before treatment was 891pg/ml (IQR 379.4 -1488). For patients treated with combination therapy (ICIs + CT), the median HGF level was 1092 pg/ml (IQR 375 -1661) before treatment. The median expression level for the CT group was 1530pg/ml (IQR 1009-2681) before treatment. We also analyzed longitudinal HGF levels according to the time, demonstrating a significant decrease in HGF levels between diagnosis and first tumor evaluation during treatment (**Figure 1**). We did not find any correlation between pMET expression and plasma HGF levels. Next, we analyzed the association between plasma HGF levels and demographic data, including age, gender, PS, tumor stage and number of metastatic sites (**Table S1**). Except for tumor histology type, there was no significant association between HGF levels and demographic or tumor aggressiveness factors including age, sex, smoking status, number of metastatic sites and PD-L1 (**Table S1**). For patients treated with CT, there was no significant association between pre-treatment plasma HGF levels and patient demographics.

### **3.3 Correlation with patient's outcomes for ICIs therapy**

For patients treated with ICIs (alone or in combination with chemotherapy), the objective response rate at the first evaluation (ORR) was 57% (n=28/49), and 16 out of 49 patients (33%) experienced early tumor progression. Patients with stable disease and tumor progression were classified as non-responders. HGF levels at treatment initiation were higher in non-responders ( $1611 \pm 432.7$ ) and progressing patients ( $1888 \pm 555.0$ ) compared to responders ( $1128 \pm 232.8$ ) and non-progressing patients ( $1076 \pm 202.6$ ) (**Table S2**). These differences were more significant in patients treated with ICIs alone including non-responders vs responders (2061 vs 790.8;  $p =$

$0.0287$ ) and progressing vs non-progressing patients ( $2408 \pm 786.9$  vs  $811.1 \pm 167.7$ ;  $p = 0.0093$ ) (**Figure 1A; Table S2**)

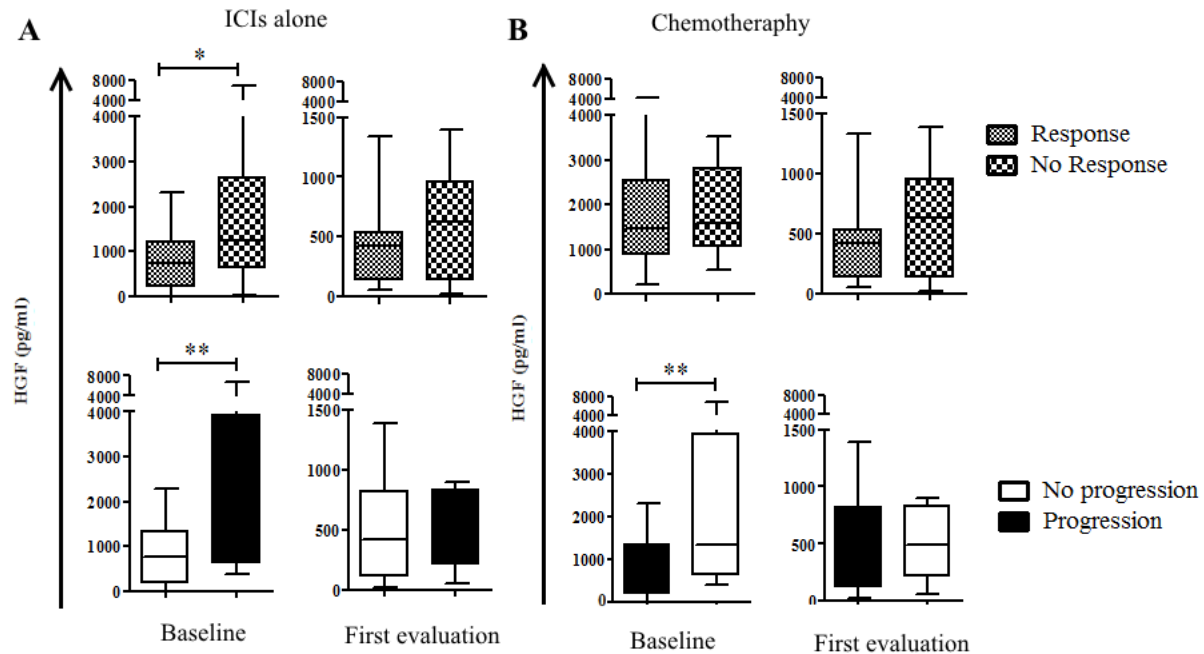


**Figure 1:** Plasma HGF levels at baseline and first evaluation according to patient's outcomes.

Plasma samples were obtained from NSCLC patients at baseline and during the first evaluation. ELISA assays were utilized to quantify HGF levels. Subsequently, expression values were categorized based on drug response and disease progression, with Panel A representing the group receiving ICIs alone and Panel B representing the group receiving chemotherapy alone.

Data are presented as mean  $\pm$  SEM. \* $p < 0.05$ ; \*\* $p < 0.01$ .

Then, we analyzed the potential correlation between HGF levels and patients' progression. In patients treated with ICIs (alone or in combination with chemotherapy), we observed that low HGF levels at baseline correlated with lower progression rate (Relative risk, RR = 0.2143; 95% CI (0.03138 - 1.463);  $p = 0.024$ ) (**Table 2A**). In patients treated with ICIs alone, no progression was observed in patients displaying lower HGF levels (RR = 0 (infinity);  $p = 0.0092$ ) (**Table 2B**). To ascertain if HGF levels in plasma samples were predictive of immunotherapy response,

we also analyzed the correlation with tumor progression in patients treated with chemotherapy alone. In these patients, no association nor correlation between HGF rate and tumor progression were observed (**Figure 1B and Table 2C-D**), confirming that HGF levels predict drug response only in patients treated with immunotherapy. Univariate analyses revealed that, in addition to HGF levels, the progression rate of patients treated with ICIs alone were also related to adenocarcinoma histology (RR = 0.2679 (0.08934 - 0.8031); p= 0.0137) (**Table S3**). Multivariate analysis based on logistic regression confirmed that adenocarcinoma histology (Hazard ratio, HR = 0.020 (0.00068 - 0.614); p = 0.025) and low baseline HGF levels (HR = 0.999 (0.998 ; 1); p = 0.041) were both predictors of low progression rate (**Table 3**).

<b>A) Immunotherapy (ICIs alone and ICIs + Chemotherapy)</b>					
Parameters		Response Rate (%)	Relative risk (RR) ; 95% CI; p-value	Progression rate (%)	Relative risk (RR) ; 95% CI; p-value
HGF Baseline (pg/mL)	Low (12)	75	1.421 (0.9063 - 2.228); p = 0.0881	8	0.2143 (0.03138 - 1.463); p = 0.024
	High (36)	53		39	
HGF First Evaluation (pg/mL)	Low (9)	78	0.7875 (0.4110 - 1.509); p = 0.227	11	0.375 (0.05402 - 2.603); p = 0.133
	High (27)	56		30	
<b>B) ICIs alone</b>					
HGF Baseline (pg/mL)	<2 (6)	85	2,143 (1.157 - 3.968); p = 0,0186	0	0(infinity); p = 0,0092
	>2 (21)	33		50	
HGF First Evaluation (pg/mL)	Yes (7)	83	1,944 (1.056 - 3.579); p = 0,0401	0	0(infinity); p = 0,0166
	No (21)	43		48	
<b>C) COMBO ( ICIs + Chemotherapy)</b>					
HGF Baseline (pg/mL)	Low (5)	60	1.309 (0.7383 - 2.321); p = 0.2164	20	0.8 (0.1140 - 5.613); p = 0.4094
	High (16)	69		25	
HGF First Evaluation (pg/mL)	Low (5)	80	1.28 (0.7167 - 2.286); p = 0.2344	20	0.8 (0.1140 - 5.613); p = 0.4094
	High (16)	63		0	
<b>D) Chemotherapy (CT)</b>					
HGF Baseline (pg/mL)	Low (10)	40	1.1 (0.4300 - 2.814); p = 0.4219	30	1.320 (0.3893 - 4.475); p = 0.3298
	High (22)	36		23	

HGF First Evaluation (pg/mL)	Low (7)	43	0.9107 (0.3373 - 2.459); p = 0.4255	14
	High (17)	47		24
			0.5313 (0.07017 - 4.022); p = 0.2601	

**Table 2: Response rate and patients' progression in univariate analysis**

**Table 3: Logistic regression analysis of response and progression rate in the ICIs alone group**

Parameters	Response			Progression		
	Hazard ratio	95% CI	p-value	Hazard ratio	95% CI	p-value
PDL1	1.035	(0.97 - 1.1)	0.292	0.966	(0.892 - 1.046)	0.395
HGF baseline (pg/ml)	0.999	(0.998 - 1)	0.041	1.002	(1.0002 - 1.003)	0.030
HGF first evaluation	0.998	(0.993 - 1.002)	0.312	0.1	0.995- 1.005	0.896
PS<1	4.733	(0.144 - 155.47)	0.383	0.373	(0.0022- 64.12)	0.707
Adenocarcinoma	0.020	(0.00068 - 0.614)	0.025	31.66	(1.056 - 949.12)	0.046
Metastasis <2	6.840	(0.274- 170.929)	0.242	8.984	(0.17- 473.93)	0.278
Presence of a mutation	0.023	(0.0003 - 1.769)	0.089	173.47	(0.187- 161045.95)	0.139

### 3.4 Correlation with patient's survival

In patients treated with ICIs (alone and in combination with chemotherapy), very low HGF (below the first quartile) concentrations at baseline were associated with longer PFS (HR= 3.048; 95% CI (1.325 – 7.013); p = 0.0103). In the group of patients treated with ICIs alone, lower levels of HGF correlated with prolonged survival (both PFS and OS) (**Figure 3A; Table S4**). In this patients' group, we found that performance status (PS) <1 and adenocarcinoma histology correlated with longer PFS and OS (**Table S5**). The COX proportional hazard models revealed that only adenocarcinoma histology and low baseline HGF levels were predictors of longer PFS and OS

(**Table 4**). There was no correlation between HGF levels and patient survival in either the chemotherapy group or the combination (COMBO) group, supporting that HGF levels were predictive of patient survival only in the ICIs alone group (**Figure 3B-C**).

**Table 4: Cox proportional hazard analysis of patients's survival**

Variable	PFS			OS		
	Relative Risk (RR)	95% CI	p-value	Relative Risk (RR)	95% CI	p-value
HGF c (pg/ml) diag	1.0009	(1.0003- 1.0013)	0.0001	1.00061	(1.0003- 1.0009)	0.0001
HGF 1ère rééval	1.0003	(0.998 - 1.002)	0.751	1.0002	(0.999- 1.001)	0.7924
PS<1-1	0.373	(0.069 - 2.0196)	0.252	0.774	(0.27- 2.218)	0.633
ADK-1	0.119	(0.000 - 0.467)	0.002	0.192	(0.000 - 0.538)	0.002

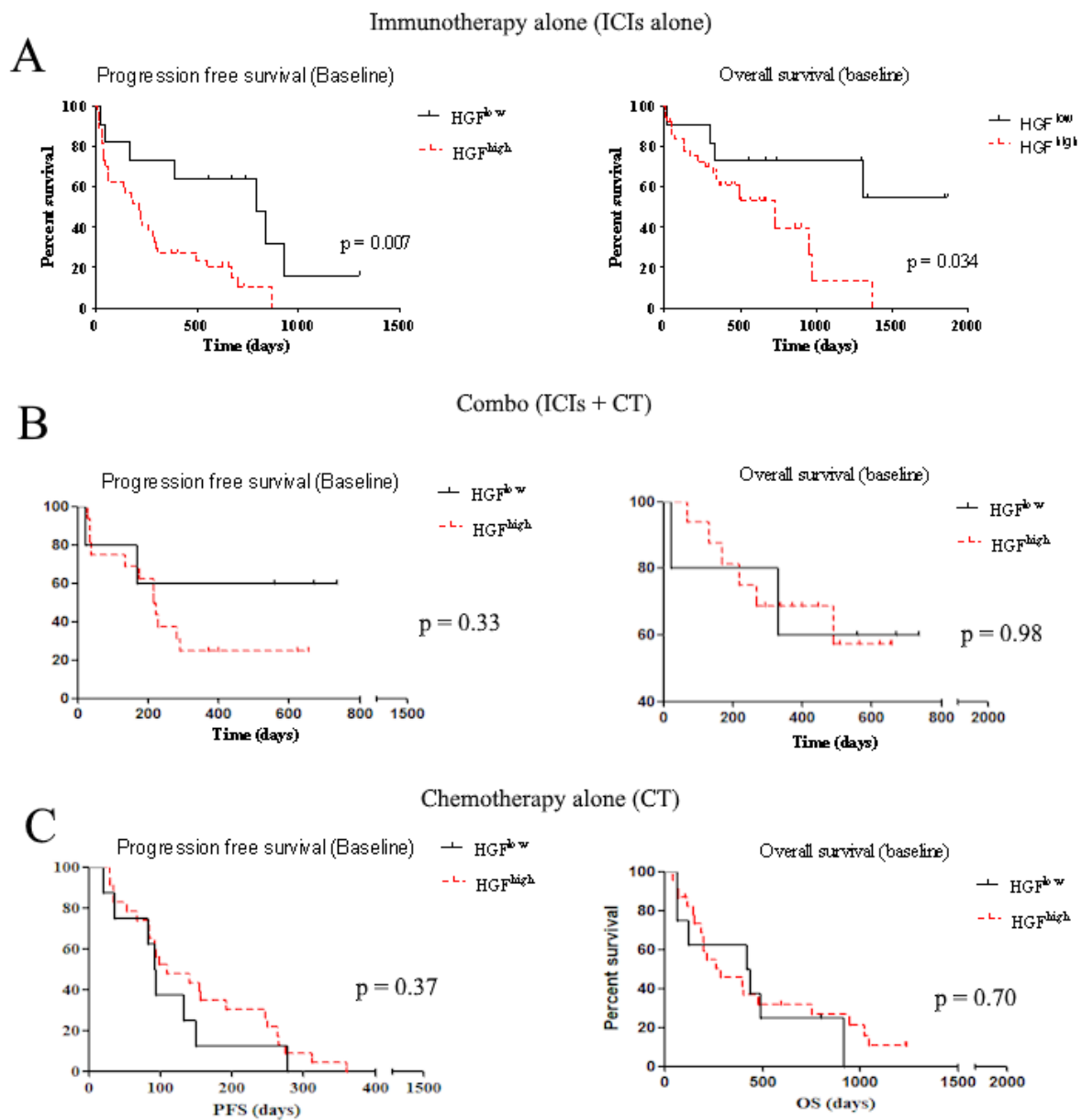


**Figure 3:** Patient's survival according to HGF expression levels.

Kaplan-Meier analyses of patient survival (PFS and OS) were conducted based on baseline HGF levels (low or high) within each treatment group, including Immunotherapy alone (A),

Immunotherapy associated with Chemotherapy (B), and Chemotherapy alone (C). The log-rank test was utilized to compare survival within each subgroup.

### **3.5 HGF suppresses lymphocyte proliferation and interferes with immunotherapy.**

We conducted a series of *in vitro* and *ex vivo* experiments to investigate the impact of the HGF/MET pathway on the modulation of ICI-mediated lymphocyte activation. Specifically, we analyzed the influence of HGF on the immune properties of immune cells in the presence and absence of pembrolizumab. First, we investigated whether NSCLC cells were a source of HGF production. Therefore, we analyzed the supernatants from A549 and H596 cell line cultures, as well as primary NSCLC cultures. Our data confirmed the production of high levels of HGF by NSCLC cells (**Figure 4A**). HGF production by primary samples was comparable to HGF levels measured in plasma samples from NSCLC patients (see 3.2), highlighting the relevance of our primary culture model in replicating HGF production in the tumor microenvironment. Then, we activated PBMC with PHA (10  $\mu$ M) and cultured them on a monolayer of primary NSCLC cells. Our findings indicated that pembrolizumab (20 nM) enhanced lymphocyte activation mediated by PHA. When lymphocytes were co-cultured with primary NSCLC cells, pembrolizumab-mediated lymphocyte activation was reduced. Furthermore, the addition of crizotinib (a MET inhibitor) into the culture medium partially restored T-cell proliferation in 3/5 of the coculture (**Figure 4B**). These experiments suggest that HGF produced by primary NSCLC cells can hinder the ability of pembrolizumab to restore LT immune activation.

To validate the immunosuppressive properties of HGF, we treated stimulated PBMC with

recombinant HGF. We compared the proliferation of LT cells in the presence of recombinant HGF and MET inhibitors (crizotinib, SGX-523). Following the administration of recombinant HGF, we observed a significant inhibition of PBMC proliferation and a decrease in IFN- $\gamma$  production compared to the control group stimulated with PHA alone (**Figure 5A-B**). These findings indicated that the presence of HGF suppressed PBMC proliferation and hampered the production of IFN- $\gamma$ , which is associated with the anti-tumor lymphocyte response. To further investigate this hypothesis, we performed flow cytometric analysis of the activated population of PBMC. The results revealed that recombinant HGF suppresses CD8+ activation, even in the presence of pembrolizumab. The CD8+ LT activation was restored using MET inhibitors (**Figure 5C-D**). These findings provide strong support for the notion that the release of HGF in the tumor microenvironment plays a significant role in immune evasion and contributes to resistance to immune checkpoint inhibitors. Consequently, the use of HGF/MET inhibitors has the potential to prevent immunosuppression and enhance the effectiveness of ICIs in the treatment of NSCLC.

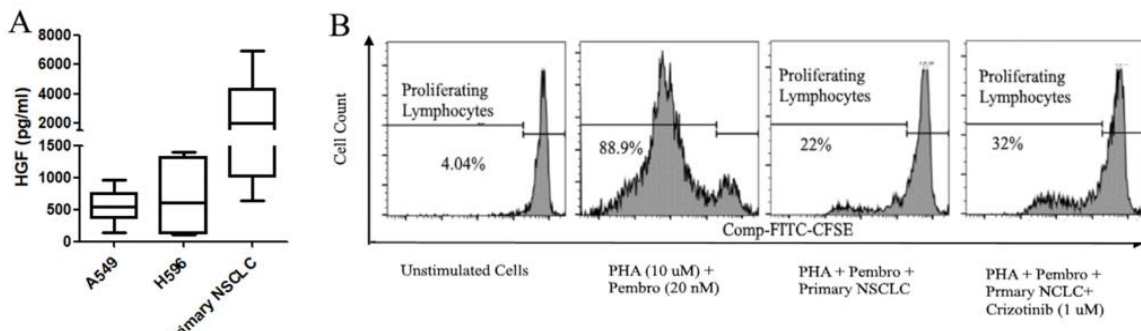


**Figure 4:** HGF production by NSCLC cells and inhibition of lymphocyte activation in the presence of pembrolizumab (“Pembro”) A) expression levels of HGF in NSCLC cell cultures were assessed using an ELISA assay. B) Peripheral blood mononuclear cells (PBMCs) were stained with CFSE and activated with phytohemagglutinin (PHA, 10  $\mu$ g/ml). These cells were then cultured either alone or on a primary NSCLC monolayer in the presence of Pembrolizumab and/or Crizotinib.

After 96 hours of incubation, CFSE-stained cells were collected and further stained with PE-Cy7-conjugated anti-CD3, BV421-conjugated anti-CD45, and APC-conjugated anti-CD8 antibodies. The cells were analyzed using flow cytometry (B). The presented data are representative of at least 6 patients.

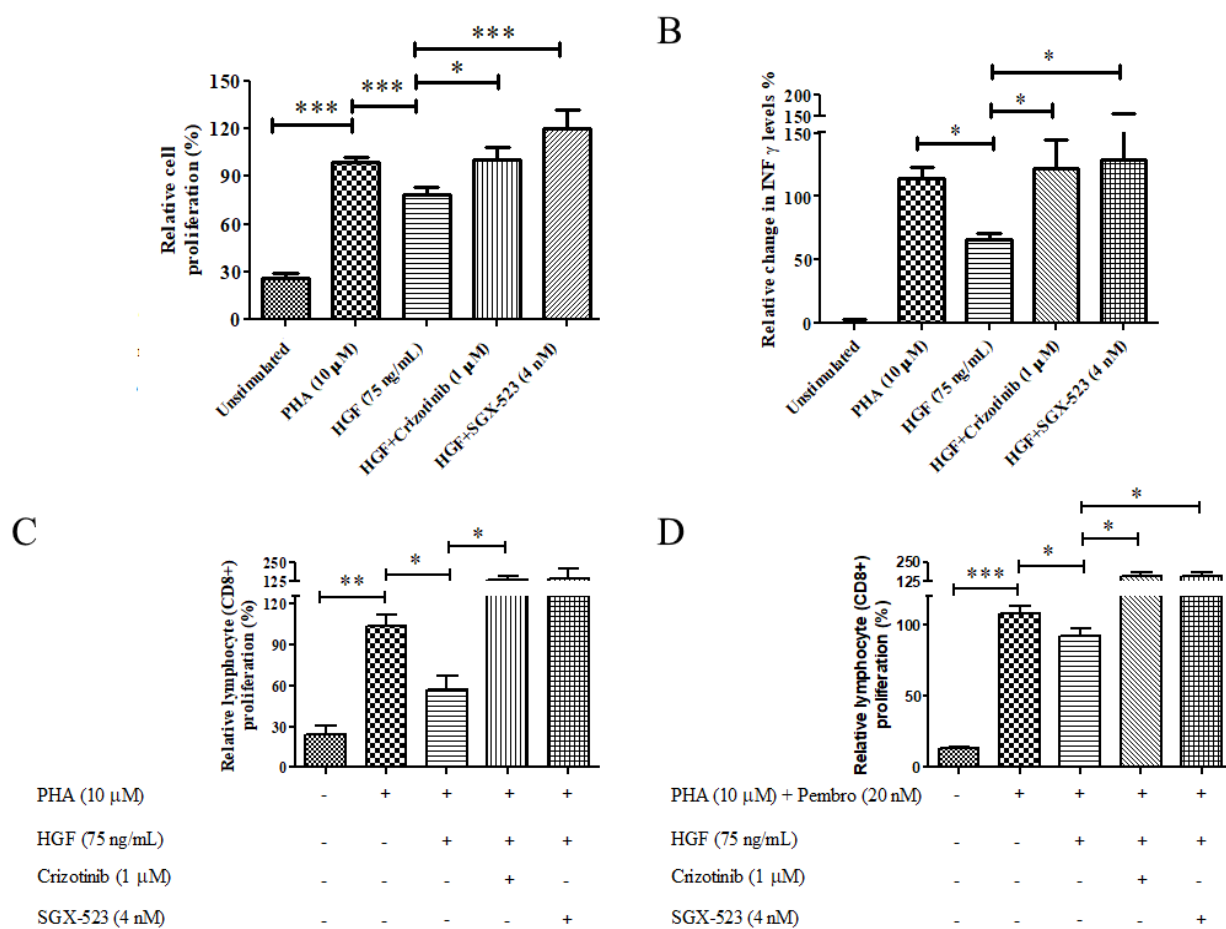


**Figure 5 :** MET inhibitors suppresses the immunosuppressive capabilities of recombinant HGF. A-B) Peripheral blood mononuclear cells (PBMCs) activated with phytohemagglutinin (PHA, 10  $\mu$ g/ml) were cultured either alone (A) or in the presence of hepatocyte growth factor (HGF, 75 ng/mL) and/or MET inhibitors (Crizotinib, SGX-523). The MTS proliferation assay was employed

to quantify lymphocyte/PBMC proliferation at 72 hours, while cell supernatants were collected at 24 hours for interferon-gamma (IFN $\gamma$ ) quantification. C-D) Activated PBMCs were stained with CFSE and treated for 96 hours with HGF (75 ng/mL) alone or in combination with Pembrolizumab (20 nm) and/or MET inhibitors (Crizotinib, SGX-523). The stained cells were collected, probed with PE-Cy7-conjugated anti-CD3, BV421-conjugated anti-CD45, and APC-conjugated anti-CD8 antibodies, and analyzed using flow cytometry. Data are presented as mean  $\pm$  SEM of at least four independent experiments. \*p < 0.05 and \*\*\*p < 0.001.

#### **4. DISCUSSION**

Identification of predictive biomarkers of IO resistance remains a significant challenge in lung cancer. In this study, we investigated the role of the HGF/MET pathway in immunotherapy resistance among NSCLC patients undergoing first-line treatment with ICIs, either alone or in combination with chemotherapy. Our data support the association of higher levels of plasma HGF with poor ORR and reduced survival among patients treated with ICIs.

The MET activation pathway plays a pivotal role in supporting the growth, survival, and drug resistance of various cancer types. Consequently, the predictive potential of HGF/MET expression has been explored across multiple malignancies<sup>12</sup>. Within the context of lung cancer, elevated MET expression and/or increased circulating HGF levels have been identified as signatures for both NSCLC and SCLC samples<sup>13,14</sup>. MET overexpression is associated with the activation of its receptor, the phosphorylated form of MET (pMET). Consistent with this pattern, we observed robust and consistent expression of pMET across most patients in the analyzed cohorts, including those treated with ICIs and chemotherapy (CT). However, as discussed by Moosavi et al.<sup>15</sup>, the

widespread and consistent expression of pMET observed across samples, while distinguishing tumor samples from normal tissues, cannot be used to stratify patients based on pMET levels, complicating the assessment of its influence on drug response and patient survival. Therefore, our investigation focused on plasma HGF levels, revealing that low levels of plasma HGF were associated with a favorable response to ICI treatment and a reduced progression rate. Similarly, patients with low HGF levels experienced significantly extended survival. These correlations were not observed in the CT group. Consequently, our results suggest that high baseline levels of HGF may not only serve as a prognostic factor, as previously suggested<sup>16,17</sup>, but also as a predictive factor for resistance to ICIs when used as first-line therapy in NSCLC.

HGF is primarily secreted by stromal cells, often through paracrine secretion, including mesenchymal cells. However, it can also be secreted directly by tumor cells, indicating autocrine secretion. This is highlighted by the presence of high levels of HGF in the supernatant of NSCLC primary cells and cell lines. The adverse prognostic significance of elevated serum HGF levels in cancer is substantiated by the fact that the activation of MET receptors located on cancer cells promotes tumor cell growth, survival, and metastatic spread<sup>16-18</sup>. In the context of the immune response and ICI therapy, the HGF/MET pathway has been reported as a mechanism of immune suppression. Through the modulation of dendritic cells, activation of regulatory T-cells, and the control of cytotoxic CD8+ T-cells<sup>19,20</sup> MET activation in tumor cells promotes various tumor properties, including the EMT, which may consequently enhance the immunosuppressive characteristics of tumor cells<sup>21,22</sup>. Notably, MET activation induces an increase in PD-L1 expression<sup>23</sup>. Interestingly, PD-L1 expression is also elevated after HGF administration, and there is a correlation between high MET activation and high PD-L1 expression<sup>24</sup>. Therefore, inhibiting MET-induced signaling could potentially block the HGF-induced PD-L1 expression<sup>25</sup>, thus

enhancing the efficacy of ICIs. Consistently, we present evidence in our work that the inhibition of MET activity using crizotinib interferes with NSCLC-mediating inhibition of CD8+ activation in the context of ICI inhibition, confirming the contribution of MET signaling in immune suppression as a mechanism of tumor-mediating resistance to ICIs. However, despite variations in HGF levels among patients, the levels of active MET in cancer cells did not differ significantly among patients, implying that MET activation in cancer cells may not be the main mechanism of immunosuppression mediated by HGF in NSCLC. In fact, it has been observed that CD8+ cytotoxic T lymphocytes (CTLs), when primed with specific antigens or exposed to the immune environment, express MET. Consequently, HGF could directly interfere with CTLs. We validated this hypothesis by demonstrating that recombinant HGF suppresses CTL activation and the production of IFN- $\gamma$ , even in the presence of pembrolizumab.

Our study supports a scenario in which HGF/MET pathway could participate in a concerted immunosuppressive mechanism within the tumor microenvironment, by enhancing the immunosuppressive properties of the microenvironment components and interfering with CTL activation. We provided evidence that the use of two MET pathway inhibitors, crizotinib and SGX-523, interferes with HGF-mediated suppression of CTL activation. Thus, the use of MET inhibitors appears to be an interesting therapeutic approach to enhance the efficacy of ICIs in patients with advanced NSCLC. Currently, various HGF/MET inhibitors are available or under development in clinical trials, including monoclonal antibodies (e.g., rilotumumab), drug-conjugated antibodies (e.g., Telisotuzumab vedotin), bi-specific antibodies (e.g., amivantamab)<sup>26</sup>, and MET-selective tyrosine kinase inhibitors (e.g., Tivantinib capmatinib, tepotinib or salvotinib).

Overall, despite the limitation in our study due to the insufficient number of available samples, notably for IHC, we managed to overcome this challenge by conducting a prospective collection

of plasma samples throughout the disease follow-up. This approach allowed us to perform a comparative analysis and longitudinally monitor the patients. Concurrently, we implemented functional in vitro and ex vivo studies using a model of primary cultures derived from surgical explants, providing a valuable representation of the tumor microenvironment. The results of these efforts collectively support the proposition that the HGF/MET pathway may serve as a potential predictive factor for the response to ICIs in advanced NSCLC.

## **CONCLUSION**

Our study's overall experiments emphasize the significant role of the HGF/MET pathway in inhibiting lymphocyte activation mediated by ICI in advanced NSCLC. In the ICI-treated patient group, we observed a correlation between high plasma HGF levels and criteria indicating tumor aggressiveness, a less favorable therapeutic response, and shorter survival. However, no such correlation was found in the group of patients treated with CT, suggesting a unique predictive role of this pathway in ICI resistance. As a result, assessing the expression of the HGF/MET pathway at the time of diagnosis, particularly through elevated plasma HGF levels, may serve as a predictive factor for a less favorable response to ICIs. Considering this, exploring the combination of HGF/MET inhibitors with ICIs in this context appears promising and warrants dedicated clinical trials for evaluation.

## **5. ETHICS, FUNDING AND DISCLOSURE**

### **5.1.Samples collection**

Primary samples were collected at Ambroise Paré Hospital after obtaining signed informed consent (CPP IDF n°8) and stored within the Centre de Ressources Biologiques (CRB) of Ambroise Paré Hospital (ID CRB 2014-A00187-40).

## **5.2.Funding**

This work was supported by Fondation du Souffle (2021)

## **5.3. Disclosure and conflict of interest**

Etienne Giroux Leprieur declare to have received honoraria/personal fees (advisory boards) from AstraZeneca, Bristol-Myers-Squibb MSD, and Roche.

The authors declare that they have no known competing financial interests or personal relationships that could have appeared to influence the work reported in this paper.

All the authors have accepted and validated the final version of this manuscript.

## **REFERENCES**

1. Pérez-Ruiz E, Melero I, Kopecka J, Sarmento-Ribeiro AB, García-Aranda M, De Las Rivas J. Cancer immunotherapy resistance based on immune checkpoints inhibitors: Targets, biomarkers, and remedies. *Drug Resist. Updat. Rev. Comment. Antimicrob. Anticancer Chemother.* 2020;53:100718. doi:10.1016/j.drup.2020.100718
2. Gandhi L, Rodríguez-Abreu D, Gadgeel S, Esteban E, Felip E, De Angelis F, Domine M, Clingan P, Hochmair MJ, Powell SF, et al. Pembrolizumab plus Chemotherapy in Metastatic Non-Small-Cell Lung Cancer. *N. Engl. J. Med.* 2018;378(22):2078–2092. doi:10.1056/NEJMoa1801005
3. Reck M, Rodríguez-Abreu D, Robinson AG, Hui R, Csőszi T, Fülöp A, Gottfried M, Peled N, Tafreshi A, Cuffe S, et al. Pembrolizumab versus Chemotherapy for PD-L1-Positive Non-Small-Cell Lung Cancer. *N. Engl. J. Med.* 2016;375(19):1823–1833. doi:10.1056/NEJMoa1606774
4. Paz-Ares L, Luft A, Vicente D, Tafreshi A, Gümüş M, Mazières J, Hermes B, Çay Şenler F, Csőszi T, Fülöp A, et al. Pembrolizumab plus Chemotherapy for Squamous Non-Small-Cell Lung Cancer. *N. Engl. J. Med.* 2018;379(21):2040–2051. doi:10.1056/NEJMoa1810865
5. Darvin P, Toor SM, Sasidharan Nair V, Elkord E. Immune checkpoint inhibitors: recent progress and potential biomarkers. *Exp. Mol. Med.* 2018;50(12):1–11. doi:10.1038/s12276-018-0191-1
6. Trusolino L, Bertotti A, Comoglio PM. MET signalling: principles and functions in development, organ regeneration and cancer. *Nat. Rev. Mol. Cell Biol.* 2010;11(12):834–848. doi:10.1038/nrm3012
7. Mazzone M, Comoglio PM. The Met pathway: master switch and drug target in cancer progression. *FASEB J. Off. Publ. Fed. Am. Soc. Exp. Biol.* 2006;20(10):1611–1621. doi:10.1096/fj.06-5947rev
8. Costantini A, Takam Kamga P, Julie C, Corjon A, Dumenil C, Dumoulin J, Ouaknine J, Giraud V, Chinet T, Rottman M, et al. Plasma Biomarkers Screening by Multiplex ELISA Assay in Patients with Advanced Non-Small Cell Lung Cancer Treated with Immune Checkpoint Inhibitors. *Cancers.* 2020;13(1):97. doi:10.3390/cancers13010097
9. Cheng Y, Wang C, Wang Y, Dai L. Soluble PD-L1 as a predictive biomarker in lung cancer: a systematic review and meta-analysis. *Future Oncol.* 2022;18(2):261–273. doi:10.2217/fon-2021-0641
10. Takam Kamga P, Mayenga M, Sebane L, Costantini A, Julie C, Capron C, Parent F, Seferian A, Guettier C, Emile J-F, et al. Colony stimulating factor-1 (CSF-1) signalling is predictive of response to immune checkpoint inhibitors in advanced non-small cell lung cancer. *Lung Cancer Amst. Neth.* 2024;188:107447. doi:10.1016/j.lungcan.2023.107447

11. Martkamchan S, Onlamoon N, Wang S, Pattanapanyasat K, Ammaranond P. The Effects of Anti-CD3/CD28 Coated Beads and IL-2 on Expanded T Cell for Immunotherapy. *Adv. Clin. Exp. Med. Off. Organ Wroclaw Med. Univ.* 2016;25(5):821–828. doi:10.17219/acem/35771
12. Gherardi E, Birchmeier W, Birchmeier C, Vande Woude G. Targeting MET in cancer: rationale and progress. *Nat. Rev. Cancer.* 2012;12(2):89–103. doi:10.1038/nrc3205
13. Tretiakova M, Salama AKS, Garrison T, Ferguson MK, Husain AN, Vokes EE, Salgia R. MET and phosphorylated MET as potential biomarkers in lung cancer. *J. Environ. Pathol. Toxicol. Oncol. Off. Organ Int. Soc. Environ. Toxicol. Cancer.* 2011;30(4):341–354. doi:10.1615/jenvironpatholtoxicoloncol.v30.i4.70
14. Arriola E, Cañadas I, Arumí-Uría M, Dómine M, Lopez-Vilariño JA, Arpí O, Salido M, Menéndez S, Grande E, Hirsch FR, et al. MET phosphorylation predicts poor outcome in small cell lung carcinoma and its inhibition blocks HGF-induced effects in MET mutant cell lines. *Br. J. Cancer.* 2011;105(6):814–823. doi:10.1038/bjc.2011.298
15. Moosavi F, Giovannetti E, Saso L, Firuzi O. HGF/MET pathway aberrations as diagnostic, prognostic, and predictive biomarkers in human cancers. *Crit. Rev. Clin. Lab. Sci.* 2019;56(8):533–566. doi:10.1080/10408363.2019.1653821
16. Masuya D, Huang C, Liu D, Nakashima T, Kameyama K, Haba R, Ueno M, Yokomise H. The tumour-stromal interaction between intratumoral c-Met and stromal hepatocyte growth factor associated with tumour growth and prognosis in non-small-cell lung cancer patients. *Br. J. Cancer.* 2004;90(8):1555–1562. doi:10.1038/sj.bjc.6601718
17. Navab R, Liu J, Seiden-Long I, Shih W, Li M, Bandarchi B, Chen Y, Lau D, Zu Y-F, Cescon D, et al. Co-overexpression of Met and Hepatocyte Growth Factor Promotes Systemic Metastasis in NCI-H460 Non-Small Cell Lung Carcinoma Cells. *Neoplasia N. Y. N.* 2009;11(12):1292–1300.
18. Tsuta K, Kozu Y, Mimae T, Yoshida A, Kohno T, Sekine I, Tamura T, Asamura H, Furuta K, Tsuda H. c-MET/phospho-MET protein expression and MET gene copy number in non-small cell lung carcinomas. *J. Thorac. Oncol. Off. Publ. Int. Assoc. Study Lung Cancer.* 2012;7(2):331–339. doi:10.1097/JTO.0b013e318241655f
19. Benkhoucha M, Santiago-Raber M-L, Schneiter G, Chofflon M, Funakoshi H, Nakamura T, Lalive PH. Hepatocyte growth factor inhibits CNS autoimmunity by inducing tolerogenic dendritic cells and CD25+Foxp3+ regulatory T cells. *Proc. Natl. Acad. Sci. U. S. A.* 2010;107(14):6424–6429. doi:10.1073/pnas.0912437107
20. Okunishi K, Dohi M, Nakagome K, Tanaka R, Mizuno S, Matsumoto K, Miyazaki J-I, Nakamura T, Yamamoto K. A novel role of hepatocyte growth factor as an immune regulator through suppressing dendritic cell function. *J. Immunol. Baltim. Md 1950.* 2005;175(7):4745–4753. doi:10.4049/jimmunol.175.7.4745

21. Rudisch A, Dewhurst MR, Horga LG, Kramer N, Harrer N, Dong M, Kuip H van der, Wernitznig A, Bernthaler A, Dolznig H, et al. High EMT Signature Score of Invasive Non-Small Cell Lung Cancer (NSCLC) Cells Correlates with NF $\kappa$ B Driven Colony-Stimulating Factor 2 (CSF2/GM-CSF) Secretion by Neighboring Stromal Fibroblasts. *PLOS ONE*. 2015;10(4):e0124283. doi:10.1371/journal.pone.0124283
22. Taki M, Abiko K, Ukita M, Murakami R, Yamanoi K, Yamaguchi K, Hamanishi J, Baba T, Matsumura N, Mandai M. Tumor Immune Microenvironment during Epithelial-Mesenchymal Transition. *Clin. Cancer Res. Off. J. Am. Assoc. Cancer Res.* 2021;27(17):4669–4679. doi:10.1158/1078-0432.CCR-20-4459
23. Garcia-Diaz A, Shin DS, Moreno BH, Saco J, Escuin-Ordinas H, Rodriguez GA, Zaretsky JM, Sun L, Hugo W, Wang X, et al. Interferon Receptor Signaling Pathways Regulating PD-L1 and PD-L2 Expression. *Cell Rep.* 2017;19(6):1189–1201. doi:10.1016/j.celrep.2017.04.031
24. Saigi M, Alburquerque-Bejar JJ, Mc Leer-Florin A, Pereira C, Pros E, Romero OA, Baixeras N, Esteve-Codina A, Nadal E, Brambilla E, et al. MET-Oncogenic and JAK2-Inactivating Alterations Are Independent Factors That Affect Regulation of PD-L1 Expression in Lung Cancer. *Clin. Cancer Res. Off. J. Am. Assoc. Cancer Res.* 2018;24(18):4579–4587. doi:10.1158/1078-0432.CCR-18-0267
25. Benkhoucha M, Tran NL, Breville G, Senoner I, Jandus C, Lalive P. c-Met enforces proinflammatory and migratory features of human activated CD4+ T cells. *Cell. Mol. Immunol.* 2021;18(8):2051–2053. doi:10.1038/s41423-021-00721-9
26. Glisson B, Besse B, Dols MC, Dubey S, Schupp M, Jain R, Jiang Y, Menon H, Nackaerts K, Orlov S, et al. A Randomized, Placebo-Controlled, Phase 1b/2 Study of Rilotumumab or Ganitumab in Combination With Platinum-Based Chemotherapy as First-Line Treatment for Extensive-Stage Small-Cell Lung Cancer. *Clin. Lung Cancer.* 2017;18(6):615–625.e8. doi:10.1016/j.cllc.2017.05.007

**Annexe #2: Predictive role of plasmatic biomarkers in advanced non-small cell lung cancer**

**treated by nivolumab**, publié dans *Oncoimmunology*. Travail de Master 2 sur le sPDL1.

Costantini A, Julie C, Dumenil C, Hélias-Rodzewicz Z, Tisserand J, Dumoulin J, Giraud V, Labrune S, Chinet T, Emile JF, Giroux Leprieur E. Predictive role of plasmatic biomarkers in advanced non-small cell lung cancer treated by nivolumab. *Oncoimmunology*. 2018 Apr 20;7(8):e1452581. doi: 10.1080/2162402X.2018.1452581. PMID: 30221046; PMCID: PMC6136870.



ORIGINAL RESEARCH

## Predictive role of plasmatic biomarkers in advanced non-small cell lung cancer treated by nivolumab

Adrien Costantini<sup>a,b</sup>, Catherine Julie<sup>a,c</sup>, Coraline Dumenil<sup>a,b</sup>, Zofia Hélias-Rodzewicz<sup>a,c</sup>, Julie Tisserand<sup>a,c</sup>, Jennifer Dumoulin<sup>a,b</sup>, Violaine Graud<sup>a,b</sup>, Sylvie Labrunie<sup>a,b</sup>, Thierry Chinet<sup>a,b</sup>, Jean-François Emile<sup>a,c</sup>, and Etienne Giroux Leprieur<sup>a,b</sup>

<sup>a</sup>EA340, UVSQ, Paris-Saclay University, Boulogne-Billancourt, France; <sup>b</sup>Department of Respiratory Diseases and Thoracic Oncology, APHP – Ambroise Paré Hospital, Boulogne-Billancourt, France; <sup>c</sup>Department of Pathology, APHP – Ambroise Paré Hospital, Boulogne-Billancourt, France

### ABSTRACT

Immune checkpoint inhibitors, as nivolumab, are used in advanced non-small cell lung cancer (NSCLC). However, no associated biomarker is validated in clinical practice with this drug. We investigated herein immune-related blood markers in patients with advanced NSCLC treated with nivolumab. Plasma of 43 consecutive patients were prospectively collected at time of the diagnosis of cancer, at the initiation of nivolumab and at the first tumour evaluation (2 months). Concentrations of PD-L1 (sPD-L1), soluble PD-L2 (sPD-L2), Interleukine-2 (sIL-2), Interferon-gamma (sIFN- $\gamma$ ), and Granzyme B (sGranB) were quantified by ELISA. Cell free RNA was quantified by Reverse Transcriptase -PCR, and plasmatic microRNAs (miRNAs) were evaluated by targeted sequencing. Expression of PD-L1 on tumour biopsies was performed by immunohistochemistry using E13LN. High sPD-L1 at 2 months and increase of sPD-L1 concentrations were associated with poor response and absence of clinical benefit (nivolumab treatment less than 6 months). The variation of sPD-L1 concentrations were confirmed by RNA quantification. sPD-L1 concentrations were not correlated with PD-L1 expression on corresponding tumour samples. Low sGranB at nivolumab initiation was also associated with poor response. High sPD-L1 and low sGranB were associated with poor progression-free survival (PFS) and overall survival (OS). Low sPD-L2, low sIL-2 and high sIFN- $\gamma$  were associated with grade 3–4 toxicities. Finally, miRNA screening showed that patients with clinical benefit ( $n = 9$ ) had down-expression of miRNA-320b and -375 compared to patients with early progression at 2 months ( $n = 9$ ). In conclusion, our results highlight the interest of circulating biomarkers in patients treated with nivolumab.

### ARTICLE HISTORY

Received 11 January 2018  
Revised 7 March 2018  
Accepted 9 March 2018

### KEYWORDS

nivolumab; non-small cell lung cancer; plasma; PD-L1; PD-L2; Granzyme B; Interleukine-2; Interferon- $\gamma$ ; microRNA; plasma; biomarker

### Introduction

Lung cancer is the leading cause of cancer related death worldwide.<sup>1</sup> Its prognosis, especially at the advanced stage, is poor with limited efficacy of cytotoxic chemotherapy (CT). Immune checkpoint inhibitors (ICIs), humanised monoclonal antibodies targeting programmed death 1 (PD-1) or programmed death-ligand 1 (PD-L1), have recently been developed. PD-L1 and programmed death-ligand (PD-L2) are membranous proteins expressed by malignant cells that interact with PD-1 expressed by T-cells. When PD-L1/PD-L2 and PD-1 bind, the T-cells' cytotoxic anti-tumour activity is down-regulated. By blocking the interaction between PD-L1 and PD-1, ICIs restore cytotoxic immune response. The Type I T helper (Th1)-related cytotoxic lymphocyte activation is mainly mediated by two effectors, interleukine-2 (IL-2) and interferon-gamma (IFN- $\gamma$ ).<sup>2,3</sup> After recognition of tumour antigens, activated CD8+ lymphocytes secrete perforins and granzymes (mainly Granzyme B) that induce tumour cell death.<sup>2</sup>

ICIs have shown their efficacy in advanced non-small cell lung cancer (NSCLC). Nivolumab, an anti-PD-1 antibody, is

currently used for second-line treatment in ALK- and EGFR-wild type advanced NSCLC.<sup>4,5</sup> There is however no biomarker predictive of nivolumab efficacy validated for clinical practice in this setting. In the two pivotal Checkmate studies,<sup>4,5</sup> PD-L1 immunohistochemistry (IHC) was performed on the tumour specimens obtained at the time of diagnosis. This analysis found that patients with non-squamous histology and high PD-L1 expression determined by IHC had longer progression-free survival (PFS) and overall survival (OS) than those with low PD-L1 expression.<sup>5</sup> These findings were not replicated in the squamous histology setting.<sup>4</sup> Patients were not stratified at randomisation according to PD-L1 IHC, which was performed retrospectively, rendering the interpretation of these results difficult. In addition, IHC was performed on the diagnostic tumour specimens whereas PD-L1 expression varies with time and especially after CT.<sup>6,7</sup> Moreover, PD-L1 IHC interpretation can be difficult, as there is a spatial heterogeneity of PD-L1 expression, within one same tumour region or between two different tumour regions (primary and metastatic).<sup>8-14</sup> There is therefore an unmet need for developing new biomarkers to

**CONTACT** Dr. Etienne Giroux Leprieur Etienne.giroux-leprieur@aphp.fr Department of Respiratory Diseases and Thoracic Oncology, APHP – Ambroise Paré Hospital, 9 avenue Charles de Gaulle, 92100 Boulogne-Billancourt, France.

Supplemental data for this article can be accessed at: <https://doi.org/10.1080/2162402X.2018.1452581>.  
© 2018 Taylor & Francis Group, LLC

predict nivolumab efficacy. Tumour mutation load or IFN- $\gamma$  signature have recently been evaluated,<sup>15,16</sup> but their use in clinical practice is still challenging.

Compared with tumour specimens, plasma has the advantage of being easily accessible, allowing sequential analysis during follow-up. Plasmatic biomarkers also have the advantage of reflecting different tumour clones present throughout the body. Circulating tumour DNA (ctDNA) has shown to be a good predictive marker of ICIs efficacy.<sup>17-19</sup> However, no study has been dedicated so far to other circulating biomarkers such as ICI-related proteins or circulating microRNA (miRNA). The presence of soluble PD-L1 (sPD-L1) has already been established in patients with NSCLC with a prognostic impact of sPD-L1 concentrations.<sup>20-22</sup> Its prognostic and predictive impact with ICIs is however still unknown.

In this study, we propose to evaluate new plasmatic biomarkers as putative predictive biomarkers associated with nivolumab efficacy and toxicity in advanced NSCLC: sPD-L1, sPD-L2, sGranzyme B (sGran B), sIL, sIFN- $\gamma$ , and circulating miRNA.

## Results

Characteristics of the 43 patients are presented in Table 1. Patients were mostly male (67%), current or former smokers (88%) and with adenocarcinoma histology (65%). They had advanced stage disease at diagnosis (93%) and mainly without EGFR-, KRAS- mutations or ALK -rearrangement (63%).

**Table 1.** Patients' characteristics.

Patient characteristics	Patients (n = 43)
Sex (%)	
Male	29 (67%)
Female	14 (33%)
Smoking history	
Current	14 (33%)
Former	24 (55%)
Non-smoker	5 (12%)
Histology	
Adenocarcinoma	28 (65%)
Squamous-cell carcinoma	9 (21%)
Sarcomatoid carcinoma	1 (2%)
Large cell carcinoma	4 (9%)
Clear cell carcinoma	1 (2%)
Stage at diagnosis	
II	3 (7%)
II-IV	40 (93%)
EGFR mutation	
KRAS mutation	
ALK rearrangement	
Other*	0 (0%)
Wild type	4 (10%)
Number of lines before nivolumab initiation	
1	23 (53%)
2	10 (23%)
3	2 (5%)
4	2 (5%)
Median age at nivolumab initiation	68 (IQR 62 - 71.5)
PS at nivolumab initiation	
0 - 1	25 (58%)
2	17 (40%)
3	1 (2%)

EGFR: Epidermal Growth Factor Receptor, ALK : Anaplastic Lymphoma Kinase, PS : Performance Status.

\*Other mutations: HER 2 (n = 1; 2%), BRAF (n = 3; 7%).

Nivolumab was given as second-line treatment in 67% of cases (further line in 33%), and patients had good PS (0 - 1) at nivolumab initiation in 58% of cases.

Objective Response Rate (ORR) with nivolumab in the global population was 40% (n = 17), and 35% (n = 15) had clinical benefit under nivolumab (as defined as still receiving nivolumab at 6 months). With a median follow-up of 16.3 months (IQR 11.7 - 21.1), 24 patients (56%) were deceased at the time of cut-off due to tumour progression, 11 patients (26%) had controlled disease, 5 (12%) were still receiving further treatment after nivolumab progression and 3 (6%) were lost during follow-up. The median nivolumab progression-free survival (PFS) was 3.0 months (IQR 1.6 - 10.1) and median overall survival (OS) was 6.2 months (IQR 2.2 - NR).

At initial diagnosis, nivolumab initiation and first tumour evaluation (2 months of treatment), median sPD-L1 concentrations were 39.81 pg/ml (IQR 29.75 - 59.21), 49.86 pg/ml (IQR 36.11 - 65.91) and 51.57 pg/ml (IQR 31.91 - 72.06), respectively; median sPD-L2 concentrations were 16390.00 pg/ml (IQR 11185.00 - 22335.50), 18250.00 pg/ml (IQR 13963.00 - 21750.00) and 17567.00 pg/ml (IQR 14384.50 - 22166.50), respectively; median sGranB concentrations were 14.06 pg/ml (IQR 9.84 - 21.13), 13.24 pg/ml (IQR 8.53 - 18.95) and 17.24 pg/ml (IQR 8.63 - 25.79), respectively; median sIL-2 concentrations were 188.00 pg/ml (IQR 113.00 - 227.50), 162.00 pg/ml (IQR 96.75 - 242.00) and 152.00 pg/ml (IQR 91.50 - 176.50), respectively; median sIFN- $\gamma$  concentrations were 0.13 pg/ml (IQR -0.03 - 0.29), 0.05 pg/ml (IQR -0.03 - 0.20) and 0.11 pg/ml (IQR -0.06 - 0.27), respectively.

## ORR, clinical benefit and survival

### sPD-L1

At initial diagnosis and at nivolumab initiation, there was no statistical difference in sPD-L1 concentrations in patients who were responders compared to non-responders to nivolumab (Supplementary Fig. 1A and 1B), and in patients presenting with clinical benefit compared to patients who did not present with clinical benefit (Supplementary Fig. 1C and 1D). However, at first tumour evaluation under nivolumab, sPD-L1 concentrations were significantly higher in non-responders with a median value of 67.64 pg/ml (IQR 46.36 - 75.14) compared to 32.94 pg/ml (IQR 24.89 - 58.91) in responders ( $p = 0.031$ ) (Fig. 1A). In the same way, median sPD-L1 concentrations were significantly higher in patients without clinical benefit with a median value of 67.64 pg/ml (IQR 42.74 - 75.45) compared to 34.14 pg/ml (IQR 24.67 - 56.48) in patients with clinical benefit ( $p = 0.024$ ) (Fig. 1B). Moreover, in case of increase of sPD-L1 concentrations between the initiation of nivolumab and first tumour evaluation ( $n = 12$ ), ORR was 17% ( $n = 2$ ) versus 68% ( $n = 13$ ) in case of decrease or stability of sPD-L1 concentrations ( $n = 19$ ) ( $p = 0.005$ ). The clinical benefit rate was 10% ( $n = 1$ ) in case of increase of sPD-L1 concentrations, versus 47% ( $n = 8$ ) in case of decrease or stability of sPD-L1 concentrations ( $n = 17$ ) ( $p = 0.049$ ).

Using ROC curves, we found a sPD-L1 cut-off concentration of 33.97 pg/ml associated with a sensitivity of 94%, a specificity of 56%, a positive predictive value (PPV) of 70% and a negative

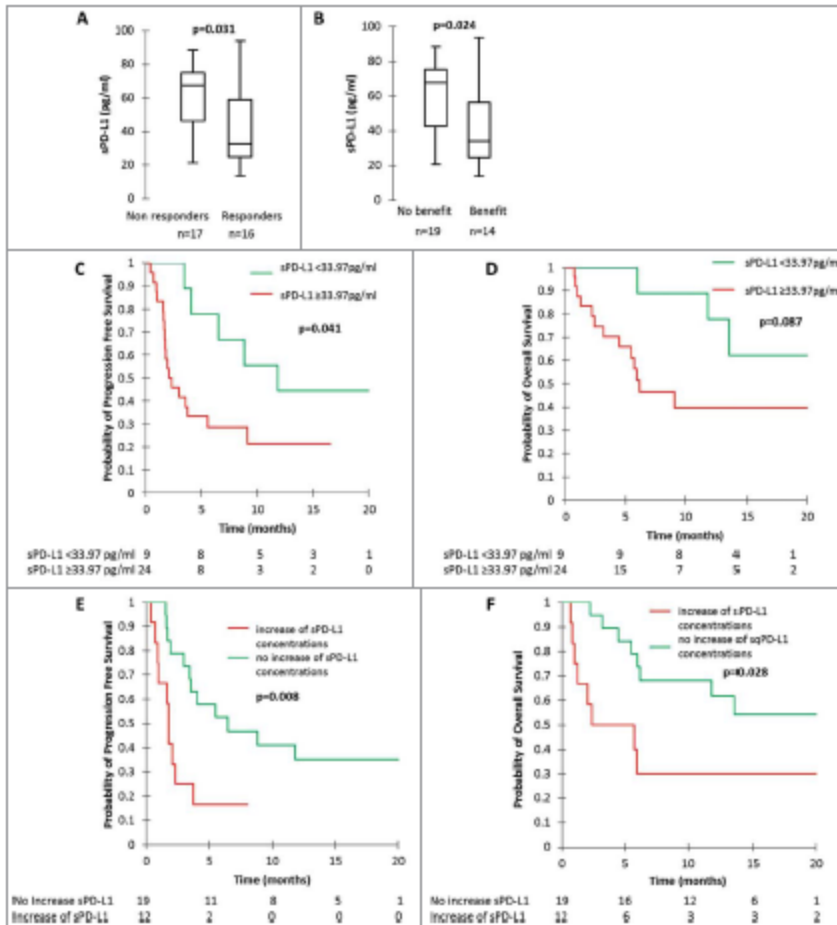


**Figure 1.** sPD-L1 and tumour response, clinical benefit, progression-free survival (PFS) and overall survival (OS). A: sPD-L1 concentrations at first tumour evaluation in patients with tumour response and patients without tumour response. B: sPD-L1 concentrations at first tumour evaluation in patients with clinical benefit and patients without clinical benefit. C and D: PFS (C) and OS (D) according to sPD-L1 concentration at first tumour evaluation. E and F: PFS (E) and OS (F) according to sPD-L1 variation between nivolumab initiation and first tumour evaluation. P-values were calculated by Mann-Whitney test (A and B) or log-rank test (C-F).

predictive value (NPV) of 90% to predict response at first tumor evaluation. Using this cut-off, we determined that patients with low sPD-L1 ( $n = 10$ ) had an ORR of 90% whilst patients who had high sPD-L1 concentrations ( $n = 23$ ) had an ORR of 30% ( $p = 0.002$ ). In the same way, we found a cut-off concentration of 36.36 pg/ml associated with a sensitivity of 84%, a specificity of 57%, a PPV of 73% and an NPV of 73% to predict clinical benefit. Using this cut-off, we determined that patients with low sPD-L1 concentrations ( $n = 11$ ) had clinical benefit in 73% of cases, whereas patients who had high sPD-L1 concentrations ( $n = 22$ ) had clinical benefit in 38% of cases ( $p = 0.013$ ).

We confirmed the variation of sPD-L1 by performing RT-PCR analysis on circulating RNA. Selecting the patients with the most important increase ( $n = 5$ ; ranging from +78% to +101%) and decrease ( $n = 5$ ; ranging from -39% to -69%) of sPD-L1 concentrations evaluated by ELISA, we showed that patients with sPD-L1 increase in ELISA had a significant

increase of PD-L1 expression ( $n = 3$ ; 2 patients without evaluable RT-PCR results). In the same way, patients with sPD-L1 decrease in ELISA had a significant decrease of PD-L1 expression ( $n = 2$ ; 3 patients without evaluable RT-PCR results) (Table 2).

High sPD-L1 concentrations at the first tumour evaluation and increase of sPD-L1 concentrations were associated with worse PFS and OS (Fig. 1 C-F). Patients with low sPD-L1 concentration at first tumour evaluation had a median PFS of 11.8 months (IQR 6.5 – NR) and median OS NR (IQR 13.6 – NR), versus median PFS of 2.2 months (IQR 1.6 – 9.1) and median OS of 6.2 months (IQR 2.4 – NR) for patients with high sPD-L1 concentrations at first tumour evaluation ( $p = 0.041$  for PFS comparison and  $p = 0.087$  for OS comparison) (Fig. 1C and 1D). Patients presenting with an increase of sPD-L1 concentrations had a median PFS of 1.8 months (IQR 0.9 – 3.0), versus 6.5 months (IQR 3.0 – NR) in patients presenting with a decrease or a stability of sPD-L1 concentrations ( $p =$

**Table 2.** Relative PD-L1 gene expression in plasma (evaluated by RT-PCR) in patients with the largest increase or decrease of sPD-L1 concentrations (evaluated by ELISA) between nivolumab initiation and first tumour evaluation.

	patients	relative change of sPD-L1 concentration (ELISA)	relative PD-L1 gene expression in plasma (RT-PCR)
patients with the largest sPD-L1 increase	patient #1	143%	NA
	patient #2	101%	5.60 ( $\pm$ 2.78)
	patient #3	93%	3.14 ( $\pm$ 0.12)
	patient #4	88%	NA
	patient #5	78%	2.05 ( $\pm$ 0.65)
patients with the largest sPD-L1 decrease	patient #1	-59%	NA
	patient #2	-51%	2.19E-17 ( $\pm$ 6.95E-19)
	patient #3	-45%	1.90E-19 ( $\pm$ 6.58E-21)
	patient #4	-41%	NA
	patient #5	-11%	NA

Relative change of sPD-L1 concentration (ELISA) is between nivolumab initiation and first tumour evaluation. Relative PD-L1 gene expression in plasma (RT-PCR) at first tumour evaluation is evaluated according to gene expression at nivolumab initiation. NA: non amplifiable RNA.

0.008). (Fig. 1E). Median OS was 5.4 months (IQR 1.1 – NR) in patients with increasing sPD-L1 concentrations, versus NR (6.0 – NR) in patients with stable or decreasing sPD-L1 concentrations ( $p = 0.028$ ). (Fig. 1F). Multivariate analysis on PFS (Table 3) confirmed the independent role of the increase of sPD-L1, with a hazard ratio (HR) at 4.85 (IC95% 1.02–NR;  $p = 0.048$ ). The only significant factor for OS in multivariate analysis was PS (PS more than 1 associated with a HR = 36.49; IC95% 4.56–291.76;  $p = 0.001$ ) (Table 4).

Finally, we analysed the outcome in patients with stable disease as best tumour response according to iRECIST ( $n = 5$ ). Interestingly, the two patients who had decreasing sPD-L1 levels had longer PFS (5.51 and 21.08 months) than patients who had increasing sPD-L1 levels (3.74, 2.33 and 2.07 months). Two examples of stable patients with differential outcome according to sPD-L1 measurements are shown in Supplementary Fig. 2.

Of the 43 patients included in the study, PD-L1 IHC was performed in 34 cases (79%) on diagnostic samples. Twenty-four patients (71%) had a positive PD-L1 expression. No association

**Table 3.** Multivariate analysis (Cox Model) on progression-free survival.

Variable	Hazard ratio (HR)	IC 95%	p-value
PS > 1	4.85	1.28–1835	0.020
sPD-L1 at first tumor evaluation (continuous variable)	0.99	0.97–1.01	0.467
sGranzyme B at nivolumab initiation (continuous variable)	0.99	0.94–1.04	0.628
Increase of sPD-L1 concentrations	4.85	1.02–NR	0.048
Increase sGranzyme B concentrations	1.82	0.61–5.43	0.284
IHC PD-L1 positive	0.79	0.26–2.42	0.681

**Table 4.** Multivariate analysis (Cox model) on overall survival.

Variable	Hazard ratio (HR)	IC 95%	p-value
PS > 1	36.49	4.56–291.76	0.001
sPD-L1 at first tumor evaluation (continuous variable)	0.98	0.95–1.01	0.129
sGranzyme B at nivolumab initiation (continuous variable)	1.00	0.94–1.07	0.966
Increase of sPD-L1 concentrations	4.15	0.64–27.03	0.136
Increase sGranzyme B concentrations	1.50	0.36–6.37	0.579
IHC PD-L1 positive	0.43	0.10–1.90	0.268

was observed between IHC positivity and sPD-L1 expression in IHC at the time of diagnosis: median sPD-L1 was 30.86 pg/ml (IQR 22.13 – 48.23) in patients with positive IHC and 36.68 pg/ml (IQR 26.10 – 55.34) in patients with negative IHC ( $p = 0.604$ ).

There was no correlation between sPD-L1 concentrations at diagnosis and level of expression of PD-L1 in IHC according to different cut-offs (Supplementary Fig. 3).

#### sGranzyme B

There was no statistical difference in sGran B concentrations measured at initial diagnosis and at first tumor evaluation in patients who were responders compared to non-responders (Supplementary Fig. 4A and 4B) and in patients presenting with clinical benefit compared to patients who did not present with clinical benefit (Supplementary Fig. 4C and 4D). However, at nivolumab initiation, responders had significantly higher median sGranzyme B concentrations than non-responders: 18.44 pg/ml (IQR 11.71 – 33.92) versus 11.88 pg/ml (IQR 7.94 – 15.41) ( $p = 0.039$ ) (Fig. 2A). In the same way, median sGran B concentrations tended to be higher in patients with clinical benefit with a median value of 67.64 pg/ml (IQR 42.74 – 75.45) compared to 34.14 pg/ml (IQR 24.67 – 56.48) in patients without clinical benefit ( $p = 0.116$ ) (Fig. 2B). There was also a trend towards a differential evolution of sGran B concentrations according to tumour response and clinical benefit: ORR was 29% ( $n = 4$ ) in case of increase of sGran B concentrations ( $n = 14$ ), versus 63% ( $n = 10$ ) in case of decrease or stability of sGran B concentrations ( $n = 16$ ) ( $p = 0.063$ ). In case of increase of sGran B concentrations ( $n = 14$ ), the clinical benefit rate was 21% ( $n = 3$ ), versus 56% ( $n = 9$ ) in case of decrease or a stability of sGran B concentrations ( $n = 16$ ) ( $p = 0.052$ ).

Using ROC curves, we found a cut-off concentration of 18.24 pg/ml associated with a sensitivity of 53%, a specificity of 87%, a PPV of 73% and an NPV of 74% to predict tumour response at nivolumab initiation. Using this cut-off, we determined that patients with high sGran B concentrations ( $n = 11$ ) had an ORR of 73%, whereas patients who had low sGran B concentrations ( $n = 27$ ) had an ORR of 26% ( $p = 0.007$ ).

Low sGran B concentrations at nivolumab initiation and increase of sGran B concentrations were also associated with worse PFS and OS (Fig. 2 C–F). Patients with high sGran B concentrations at nivolumab initiation had a median PFS of 8.8 months (IQR 3.7 – NR) and median OS NR (IQR 9.0 – NR), versus median PFS of 1.8 months (IQR 1.1 – 3.7) and median OS of 4.5 months (IQR 1.8 – NR) for patients with low sGran B

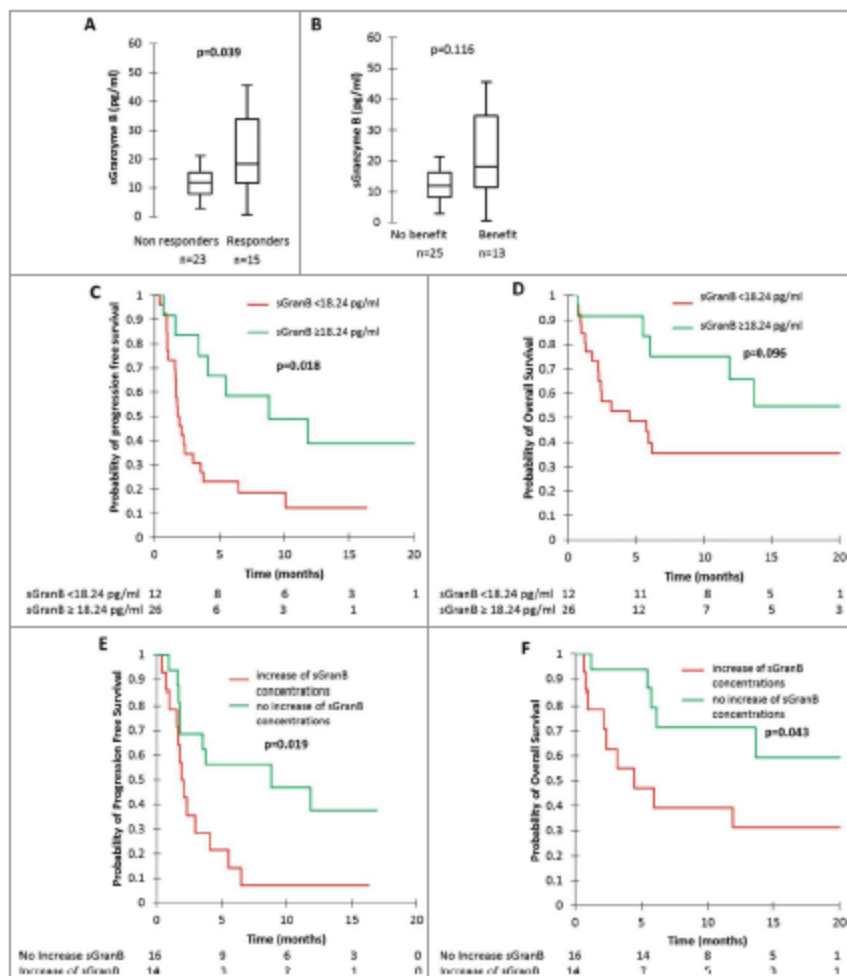


**Figure 2.** sGranzyme B (sGran B) and tumour response, clinical benefit, progression-free survival (PFS) and overall survival (OS). A: sGran B concentrations at nivolumab initiation in patients with tumour response and patients without tumour response. B: sGran B concentrations at nivolumab initiation in patients with clinical benefit and patients without clinical benefit. C and D: PFS (E) and OS (F) according to sGran B concentrations at nivolumab initiation. E and F: PFS (E) and OS (F) according to sGran B variation between nivolumab initiation and first tumour evaluation. P-values were calculated by Mann-Whitney test (A and B) or log-rank test (C-F).

concentrations at nivolumab initiation ( $p = 0.018$  for PFS comparison, and  $p = 0.096$  for OS comparison) (Fig. 3C and 3D). Patients presenting with an increase in sGran B concentrations had a median PFS of 2.0 months (IQR 1.6 – 4.1), versus 8.8 months (IQR 1.8–NR) in patients presenting with a decrease or a stability of sGran B concentrations ( $p = 0.019$ ) (Fig. 2E). Median OS was 4.5 months (IQR 2.2 – NR) in patients with increasing sGran B concentrations, versus NR (IQR 6.2 – NR) in patients with stable or decreasing sGranzyme B concentrations ( $p = 0.043$ ) (Fig. 2F).

#### sPD-L2, sIL-2 and sIFN- $\gamma$

There was no impact of sPD-L2, sIL-2 and sIFN- $\gamma$  concentrations and variations on ORR, clinical benefit, PFS or OS, at any time of analysis (Supplementary Figs. 5 and 6).

#### Immune related adverse events (irAEs)

Eight patients (19%) experienced grade 3–4 irAEs whilst receiving nivolumab: hypophysitis ( $n = 1$ ), arthro-myalgia ( $n = 1$ ), auto-immune cholangitis ( $n = 1$ ), auto-immune hepatitis ( $n = 1$ ), auto-immune kidney failure ( $n = 1$ ), interstitial pneumonia ( $n = 1$ ), skin toxicity ( $n = 1$ ), auto-immune colitis ( $n = 1$ ).

Of all the tested biomarkers, sPD-L2 at initial diagnosis and at nivolumab initiation, sIL-2 at nivolumab initiation and sIFN- $\gamma$  at first tumor evaluation were significantly associated with grade 3–4 irAEs with nivolumab (Fig. 3 and Supplementary Fig. 7).

#### miRNA

We performed miRNA screening on plasma at nivolumab initiation, and compared the miRNA profile between patients with

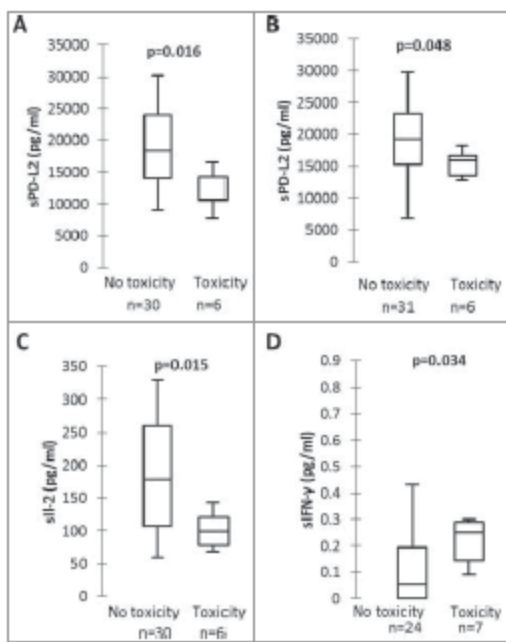


**Figure 3.** sPD-L2, sIL-2, sIFN- $\gamma$  and grade 3–4 toxicity with nivolumab. **A** and **B**: sPD-L2 concentrations at initial diagnosis (**A**) and at nivolumab initiation (**B**) in patients with grade 3–4 toxicity and patients without grade 3–4 toxicity. **C**: sIL-2 concentrations at nivolumab initiation in patients with grade 3–4 toxicity and patients without grade 3–4 toxicity. **D**: sIFN- $\gamma$  concentrations at first tumour evaluation in patients with grade 3–4 toxicity and patients without grade 3–4 toxicity. P-values were calculated by Mann-Whitney test.

clinical benefit ( $n = 9$ ) and patients with early progression (at first tumour evaluation) under nivolumab ( $n = 9$ ). We showed a differential expression of 2 miRNA between the 2 groups of patients (Supplementary Fig. 8), corresponding to miRNA-320b and miRNA-375. Patients with clinical benefit had a down-expression of both miRNA-320b (fold change -3.1) and -375 (fold change -3.2), compared to patients with early progression ( $p < 0.05$  for both miRNA). When analyzing target genes using miRecords, miRTarBase and TarBase databases, we found that miRNA-320b was notably associated with proliferation (*MYC*, *TUBB1*) genes, while miRNA-375 was notably associated with immune-related genes (*JAK2*, *TGF- $\beta$ 2*), Wnt pathway (*FZD4*, *FZD8*), proliferation (*MYC*), Hippo pathway (*YAP1*) and tumor migration (*NCAM1*, *CDH2*) genes.

## Discussion

This study reports for the first time the predictive role of plasmatic immune-related biomarkers and circulating miRNA in NSCLC patients treated with nivolumab. We showed that sPD-L1 and sGran B were associated with outcome, whereas sPD-L2, sIL-2 and sIFN- $\gamma$  were associated with nivolumab-related grade 3–4 toxicity. Finally, we observed that the plasmatic miRNA profile at the beginning of treatment was different between patients with objective response and patients with early progression under nivolumab.

Our results suggest that sPD-L1 may play an important part in evaluating response, survival and clinical benefit under nivolumab. sPD-L1 concentrations at first tumour evaluation and the variation of sPD-L1 concentrations at the beginning of treatment were associated with ORR and clinical benefit at six months. sPD-L1 also strongly impacted PFS and OS, with longer median PFS and OS in case of low sPD-L1 concentrations at first tumour evaluation or in case of decrease or stability of sPD-L1 concentrations between initiation of nivolumab and first tumour evaluation. sPD-L1 has already been studied in NSCLC, with results showing a higher sPD-L1 expression in patients with NSCLC than in healthy controls, and that patients had a better prognosis in case of higher sPD-L1 concentrations.<sup>20,21</sup> However, patients did not receive ICIs treatment in these studies. Furthermore, the patients did not have multiple sPD-L1 measurements and no dynamic analysis was performed. Finally, the moment of sampling was not specified beforehand with samples taken at different times (diagnosis, during treatment) rendering comparisons difficult. Another report studied the variation of sPD-L1 in patients with locally advanced or inoperable NSCLC undergoing radiotherapy.<sup>22</sup> This study showed that sPD-L1 levels measured after 2 and 4 weeks of radiotherapy significantly decreased compared to pre-radiotherapy levels and that patients with lower baseline sPD-L1 levels had longer OS than those with higher sPD-L1 levels.

We did not show a correlation between the sPD-L1 concentrations and the expression of PD-L1 in IHC performed on the initial biopsy. This can in part be explained by the use of two different antibodies for ELISA (28-8 clone) and for IHC (E13LN clone). However, recent publications have shown a good concordance between these two antibodies for PD-L1 expression in tumour cells.<sup>23</sup> The difference between ELISA and IHC could also be explained by the fact that plasma reflects the entire tumour heterogeneity, whereas PD-L1 expression can be heterogeneous within one tumour site, but also between different tumour sites.<sup>8–14</sup> Finally, sPD-L1 could also be secreted by cells other than tumour cells, such as immune cells. Interestingly, we confirmed the variation of sPD-L1 concentrations by RT-PCR from circulating RNA in patients with the largest variations of sPD-L1 concentrations. Circulating RNA is a mix of RNA from tumour cells and from other cells (immune cells, stroma cells...), so our results cannot precisely determine the source of sPD-L1. Little data is currently available on the origin and function of sPD-L1. The first hypothesis is that sPD-L1 concentrations reflect the tumour mass and that its presence in peripheral blood is due to the lysis of tumour cells. A high level of sPD-L1 would be the reflection of high tumour mass and the increase of sPD-L1 concentrations under nivolumab associated with poorer response could simply reflect the increase of the tumour volume. The second hypothesis is that sPD-L1 has its own biological effect. It could interfere with nivolumab by binding with PD-1 expressed by T lymphocytes and induce a competing effect with nivolumab. The low sPD-L1 concentrations at the beginning of treatment associated with better efficacy of nivolumab is compatible with such a hypothesis. A study is currently underway to try to determine which cells produce sPD-L1 in various malignancies (NCT01660776).

Granzyme B is a serine protease that is a mediator of target-cell apoptosis by cells such as NK cells and cytotoxic CD8+ T cells. Granzymes are delivered to the target cells via cytotoxic granules and are responsible for caspase-dependant apoptosis.<sup>24,25</sup> Soluble Granzyme B has already been explored in the context of auto-immune diseases, showing that high levels of sGran B were associated with rheumatoid arthritis, myocardial infarction and lipid-rich carotid plaques.<sup>26-28</sup> To our knowledge, this is the first time that sGran B concentrations have been evaluated in the plasma of NSCLC patients treated with nivolumab. We found that patients who presented with an objective response to nivolumab had significantly higher sGran B concentrations at nivolumab initiation than patients who were non-responders. This could reflect the activation of the CD8+ cytotoxic immune response, known to be associated with better response with ICIs. When analysing the variation of sGran B concentrations between nivolumab initiation and first tumour evaluation we found a tendency favouring patients with stable or decreasing concentrations for ORR, clinical benefit, OS and PFS. As for sPD-L1, an increase of sGran B at the beginning of the treatment could be the reflection of the persistence of a high tumour volume, with persistent CD8 lymphocytes activation and Granzyme B secretion. However, these hypotheses need to be validated in further studies.

The prediction of severe adverse events with ICIs remains a daily challenge. Even if grade 3–4 adverse events are rare with nivolumab,<sup>43</sup> they can be severe, impacting quality of life, sometimes life-threatening, and can lead to treatment interruption. We found that several immune-related plasmatic biomarkers were associated with grade 3–4 toxicity. Patients presenting grade 3–4 toxicity under nivolumab had lower sPD-L1 concentrations at initial diagnosis and at nivolumab initiation, lower sIL-2 concentrations at nivolumab initiation, and higher sIFN- $\gamma$  concentrations at first tumour evaluation. If confirmed, these results could help predict which patients are at risk for high-grade toxicity as early as the beginning of treatment, leading to close follow-up of such patients.

miRNA are non-coding RNA fragments with biological activity. Their role in solid cancers has been widely studied, and they have been shown to be involved in chemo-resistance.<sup>29</sup> Some publications have suggested an implication of miRNA in immune response regulation as well as PD-L1 and PD-1 expression regulation.<sup>30-41</sup> We report for the first time the association of down-regulation of circulating miRNA-320b and -375 expression and response to ICIs. miRNA-320b is down-regulated in various cancers, and it is associated with tumorigenesis and poor prognosis in glioma.<sup>42</sup> miRNA-375 was also shown to be often down-regulated in NSCLC,<sup>43,44</sup> breast cancer,<sup>45</sup> colorectal cancer,<sup>46-49</sup> oesophageal cancer,<sup>50,51</sup> gastric cancer,<sup>52,53</sup> and pancreatic cancer.<sup>54,55</sup> It is associated with tumour proliferation and metastases.<sup>44,48,51,54,56-59</sup> In NSCLC, miRNA-375 is associated with poor prognosis.<sup>43,44,60</sup> Interestingly, miRNA-375 is strongly associated with the Wnt/ $\beta$ -catenine pathway<sup>49</sup> and the Hippo pathway,<sup>59,61-63</sup> known to be involved in ICIs resistance.<sup>64-70</sup> Moreover, miRNA-375 targets the JAK2 gene,<sup>62,71</sup> involved in the IFN- $\gamma$  and TNF- $\alpha$  pathways, key-regulators of cytotoxic CD8+ immune response.<sup>72</sup> Taken together, these data, highlighted by our results, suggest an implication of both miRNA-320b and miRNA-375 in anti-

tumour immune response with ICIs, and the potential utility of screening for these miRNA in plasma before beginning nivolumab to select patients who will have response and clinical benefit with this treatment.

This study has several limitations. It is a monocentric study of small size, with a possibility of lack of power for some statistical analyses, especially for multivariate analyses. Nevertheless, despite this small population, we observed significant results on ORR, clinical benefit, survival and toxicity. Finally, to confirm the predictive value of sPD-L1 and sGran B it would be necessary to use a validation cohort with a control group. This study also has several strengths. We used a prospective cohort of patients with plasma samples. These samples were well characterised beforehand and underwent rigorous pre-analytical conditioning. Furthermore, our study presents multiple samples for each patient allowing dynamic analyses.

In conclusion, sPD-L1 and sGran B seem to be promising biomarkers associated with tumour response and clinical benefit with nivolumab, while sPD-L2, sIL-2 and sIFN- $\gamma$  were effective in predicting immune-related toxicities. Furthermore, the screening of circulating miRNA also seems to be an exciting research possibility. If confirmed, our results suggest that an approach integrating plasmatic immune-related biomarkers such as sPD-L1, sGran B or circulating miRNA could help us to rapidly detect patients who truly benefit from immunotherapy and, on the contrary, consider a rapid change of strategy in case of no anticipated clinical benefit. Further studies are needed, for validation of these biomarkers in a different cohort of patients and evaluation in other ICIs treatment settings (first-line treatment, combination of ICIs, ICIs and chemotherapy combined treatment).

## Materials and methods

### Experimental design

This study was an exploratory study, based on the analysis of consecutive patients prospectively included in the Department of Respiratory Medicine and Thoracic Oncology (APHP – Ambroise Paré Hospital) between July 2015 and September 2017. Exploratory endpoints were ORR, clinical benefit (*i.e.* complete response, partial response or stability, according to iRECIST, lasting 6 months or more after initiation of nivolumab treatment), PFS, OS, grade 3–4 toxicity (according to CTCAE v4.0), according to plasmatic concentrations of various circulating biomarkers. Differential analysis of plasmatic miRNA profiles between responders and patients with early progression with nivolumab was also planned.

### Patients and plasma

Tumour response was evaluated every two months using iRECIST criteria. Medical records were reviewed, and data retrospectively extracted on clinical and pathological features as well as treatment history. Plasma samples were taken at diagnosis, just before the first injection of nivolumab (C1), and at the first

tumour evaluation (at 2 months, M2) (Supplementary Fig. 9). Two 10ml-EDTA tubes of peripheral blood were taken, and plasma was isolated within one hour after and immediately conserved at -80°C.

#### Ethical considerations

All patients signed an informed consent allowing blood to be drawn and stored within the *Centre de Ressources Biologiques* (CRB) of the Ambroise Paré University Hospital during their follow-up and treatment. The protocol was approved by the Institutional Review Board CPP IDF n°8 (ID CRB 2014-A00187-40).

#### ELISA technique

sPD-L1, sPD-L2, sGran B, sIL-2, sIFN- $\gamma$  concentrations were calculated by ELISA. ELISA tests were performed using commercial kits (ab214565 Human PD-L1 [28-8] ELISA Kit, Abcam; BMS 2215 Human PD-L2 Platinum ELISA, Thermo Fisher Scientific; BMS 2027 Human Granzyme b Coated ELISA Kit, Thermo Fisher Scientific; ab174443 Human IFN gamma ELISA Kit, Abcam; ab174444 Human IL-2 ELISA Kit, Abcam) according to manufacturer's instructions. Corresponding recombinant proteins were used for each test at pre-specified concentrations to build standard curves. The results were obtained using a spectrophotometer (reading at 450nm), and concentrations were calculated according to the standard curves. All samples, standards and negative controls were tested in duplicate.

#### IHC technique

IHC was performed using an automated method (Leica) and the E13LN anti-PD-L1 antibody (Cell signalling Technology) diluted to the 1/80th on 4 $\mu$ m-slides from the treatment-naïve diagnostic samples. The assay was performed using human amygdala as positive control, and IgG as isotype negative control. The IHC was considered as being positive if at least one tumour cell out of 100 analysed tumour cells was positively stained.

#### Quantitative reverse-transcriptase polymerase chain reaction (RT-PCR)

Plasmatic RNAs were extracted using miRNeasy Serum/Plasma kit (Qiagen), according to manufacturer's instructions. RNA concentrations were evaluated by Nanodrop. cDNA was synthesized using iScript cDNA Synthesis Kit (Bio-Rad) according to the manufacturer's instructions. RT-PCR for PD-L1 gene expression was performed using specific Taqman primers and probes (Hs00204257\_m1, ThermoFisher) on 7900HT Fast Real-Time PCR System (Applied Biosystems). Gene expression analysis was calculated with the delta-delta CT method normalized to an endogenous control (RPLP0). All samples were tested in triplicate.

#### miRNA screening

Plasmatic miRNA were extracted using miRNeasy Serum/Plasma kit (Qiagen), according to manufacturer's instructions. miRNA concentrations were evaluated by BioAnalyzer. Screening of plasmatic miRNA was performed by targeted sequencing using TruSeq Small RNA kit (Illumina). Briefly, after a ligation step of miRNA with specific Illumina adapters, a RT-PCR was run. Banks of sequences were then analysed on HiSeq2500 (single read mode), with reading of 50 nucleotides (enough to cover the 19 to 22 bases of miRNA). After normalization and a trimmed mean calculation step,<sup>73</sup> a differential analysis of expressed miRNA between patients with clinical benefit and patients with early progression with nivolumab was performed.<sup>74,75</sup> After identification of miRNA differentially expressed, corresponding target genes were identified using miRecords, miRTarBase and TarBase databases.<sup>76</sup>

#### Statistical analysis

Median soluble concentrations of all the tested biomarkers were analysed according to ORR, clinical benefit, grade 3-4 toxicities. The comparison of median biomarker levels between groups was performed using Mann-Whitney test and interquartile range (IQR) is given for each value. Receiving Operating Curve (ROC) method was used to determine a cut-off level for each biomarker with a significant difference for endpoints with the Mann-Whitney test. Kaplan-Meier method was used to determine OS and PFS. Comparison between survival curves was performed using log-rank method. Multivariate analysis was performed using Cox proportional hazards model (PFS, OS), integrating experimental variables with significant result in univariate analyses, and known prognostic and predictive associated with ICIs (PS, PD-L1 IHC). Data analysis was computed using XIStat v 19.4 (Addinsoft). P-values were considered as significant if <0.05.

#### Disclosure statement

EGL received research funding from Bristol-Myers Squibb. Other authors did not have conflict of interest related to this project.

#### Funding

This work was supported by Bristol-Myers-Squibb.

#### References

1. Siegel RL, Miller KD, Jemal A. Cancer statistics, 2016. CA Cancer J Clin. 2016;66:7-30. doi:10.3322/caac.21332.
2. Martinez-Lostao L, Andl A, Pardo J. How Do Cytotoxic Lymphocytes Kill Cancer Cells? Clin Cancer Res. 2015;21:5047-56. doi:10.1158/1078-0432.CCR-15-0685. PMID:26567364.
3. Balkhi MY, Ma Q, Ahmad S, Junghans RP. T cell exhaustion and Interleukin 2 downregulation. Cytokine. 2015;71:339-47. doi:10.1016/j.cyto.2014.11.024. PMID:25516298.
4. Brahmer J, Reckamp KL, Baas P, Crino L, Eberhardt WEE, Poddubskaya E, Antonia S, Pluzanski A, Vokes EE, Holgado E, et al. Nivolumab versus Docetaxel in Advanced Squamous-Cell Non-Small-Cell Lung Cancer. N Engl J Med. 2015;373:123-35. doi:10.1056/NEJMoa1504627. PMID:26028407.

5. Borghaei H, Paz-Ares L, Horn L, Spigel DR, Steins M, Ready NE, Chow LQ, Vokes EE, Felip E, Holgado E, et al. Nivolumab versus Docetaxel in Advanced Nonsquamous Non-Small-Cell Lung Cancer. *N Engl J Med.* 2015;373:1627–39. doi:10.1056/NEJMoa1507643. PMID:26412456.
6. Sheng J, Fang W, Yu J, Chen N, Zhan J, Ma Y, Yang Y, Huang Y, Yan-huang null, Zhao H, et al. Expression of programmed death ligand-1 on tumor cells varies pre and post chemotherapy in non-small cell lung cancer. *Sci Rep.* 2016;6:20090. doi:10.1038/srep20090. PMID:26822379.
7. Lim SH, Hong M, Ahn S, Choi Y-L, Kim K-M, Oh D, Ahn YC, Jung S-H, Ahn M-J, Park K, et al. Changes in tumour expression of programmed death-ligand 1 after neoadjuvant concurrent chemoradiotherapy in patients with squamous oesophageal cancer. *Eur J Cancer* Oxf Engl 1990. 2016;52:1–9.
8. Kim S, Kim M-Y, Koh J, Go H, Lee DS, Jeon YK, Chung DH. Programmed death-1 ligand 1 and 2 are highly expressed in pleomorphic carcinomas of the lung: Comparison of sarcomatous and carcinomatous areas. *Eur J Cancer* Oxf Engl 1990. 2015;51:698–707.
9. Ilie M, Long-Mira E, Beno C, Butori C, Lassalle S, Bouhlel I, Fazzalari L, Zahaf K, Lalvée S, Washetine K, et al. Comparative study of the PD-L1 status between surgically resected specimens and matched biopsies of NSCLC patients reveal major discordances: a potential issue for anti-PD-L1 therapeutic strategies. *Ann Oncol Off J Eur Soc Med Oncol.* 2016;27:147–53. doi:10.1093/annonc/mdv489.
10. Li C, Huang C, Mok TS, Zhuang W, Xu H, Miao Q, Fan X, Zhu W, Huang Y, Lin X, et al. Comparison of 22C3 PD-L1 Expression between Surgically Resected Specimens and Paired Tissue Microarrays in Non-Small Cell Lung Cancer. *J Thorac Oncol Off Publ Int Assoc Study Lung Cancer.* 2017;12:1536–43.
11. Casadevall D, Clavé S, Taus Á, Hardy-Werbin M, Rocha P, Lorenzo M, Menéndez S, Salido M, Alband J, Pijuan I, et al. Heterogeneity of Tumor and Immune Cell PD-L1 Expression and Lymphocyte Counts in Surgical NSCLC Samples. *Clin Lung Cancer.* 2017;18:682–91.e5. doi:10.1016/j.cllc.2017.04.014. PMID:28549836.
12. Uruga H, Bozkurtlar E, Huynh TG, Muzikansky A, Goto Y, Gomez-Caraballo M, Hata AN, Gainor JF, Mark EJ, Engelman JA, et al. Programmed Cell Death Ligand (PD-L1) Expression in Stage II and III Lung Adenocarcinomas and Nodal Metastases. *J Thorac Oncol Off Publ Int Assoc Study Lung Cancer.* 2017;12:458–66.
13. Pinato DJ, Shiner RJ, White SDT, Black JRM, Trivedi P, Stebbing J, Sharma R, Mauri FA. Intra-tumoral heterogeneity in the expression of programmed-death (PD) ligands in isogenic primary and metastatic lung cancer: Implications for immunotherapy. *Oncoimmunology.* 2016;5:e1213934. doi:10.1080/2162402X.2016.1213934. PMID:27757309.
14. Mansfield AS, Aubry MC, Moser JC, Harrington SM, Dronca RS, Park SS, Dong H. Temporal and spatial discordance of programmed cell death-ligand 1 expression and lymphocyte tumor infiltration between paired primary lesions and brain metastases in lung cancer. *Ann Oncol Off J Eur Soc Med Oncol.* 2016;27:1953–8. doi:10.1093/annonc/mdw289.
15. Van Allen EM, Miao D, Schilling B, Shukla SA, Blank C, Zimmer L, Sucker A, Hillen U, Foppen MHG, Goldinger SM, et al. Genomic correlates of response to CTLA-4 blockade in metastatic melanoma. *Science.* 2015;350:207–11. doi:10.1126/science.aad0095. PMID:26359337.
16. Garcia-Diaz A, Shin DS, Moreno BH, Saco J, Escuin-Ordinés H, Rodriguez GA, Zaretsky JM, Sun L, Hugo W, Wang X, et al. Interferon Receptor Signaling Pathways Regulating PD-L1 and PD-L2 Expression. *Cell Rep.* 2017;19:1189–201. doi:10.1016/j.ccr.2017.04.031. PMID:28494868.
17. Cabel L, Riva F, Servois V, Livartowski A, Daniel C, Rampanou A, Lantz O, Romano E, Milder M, Buescher B, et al. Circulating tumor DNA changes for early monitoring of anti-PD1 immunotherapy: a proof-of-concept study. *Ann Oncol.* 2017;28:1996–2001. doi:10.1093/annonc/mdw212. PMID:28459943.
18. Iijima Y, Hirotsu Y, Amemiya K, Ooka Y, Mochizuki H, Oyama T, Nakagomi T, Uchida Y, Kobayashi Y, Tsutsui T, et al. Very early response of circulating tumour-derived DNA in plasma predicts efficacy of nivolumab treatment in patients with non-small cell lung cancer. *Eur J Cancer* Oxf Engl 1990. 2017;86:349–57.
19. Giroux Leprieur E, Herbetrau G, Dumenuil C, Julie C, Giraud V, Labrune S, Dumoulin J, Tisserand J, Emile J-F, Blons H, et al. Circulating tumor DNA evaluated by Next-Generation Sequencing is predictive of tumor response and prolonged clinical benefit with nivolumab in advanced non-small cell lung cancer. *OncoImmunology.* 2018. doi:10.1080/2162402X.2018.1424675.
20. Zhang J, Gao J, Li Y, Nie J, Dai L, Hu W, Chen X, Han J, Ma X, Tian G, et al. Circulating PD-L1 in NSCLC patients and the correlation between the level of PD-L1 expression and the clinical characteristics. *Thorac Cancer.* 2015;6:534–8. doi:10.1111/1759-7714.12247. PMID:26273411.
21. Okuma Y, Hosomi Y, Nakahara Y, Watanabe K, Sagawa Y, Homma S. High plasma levels of soluble programmed cell death ligand 1 are prognostic for reduced survival in advanced lung cancer. *Lung Cancer Amst Neth.* 2017;104:1–6. doi:10.1016/j.jlungcan.2016.11.023.
22. Zhao J, Zhang P, Wang J, Xi Q, Zhao X, Ji M, Hu G. Plasma levels of soluble programmed death ligand-1 may be associated with overall survival in nonsmall cell lung cancer patients receiving thoracic radiotherapy. *Medicine (Baltimore).* 2017;96:e6102. doi:10.1097/MD.000000000000102. PMID:28207525.
23. Adam J, Rouquette I, Damotte D, Badoval C, Daniel C, Damiola F, Penault-Llorca F, Lantuejoul S. Multicentric French Harmonization Study for PD-L1 IHC Testing in NSCLC. *J Thorac Oncol Off Publ Int Assoc Study Lung Cancer.* 2017;12 (Is)ePL04a.04.
24. Trapani JA, Sutton VR. Granzyme B: pro-apoptotic, antiviral and antitumor functions. *Curr Opin Immunol.* 2003;15:533–43. doi:10.1016/S0952-7915(03)00107-9. PMID:14499262.
25. Waterhouse NJ, Sutton VR, Sedelies KA, Ciccone A, Jenkins M, Turner SJ, Bird PI, Trapani JA. Cytotoxic T lymphocyte-induced killing in the absence of granzymes A and B is unique and distinct from both apoptosis and perforin-dependent lysis. *J Cell Biol.* 2006;173:133–44. doi:10.1083/jcb.200510072. PMID:16606695.
26. Tak PP, Spaeny-Dekking L, Kraan MC, Breedveld FC, Froelich CJ, Hack CE. The levels of soluble granzyme A and B are elevated in plasma and synovial fluid of patients with rheumatoid arthritis (RA). *Clin Exp Immunol.* 1999;116:366–70. doi:10.1046/j.1365-2249.1999.00881.x. PMID:10337032.
27. Kondo H, Hojo Y, Tsuru R, Nishimura Y, Shimizu H, Takahashi N, Hirose M, Ikemoto T, Ohya K-I, Katsuki T, et al. Elevation of plasma granzyme B levels after acute myocardial infarction. *Circ J Off J Jpn Circ Soc.* 2009;73:503–7.
28. Skjelland M, Michelsen AE, Krohg-Sorensen K, Terme B, Dahl A, Bakke S, Brostad F, Damis JK, Russell D, Halvorsen B, et al. Plasma levels of granzyme B are increased in patients with lipid-rich carotid plaques as determined by echogenicity. *Atherosclerosis.* 2007;195:e142–146. doi:10.1016/j.atherosclerosis.2007.05.001. PMID:17568588.
29. Naidu S, Garofalo M. microRNAs: An Emerging Paradigm in Lung Cancer Chemoresistance. *Front Med.* 2015;2:77. doi:10.3389/fmed.2015.00077..
30. Zhou S, Dong X, Zhang C, Chen X, Zhu J, Li W, Song X, Xu Z, Zhang W, Yang X, et al. MicroRNAs are implicated in the suppression of CD4+CD25+ conventional T cell proliferation by CD4+CD25+ regulatory T cells. *Mol Immunol.* 2015;63:464–72. doi:10.1016/j.molimm.2014.10.001. PMID:25457879.
31. Wei J, Ndoum EK, Kong L-Y, Hashimoto Y, Xu S, Gabrusiewicz K, Ling X, Huang N, Qiao W, Zhou S, et al. MiR-138 exerts anti-glioma efficacy by targeting immune checkpoints. *Neuro-Oncol.* 2016;18:639–48. doi:10.1093/neuonc/nov292. PMID:26658052.
32. Ali MA, Matboli M, Tarek M, Reda M, Kamal KM, Nouh M, Ashry AM, El-Bah AF, Mesalam HA, Shafei AE-S, et al. Epigenetic regulation of immune checkpoints: another target for cancer immunotherapy? *Immunotherapy.* 2017;9:99–108. doi:10.2217/imt-2016-0111. PMID:28000527.
33. Cioffi M, Trabulo SM, Vallespinos M, Raj D, Kheir TB, Lin M-L, Begum J, Baker A-M, Amgheib A, Saif J, et al. The miR-25-93-106b cluster regulates tumor metastasis and immune evasion via modulation of CXCL12 and PD-L1. *Oncotarget.* 2017;8:21609–25. doi:10.1863/oncotarget.15450. PMID:28423491.

34. Khorrami S, Zavarani Hosseini A, Mowla SJ, Soleimani M, Rakhshani N, Malekzadeh R. MicroRNA-146a induces immune suppression and drug-resistant colorectal cancer cells. *Tumour Biol J Int Soc Oncodevelopmental Biol Med*. 2017;39:1010428317698365. doi:10.1177/1010428317698365.
35. Xu C, Zhang Y, Wang Q, Xu Z, Jiang J, Gao Y, Gao M, Kang J, Wu M, Xiong J, et al. Long non-coding RNA GASS controls human embryonic stem cell self-renewal by maintaining NODAL signalling. *Nat Commun*. 2016;7:13287. doi:10.1038/ncomms13287. PMID:27811843.
36. Yeo D, Shah KM, Coles MC, Sharp TV, Lagoor D. MicroRNA-155 induction via TNF- $\alpha$  and IFN- $\gamma$  suppresses expression of programmed death ligand-1 (PD-L1) in human primary cells. *J Biol Chem*. 2017;292:20683–93. doi:10.1074/jbc.M117.809053. PMCID:PMC5733604.
37. Cortez MA, Ivan C, Valdecamas D, Wang X, Peltier HJ, Ye Y, Araujo I, Carbone DP, Shilo K, Giri DK, et al. PDL1 Regulation by p53 via miR-34. *J Natl Cancer Inst*. 2016;108:dvj303. doi:10.1093/jnci/dvj303. PMID:26577528.
38. Zhao L, Yu H, Yi S, Peng X, Su P, Xiao Z, Liu R, Tang A, Li X, Liu F, et al. The tumor suppressor miR-138-5p targets PD-L1 in colorectal cancer. *Oncotarget*. 2016;7:45370–84. PMID:27248318.
39. Zhu J, Chen L, Zou L, Yang P, Wu R, Mao Y, Zhou H, Li R, Wang K, Wang W, et al. MiR-20b, -21, and -130b inhibit PTEN expression resulting in B7-H1 over-expression in advanced colorectal cancer. *Hum Immunol*. 2014;75:348–53. doi:10.1016/j.humimm.2014.01.006. PMID:24468585.
40. Li Q, Johnston N, Zheng X, Wang H, Zhang X, Gao D, Min W. miR-28 modulates exhaustive differentiation of T cells through silencing programmed cell death-1 and regulating cytokine secretion. *Oncotarget*. 2016;7:53735–50. PMID:27447564.
41. Wang X, Li J, Dong K, Lin F, Long M, Ouyang Y, Wei J, Chen X, Weng Y, He T, et al. Tumor suppressor miR-34a targets PD-L1 and functions as a potential immunotherapeutic target in acute myeloid leukemia. *Cell Signal*. 2015;27:443–52. doi:10.1016/j.cellsig.2014.12.003. PMID:25499621.
42. Lv Q-L, Du H, Liu Y-L, Huang Y-T, Wang G-H, Zhang X, Chen S-H, Zhou H-H. Low expression of microRNA-320b correlates with tumorigenesis and unfavorable prognosis in glioma. *Oncol Rep*. 2017;38:959–66. doi:10.3892/or.2017.5762. PMID:28656255.
43. Li Y, Jiang Q, Xia N, Yang H, Hu C. Decreased expression of microRNA-375 in nonsmall cell lung cancer and its clinical significance. *J Int Med Res*. 2012;40:1662–9. doi:10.1177/030006051204000505. PMID:23206448.
44. Chen L-J, Li X-Y, Zhao Y-Q, Liu W-J, Wu H-J, Liu J, Mu X-Q, Wu H-B. Down-regulated microRNA-375 expression as a predictive biomarker in non-small cell lung cancer brain metastasis and its prognostic significance. *Pathol Res Pract*. 2017;213:882–8. doi:10.1016/j.prp.2017.06.012. PMID:28688608.
45. Zou Q, Yi W, Huang J, Fu F, Chen G, Zhong D. MicroRNA-375 targets PAX6 and inhibits the viability, migration and invasion of human breast cancer MCF-7 cells. *Exp Ther Med*. 2017;14:1198–204. doi:10.3892/etm.2017.4593. PMID:28810579.
46. Dai X, Chiang Y, Wang Z, Song Y, Lu C, Gao P, Xu H. Expression levels of microRNA-375 in colorectal carcinoma. *Mol Med Rep*. 2012;5:1299–304. PMID:22377847.
47. Xu L, Li M, Wang M, Yan D, Feng G, An G. The expression of microRNA-375 in plasma and tissue is matched in human colorectal cancer. *BMC Cancer*. 2014;14:714. doi:10.1186/1471-2407-14-714. PMID:25255814.
48. Alami KJ, Mo J-S, Han S-H, Park W-C, Kim H-S, Yun K-J, Chae S-C. MicroRNA 375 regulates proliferation and migration of colon cancer cells by suppressing the CTGF-EGFR signaling pathway. *Int J Cancer*. 2017;141:1614–29. doi:10.1002/ijc.30861. PMID:28670764.
49. Xu L, Wen T, Liu Z, Xu F, Yang L, Liu J, Feng G, An G. MicroRNA-375 suppresses human colorectal cancer metastasis by targeting Frizzled 8. *Oncotarget*. 2016;7:40644–56. PMID:27276676.
50. Lv H, He Z, Wang H, Du T, Pang Z. Differential expression of miR-21 and miR-75 in esophageal carcinoma patients and its clinical implication. *Am J Transl Res*. 2016;8:3288–98. PMID:27508050.
51. Hu G, Lv L, Peng J, Liu D, Wang X, Zhou Y, Huo J. MicroRNA-375 suppresses esophageal cancer cell growth and invasion by repressing metadherin expression. *Oncol Lett*. 2017;13:4769–75. doi:10.3892/ol.2017.6098. PMID:28599478.
52. Lee SW, Park KC, Kim JG, Moon SJ, Kang SB, Lee DS, Sul HJ, Ji JS, Jeong HY. Dysregulation of MicroRNA-196b-5p and MicroRNA-375 in Gastric Cancer. *J Gastric Cancer*. 2016;16:221–9. doi:10.5230/jgc.2016.16.4.221. PMID:28053808.
53. Lian S, Park JS, Xia Y, Nguyen TT, Joo YE, Kim KK, Kim HK, Jung YD. MicroRNA-375 Functions as a Tumor-Suppressor Gene in Gastric Cancer by Targeting Recepteur d'Origine Nantais. *Int J Mol Sci*. 2016;17:p. 1633. doi:10.3390/ijms17101633.
54. Zhou J, Song S, Cen J, Zhu D, Li D, Zhang Z. MicroRNA-375 is downregulated in pancreatic cancer and inhibits cell proliferation in vitro. *Oncol Res*. 2012;20:197–203. doi:10.3727/096504013X13589503482734. PMID:23581226.
55. Song S, Zhou J, He S, Zhu D, Zhang Z, Zhao H, Wang Y, Li D. Expression levels of microRNA-375 in pancreatic cancer. *Biomed Rep*. 2013;1:393–8. doi:10.3892/br.2013.88. PMID:24648956.
56. Cui F, Wang S, Lao I, Zhou C, Kong H, Bayaxi N, Li J, Chen Q, Zhu T, Zhu H. miR-375 inhibits the invasion and metastasis of colorectal cancer via targeting SPI1 and regulating EMT-associated genes. *Oncol Rep*. 2016;36:487–93. doi:10.3892/or.2016.4834. PMID:27222350.
57. Yang D, Yan R, Zhang X, Zhu Z, Wang C, Liang C, Zhang X. Derepression of MicroRNA-375 inhibits cancer proliferation, migration and chemosensitivity in pancreatic cancer through the association of HOXB3. *Am J Transl Res*. 2016;8:1551–9. PMID:27186281.
58. Kong KI, Kwong DLW, Chan TH-M, Law SY-K, Chen I, Li Y, Qin Y-R, Guan X-Y. MicroRNA-375 inhibits tumour growth and metastasis in oesophageal squamous cell carcinoma through repressing insulin-like growth factor 1 receptor. *Gut*. 2012;61:33–42. doi:10.1136/gutjnl-2011-300178. PMID:21813472.
59. Liu AM, Poon RTP, Luk JM. MicroRNA-375 targets Hippo-signaling effector YAP in liver cancer and inhibits tumor properties. *Biophys Res Commun*. 2010;394:623–7. doi:10.1016/j.bbrc.2010.03.036. PMID:20226166.
60. Shao Y, Geng Y, Gu W, Huang J, Ning Z, Pei H. Prognostic significance of microRNA-375 downregulation in solid tumors: a meta-analysis. *Dis Markers*. 2014;2014:626185. doi:10.1155/2014/626185. PMID:25404787.
61. Hu Y, Wang L, Gu J, Qu K, Wang Y. Identification of microRNA differentially expressed in three subtypes of non-small cell lung cancer and in silico functional analysis. *Oncotarget*. 2017;8:74554–66. PMID:29088807.
62. Chen X, Li B, Liao R, Cai S, Zhang C, Cao X. Analysis of the function of microRNA-375 in humans using bioinformatics. *Biomed Rep*. 2017;6:561–6. doi:10.3892/br.2017.889. PMID:28515914.
63. Selth LA, Das R, Townley SL, Coutinho I, Hanson AR, Centenera MM, Stylianou N, Sweeney K, Soekmadji C, Jovanovic I, et al. A ZEB1-miR-375-YAP1 pathway regulates epithelial plasticity in prostate cancer. *Oncogene*. 2017;36:24–34. doi:10.1038/onc.2016.185. PMID:27270433.
64. Spranger S, Gajewski TF. A new paradigm for tumor immune escape:  $\beta$ -catenin-driven immune exclusion. *J Immunother Cancer*. 2015;3:43. doi:10.1186/40425-015-0089-6. PMID:26380088.
65. Ramor RN, Piaggio E, Romano E. Mechanisms of Resistance to Immune Checkpoint Antibodies. *Handb Exp Pharmacol*. 2017; doi:10.1007/164\_2017\_11. PMID:28315073. [Epub ahead of print]
66. Moroishi T, Hayashi T, Pan W-W, Fujita Y, Holt MV, Qin J, Carson DA, Guan K-L. The Hippo Pathway Kinases LATS1/2 Suppress Cancer Immunity. *Cell*. 2016;167:1525–39.e17. doi:10.1016/j.cell.2016.05.017. PMID:27044666.
67. Siemers NO, Holloway JL, Chang H, Chasalow SD, Ross-McDonald PB, Voliva CF, Szustakowski JD. Genome-wide association analysis identifies genetic correlates of immune infiltrates in solid tumors. *PLoS One*. 2017;12:e0179726. doi:10.1371/journal.pone.0179726. PMID:28749946.
68. Kakavandi H, Rawson RV, Pupo GM, Yang JYH, Menzies AM, Carlino MS, Kefford RF, Howle JR, Saw RPM, Thompson JE, et al. PD-L1 Expression and Immune Escape in Melanoma Resistance to MAPK

- Inhibitors. *Clin Cancer Res Off J Am Assoc Cancer Res.* 2017;23:6054–61. doi:10.1158/1078-0432.CCR-16-1688.
69. Pai SG, Carneiro BA, Mota JM, Costa R, Leite CA, Barroso-Sousa R, Kaplan JB, Chae YK, Giles FJ. Wnt/beta-catenin pathway: modulating anticancer immune response. *J Hematol Oncol Hematol Oncol.* 2017;10:101. doi:10.1186/s13045-017-0471-6..
70. Massi D, Romano E, Rulli E, Merelli B, Nassini R, De Logu F, Bieche I, Baroni G, Cattaneo I, Xue G, et al. Baseline  $\beta$ -catenin, programmed death-ligand 1 expression and tumour-infiltrating lymphocytes predict response and poor prognosis in BRAF inhibitor-treated melanoma patients. *Eur J Cancer Oxf Engl 1990.* 2017;78:70–81.
71. Wei R, Yang Q, Han B, Li Y, Yao K, Yang X, Chen Z, Yang S, Zhou J, Li M, et al. microRNA-375 inhibits colorectal cancer cells proliferation by downregulating JAK2/STAT3 and MAP3K8/ERK signaling pathways. *Oncol Lett.* 2017;8:16633–41. PMID:28186962.
72. Wang J, Huang H, Wang C, Liu X, Hu F, Liu M. MicroRNA-375 sensitizes tumour necrosis factor-alpha (TNF- $\alpha$ )-induced apoptosis in head and neck squamous cell carcinoma in vitro. *Int J Oral Maxillofac Surg.* 2013;42:949–55. doi:10.1016/j.ijom.2013.04.016. PMID:23726271.
73. Robinson MD, Oshlack A. A scaling normalization method for differential expression analysis of RNA-seq data. *Genome Biol.* 2010;11:R25. doi:10.1186/gb-2010-11-3-r25. PMID:20196867.
74. Robinson MD, McCarthy DJ, Smyth GK. edgeR: a Bioconductor package for differential expression analysis of digital gene expression data. *Bioinformatics.* 2010;26:139–40. doi:10.1093/bioinformatics/btp616. PMID:19910308.
75. McCarthy DJ, Chen Y, Smyth GK. Differential expression analysis of multifactor RNA-Seq experiments with respect to biological variation. *Nucleic Acids Res.* 2012;40:4288–97. doi:10.1093/nar/gks042. PMID:22287627.
76. Ru Y, Kechriz KJ, Tabakoff B, Hoffman P, Radcliffe RA, Bowler R, Mahafey S, Rossi S, Calin GA, Bemis L, et al. The multiMiR R package and database integration of microRNA-target interactions along with their disease and drug associations. *Nucleic Acids Res.* 2014;42:e133–e133. doi:10.1093/nar/gku631. PMID:25063298.

**Annexe #3: Plasma Biomarkers and Immune Checkpoint Inhibitors in Non-Small Cell Lung Cancer: New Tools for Better Patient Selection?** Publié dans *Cancers*. Revue de la literature sur les biomarqueurs plasmatiques et immunothérapie (1e auteur).

Costantini A, Takam Kamga P, Dumenil C, Chinet T, Emile JF, Giroux Leprieur E. Plasma Biomarkers and Immune Checkpoint Inhibitors in Non-Small Cell Lung Cancer: New Tools for Better Patient Selection? *Cancers* (Basel). 2019 Aug 29;11(9):1269. doi: 10.3390/cancers11091269. PMID: 31470546; PMCID: PMC6769436.

*Review*

# Plasma Biomarkers and Immune Checkpoint Inhibitors in Non-Small Cell Lung Cancer: New Tools for Better Patient Selection?

Adrien Costantini <sup>1,2</sup> , Paul Takam Kamga <sup>2</sup> , Coraline Dumenil <sup>1,2</sup> , Thierry Chinet <sup>1,2</sup> , Jean-François Emile <sup>2,3</sup>  and Etienne Giroux Leprieur <sup>1,2,\*</sup>

<sup>1</sup> Department of Respiratory Diseases and Thoracic Oncology, APHP—Hôpital Ambroise Paré, 92100 Boulogne-Billancourt, France

<sup>2</sup> EA 4340 BECCOH, UVSQ, Université Paris Saclay, 92100 Boulogne-Billancourt, France

<sup>3</sup> Department of Pathology, APHP—Hôpital Ambroise Paré, 92100 Boulogne-Billancourt, France

\* Correspondence: etienne.giroux-leprieur@aphp.fr; Tel.: +33-149-095-802; Fax: +33149095806



Received: 31 July 2019; Accepted: 22 August 2019; Published: 29 August 2019

**Abstract:** Immune checkpoint inhibitors (ICIs) have transformed the treatment landscape for patients with non-small cell lung cancer (NSCLC). Although some patients can experience important response rates and improved survival, many others do not benefit from ICIs developing hyper-progressive disease or immune-related adverse events. This underlines the need to select biomarkers for ICIs use in order to better select patients. There is currently no universally validated robust biomarker for daily use of ICIs. Programmed death-ligand 1 (PD-L1) or tumor mutational burden (TMB) are sometimes used but still have several limitations. Plasma biomarkers are a promising approach in ICI treatment. This review will describe the development of novel plasma biomarkers such as soluble proteins, circulating tumor DNA (ctDNA), blood TMB, and blood microbiome in NSCLC patients treated with ICIs and their potential use in predicting response and toxicity.

**Keywords:** non-small cell lung cancer; plasma; biomarkers; immune checkpoint inhibitor

## 1. Introduction

Immune checkpoint inhibitors (ICIs) are humanized monoclonal antibodies that mainly target programmed death 1 (PD-1), programmed death-ligand 1 (PD-L1), or cytotoxic T-lymphocyte-associated protein 4 (CTLA-4). They are currently transforming treatment strategies across numerous cancer types and especially advanced non-small cell lung cancer (NSCLC) [1–7].

PD-L1 and programmed death-ligand 2 (PD-L2) are membranous proteins expressed by malignant cells that interact with PD-1 expressed by T-cells. When PD-L1/PD-L2 and PD-1 bind, the T-cells' cytotoxic anti-tumor activity is down-regulated. By blocking the interaction between PD-L1 and PD-1, anti-PD-1 and anti-PD-L1 antibodies restore cytotoxic immune response.

Although this approach has changed the treatment strategy in advanced NSCLC (first-line setting, second-line setting, and beyond) as well as in locally advanced NSCLC (consolidation setting after chemo-radiotherapy) [1–8], a large proportion of patients will not benefit from ICIs and patient selection is still a challenge. At the moment, immunohistochemistry (IHC) is the standard biomarker used to evaluate PD-L1 expression on tumor cells and not only informs treatment decisions but also regulatory approval, with a threshold at 50% of positive tumor cells for pembrolizumab in first-line treatment for advanced NSCLC, and 1% for pembrolizumab in second-line or durvalumab in consolidation after chemo-radiotherapy in locally advanced NSCLC.

However, the use of PD-L1 as a predictive biomarker remains challenging, as some patients experience tumor response with low/negative PD-L1 IHC expression [1,2,4,8]. There is also a spatial

intra-tumor and inter-tumor heterogeneity [9–15] as well as temporal variation of PD-L1 expression, especially after chemotherapy [16,17].

There is currently an unmet need for new biomarkers in order to better select patients who will benefit from ICIs. Research is currently focusing on tissue-based biomarkers such as PD-L1 IHC or the tissue tumor mutational burden (tTMB) but also on plasma biomarkers. The advantages of plasma biomarkers are numerous: plasma is easily accessible, less invasive than tissue biopsies, and represents the entire tumor burden present within the patient.

The aim of this review is to describe the development of novel plasma biomarkers such as soluble proteins, circulating tumor DNA (ctDNA), blood TMB (bTMB), and blood microbiome in NSCLC patients treated with ICIs, and their potential use in predicting response and toxicity.

## 2. Circulating PD-L1

PD-1 is an immunoglobulin superfamily type 1 transmembrane glycoprotein consisting of 288 amino acids. It is expressed on tumor cells and different immune cells such as T cells [18]. PD-L1 is a ligand of PD-1 and can be expressed in two forms: membrane-bound (mPD-L1) and in a soluble form (sPD-L1), which is present in the peripheral blood of patients with solid tumors. It has been shown that patients affected with lung cancer have higher levels of sPD-L1 than healthy controls [19].

### 2.1. Prognostic Role of sPD-L1 in NSCLC

Several studies have described the prognostic role of sPD-L1 in NSCLC. Zhang et al. included 109 patients with advanced NSCLC and 65 healthy controls. Enzyme-linked immunosorbent assay determination (ELISA) was used to measure sPD-L1 levels [19]. The authors determined a sPD-L1 cut-off at 0.636 ng/mL to distinguish patients with high ( $n = 61$ ) and low ( $n = 48$ ) sPD-L1 concentrations. When comparing overall survival (OS) between these two groups, it was found that patients with low sPD-L1 concentrations had longer median OS: 26.8 months vs. 18.7 months for patients with high sPD-L1 concentrations ( $p < 0.001$ ). Finally, when comparing sPD-L1 levels and clinical-pathological features it was found that sPD-L1 was associated with abdominal organ metastasis ( $p = 0.004$ ). No other statistically significant association was observed.

Another study [20] included 96 patients with advanced or post-surgical recurrent lung cancer. ELISA was used to measure sPD-L1 levels (mean sPD-L1 concentration of 6.95 ng/mL). A cut-off was determined at 7.23 ng/mL to separate patients into high ( $n = 40$ ) and low ( $n = 56$ ) sPD-L1 concentrations. Again, patients with high sPD-L1 concentrations had shorter OS than patients with low sPD-L1 concentrations: 13.0 months vs. 20.4 months ( $p = 0.037$ ). No correlation was noted between sPD-L1 levels and clinical-pathological features. However, when multivariate analysis was performed, patient age, performance status (PS), use of steroids, and sPD-L1 levels were independently associated with survival.

These two studies bring relevant data: sPD-L1 is present in the plasma of healthy controls and at higher levels in patients with advanced NSCLC. Higher sPD-L1 concentrations seem to be associated with worse survival. However, these studies were performed before the immunotherapy era and although patient treatment was not specified it is likely that they received chemotherapy. Furthermore, we do not have the detail as to when the plasma sample was drawn (at diagnosis or during chemotherapy) rendering the interpretation of these findings difficult.

Two reviews, both associated with a meta-analysis [21,22], assessed the prognostic significance of sPD-L1 in 1102 and 1040 patients respectively with advanced solid tumors. The two meta-analyses did not include the same studies and different cancer types were present (hepatocellular carcinoma, diffuse large B cell lymphoma, NSCLC, gastric adenocarcinoma, biliary tract cancer, multiple myeloma, renal cell carcinoma). However, both studies showed that patients with high sPD-L1 levels had shorter OS than patients with low sPD-L1 levels: hazard ratio (HR) at 1.60 (95% CI: 1.21–1.99,  $p < 0.01$ ) and 2.26 (95% CI: 1.83–2.80,  $p < 0.001$ ), respectively.

## 2.2. sPD-L1 in NSCLC Patients Treated with Radiotherapy

sPD-L1 has also been evaluated in patients with locally advanced or inoperable NSCLC treated with thoracic radiotherapy (TRT) alone or with concurrent chemo-radiotherapy [23]. Zhao et al. performed dynamic measures of sPD-L1, at diagnosis (before initiating TRT), during TRT (week 2 and week 4), and after radiotherapy treatment (within three months of the last TRT treatment day). The study included 126 patients and found that sPD-L1 levels were significantly lower at week 2 and week 4 when compared to baseline ( $p < 0.001$  and  $p < 0.001$ ). As had been previously reported, low sPD-L1 concentrations at diagnosis were associated with longer OS as compared to high sPD-L1 concentrations. In this study, the optimal cut-off for sPD-L1 at diagnosis was 0.0965 ng/mL and the median OS for patients with low sPD-L1 levels was 27.8 months vs. 15.5 months ( $p = 0.005$ ) for other patients.

## 2.3. sPD-L1 in NSCLC Patients Treated with ICIs

Several recent publications have focused on sPD-L1 in patients treated with ICIs. Okuma et al. included 39 Japanese patients with stage IV or recurrent NSCLC treated with an anti-PD-1 antibody (nivolumab, 3 mg/kg every two weeks) in the second-line setting or more [24]. Plasma samples were drawn at baseline and sPD-L1 levels were measured by ELISA. The median sPD-L1 concentration was 2.24 ng/mL and the sPD-L1 cut-off to differentiate low and high sPD-L1 concentrations was 3.357 ng/mL. Patients with high sPD-L1 concentrations had shorter OS and shorter time to treatment failure (TTF) compared to patients with low sPD-L1 concentrations: respectively 7.20 months vs. not reached ( $p = 0.040$ ) for OS and 1.48 months vs. 5.36 months ( $p = 0.032$ ) for TTF. Furthermore, the overall response rate (ORR) with nivolumab was greater in the group with low sPD-L1 concentrations compared to high sPD-L1 concentrations (59% vs. 25%,  $p = 0.0069$ ). In univariate analysis, there was a statistically significant difference in sPD-L1 concentrations between patients achieving CR/PR/SD compared to patients presenting with progressive disease (PD) ( $p = 0.0066$ ), no other difference with regards to clinical-pathological features was found. In multivariate analysis, sPD-L1 levels (low vs. high) remained associated with TTF (HR: 0.37,  $p = 0.041$ ).

We recently reported [25] a single-center study that included 43 patients with advanced NSCLC treated with nivolumab (3 mg/kg every two weeks) in second-line treatment or more. Plasma was not only drawn before nivolumab initiation but also at the first tumor evaluation (two months), giving a dynamic view of sPD-L1 variations during treatment. ELISA was performed on plasma samples drawn at different time points during nivolumab. sPD-L1 concentrations at the first tumor evaluation were significantly higher in non-responders with a median value of 67.64 pg/mL (IQR 46.36–75.14) compared to 32.94 pg/mL (IQR 24.89–58.91) in responders ( $p = 0.031$ ). In the same way, it was found that patients who had a clinical benefit from nivolumab (CR, PR, or stability according to RECIST lasting six months or more after nivolumab initiation) had significantly lower sPD-L1 concentrations at the first tumor evaluation under nivolumab (median value of 0.06764 pg/mL) than patients without clinical benefit (median value of 0.03414 pg/mL,  $p = 0.024$ ). A cut-off level of sPD-L1 concentration at the first tumor evaluation was determined at 0.03397 ng/mL. Patients with high sPD-L1 concentrations at two months of nivolumab had a significantly shorter median PFS (2.2 months vs. 11.8 months,  $p = 0.041$ ) and shorter median OS (6.2 months vs. NR,  $p = 0.087$ ) than other patients. Moreover, patients who had an increase in sPD-L1 concentrations between nivolumab initiation and first tumor evaluation had worse ORR (17% vs. 68%,  $p = 0.005$ ), lower rates of clinical benefit (10% vs. 47%,  $p = 0.047$ ), shorter median PFS (1.8 months vs. 6.5 months,  $p = 0.008$ ), and shorter median OS (5.4 months vs. NR,  $p = 0.028$ ) than patients who had decreasing or stable sPD-L1 concentrations.

These different studies bring consistent data relative to the value of sPD-L1 as a prognostic biomarker, at first in patients treated with CT but now also in patients receiving ICIs. Furthermore, some results suggest that sPD-L1 could be used to monitor the efficacy of ICIs and might help to anticipate which patients will benefit from the treatment. These different studies are summarized in Table 1.

A major limitation in the translation to clinics for sPD-L1 is the current absence of standardization of sPD-L1 measurement, with several ELISA kits used in the studies, with different thresholds.

**Table 1.** Comparison of the different studies testing soluble programmed death-ligand 1 (sPD-L1).

Study	Patients (n)	Time of sPD-L1 Measure	sPD-L1 Cut-Off	Treatment	Main Results
Zhang et al. [19]	Advanced NSCLC (109), healthy controls (65)	Diagnosis	0.636 ng/mL	NS	Higher sPD-L1 levels in patients than controls Shorter OS in high sPD-L1 patients
Okuma et al. [20]	Advanced or postsurgical recurrent lung cancer (96)	Before initiation of CT or at least 3–4 weeks after last CT	7.32 ng/mL	CT	Shorter OS in high sPD-L1 patients
Zhao et al. [23]	Locally advanced or inoperable NSCLC (126)	Diagnosis, Week 2 and 4 of treatment	0.0965 ng/mL	TRT ± CT	Decrease of sPD-L1 during TRT Shorter OS in high sPD-L1 patients
Okuma et al. [24]	Advanced or recurrent NSCLC (39)	Baseline	3.357 ng/mL	nivolumab	Shorter OS TTF in high sPD-L1 patients Higher rates of CR, PR, and SD in low sPD-L1 patients
Costantini et al. [25]	Advanced NSCLC (43)	At initial diagnosis, at nivolumab initiation, at first tumor evaluation	0.0337 ng/mL	nivolumab	sPD-L1 at first tumor evaluation higher in non-responders Patients with clinical benefit had lower sPD-L1 levels at first tumor evaluation Patients with increasing sPD-L1 levels had worse ORR, lower rates of clinical benefit, shorter PFS and OS

NSCLC: Non-small cell lung cancer. CT: Chemotherapy. TRT: Thoracic radiotherapy. NS: Not specified.

#### 2.4. Source and Biological Activity of sPD-L1

The studies presented above have shown that a soluble form of PD-L1 can be detected in the blood/plasma of healthy controls as well as in that of patients affected with NSCLC. However, several questions remain, such as the biological origin and activity of sPD-L1.

Frigola et al. [18] demonstrated that sPD-L1 was detected in the culture supernatants of PD-L1 positive tumor cell lines but not in that of PD-L1 negative tumor cell lines. This result, obtained in vitro, shows that tumor cells release sPD-L1, but the release mechanism remains unclear. sPD-L1 could be actively shed by tumor cells or could be released by dying tumor cells. Although little data is currently available, we can hypothesize that sPD-L1 is actively shed by tumor cells as it was found that patients with decreasing sPD-L1 levels after nivolumab initiation presented with better outcomes [25]. The protein sequence of sPD-L1 has also been studied [18] by performing affinity chromatography using cell culture supernatants of PD-L1 positive tumor cells. The eluted fractions were tested with ELISA and the fractions with the highest sPD-L1 concentrations were pooled and subjected to protein electrophoresis and immunoblotting revealing a 45kDa band. Protein sequencing of this band revealed that it corresponded to the N-terminus part of PD-L1 and contained the Ig-V ligand-binding domain required for interaction with PD-1 on T-cells and delivering immunoinhibitory signals. Other studies [26] have shown that human peripheral blood mononuclear cells (PBMC), challenged with the mitogen PHA, released sPD-L1, suggesting that immune cell activation might be needed in order to produce sPD-L1. To further determine which cells secreted sPD-L1, PBMC were separated into plastic and non-plastic adherent cell. Plastic adherent cells (monocytes, macrophages, and DCs) released sPD-L1, but non-plastic adherent ones (T cells) did not. Moreover, activated CD3+ T-cells expressed mPD-L1 but did not release sPD-L1. These in vitro results strongly suggest that, among immune cells, sPD-L1 is secreted by monocytes, macrophages, and DCs, but not by T lymphocytes. Functional analyses showed that sPD-L1 increased the apoptotic activity of activated CD4 T cells and, to a lesser degree, of CD8 T cells. This suggests that sPD-L1 has biological activity

and can deliver immunosuppressive signals to activated T cells [18]. Furthermore, as sPD-L1 has similar structural points to mPD-L1, we can hypothesize that it could bind with anti-PD-L1 drugs and, thus, exert a competing effect, explaining why patients with high levels of sPD-L1 have worse outcomes. Data to support this hypothesis has been reported by Gong et al. [27]. They found that patients who were resistant to ICIs had sPD-L1 variants that were secreted. These variants lacked the transmembrane domain usually present and cause ICI inefficacy by binding to the monoclonal antibodies and inhibiting their usual activity. These results are of the utmost interest and further studies are needed to confirm and validate them.

### 3. Other Soluble Proteins

#### 3.1. Granzyme B

Granzyme B is a serine protease secreted by NK cells and cytotoxic CD8+ T cells, with a key role for immune-induced apoptosis. Granzyme proteins are delivered to the target cells via cytotoxic granules and are responsible for caspase-dependent apoptosis [28,29]. Several studies [30,31] have evaluated granzyme B activity through dedicated PET imaging in pre-clinical models showing that granzyme B activity can be used to predict response to ICIs and that tumors classified as high-signal with regards to granzyme B uptake presented with good response to ICIs.

Costantini et al. [25] found that soluble granzyme B (sGranzyme B) concentrations at nivolumab initiation in NSCLC patients were higher in patients who were responders than in non-responders (18.44 pg/mL vs. 11.88 pg/mL,  $p = 0.039$ ). Significant results were also found when analyzing the variation of sGranzyme B during nivolumab treatment: patients with increasing concentrations of sGranzyme B between nivolumab initiation and the first tumor evaluation had worse outcomes with lower rates of ORR, shorter PFS (2.0 months vs. 8.8 months,  $p = 0.019$ ), and OS (4.5 months vs. NR,  $p = 0.043$ ) than patients with stable or decreasing concentrations. At nivolumab initiation, patients with high sGranzymeB concentrations had a non-reached median OS and a median PFS of 8.8 months, versus 4.5 months ( $p = 0.096$ ) and 1.8 months ( $p = 0.018$ ) respectively, for patients with low sGranzymeB concentrations. We hypothesize that high levels of pre-treatment sGranzyme B reflect an activated and efficient CD8+ cytotoxic immune response. The increase in sGranzyme B could be the reflection of an increasing yet ineffective T-cell response leading to T-cell exhaustion.

#### 3.2. PD-L2, IL-2, IFN-Gamma

There is little data available on other soluble immune-related biomarkers, such as sPD-L2, interleukine (IL), or interferon-gamma (IFN- $\gamma$ ). We were not able to find any impact of the concentrations or dynamic evolution of these soluble proteins during nivolumab treatment on the efficacy of ICIs [25]. However, we showed that sPD-L2, sIL-2, and sIFN- $\gamma$  concentrations at the early stages of nivolumab treatment were associated with the occurrence of an immune grade 3–4 toxicity with nivolumab. Another study [32] included 34 patients with advanced NSCLC who had failed at least one prior chemotherapy regimen and subsequently received nivolumab monotherapy (3 mg/kg every two weeks). Blood samples were collected at baseline, at week four, eight, twelve, and at the time of progression. Serum proteins were quantified by Milliplex MAP assay using human cytokine/chemokine panel 1, human angiogenesis/ growth factor panel 1, and a multi-species TGF- $\beta$  panel (Millipore, Billerica, MA, USA). At week four, three proteins had different levels of expression between patients with irAEs and patients without irAEs: G-CSF, leptin, and RANTES. Multivariate analysis revealed that only the levels of RANTES were associated with irAEs. It was also shown that RANTES levels decreased after corticosteroid initiation. RANTES, also known as CCL5 (Chemokine ligand 5), plays an active role in recruiting leukocytes into inflammatory sites. It can also induce the proliferation and activation of natural killer (NK) cells using cytokines such as IL-2 or IFN- $\gamma$  secreted by T-cells. Finally, IL-8 has been studied in melanoma and advanced NCLC patients [33]. Nineteen patients with NSCLC treated with nivolumab or pembrolizumab were included and it was found that responders had significantly

decreasing levels of IL-8 between baseline and the first tumor evaluation while non-responders had significantly increasing levels of IL-8. Furthermore, an early decrease in IL-8 levels was associated with longer OS (not reached vs. 8.0 months 95% CI: 0–19.7,  $p = 0.015$ ) compared to patients with early increasing levels of IL-8.

These results are mostly exploratory. However, the high levels of RANTES measured at week four in the study by Oyanagi et al. found to be associated with irAEs and the elevated concentrations of sIFN- $\gamma$  found to be associated with irAEs by Costantini et al. are coherent results. In fact, an excessive T-cell reaction via a RANTES-mediated mechanism could lead to the excessive secretion of cytokines such as IL-2 and IFN- $\gamma$ . The relatively high incidence of high-grade irAEs with ICIs (around 10–15%), sometimes associated with severe morbi-mortality or the interruption of ICI treatment underlines the necessity for the early detection of patients at risk for such complications.

#### 4. Circulating Tumor DNA (ctDNA)

Circulating cell-free DNAs (cfcDNA) are short DNA fragments that are derived from dying cells. These fragments are present in healthy subjects where they are mostly derived from hematopoietic cells as well as in patients with cancer where a fraction can be derived from cancer cells [34]. In this case, the DNA fragments are called circulating tumor DNA (ctDNA). ctDNA can be explored by different ways: a quantitative approach in which ctDNA concentration is measured; a targeted sequencing approach (mostly by digital droplet PCR, ddPCR), to determine specific mutation profile as epidermal growth factor receptor (EGFR) mutations for example, or large ctDNA sequencing (next-generation sequencing, whole-exome sequencing) to have an extended view on mutational tumor profile and evaluate the mutational burden, also defined as blood tumor mutational burden (bTMB).

##### 4.1. ctDNA Quantitative Approach and ICIs in NSCLC

A study by Cabel et al. [35] investigated whether ctDNA changes were correlated with outcomes in patients treated with anti-PD-1 therapy. This small study included 15 patients (10 treated for metastatic NSCLC, three treated for metastatic uveal melanoma and two treated for metastatic micro-satellite instable colorectal cancer) all receiving either nivolumab (3 mg/kg every 2 weeks) or pembrolizumab (2 mg/kg every three weeks). Plasma samples were prospectively collected at week 0 and week 8. In the case of a detectable mutation available in the patients' record, it was used as the target to monitor plasma ctDNA using ddPCR or Bi-PAP depending on the mutation type. If no mutation was known, cfcDNA was submitted to targeted NGS. At baseline, ctDNA was detected in 10 out of the 15 patients (67%) and no association was found between baseline ctDNA levels and clinical characteristics. When analyzing ctDNA levels and tumor size change between week 0 and week 8, a statistically significant association was found (Spearman correlation  $r = 0.86$ ,  $p = 0.002$ ). Furthermore, patients with undetectable ctDNA at week 8 had significantly longer PFS than patients with detectable ctDNA (median PFS 11 vs. 2 months HR = 10.2, 95% CI: 2.5–41,  $p = 0.001$ ) and OS (HR = 15, 95% CI: 2.5–95,  $p = 0.004$ ). At baseline, patients with undetectable ctDNA levels had significantly longer OS durations (HR = 6.8, 95% CI: 1.1–41.0,  $p = 0.03$ ) but no difference was found in terms of PFS.

These results were confirmed in another study where 49 patients with metastatic NSCLC treated with ICIs were included [36]. Plasma was drawn at baseline and then regularly throughout the follow-up period. Somatic mutations within cfcDNA were identified and quantified using a deep sequencing method and ctDNA was quantified using the allelic fraction of mutant tumor-derived DNA within total cfcDNA. If two mutants were detected, the one with the highest allelic fraction was used. Included in the study were 28 patients that had somatic mutations identified in their baseline plasma. ctDNA response was defined as a drop in ctDNA level to <50% of baseline confirmed by a second successive measurement. A strong correlation was found between ctDNA response and best radiographic response (Cohen's kappa statistic [ $k = 0.753$ ; 95% confidence interval (CI): 0.501–1.000,  $p < 0.001$ ]). Out of the 24 patients achieving PR, 10 had a ctDNA response. The magnitude of the decrease in ctDNA levels was also greater in responders compared to non-responders ( $p = 0.002$ ).

Of interest, ctDNA response seemed to be achieved earlier than radiological response (24.5 days since the start of treatment vs. 72.5 days for radiological assessment). Finally, ctDNA responders had a longer duration of immunotherapy treatment (205.5 vs. 69 days,  $p < 0.001$ ) and presented with a significantly lower risk of disease progression (HR = 0.29, 95% CI: 0.09–0.89,  $p = 0.03$ ) and a lower, but not significantly, risk of death (HR = 0.22, 95% CI: 0.05–1.02,  $p = 0.053$ ).

Finally, two studies have focused on patients with advanced NSCLC treated with nivolumab. The first study [37] calculated tumor volume (TV) by summing the diameter of five target lesions. Tumor tissue was obtained for all 14 patients included and plasma was drawn at baseline and at 1, 2, 4, 6, and 8 weeks after initiation of nivolumab treatment. The study found a significant correlation between TV and ctDNA levels ( $p = 0.02$ ) and showed that ctDNA levels in responders usually decreased during follow-up whereas ctDNA in non-responders remained high after treatment initiation. The final study [38] included 20 patients with plasma drawn at initial diagnosis, at nivolumab initiation, and at first tumor evaluation. At baseline, ctDNA concentrations were not different between patients with objective response (OR) and patients without OR and were not correlated with baseline tumor burden. At first tumor evaluation, patients with OR had lower ctDNA concentrations than patients without OR ( $p = 0.032$ ). Furthermore, responders all had decreasing ctDNA levels whereas 60% of non-responders had increasing ctDNA levels ( $p = 0.025$ ). Finally, a ctDNA cut-off was determined at first tumor evaluation (0.006 ng/ $\mu$ L) with significantly longer PFS ( $p = 0.003$ ) and OS ( $p = 0.044$ ) in patients with lower ctDNA levels.

Taken together, these results support the fact that ctDNA could be a useful biomarker to predict response to ICIs in patients with advanced NSCLC. However, larger dedicated prospective trials are urgently needed, as so far data has only been collected from very small cohorts of patients, mostly in a retrospective way. Some technical limitations remain as ctDNA is not detected in all patients with advanced NSCLC and there is a need for standardization of the different ctDNA detection techniques. Finally, there seems to be little data [39] on the behavior of ctDNA in cases of particular progression patterns such as pseudo-progression or hyper-progressive disease.

#### 4.2. Tumor Mutational Burden (TMB)

Tumor mutational burden can be defined as the number of somatic missense mutations present in a tumor sample. The optimal tool for measuring TMB is whole-exome sequencing (WES). As this is expensive and not widely available, NGS using cancer-gene panels (CGP) has also been used. Several CGP currently exist, such as Memorial Sloan Kettering Cancer Center's Integrated Mutation Profiling of Actionable Cancer Targets (MSK-IMPACT), Foundation One CDx (FICDx), Guardant 360, PlasmaSELECT 64, and Foundation ACT.

TMB has revealed itself as a potential biomarker in melanoma, urothelial carcinoma, and lung cancer [40–43]. TMB was notably analyzed in an exploratory analysis of the Checkmate-026 study [41] which compared nivolumab to platinum-based immunotherapy in patients with PD-L1 positive advanced NSCLC. The study was negative on PFS (primary objective) among patients with a PD-L1 expression level of 5% or more (median PFS of 4.2 months with nivolumab versus 5.9 months with chemotherapy,  $p = 0.25$ ). However, patients with high TMB ( $\geq 243$  mutations as determined by WES) had improved PFS and ORR when they received nivolumab, compared to patients treated with chemotherapy. In Checkmate-227, NSCLC patients received either nivolumab-ipilimumab combination therapy or platinum-based chemotherapy in first-line treatment [42]. PFS was used as an endpoint in patients with high TMB (defined as  $\geq 10$  mutations/megabase determined by the FoundationOne CDx assay). In this population, immunotherapy combination was superior to chemotherapy with regards to PFS: HR = 0.58 (97.5% CI, 0.41–0.81),  $p < 0.001$ . However, analyses on TMB was not pre-defined, patients were not stratified on TMB, and only 57.7% of patients had TMB results available, making definitive conclusions on these results difficult.

Although promising, the clinical use of tissue TMB (tTMB) remains currently challenging, as it requires large amounts of tissue in order to perform effective sequencing, and there is still no standardization in term of technics or thresholds.

Less invasive methods have been sought, such as measuring TMB on ctDNA (bloodTMB or bTMB). Wang et al. [44] evaluated bTMB in patients with NSCLC using an NGS cancer gene panel. The study contained four sections: panel design, virtual validation, technical validation, and clinical validation. The CGP used was called NCC-GP150 and was designed by selecting cancer-related genes. In order to create the CGP, WES data from 9205 samples from The Cancer Genome Atlas (TCGA) were used and genes were randomly extracted to generate panels for TMB extraction. The more genes included, the higher the correlation between the CGP and the WES-based TMB. When 150 genes were used (NCC-GP150), a plateau was reached when evaluating the correlation between the CGP and the WES-based TMB. A validation cohort was used on 48 patients with advanced NSCLC and treated with anti-PD-1 ICI, showing a good correlation between NCC-GP150 and WES results, and a bTMB cut-off of six or higher for an optimal Youden index of 0.59 (0.88 sensitivity and 0.71 specificity). Finally, to evaluate the clinical significance of NCC-GP150, an independent cohort of 50 patients with advanced NSCLC and treated with anti-PD-1 or PD-L1 agents was analyzed. It was found that patients with high bTMB ( $>6$ ) had longer PFS when compared to patients with low bTMB: median not reached vs. 2.9 months (HR = 0.39, 95% CI: 0.18–0.84,  $p = 0.01$ ).

Another study [45] reported bTMB results using more than 1000 prospectively collected plasma samples from patients of the POPLAR [46] and OAK [4] studies. POPLAR was a phase II study that compared atezolizumab and docetaxel in the second-line setting for patients with previously treated advanced NSCLC. The OAK study was a randomized phase III trial with a similar setting. Both studies showed the superiority of atezolizumab versus docetaxel, in terms of OS regardless of PD-L1 expression or histology. tTMB and bTMB were evaluated by FoundationOne CDx NGS assay. Exploratory analyses from a subset of POPLAR and OAK samples showed a positive correlation between bTMB and tTMB (Spearman rank correlation = 0.64; 95% confidence interval (CI): 0.56–0.71). Patients with higher bTMB had improved PFS and OS benefit. For example, in the POPLAR study ( $n = 273$ ), at the bTMB cut-off of 16 mutation/megabase, the median PFS in patients with bTMB  $>16$  was 4.2 months in the atezolizumab arm and 2.9 months in the docetaxel arm with a HR of 0.57 (95% CI: 0.33–0.99). Similar results were found when using data from the OAK study.

#### 4.3. Current Limitations for ctDNA and bTMB Use as Biomarkers for ICIs in NSCLC

Using ctDNA or bTMB to predict and track early response to ICIs is a promising approach. The studies described above and summarized in Table 2 have shown that the quantitative approach to ctDNA can help to predict responses to ICIs as early as the baseline and, maybe even more importantly, the early variation of ctDNA precisely predicts the response to immunotherapy. bTMB has also brought promising results, showing good correlation with tTMB and helping to predict response to ICIs in patients with high bTMB. However, these methods still present several limitations. First, ctDNA needs to be detected in the patients' plasma. Furthermore, there are currently several panels used to determine bTMB, all using different gene targets, sequences, and thresholds leading to a lack of harmonization of research results. This is also an expensive technique and most data available to date is retrospective. Efforts are needed to improve the ctDNA detection rate, harmonize the different assays used, and to build clinical trials that will prospectively evaluate ctDNA and bTMB as a biomarker in lung cancer patients treated with ICIs.

**Table 2.** Comparison of the different studies testing circulating tumor DNA (ctDNA) and blood tumor mutational burden (bTMB).

Study	Patients (n)	Variable Measured	Cut-Off Used for bTMB	Treatment	Positive Findings
Cabel et al. [34]	NSCLC, uveal melanoma, MSI colorectal cancer (10)	ctDNA concentrations	NA	nivolumab, pembrolizumab	PFS, OS
Goldberg et al. [35]	Metastatic NSCLC (28)	ctDNA concentrations	NA	Anti PD-1, anti-PD-L1 alone or in combination	Time on treatment, PFS, OS
Iijima et al. [36]	Advanced NSCLC (14)	ctDNA concentrations	NA	nivolumab	Durable response
Giroux-Leprieur et al. [37]	Advanced NSCLC (15)	ctDNA concentrations by NGS	NA	nivolumab	PFS, clinical benefit
Wang et al. [43]	Advanced NSCLC (50)	NCC-GPI50 (150 genes)	bTMB ≥ 6	Anti-PD-1 Anti-PD-L1	PFS ORR
Gandara et al. [44]	Advanced NSCLC (273)	NGS	bTMB ≥ 16	Atezolizumab (anti-PD-L1)	PFS

PPS: Progression-free survival. NSCLC: Non-small cell lung cancer. ORR: Objective response rate. bTMB: Blood tumor mutational burden. NA: Not applicable.

## 5. New Plasma Biomarkers: Blood Microbiome and Plasma Marker of the Intestinal Barrier

It has been shown that gut microbiome influences the efficacy of PD-1-based immunotherapy in epithelial tumors [47]. As with the previous biomarkers reviewed, the blood microbiome is easily accessible and manageable as compared to fecal microbiome measurement [48–50]. Moreover, early use of antibiotics (EUA) has been proven to be associated with worse outcomes with ICIs, probably due to alteration in the intestinal barrier, modification of fecal microbiota, bacterial translocation, and modification of the anti-tumor immune response.

A recent pilot study described the plasma evaluation of the intestinal barrier and blood microbiome in a cohort of NSCLC patients treated with nivolumab. Ouaknine et al [51] included 72 consecutive patients with advanced NSCLC treated with nivolumab in a second-line setting or more. EUA was defined as oral or intravenous anti-biotherapy given two months before until one month after the beginning of nivolumab. Plasma citrulline, secreted by enterocytes and proven to be a biomarker of the intestinal barrier [52] was prospectively evaluated at months (M) M0, M1, M2, M4, and M6. The blood microbiome was assessed at baseline. It was found that patients with EUA had a shorter median OS (5.1 months vs. 13.4 months,  $p = 0.03$ ) compared to patients without EUA. High baseline citrulline rates ( $\geq 20 \mu\text{M}$ ) were associated with clinical benefit ( $p = 0.002$ ), longer PFS ( $p < 0.0001$ ), and longer OS ( $p < 0.0001$ ). Patients with EUA had lower citrulline concentrations. Finally, different blood microbiome compositions were determined according to the tumor response and clinical benefit with nivolumab. For example, the presence of Gemmatimonadaceae DNA was associated with both low response rates (14% vs. 50% for other patients,  $p = 0.09$ ) and high rates of progression at M2 (86% vs. 29% for other patients,  $p = 0.006$ ). In multivariate analysis, low citrulline concentrations (HR = 3.8, 95%CI: 1.4–99.9,  $p = 0.008$ ) was associated with worse PFS, and the presence of Gemmatimonadaceae DNA (HR = 16.4, 95% CI: 3.9–68.5,  $p < 0.001$ ) and EUA (HR = 2.2, 95% CI: 1.1–4.8,  $p = 0.038$ ) were associated with worse OS. Finally, a response-associated blood microbiome profile was more frequent in patients who did not receive EUA.

These preliminary results need to be confirmed in a prospective way, but open exciting new perspectives in ICI-related plasma biomarkers.

## 6. Future Directions and Conclusions

Throughout this review, we have covered potential new plasma biomarkers such as soluble proteins, ctDNA, bTMB, citrulline, and blood microbiome (Figure 1). These biomarkers can help to better select patients who might respond to immunotherapy, they can help to determine an early response, prior to clinical or radiological evaluation and might even help in anticipating adverse events. Most of the available results are preliminary and cannot be implemented into daily clinical practice. The next step will be to develop prospective clinical trials testing different biomarkers, alone or in combination, in order to determine thresholds and different strategies to adopt. Challenges remain, as with PD-L1 IHC, a harmonization process will be needed for all biomarkers. As things stand, good quality biopsies are still required to choose the optimal treatment options. Available data suggest a comparable efficacy of tissue-based biomarkers for predicting ICI efficacy [53]. However, it is plausible that soluble biomarkers will soon be used as tools to help clinicians treating patients with advanced NSCLC receiving immunotherapy.

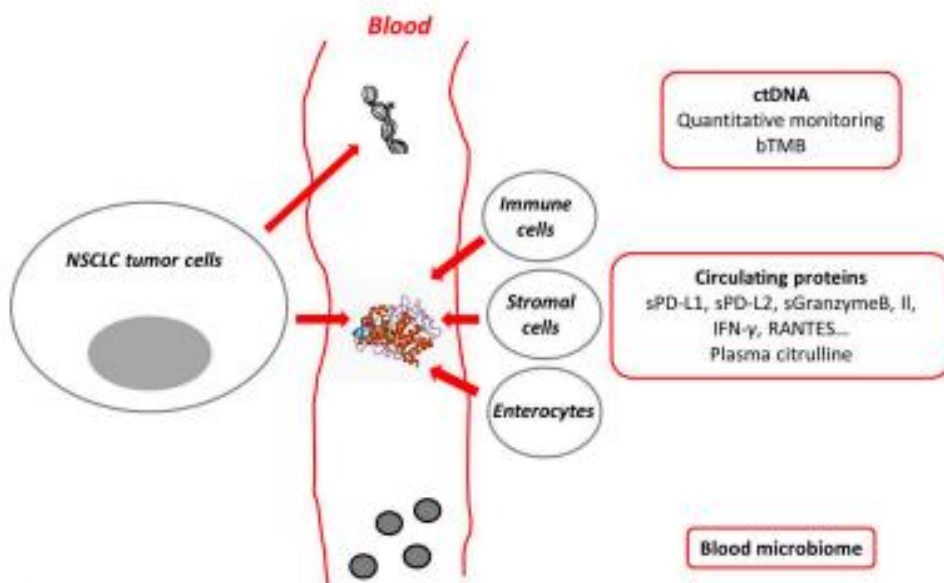


**Figure 1.** Plasma biomarkers and immune checkpoint inhibitors in non-small cell lung cancer.

**Author Contributions:** Conceptualization: A.C., E.G.-L.; investigation: A.C.; writing—original draft preparation: A.C.; writing—review and editing: A.C., P.T.K., C.D., J.F.E., T.C., E.G.-L.; supervision: E.G.-L.

**Funding:** This research received no external funding.

**Conflicts of Interest:** A.C.: none; P.T.K.: none; C.D.: none; T.C.: AstraZeneca, Boehringer-Ingelheim, Chiesi, Novartis, Pfizer, GSK; J.F.E.: Bristol-Myers-Squibb; E.G.-L.: AstraZeneca, Boehringer-Ingelheim, Bristol-Myers-Squibb, MSD, Novartis, Roche.

## References

- Brahmer, J.; Reckamp, K.L.; Baas, P.; Crino, L.; Eberhardt, W.E.; Poddubskaya, E.; Antonia, S.; Pluzanski, A.; Vokes, E.E.; Holgado, E.; et al. Nivolumab versus docetaxel in advanced squamous-cell non-small-cell lung cancer. *N. Engl. J. Med.* **2015**, *373*, 123–135. [[CrossRef](#)] [[PubMed](#)]
- Borghaei, H.; Paz-Ares, L.; Horn, L.; Spigel, D.R.; Steins, M.; Ready, N.E.; Chow, L.Q.; Vokes, E.E.; Felip, E.; Holgado, E.; et al. Nivolumab versus docetaxel in advanced nonsquamous non-small-cell lung cancer. *N. Engl. J. Med.* **2015**, *373*, 1627–1639. [[CrossRef](#)] [[PubMed](#)]

3. Reck, M.; Rodríguez-Abreu, D.; Robinson, A.G.; Hui, R.; Csősz, T.; Fülöp, A.; Gottfried, M.; Peled, N.; Tafreshi, A.; Cuffe, S.; et al. Pembrolizumab versus chemotherapy for PD-L1-positive non-small-cell lung cancer. *N. Engl. J. Med.* **2016**, *375*, 1823–1833. [[CrossRef](#)] [[PubMed](#)]
4. Rittmeyer, A.; Barlesi, F.; Waterkamp, D.; Park, K.; Ciardiello, F.; von Pawel, J.; Gadgeel, S.M.; Hida, T.; Kowalski, D.M.; Dols, M.C.; et al. Atezolizumab versus docetaxel in patients with previously treated non-small-cell lung cancer (OAK): A phase 3, open-label, multicentre randomised controlled trial. *Lancet* **2017**, *389*, 255–265. [[CrossRef](#)]
5. Gandhi, L.; Rodriguez-Abreu, D.; Gadgeel, S.; Esteban, E.; Felip, E.; De Angelis, F.; Domine, M.; Clingan, P.; Hochmair, M.J.; Powell, S.F.; et al. Pembrolizumab plus chemotherapy in metastatic non-small-cell lung cancer. *N. Engl. J. Med.* **2018**, *378*, 2078–2092. [[CrossRef](#)] [[PubMed](#)]
6. Paz-Ares, L.; Luft, A.; Vicente, D.; Tafreshi, A.; Gümuş, M.; Mazières, J.; Hermes, B.; Çay Şenler, F.; Csősz, T.; Fülöp, A.; et al. Pembrolizumab plus chemotherapy for squamous non-small-cell lung cancer. *N. Engl. J. Med.* **2018**, *379*, 2040–2051. [[CrossRef](#)] [[PubMed](#)]
7. Socinski, M.A.; Jotte, R.M.; Cappuzzo, F.; Orlandi, F.; Stroyakovskiy, D.; Nogami, N.; Rodriguez-Abreu, D.; Moro-Sibilot, D.; Thomas, C.A.; Barlesi, F.; et al. Atezolizumab for first-line treatment of metastatic nonsquamous NSCLC. *N. Engl. J. Med.* **2018**, *378*, 2288–2301. [[CrossRef](#)]
8. Antonia, S.J.; Villegas, A.; Daniel, D.; Vicente, D.; Murakami, S.; Hui, R.; Kurata, T.; Chiappori, A.; Lee, K.H.; de Wit, M.; et al. Overall survival with durvalumab after chemoradiotherapy in stage III NSCLC. *N. Engl. J. Med.* **2017**, *377*, 1919–1929. [[CrossRef](#)]
9. Kim, S.; Kim, M.Y.; Koh, J.; Go, H.; Lee, D.S.; Jeon, Y.K.; Chung, D.H. Programmed death-1 ligand 1 and 2 are highly expressed in pleomorphic carcinomas of the lung: Comparison of sarcomatous and carcinomatous areas. *Eur. J. Cancer* **2015**, *51*, 2698–2707. [[CrossRef](#)]
10. Ilie, M.; Long-Mira, E.; Bence, C.; Butori, C.; Lassalle, S.; Bouhlel, L.; Fazzalari, L.; Zahaf, K.; Lalvée, S.; Washetine, K.; et al. Comparative study of the PD-L1 status between surgically resected specimens and matched biopsies of NSCLC patients reveal major discordances: A potential issue for anti-PD-L1 therapeutic strategies. *Ann. Oncol.* **2016**, *27*, 147–153. [[CrossRef](#)]
11. Li, C.; Huang, C.; Mok, T.S.; Zhuang, W.; Xu, H.; Miao, Q.; Fan, X.; Zhu, W.; Huang, Y.; Lin, X.; et al. Comparison of 22C3 PD-L1 Expression between Surgically Resected Specimens and Paired Tissue Microarrays in Non-Small Cell Lung Cancer. *J. Thorac. Oncol.* **2017**, *12*, 1536–1543. [[CrossRef](#)] [[PubMed](#)]
12. Casadevall, D.; Clavé, S.; Taus, Á.; Hardy-Werbin, M.; Rocha, P.; Lorenzo, M.; Menéndez, S.; Salido, M.; Albane, J.; Pijuan, L.; et al. Heterogeneity of Tumor and Immune Cell PD-L1 Expression and Lymphocyte Counts in Surgical NSCLC Samples. *Clin. Lung Cancer* **2017**, *18*, 682–691.e5. [[CrossRef](#)] [[PubMed](#)]
13. Uruga, H.; Bozkurtlar, E.; Huynh, T.G.; Muzikansky, A.; Goto, Y.; Gomez-Carballo, M.; Hata, A.N.; Gainor, J.F.; Mark, E.J.; Engelman, J.A.; et al. Programmed Cell Death Ligand (PD-L1) Expression in Stage II and III Lung Adenocarcinomas and Nodal Metastases. *J. Thorac. Oncol.* **2017**, *12*, 458–466. [[CrossRef](#)] [[PubMed](#)]
14. Pinato, D.J.; Shiner, R.J.; White, S.D.; Black, J.R.; Trivedi, P.; Stebbing, J.; Sharma, R.; Mauri, F.A. Intra-tumoral heterogeneity in the expression of programmed-death (PD) ligands in isogenic primary and metastatic lung cancer: Implications for immunotherapy. *Oncimmunology* **2016**, *5*, e1213934, eCollection 2016. [[CrossRef](#)] [[PubMed](#)]
15. Mansfield, A.S.; Aubry, M.C.; Moser, J.C.; Harrington, S.M.; Dronca, R.S.; Park, S.S.; Dong, H. Temporal and spatial discordance of programmed cell death-ligand 1 expression and lymphocyte tumor infiltration between paired primary lesions and brain metastases in lung cancer. *Ann. Oncol.* **2016**, *27*, 1953–1958. [[CrossRef](#)] [[PubMed](#)]
16. Sheng, J.; Fang, W.; Yu, J.; Chen, N.; Zhan, J.; Ma, Y.; Yang, Y.; Huang, Y.; Zhao, H.; Zhang, L. Expression of programmed death ligand-1 on tumor cells varies pre and post chemotherapy in non-small cell lung cancer. *Sci. Rep.* **2016**, *6*, 20090. [[CrossRef](#)] [[PubMed](#)]
17. Lim, S.H.; Hong, M.; Ahn, S.; Choi, Y.L.; Kim, K.M.; Oh, D.; Ahn, Y.C.; Jung, S.H.; Ahn, M.J.; Park, K.; et al. Changes in tumour expression of programmed death-ligand 1 after neoadjuvant concurrent chemoradiotherapy in patients with squamous oesophageal cancer. *Eur. J. Cancer* **2016**, *52*, 1–9. [[CrossRef](#)] [[PubMed](#)]

18. Frigola, X.; Inman, B.A.; Lohse, C.M.; Krco, C.J.; Cheville, J.C.; Thompson, R.H.; Leibovich, B.; Blute, M.L.; Dong, H.; Kwon, E.D. Identification of a soluble form of B7-H1 that retains immunosuppressive activity and is associated with aggressive renal cell carcinoma. *Clin. Cancer Res.* **2011**, *17*, 1915–1923. [CrossRef] [PubMed]
19. Zhang, J.; Gao, J.; Li, Y.; Nie, J.; Dai, L.; Hu, W.; Chen, X.; Han, J.; Ma, X.; Tian, G.; et al. Circulating PD-L1 in NSCLC patients and the correlation between the level of PD-L1 expression and the clinical characteristics. *Thorac. Cancer* **2015**, *6*, 534–538. [CrossRef]
20. Okuma, Y.; Hosomi, Y.; Nakahara, Y.; Watanabe, K.; Sagawa, Y.; Homma, S. High plasma levels of soluble programmed cell death ligand 1 are prognostic for reduced survival in advanced lung cancer. *Lung Cancer* **2017**, *104*, 1–6. [CrossRef]
21. Ding, Y.; Sun, C.; Li, J.; Hu, L.; Li, M.; Liu, J.; Pu, L.; Xiong, S. The prognostic significance of soluble programmed death ligand 1 expression in cancers: A systematic review and meta-analysis. *Scand. J. Immunol.* **2017**, *86*, 361–367. [CrossRef] [PubMed]
22. Wei, W.; Xu, B.; Wang, Y.; Wu, C.; Jiang, J.; Wu, C. Prognostic significance of circulating soluble programmed death ligand 1 in patients with solid tumors: A meta-analysis. *Medicine (Baltimore)* **2018**, *97*, e9617. [CrossRef] [PubMed]
23. Zhao, J.; Zhang, P.; Wang, J.; Xi, Q.; Zhao, X.; Ji, M.; Hu, G. Plasma levels of soluble programmed death ligand-1 may be associated with overall survival in nonsmall cell lung cancer patients receiving thoracic radiotherapy. *Medicine (Baltimore)* **2017**, *96*, e6102. [CrossRef] [PubMed]
24. Okuma, Y.; Wakui, H.; Utsumi, H.; Sagawa, Y.; Hosomi, Y.; Kuwano, K.; Homma, S. Soluble Programmed Cell Death Ligand 1 as a Novel Biomarker for Nivolumab Therapy for Non-Small-cell Lung Cancer. *Clin. Lung Cancer* **2018**, *19*, 410–417.e1. [CrossRef] [PubMed]
25. Costantini, A.; Julie, C.; Dumenil, C.; Hélias-Rodziewicz, Z.; Tisserand, J.; Dumoulin, J.; Giraud, V.; Labrune, S.; Chinet, T.; Emile, J.F.; et al. Predictive role of plasmatic biomarkers in advanced non-small cell lung cancer treated by nivolumab. *Oncoimmunology* **2018**, *7*, e1452581. [CrossRef] [PubMed]
26. Frigola, X.; Inman, B.A.; Krco, C.J.; Liu, X.; Harrington, S.M.; Bulur, P.A.; Dietz, A.B.; Dong, H.; Kwon, E.D. Soluble B7-H1: Differences in production between dendritic and T cells. *Immunol. Lett.* **2012**, *142*, 78–82. [CrossRef] [PubMed]
27. Gong, B.; Kiyotani, K.; Sakata, S.; Nagano, S.; Kumebara, S.; Baba, S.; Besse, B.; Yanagitani, N.; Friboulet, L.; Nishio, M.; et al. Secreted PD-L1 variants mediate resistance to PD-L1 blockade therapy in non-small cell lung cancer. *J. Exp. Med.* **2019**, *216*, 982–1000. [CrossRef]
28. Trapani, J.A.; Sutton, V.R. Granzyme B: Pro-apoptotic, antiviral and antitumor functions. *Curr. Opin. Immunol.* **2003**, *15*, 533–543. [CrossRef]
29. Waterhouse, N.J.; Sutton, V.R.; Sedelies, K.A.; Ciccone, A.; Jenkins, M.; Turner, S.J.; Bird, P.I.; Trapani, J.A. Cytotoxic T lymphocyte-induced killing in the absence of granzymes A and B is unique and distinct from both apoptosis and perforin-dependent lysis. *J. Cell Biol.* **2006**, *173*, 133–144. [CrossRef]
30. Larimer Wehrenberg-Klee, E.; Dubois, F.; Mehta, A.; Kalomeris, T.; Flaherty, K.; Boland, G.; Mahmood, U. Granzyme B PET Imaging as a Predictive Biomarker of Immunotherapy Response. *Cancer Res.* **2017**, *77*, 2318–2327. [CrossRef]
31. Larimer, B.M.; Bloch, E.; Nesti, S.; Austin, E.E.; Wehrenberg-Klee, E.; Boland, G.; Mahmood, U. The Effectiveness of Checkpoint Inhibitor Combinations and Administration Timing Can Be Measured by Granzyme B PET Imaging. *Clin. Cancer Res.* **2019**, *25*, 1196–1205. [CrossRef] [PubMed]
32. Oyanagi, J.; Koh, Y.; Sato, K.; Mori, K.; Teraoka, S.; Akamatsu, H.; Kanai, K.; Hayata, A.; Tokudome, N.; Akamatsu, K.; et al. Predictive value of serum protein levels in patients with advanced non-small cell lung cancer treated with nivolumab. *Lung Cancer* **2019**, *132*, 107–113. [CrossRef] [PubMed]
33. Sanmamed, M.F.; Perez-Gracia, J.L.; Schalper, K.A.; Fusco, J.P.; Gonzalez, A.; Rodriguez-Ruiz, M.E.; Oñate, C.; Perez, G.; Alfaro, C.; Martin-Algarra, S.; et al. Changes in serum interleukin-8 (IL-8) levels reflect and predict response to anti-PD-1 treatment in melanoma and non-small-cell lung cancer patients. *Am. J. Oncol.* **2017**, *28*, 1988–1995. [CrossRef] [PubMed]
34. Cabel, L.; Proudhon, C.; Romano, E.; Girard, N.; Lantz, O.; Stern, M.H.; Pierga, J.Y.; Bidard, F.C. Clinical potential of circulating tumour DNA in patients receiving anticancer immunotherapy. *Nat. Rev. Clin. Oncol.* **2018**, *15*, 639–650. [CrossRef]

35. Cabel, L.; Riva, F.; Servois, V.; Livartowski, A.; Daniel, C.; Rampanou, A.; Lantz, O.; Romano, E.; Milder, M.; Buecher, B.; et al. Circulating tumor DNA changes for early monitoring of anti-PD1 immunotherapy: A proof-of-concept study. *Ann. Oncol.* **2017**, *28*, 1996–2001. [CrossRef]
36. Goldberg, S.; Narayan, A.; Kole, A.J.; Decker, R.H.; Teysir, J.; Carriero, N.J.; Lee, A.; Nemati, R.; Nath, S.K.; Mane, S.M.; et al. Early assessment of lung cancer immunotherapy response via circulating tumor DNA. *Clin. Cancer Res.* **2018**, *24*, 1872–1880. [CrossRef]
37. Iijima, Y.; Hirotsu, Y.; Amemiya, K.; Ooka, Y.; Mochizuki, H.; Oyama, T.; Nakagomi, T.; Uchida, Y.; Kobayashi, Y.; Tsutsui, T.; et al. Very early response of circulating tumour-derived DNA in plasma predicts efficacy of nivolumab treatment in patients with non-small cell lung cancer. *Eur. J. Cancer* **2017**, *86*, 349–357. [CrossRef]
38. Gérard Leprieur, E.; Herbretau, G.; Dumenil, C.; Julie, C.; Giraud, V.; Labrune, S.; Dumoulin, J.; Tisserand, J.; Emile, J.F.; Blons, H.; et al. Circulating tumor DNA evaluated by next-generation sequencing is predictive of tumor response and prolonged clinical benefit with nivolumab in advanced non-small cell lung cancer. *Oncotarget* **2018**, *7*, e1424675. [CrossRef]
39. Guibert, N.; Mazieres, J.; Delaunay, M.; Casanova, A.; Farella, M.; Keller, L.; Favre, G.; Pradines, A. Monitoring of KRAS-mutated ctDNA to discriminate pseudo-progression from true progression during anti-PD-1 treatment of lung adenocarcinoma. *Oncotarget* **2017**, *8*, 38056–38060. [CrossRef]
40. Rizvi, N.A.; Hellmann, M.D.; Snyder, A.; Kvistborg, P.; Makarov, V.; Havel, J.J.; Lee, W.; Yuan, J.; Wong, P.; Ho, T.S.; et al. Cancer immunology: Mutational landscape determines sensitivity to PD-1 blockade in non-small cell lung cancer. *Science* **2015**, *348*, 124–128. [CrossRef]
41. Carbone, D.P.; Reck, M.; Paz-Ares, L.; Creelan, B.; Horn, L.; Steins, M.; Felip, E.; van den Heuvel, M.M.; Ciuleanu, T.E.; Badin, F.; et al. First-line nivolumab in stage IV or recurrent non-small-cell lung cancer. *N. Engl. J. Med.* **2017**, *376*, 2415–2426. [CrossRef] [PubMed]
42. Hellmann, M.D.; Ciuleanu, T.E.; Pluzanski, A.; Lee, J.S.; Otterson, G.A.; Audigier-Valette, C.; Minenza, E.; Linardiou, H.; Burgers, S.; Salman, P.; et al. Nivolumab plus ipilimumab in lung cancer with a high tumor mutational burden. *N. Engl. J. Med.* **2018**, *378*, 2093–2104. [CrossRef] [PubMed]
43. Hellmann, M.D.; Callahan, M.K.; Awad, M.M.; Calvo, E.; Ascierto, P.A.; Atmaca, A.; Rizvi, N.A.; Hirsch, F.R.; Selvaggi, G.; Szustakowski, J.D.; et al. Tumor mutational burden and efficacy of nivolumab monotherapy and in combination with ipilimumab in small-cell lung cancer. *Cancer Cell* **2018**, *33*, 853–861.e4. [CrossRef] [PubMed]
44. Wang, Z.; Duan, J.; Cai, S.; Han, M.; Dong, H.; Zhao, J.; Zhu, B.; Wang, S.; Zhuo, M.; Sun, J.; et al. Assessment of Blood Tumor Mutational Burden as a Potential Biomarker for Immunotherapy in Patients with Non-Small Cell Lung Cancer With Use of a Next-Generation Sequencing Cancer Gene Panel. *JAMA Oncol.* **2019**, *5*, 696–702. [CrossRef] [PubMed]
45. Gandara, D.R.; Paul, S.M.; Kowanetz, M.; Schleifman, E.; Zou, W.; Li, Y.; Rittmeyer, A.; Fehrenbacher, L.; Otto, G.; Malboeuf, C.; et al. Blood-based tumor mutational burden as a predictor of clinical benefit in non-small-cell lung cancer patients treated with atezolizumab. *Nat. Med.* **2018**, *24*, 1441–1448. [CrossRef] [PubMed]
46. Fehrenbacher, L.; Spira, A.; Ballinger, M.; Kowanetz, M.; Vansteenkiste, J.; Mazieres, J.; Park, K.; Smith, D.; Artal-Cortes, A.; Lewanski, C.; et al. Atezolizumab versus docetaxel for patients with previously treated non-small-cell lung cancer (POPLAR): A multicentre, open-label, phase 2 randomised controlled trial. *Lancet* **2016**, *387*, 1837–1846. [CrossRef]
47. Routy, B.; Le Chatelier, E.; Derosa, L.; Duong, C.P.M.; Alou, M.T.; Daillère, R.; Flückiger, A.; Messaoudene, M.; Rauber, C.; Roberti, M.P.; et al. Gut microbiome influences efficacy of PD-1-based immunotherapy against epithelial tumors. *Science* **2018**, *359*, 91–97. [CrossRef] [PubMed]
48. Païssé, S.; Valle, C.; Servant, F.; Courtney, M.; Burcelin, R.; Amar, J.; Lelouvier, B. Comprehensive description of blood microbiome from healthy donors assessed by 16S targeted metagenomic sequencing. *Transfusion* **2016**, *56*, 1138–1147. [CrossRef]
49. Amar, J.; Chabo, C.; Waget, A.; Klopp, P.; Vachoux, C.; Bermúdez-Humarán, L.G.; Smirnova, N.; Berge, M.; Sulpice, T.; Lahtinen, S.; et al. Intestinal mucosal adherence and translocation of commensal bacteria at the early onset of type 2 diabetes: Molecular mechanisms and probiotic treatment. *EMBO Mol. Med.* **2011**, *3*, 559–572. [CrossRef]

50. Amar, J.; Lange, C.; Payros, G.; Garret, C.; Chabo, C.; Lantieri, O.; Courtney, M.; Marre, M.; Charles, M.A.; Balkau, B.; et al. Blood microbiota dysbiosis is associated with the onset of cardiovascular events in a large general population: The D.E.S.I.R. study. *PLoS ONE* **2013**, *8*, e54461. [[CrossRef](#)]
51. Ouaknine Krief, J.; Helly de Tauriers, P.; Dumenil, C.; Neveux, N.; Dumoulin, J.; Giraud, V.; Labrune, S.; Tisserand, J.; Julie, C.; Emile, J.F.; et al. Role of antibiotic use, plasma citrulline and blood microbiome in advanced non-small cell lung cancer patients treated with nivolumab. *J. Immunother. Cancer* **2019**, *7*, 176. [[CrossRef](#)] [[PubMed](#)]
52. Cremm, P.; Messing, B.; Cynober, L. Citrulline as a biomarker of intestinal failure due to enterocyte mass reduction. *Clin. Nutr.* **2008**, *27*, 328–339. [[CrossRef](#)] [[PubMed](#)]
53. Lu, S.; Stein, J.E.; Rimm, D.L.; Wang, D.W.; Bell, J.M.; Johnson, D.B.; Sosman, J.; Schalper, K.A.; Anders, R.A.; Wang, H.; et al. Comparison of Biomarker Modalities for Predicting Response to PD-1/PD-L1 Checkpoint Blockade: A Systematic Review and Meta-analysis. *JAMA Oncol.* **2019**. [[CrossRef](#)] [[PubMed](#)]



© 2019 by the authors. Licensee MDPI, Basel, Switzerland. This article is an open access article distributed under the terms and conditions of the Creative Commons Attribution (CC BY) license (<http://creativecommons.org/licenses/by/4.0/>).

## **BIBLIOGRAPHIE**

**A**i J, Chen Y, Peng X, Ji Y, Xi Y, Shen Y, Yang X, Su Y, Sun Y, Gao Y, Ma Y, Xiong B, Shen J, Ding J, Geng M. Preclinical Evaluation of SCC244 (Glumetinib), a Novel, Potent, and Highly Selective Inhibitor of c-Met in MET-dependent Cancer Models. *Mol Cancer Ther.* 2018 Apr;17(4):751-762. doi: 10.1158/1535-7163.MCT-17-0368. Epub 2017 Dec 13. PMID: 29237805

Alrehaili AA, Gharib AF, Almalki A, Alghamdi A, Hawsawi NM, Bakuraysah MM, Alhuthali HM, Etewa RL, Elsawy WH. Soluble Programmed Death-Ligand 1 (sPD-L1) as a Promising Marker for Head and Neck Squamous Cell Carcinoma: Correlations With Clinical and Demographic Characteristics. *Cureus.* 2023 Aug 29;15(8):e44338. doi: 10.7759/cureus.44338. eCollection 2023 Aug. PMID: 37779773

Altorki NK, Yip R, Hanaoka T, Bauer T, Aye R, Kohman L, Sheppard B, Thurer R, Andaz S, Smith M, Mayfield W, Grannis F, Korst R, Pass H, Straznicka M, Flores R, Henschke CI; I-ELCAP Investigators. Sublobar resection is equivalent to lobectomy for clinical stage 1A lung cancer in solid nodules. *J Thorac Cardiovasc Surg.* 2014 Feb;147(2):754-62; Discussion 762-4. doi: 10.1016/j.jtcvs.2013.09.065. Epub 2013 Nov 23. PMID: 24280722

Anagnostou V, Smith KN, Forde PM, Niknafs N, Bhattacharya R, White J, Zhang T, Adleff V, Phallen J, Wali N, Hruban C, Guthrie VB, Rodgers K, Naidoo J, Kang H, Sharfman W, Georgiades C, Verde F, Illei P, Li QK, Gabrielson E, Brock MV, Zahnow CA, Baylin SB, Scharpf RB, Brahmer JR, Karchin R, Pardoll DM, Velculescu VE. Evolution of Neoantigen Landscape during Immune Checkpoint Blockade in Non-Small Cell Lung Cancer. *Cancer Discov.* 2017 Mar;7(3):264-276. doi: 10.1158/2159-8290.CD-16-0828. Epub 2016 Dec 28. PMID: 28031159

Ancın B, Özercan MM, Yılmaz YM, Uysal S, Kumbasar U, Saribaş Z, Dikmen E, Doğan R, Demircin M. The correlation of serum sPD-1 and sPD-L1 levels with clinical, pathological characteristics and lymph node metastasis in nonsmall cell lung cancer patients. *Turk J Med Sci.* 2022 Aug;52(4):1050-1057. doi: 10.55730/1300-0144.5407. Epub 2022 Aug 10. PMID: 36326416

Ando K, Hamada K, Watanabe M, Ohkuma R, Shida M, Onoue R, Kubota Y, Matsui H, Ishiguro T, Hirasawa Y, Ariizumi H, Tsurutani J, Yoshimura K, Tsunoda T, Kobayashi S, Wada S. Plasma Levels of Soluble PD-L1 Correlate With Tumor Regression in Patients With Lung and Gastric Cancer Treated With Immune Checkpoint Inhibitors. *Anticancer Res.* 2019 Sep;39(9):5195-5201. doi: 10.21873/anticanres.13716. PMID: 31519633

Antoniou AN, Ford S, Pilley ES, Blake N, Powis SJ. Interactions formed by individually expressed TAP1 and TAP2 polypeptide subunits. *Immunology.* 2002 Jun;106(2):182-9. doi: 10.1046/j.1365-2567.2002.01415.x. PMID: 12047747

Arriagada R, Bergman B, Dunant A, Le Chevalier T, Pignon JP, Vansteenkiste J; International Adjuvant Lung Cancer Trial Collaborative Group. Cisplatin-based adjuvant chemotherapy in patients with completely resected non-small-cell lung cancer. *N Engl J Med.* 2004 Jan 22;350(4):351-60. doi: 10.1056/NEJMoa031644.PMID: 14736927

Arriagada R, Dunant A, Pignon JP, Bergman B, Chabowski M, Grunenwald D, Kozlowski M, Le Péchoux C, Pirker R, Pinel MI, Tarayre M, Le Chevalier T. Long-term results of the international adjuvant lung cancer trial evaluating adjuvant Cisplatin-based chemotherapy in resected lung cancer. *J Clin Oncol.* 2010 Jan 1;28(1):35-42. doi: 10.1200/JCO.2009.23.2272. Epub 2009 Nov 23.PMID: 19933916

Atkins D, Breuckmann A, Schmahl GE, Binner P, Ferrone S, Krummenauer F, Storkel S, Seliger B. MHC class I antigen processing pathway defects, ras mutations and disease stage in colorectal carcinoma. *Int J Cancer.* 2004; 109:265-73; PMID:14750179; <http://dx.doi.org/10.1002/ijc.1168116>.

**B**aldacci S, Besse B, Avrillon V, Mennecier B, Mazieres J, Dubray-Longeras P, Cortot AB, Descourt R, Doubre H, Quantin X, Duruisseaux M, Monnet I, Moro-Sibilot D, Cadranell J, Clément-Duchêne C, Cousin S, Ricordel C, Merle P, Otto J, Schneider S, Langlais A, Morin F, Westeel V, Girard N. Lorlatinib for advanced anaplastic lymphoma kinase-positive non-small cell lung cancer: Results of the IFCT-1803 LORLATU cohort. *Eur J Cancer.* 2022 May;166:51-59. doi: 10.1016/j.ejca.2022.01.018. Epub 2022 Mar 9.PMID: 35278825

Ball D, Mai GT, Vinod S, Babington S, Ruben J, Kron T, Chesson B, Herschtal A, Vanevski M, Rezo A, Elder C, Skala M, Wirth A, Wheeler G, Lim A, Shaw M, Schofield P, Irving L, Solomon B; TROG 09.02 CHISEL investigators. Stereotactic ablative radiotherapy versus standard radiotherapy in stage 1 non-small-cell lung cancer (TROG 09.02 CHISEL): a phase 3, open-label, randomised controlled trial. *Lancet Oncol.* 2019 Apr;20(4):494-503. doi: 10.1016/S1470-2045(18)30896-9. Epub 2019 Feb 12.PMID: 30770291

Bangia N, Lehner PJ, Hughes EA, Surman M, Cresswell P. The N-terminal region of tapasin is required to stabilize the MHC class I loading complex..*Eur J Immunol.* 1999 Jun;29(6):1858-70. doi:10.1002/(SICI)1521-4141(199906)29:06<1858::AID-IMMU1858>3.0.CO;2 C.PMID: 10382748

Besaratinia A, Pfeifer GP. Second-hand smoke and human lung cancer. *Lancet Oncol.* 2008 Jul;9(7):657-66. doi: 10.1016/S1470-2045(08)70172-4.PMID: 18598930

Blees A, Januliene D, Hofmann T, Koller N, Schmidt C, Trowitzsch S, Moeller A, Tampé R. Structure of the human MHC-I peptide-loading complex. *Nature.* 2017 Nov 23;551(7681):525-528. doi: 10.1038/nature24627. Epub 2017 Nov 6.PMID: 29107940

Bonomi M, Ahmed T, Addo S, Kooshki M, Palmieri D, Levine BJ, Ruiz J, Grant S, Petty WJ, Triozzi PL. Circulating immune biomarkers as predictors of the response to pembrolizumab and weekly low dose carboplatin and paclitaxel in NSCLC and poor PS: An interim analysis. *Oncol Lett.* 2019 Jan;17(1):1349-1356. doi: 10.3892/ol.2018.9724. Epub 2018 Nov 19. PMID: 30655905

Bottaro DP, Rubin JS, Faletto DL, Chan AM, Kmiecik TE, Vande Woude GF, Aaronson SA. Identification of the hepatocyte growth factor receptor as the c-met proto-oncogene product. *Science.* 1991 Feb 15;251(4995):802-4. doi: 10.1126/science.1846706. PMID: 1846706

Brun SS, Hansen TF, Wen SWC, Nyhus CH, Bertelsen L, Jakobsen A, Hansen TS, Nederby L. Soluble programmed death ligand 1 as prognostic biomarker in nonsmall cell lung cancer patients receiving nivolumab, pembrolizumab or atezolizumab therapy. *Sci Rep.* 2024 Apr 18;14(1):8993. doi: 10.1038/s41598-024-59791-0. PMID: 38637655

**C**allaghan RC, Allebeck P, Sidorchuk A. Marijuana use and risk of lung cancer: a 40-year cohort study. *Cancer Causes Control.* 2013 Oct;24(10):1811-20. doi: 10.1007/s10552-013-0259-0. Epub 2013 Jul 12. PMID: 23846283

Camidge DR, Bar J, Horinouchi H, Goldman J, Moiseenko F, Filippova E, Cicin I, Ciuleanu T, Daaboul N, Liu C, Bradbury P, Moskovitz M, Katgi N, Tomasini P, Zer A, Girard N, Cuppens K, Han JY, Wu SY, Baijal S, Mansfield AS, Kuo CH, Nishino K, Lee SH, Planchard D, Baik C, Li M, Ansell P, Xia S, Bolotin E, Looman J, Ratajczak C, Lu S. Telisotuzumab Vedotin Monotherapy in Patients With Previously Treated c-Met Protein-Overexpressing Advanced Nonsquamous EGFR-Wildtype Non-Small Cell Lung Cancer in the Phase II LUMINOSITY Trial. *J Clin Oncol.* 2024 Sep 1;42(25):3000-3011. doi: 10.1200/JCO.24.00720. Epub 2024 Jun 6. PMID: 38843488

Camidge DR, Kim HR, Ahn MJ, Yang JCH, Han JY, Hochmair MJ, Lee KH, Delmonte A, Garcia Campelo MR, Kim DW, Griesinger F, Felip E, Califano R, Spira AI, Gettinger SN, Tiseo M, Lin HM, Liu Y, Vranceanu F, Niu H, Zhang P, Popat S. Brigatinib Versus Crizotinib in ALK Inhibitor-Naive Advanced ALK-Positive NSCLC: Final Results of Phase 3 ALTA-1L Trial. *J Thorac Oncol.* 2021 Dec;16(12):2091-2108. doi: 10.1016/j.jtho.2021.07.035. Epub 2021 Sep 16. PMID: 34537440  
Cancer Discov. 2024 Sep 13:OF1-OF20. doi: 10.1158/2159-8290.CD-24-0231. Online ahead of print. PMID: 39269178

Casadevall D., Clavé S., Taus Á., Hardy-Werbin M., Rocha P., Lorenzo M., Menéndez S., Salido M., Albanell J., Pijuan L., et al. Heterogeneity of Tumor and Immune Cell PD-L1 Expression and Lymphocyte Counts in Surgical NSCLC Samples. *Clin. Lung Cancer.* 2017;18:682-691.e5. doi: 10.1016/j.cllc.2017.04.014

Cascone T, Awad MM, Spicer JD, He J, Lu S, Sepesi B, Tanaka F, Taube JM, Cornelissen R, Havel L, Karaseva N, Kuzdzal J, Petruzelka LB, Wu L, Pujol JL, Ito H, Ciuleanu TE, de Oliveira Muniz Koch L, Janssens A, Alexandru A, Bohnet S, Moiseyenko FV, Gao Y, Watanabe Y, Coronado Erdmann C, Sathyaranayana P, Meadows-Shropshire S, Blum SI, Provencio Pulla M; CheckMate 77T Investigators. Perioperative Nivolumab in Resectable Lung Cancer. *N Engl J Med.* 2024 May 16;390(19):1756-1769. doi: 10.1056/NEJMoa2311926.PMID: 38749033

Castello A, Rossi S, Toschi L, Mansi L, Lopci E. Soluble PD-L1 in NSCLC Patients Treated with Checkpoint Inhibitors and Its Correlation with Metabolic Parameters. *Cancers (Basel).* 2020 May 27;12(6):1373. doi: 10.3390/cancers12061373.PMID: 32471030

Champiat S, Dercle L, Ammari S, Massard C, Hollebecque A, Postel-Vinay S, Chaput N, Eggermont A, Marabelle A, Soria JC, Ferté C. Hyperprogressive Disease Is a New Pattern of Progression in Cancer Patients Treated by Anti-PD-1/PD-L1. *Clin Cancer Res.* 2017 Apr 15;23(8):1920-1928. doi: 10.1158/1078-0432.CCR-16-1741. Epub 2016 Nov 8.PMID: 27827313

Chang JY, Mehran RJ, Feng L, Verma V, Liao Z, Welsh JW, Lin SH, O'Reilly MS, Jeter MD, Balter PA, McRae SE, Berry D, Heymach JV, Roth JA; STARS Lung Cancer Trials Group. Stereotactic ablative radiotherapy for operable stage I non-small-cell lung cancer (revised STARS): long-term results of a single-arm, prospective trial with prespecified comparison to surgery. *Lancet Oncol.* 2021 Oct;22(10):1448-1457. doi: 10.1016/S1470-2045(21)00401-0. Epub 2021 Sep 13.PMID: 34529930

Chang JY, Senan S, Paul MA, Mehran RJ, Louie AV, Balter P, Groen HJ, McRae SE, Widder J, Feng L, van den Borne BE, Munsell MF, Hurkmans C, Berry DA, van Werkhoven E, Kresl JJ, Dingemans AM, Dawood O, Haasbeek CJ, Carpenter LS, De Jaeger K, Komaki R, Slotman BJ, Smit EF, Roth JA. Stereotactic ablative radiotherapy versus lobectomy for operable stage I non-small-cell lung cancer: a pooled analysis of two randomised trials. *Lancet Oncol.* 2015 Jun;16(6):630-7. doi: 10.1016/S1470-2045(15)70168-3. Epub 2015 May 13.PMID: 25981812

Cheng Y, Wang C, Wang Y, Dai L. Soluble PD-L1 as a predictive biomarker in lung cancer: a systematic review and meta-analysis. *Future Oncol.* 2022 Jan;18(2):261-273. doi: 10.2217/fon-20210641. Epub 2021 Dec 7.PMID: 34874185

Chew GL, Campbell AE, De Neef E, Sutliff NA, Shadle SC, Tapscott SJ, et al. . DUX4 suppresses MHC class I to promote cancer immune evasion and resistance to checkpoint blockade. *Dev Cell* 2019;50:658–71

Chiarucci C, Cannito S, Daffinà MG, Amato G, Giacobini G, Cutaia O, Lofiego MF, Fazio C, Giannarelli D, Danielli R, Di Giacomo AM, Coral S, Calabò L, Maio M, Covre A. Circulating Levels of PD-L1 in Mesothelioma Patients from the NIBIT-MESO-1 Study: Correlation with Survival. *Cancers (Basel).* 2020 Feb 5;12(2):361. doi: 10.3390/cancers12020361.PMID: 32033266

Chivu-Economescu M, Herlea V, Dima S, Sorop A, Pechianu C, Procop A, Kitahara S, Necula L, Matei L, Dragu D, Neagu AI, Bleotu C, Diaconu CC, Popescu I, Duda DG. Soluble PD-L1 as a diagnostic and prognostic biomarker in resectable gastric cancer patients. *Gastric Cancer*. 2023 Nov;26(6):934-946. doi: 10.1007/s10120-023-01429-7. Epub 2023 Sep 5. PMID: 37668884

Chmielewska I, Grenda A, Krawczyk P, Frąk M, Kuźnar Kamińska B, Mitura W, Milanowsk J. The influence of plasma sPD-L1 concentration on the effectiveness of immunotherapy in advanced NSCLC patients. *Cancer Immunol Immunother*. 2023 Dec;72(12):4169-4177. doi: 10.1007/s00262-023-03552-x. Epub 2023 Oct 10. PMID: 37816808

Cho BC, Lu S, Felip E, Spira AI, Girard N, Lee JS, Lee SH, Ostapenko Y, Danchaivijitr P, Liu B, Alip A, Korbenfeld E, Mourão Dias J, Besse B, Lee KH, Xiong H, How SH, Cheng Y, Chang GC, Yoshioka H, Yang JC, Thomas M, Nguyen D, Ou SI, Mukhedkar S, Prabhash K, D'Arcangelo M, Alatorre-Alexander J, Vázquez Limón JC, Alves S, Stroyakovskiy D, Peregudova M, Şendur MAN, Yazici O, Califano R, Gutiérrez Calderón V, de Marinis F, Passaro A, Kim SW, Gadgeel SM, Xie J, Sun T, Martinez M, Ennis M, Fennema E, Daksh M, Millington D, Leconte I, Iwasawa R, Lorenzini P, Baig M, Shah S, Baum JM, Shreeve SM, Sethi S, Knoblauch RE, Hayashi H; MARIPOSA Investigators. Amivantamab plus Lazertinib in Previously Untreated EGFR-Mutated Advanced NSCLC. *N Engl J Med*. 2024 Jun 26. doi: 10.1056/NEJMoa2403614. Online ahead of print. PMID: 38924756

Coe H, Michalak M. ERp57, a multifunctional endoplasmic reticulum resident oxidoreductase. *Int J Biochem Cell Biol*. 2010 Jun;42(6):796-9. doi: 10.1016/j.biocel.2010.01.009. Epub 2010 Jan 15. PMID: 20079872

Comoglio PM, Trusolino L, Boccaccio C. Known and novel roles of the MET oncogene in cancer: a coherent approach to targeted therapy. *Nat Rev Cancer*. 2018 Jun;18(6):341-358. doi: 10.1038/s41568-018-0002-y. PMID: 29674709

Coppolino M, Leung-Hagesteijn C, Dedhar S, Wilkins J. Inducible interaction of integrin alpha 2 beta 1 with calreticulin. Dependence on the activation state of the integrin. *J. Biol. Chem.* 1995;270:23132–23138

Coppolino MG. Calreticulin is essential for integrin-mediated calcium signalling and cell adhesion. *Nature*. 1997;386:843–847.

Costantini A, Julie C, Dumenil C, Hélias-Rodzewicz Z, Tisserand J, Dumoulin J, Giraud V, Labrune S, Chinet T, Emile JF, Giroux Leprieur E. Predictive role of plasmatic biomarkers in advanced non-small cell lung cancer treated by nivolumab. *Oncoimmunology*. 2018 Apr 20;7(8):e1452581. doi: 10.1080/2162402X.2018.1452581. eCollection 2018. PMID: 30221046

Costantini A, Takam Kamga P, Dumenil C, Chinet T, Emile JF, Giroux Leprieur E. Plasma Biomarkers and Immune Checkpoint Inhibitors in Non-Small Cell Lung Cancer: New Tools for Better Patient Selection? *Cancers (Basel)*. 2019 Aug 29;11(9):1269. doi: 10.3390/cancers11091269. PMID: 31470546

Couraud S, Swalduz A, Pierret T, Ranchon F, Forest F, Le Bon M, Galvaing G, Merle P, Souquet P-J, Toffart A-C, et le comité de rédaction des référentiels Auvergne Rhône-Alpes en oncologie thoracique. Référentiel sur le cancer bronchique non à petites-cellules : actualisation 2024. ARISTOT 2024. Accessible sur <http://referentiels-aristot.com/>

Cui Q, Li W, Wang D, Wang S, Yu J. Prognostic significance of blood-based PD-L1 analysis in patients with non-small cell lung cancer undergoing immune checkpoint inhibitor therapy: a systematic review and meta-analysis. *World J Surg Oncol.* 2023 Oct 11;21(1):318. doi: 10.1186/s12957-023-03215-2.PMID: 37821941

Datar IJ, Hauc SC, Desai S, Gianino N, Henick B, Liu Y, Syrigos K, Rimm DL, Kavathas P, Ferrone S, Schalper KA. Spatial Analysis and Clinical Significance of HLA Class-I and Class-II Subunit Expression in Non-Small Cell Lung Cancer. *Clin Cancer Res.* 2021 May 15;27(10):2837-2847. doi: 10.1158/1078-0432.CCR-20-3655. Epub 2021 Feb 18.PMID: 33602682

de Langen AJ, Johnson ML, Mazieres J, Dingemans AC, Mountzios G, Pless M, Wolf J, Schuler M, Lena H, Skoulidis F, Yoneshima Y, Kim SW, Linardou H, Novello S, van der Wekken AJ, Chen Y, Peters S, Felip E, Solomon BJ, Ramalingam SS, Dooms C, Lindsay CR, Ferreira CG, Blais N, Obiozor CC, Wang Y, Mehta B, Varriuer T, Ngarmchamnanirth G, Stollenwerk B, Waterhouse D, Paz-Ares L; CodeBreak 200 Investigators. Sotorasib versus docetaxel for previously treated non-small-cell lung cancer with KRAS<sup>G12C</sup> mutation: a randomised, open-label, phase 3 trial. *Lancet.* 2023 Mar 4;401(10378):733-746. doi: 10.1016/S0140 6736(23)00221-0. Epub 2023 Feb 7.PMID: 36764316

Defossez G, Le Guyader-Peyrou S, Uhry Z, Grosclaude P, Colonna M, Dantony E, et al. Estimations nationales de l'incidence et de la mortalité par cancer en France métropolitaine entre 1990 et 2018. Volume 1 – Tumeurs solides. Saint-Maurice (Fra) : Santé publique France, 2019. 372 p.

Dick TP, Bangia N, Peaper DR, Cresswell P. Disulfide bond isomerization and the assembly of MHC class I-peptide complexes. *Immunity.* 2002 Jan;16(1):87-98. doi: 10.1016/s1074-7613(02)00263-7.PMID: 11825568

Ding XC, Wang LL, Zhu YF, Li YD, Nie SL, Yang J, Liang H, Weichselbaum RR, Yu JM, Hu M. The Change of Soluble Programmed Cell Death-Ligand 1 in Glioma Patients Receiving Radiotherapy and Its Impact on Clinical Outcomes. *Front Immunol.* 2020 Oct 30;11:580335. doi: 10.3389/fimmu.2020.580335. eCollection 2020.PMID: 33224142

Dissemont J, Kothen T, Mors J, Weimann TK, Lindeke A, Goos M, Wagner SN. Downregulation of tapasin expression in progressive human malignant melanoma. *Arch Dermatol Res* 2003; 295:43-9;PMID:12682852; <http://dx.doi.org/10.1007/s00403-003-0393-811>.

Doll R, Peto R, Wheatley K, Gray R, Sutherland I. Mortality in relation to smoking: 40 years' observations on male British doctors. *BMJ* 1994;309:901-11.

Dong C, Hui K, Gu J, Wang M, Hu C, Jiang X. Plasma sPD-L1 and VEGF levels are associated with the prognosis of NSCLC patients treated with combination immunotherapy. *Anticancer Drugs*. 2024 Jun 1;35(5):418-425. doi: 10.1097/CAD.0000000000001576. Epub 2024 Feb 23. PMID: 38386011

Dong G, Wearsch PA, Peaper DR, Cresswell P, Reinisch KM. Insights into MHC class I peptide loading from the structure of the tapasin-ERp57 thiol oxidoreductase heterodimer. *Immunity*. 2009 Jan 16;30(1):21-32. doi: 10.1016/j.jimmuni.2008.10.018. PMID: 19119025

Dong H, Zhu G, Tamada K, Chen L. B7-H1, a third member of the B7 family, co-stimulates T-cell proliferation and interleukin-10 secretion. *Nat Med*. 1999 Dec;5(12):1365-9. doi: 10.1038/70932. PMID: 10581077

Drilon A, Clark JW, Weiss J, Ou SI, Camidge DR, Solomon BJ, Otterson GA, Villaruz LC, Riely GJ, Heist RS, Awad MM, Shapiro GI, Satouchi M, Hida T, Hayashi H, Murphy DA, Wang SC, Li S, Usari T, Wilner KD, Paik PK. Antitumor activity of crizotinib in lung cancers harboring a MET exon 14 alteration. *Nat Med*. 2020 Jan;26(1):47-51. doi: 10.1038/s41591-019-0716-8. Epub 2020 Jan 13. PMID: 3193280

Drilon A, Camidge DR, Lin JJ, Kim SW, Solomon BJ, Dziadziszko R, Besse B, Goto K, de Langen AJ, Wolf J, Lee KH, Popat S, Springfield C, Nagasaka M, Felip E, Yang N, Velcheti V, Lu S, Kao S, Dooms C, Krebs MG, Yao W, Beg MS, Hu X, Moro-Sibilot D, Cheema P, Stopatschinskaja S, Mehta M, Trone D, Gruber A, Sims G, Yuan Y, Cho BC; TRIDENT-1 Investigators. Repotrectinib in ROS1 Fusion-Positive Non-Small-Cell Lung Cancer. *N Engl J Med*. 2024 Jan 11;390(2):118-131. doi: 10.1056/NEJMoa2302299. PMID: 38197815

Drilon A, Siena S, Dziadziszko R, Barlesi F, Krebs MG, Shaw AT, de Braud F, Rolfo C, Ahn MJ, Wolf J, Seto T, Cho BC, Patel MR, Chiu CH, John T, Goto K, Karapetis CS, Arkenau HT, Kim SW, Ohe Y, Li YC, Chae YK, Chung CH, Otterson GA, Murakami H, Lin CC, Tan DSW, Prenen H, Riehl T, Chow-Maneval E, Simmons B, Cui N, Johnson A, Eng S, Wilson TR, Doebele RC; trial investigators. Entrectinib in ROS1 fusion-positive non-small-cell lung cancer: integrated analysis of three phase 1-2 trials. *Lancet Oncol*. 2020 Feb;21(2):261-270. doi: 10.1016/S1470-2045(19)30690-4. Epub 2019 Dec 11. PMID: 31838015

Du S, McCall N, Park K, Guan Q, Fontina P, Ertel A, Zhan T, Dicker AP, Lu B. Blockade of Tumor-Expressed PD-1 promotes lung cancer growth. *Oncoimmunology*. 2018 Jan 29;7(4):e1408747. doi: 10.1080/2162402X.2017.1408747. eCollection 2018. PMID: 29632720

Duplaquet L, Kherrouche Z, Baldacci S, Jamme P, Cortot AB, Copin MC, Tulasne D. The multiple paths towards MET receptor addiction in cancer. *Oncogene*. 2018 Jun;37(24):3200-3215. doi: 10.1038/s41388-018-0185-4. Epub 2018 Mar 19. PMID: 29551767

**F**acoetti A, Nano R, Zelini P, Morbini P, Benericetti E, Ceroni M, Campoli M, Ferrone S. Human leukocyte antigen and antigen processing machinery component defects in astrocytic tumors. Clin Cancer Res 2005; 11:8304-11; PMID:16322289; <http://dx.doi.org/10.1158/1078-0432.CCR-04-258817>.

Fang MY, Wang SY, Zheng YB, Gong LY, Bao WL, Gu DL, Mao WM. Prognostic and predictive significance of plasma hepatocyte growth factor and carcinoembryonic antigen in non-small lung cancer after surgery. Eur Rev Med Pharmacol Sci. 2014;18(3):398-403. PMID: 24563441

Fei Y, Yu J, Li Y, Li L, Zhou S, Zhang T, Li L, Qiu L, Meng B, Pan Y, Ren X, Qian Z, Wang X, Zhang H. Plasma soluble PD-L1 and STAT3 predict the prognosis in diffuse large B cell lymphoma patients. J Cancer. 2020 Oct 17;11(23):7001-7008. doi: 10.7150/jca.47816. eCollection 2020. PMID: 33123290

Felip E, Altorki N, Zhou C, Csőzsi T, Vynnychenko I, Goloborodko O, Luft A, Akopov A, Martinez-Marti A, Kenmotsu H, Chen YM, Chella A, Sugawara S, Voong D, Wu F, Yi J, Deng Y, McCleland M, Bennett E, Gitlitz B, Wakelee H; IMpower010 Investigators. Adjuvant atezolizumab after adjuvant chemotherapy in resected stage IB-IIIA non-small-cell lung cancer (IMpower010): a randomised, multicentre, open-label, phase 3 trial. Lancet. 2021 Oct 9;398(10308):1344-1357. doi: 10.1016/S0140-6736(21)02098-5. Epub 2021 Sep 20. PMID: 34555333

Felip E, Altorki N, Zhou C, Vallières E, Martínez-Martí A, Rittmeyer A, Chella A, Reck M, Goloborodko O, Huang M, Belleli R, McNally V, Srivastava MK, Bennett E, Gitlitz BJ, Wakelee HA. Overall survival with adjuvant atezolizumab after chemotherapy in resected stage II-IIIA non-small-cell lung cancer (IMpower010): a randomised, multicentre, open-label, phase III trial. Ann Oncol. 2023 Oct;34(10):907-919. doi: 10.1016/j.annonc.2023.07.001. Epub 2023 Jul 17. PMID: 37467930

Fois SS, Paliogiannis P, Zinelli A, Fois AG, Cossu A, Palmieri G. Molecular Epidemiology of the Main Druggable Genetic Alterations in Non Small Cell Lung Cancer. Int J Mol Sci. 2021 Jan 9;22(2):612. doi: 10.3390/ijms22020612. PMID: 33435440

Forde PM, Spicer J, Lu S, Provencio M, Mitsudomi T, Awad MM, Felip E, Broderick SR, Brahmer JR, Swanson SJ, Kerr K, Wang C, Ciuleanu TE, Sailors GB, Tanaka F, Ito H, Chen KN, Liberman M, Vokes EE, Taube JM, Dorange C, Cai J, Fiore J, Jarkowski A, Balli D, Sausen M, Pandya D, Calvet CY, Girard N; CheckMate 816 Investigators. Neoadjuvant Nivolumab plus Chemotherapy in Resectable Lung Cancer. N Engl J Med. 2022 May 26;386(21):1973-1985. doi: 10.1056/NEJMoa2202170. Epub 2022 Apr 11. PMID: 35403841

Frigola X, Inman BA, Krco CJ, Liu X, Harrington SM, Bultur PA, Dietz AB, Dong H, Kwon ED. Soluble B7-H1: differences in production between dendritic cells and T cells. Immunol Lett. 2012 Feb 29;142(1-2):78-82. doi: 10.1016/j.imlet.2011.11.001. Epub 2011 Nov 25. PMID: 22138406

[Frigola X](#), Inman [BA](#), Lohse [CM](#), Krco [CJ](#), Cheville [JC](#), Thompson [RH](#), Leibovich [B](#), Blute [ML](#), Dong H, Kwon [ED](#). Identification of a soluble form of B7-H1 that retains immunosuppressive activity and is associated with aggressive renal cell carcinoma. *Clin Cancer Res.* 2011 Apr 1;17(7):1915-23. doi: 10.1158/1078-0432.CCR-10-0250. Epub 2011 Feb 25.

Fucikova J, Spisek R, Kroemer G, Galluzzi L. Calreticulin and cancer. *Cell Res.* 2021 Jan;31(1):5-16. doi: 10.1038/s41422-020-0383-9. Epub 2020 Jul 30. PMID: 32733014

Fukushima T, Uchiyama S, Tanaka H, Kataoka H. Hepatocyte Growth Factor Activator: A Proteinase Linking Tissue Injury with Repair. *Int J Mol Sci.* 2018 Nov 1;19(11):3435. doi: 10.3390/ijms19113435. PMID: 30388869

**G**álffy G, Morócz É, Korompay R, Hécz R, Bujdosó R, Puskás R, Lovas T, Gáspár E, Yahya K, Király P, Lohinai Z. [Targeted therapeutic options in early and metastatic NSCLC-overview](#). *Pathol Oncol Res.* 2024 Mar 28;30:1611715. doi: 10.3389/pore.2024.1611715. eCollection 2024. PMID: 38605928

Gambarotta G, Boccaccio C, Giordano S, Andő M, Stella MC, Comoglio PM. Ets up-regulates MET transcription. *Oncogene.* 1996 Nov 7;13(9):1911-7. PMID: 8934537

Gandhi L, Rodríguez-Abreu D, Gadgeel S, Esteban E, Felip E, De Angelis F, Domine M, Clingen P, Hochmair MJ, Powell SF, Cheng SY, Bischoff HG, Peled N, Grossi F, Jennens RR, Reck M, Hui R, Garon EB, Boyer M, Rubio-Viqueira B, Novello S, Kurata T, Gray JE, Vida J, Wei Z, Yang J, Raftopoulos H, Pietanza MC, Garassino MC; KEYNOTE-189 Investigators. Pembrolizumab plus Chemotherapy in Metastatic Non-Small-Cell Lung Cancer. *N Engl J Med.* 2018 May 31;378(22):2078-2092. doi: 10.1056/NEJMoa1801005. Epub 2018 Apr 16. PMID: 29658856

[Garbi N](#), [Tiwari N](#), [Momburg F](#), [Hämmerling GJ](#). A major role for tapasin as a stabilizer of the TAP peptide transporter and consequences for MHC class I expression. *Eur J Immunol.* 2003 Jan;33(1):264-73. doi: 10.1002/immu.200390029.

Garnett J, Chumbalkar V, Vaillant B, Gururaj AE, Hill KS, Latha K, Yao J, Priebe W, Colman H, Elferink LA, Bogler O. Regulation of HGF expression by deltaEGFR-mediated c-Met activation in glioblastoma cells. *Neoplasia.* 2013 Jan;15(1):73-84. doi: 10.1593/neo.121536. PMID: 23359207

Garrido F. MHC/HLA class I loss in cancer cells. *Adv Exp Med Biol* 2019;1151:15–78. - Geiger K, Joerger M, Roessler M, Hettwer K, Ritter C, Simon K, Uhlig S, Holdenrieder S. Missing prognostic value of soluble PD-1, PD-L1 and PD-L2 in lung cancer patients undergoing chemotherapy - A CEPAC-TDM biomarker substudy.. *Tumour Biol.* 2024;46(s1):S355-S367. doi: 10.3233/TUB-230015. PMID: 38277316

Genova C, Tasso R, Rosa A, Rossi G, Reverberi D, Fontana V, Marconi S, Croce M, Dal Bello MG, Dellepiane C, Tagliamento M, Ciferri MC, Zullo L, Fedeli A, Alama A, Cortese K, Gentili C, Cella E, Anselmi G, Mora M, Barletta G, Rijavec E, Grossi F, Pronzato P, Coco S. Prognostic Role of Soluble and Extracellular Vesicle-Associated PD-L1, B7-H3 and B7-H4 in NonSmall Cell Lung Cancer Patients Treated with Immune Checkpoint Inhibitors. *Cells.* 2023 Mar 8;12(6):832. doi: 10.3390/cells12060832.PMID: 36980174

Gettinger S, Choi J, Hastings K, Truini A, Datar I, Sowell R, Wurtz A, Dong W, Cai G, Melnick MA, Du VY, Schlessinger J, Goldberg SB, Chiang A, Sanmamed MF, Melero I, Agorreta J, Montuenga LM, Lifton R, Ferrone S, Kavathas P, Rimm DL, Kaech SM, Schalper K, Herbst RS, Politi K. Impaired HLA Class I Antigen Processing and Presentation as a Mechanism of Acquired Resistance to Immune Checkpoint Inhibitors in Lung Cancer. *Cancer Discov.* 2017 Dec;7(12):1420-1435. doi: 10.1158/2159-8290.CD-17-0593. Epub 2017 Oct 12.PMID: 29025772

Giroux Leprieur E, Hélias-Rodzewicz Z, Takam Kamga P, Costantini A, Julie C, Corjon A, Dumenil C, Dumoulin J, Giraud V, Labrune S, Garinet S, Chinet T, Emile JF. Sequential ctDNA whole-exome sequencing in advanced lung adenocarcinoma with initial durable tumor response on immune checkpoint inhibitor and late progression. *J Immunother Cancer.* 2020 Jun;8(1):e000527. doi: 10.1136/jitc-2020-000527.PMID: 32581058

Gogishvili M, Melkadze T, Makharadze T, Giorgadze D, Dvorkin M, Penkov K, Laktionov K, Nemsadze G, Nechaeva M, Rozhkova I, Kalinka E, Gessner C, Moreno-Jaime B, Passalacqua R, Li S, McGuire K, Kaul M, Paccaly A, Quek RGW, Gao B, Seebach F, Weinreich DM, Yancopoulos GD, Lowy I, Gullo G, Rietschel P. Cemiplimab plus chemotherapy versus chemotherapy alone in non-small cell lung cancer: a randomized, controlled, double-blind phase 3 trial. *Nat Med.* 2022 Nov;28(11):2374-2380. doi: 10.1038/s41591-022-01977-y. Epub 2022 Aug 25.PMID: 36008722

Goss G, G.E. Darling GE, Westeel V, Nakagawa K, Massuti Sureda B, Perrone F, McLachlan S, Kang JH, Wu Y, Dingemans AC, Dziadziuszko R, Okada M, Greillier L, Audigier-Valette C, Sugawara S, Nadal E, Catino<sup>1</sup> A, Stockler MR, Ding K, O'Callaghan C LBA48 - CCTG BR.31: A global, double-blind placebo-controlled, randomized phase III study of adjuvant durvalumab in completely resected non-small cell lung cancer (NSCLC). *Annals of Oncology* (2024) 35 (suppl\_2): 1-72. 10.1016/annonc/annonc1623

Guo X, Wang J, Jin J, Chen H, Zhen Z, Jiang W, Lin T, Huang H, Xia Z, Sun X. High Serum Level of Soluble Programmed Death Ligand 1 is Associated With a Poor Prognosis in Hodgkin Lymphoma. *Transl Oncol.* 2018 Jun;11(3):779-785. doi: 10.1016/j.tranon.2018.03.012. Epub 2018 Apr 24.PMID: 29698935

**H**an B, Dong L, Zhou J, Yang Y, Guo J, Xuan Q, Gao K, Xu Z, Lei W, Wang J, Zhang Q. The clinical implication of soluble PD-L1 (sPD-L1) in patients with breast cancer and its biological function in regulating the function of T lymphocyte. *Cancer Immunol Immunother.* 2021 Oct;70(10):2893-2909. doi: 10.1007/s00262-021-02898-4. Epub 2021 Mar 10.PMID: 33688997

Hanagiri T, Shigematsu Y, Shinohara S, Takenaka M, Oka S, Chikaishi Y, Nagata Y, Baba T, Uramoto H, So T, Yamada S. [Clinical significance of expression of cancer/testis antigen and down-regulation of HLA class-I in patients with stage I non-small cell lung cancer.](#) Anticancer Res. 2013 May;33(5):2123-8. PMID: 23645764

Hayashi H, Chamoto K, Hatae R, Kurosaki T, Togashi Y, Fukuoka K, Goto M, Chiba Y, Tomida S, Ota T, Haratani K, Takahama T, Tanizaki J, Yoshida T, Iwasa T, Tanaka K, Takeda M, Hirano T, Yoshida H, Ozasa H, Sakamori Y, Sakai K, Higuchi K, Uga H, Suminaka C, Hirai T, Nishio K, Nakagawa K, Honjo T. Soluble immune checkpoint factors reflect exhaustion of antitumor immunity and response to PD-1 blockade. J Clin Invest. 2024 Apr 1;134(7):e168318. doi: 10.1172/JCI168318. PMID: 38557498

He J, Pan Y, Guo Y, Li B, Tang Y. Study on the Expression Levels and Clinical Significance of PD-1 and PD-L1 in Plasma of NSCLC Patients. J Immunother. 2020 Jun;43(5):156-164. doi: 10.1097/CJI.0000000000000315. PMID: 32168233

Herbst RS, Giaccone G, de Marinis F, Reinmuth N, Vergnenegre A, Barrios CH, Morise M, Felip E, Andric Z, Geater S, Özgüroğlu M, Zou W, Sandler A, Enquist I, Komatsubara K, Deng Y, Kuriki H, Wen X, McCleland M, Mocci S, Jassem J, Spigel DR. [Atezolizumab for First-Line Treatment of PD-L1-Selected Patients with NSCLC.](#) N Engl J Med. 2020 Oct 1;383(14):1328-1339. doi: 10.1056/NEJMoa1917346. PMID: 32997907

Herbst RS, Wu YL, John T, Grohe C, Majem M, Wang J, Kato T, Goldman JW, Laktionov K, Kim SW, Yu CJ, Vu HV, Lu S, Lee KY, Mukhametshina G, Akewanlop C, de Marinis F, Bonanno L, Domine M, Shepherd FA, Urban D, Huang X, Bolanos A, Stachowiak M, Tsuboi M. Adjuvant Osimertinib for Resected EGFR-Mutated Stage IB-IIIA Non-Small-Cell Lung Cancer: Updated Results From the Phase III Randomized ADAURA Trial. J Clin Oncol. 2023 Apr 1;41(10):1830-1840. doi: 10.1200/JCO.22.02186. Epub 2023 Jan 31. PMID: 36720083

Heymach J, Opdam F, Barve M, Gibson N, Sadrolhefazi B, Serra J, Yamamoto N. A Phase I, Open-Label, Dose Confirmation, Escalation, and Expansion Trial of BI 1810631 as Monotherapy in Patients With Advanced or Metastatic Solid Tumors With HER2 Aberrations. [Clin Lung Cancer.](#) 2023 Mar;24(2):e65-e68. doi: 10.1016/j.cllc.2022.10.008. Epub 2022 Nov 11. PMID: 36528522 Free article.

Heymach JV, Harpole D, Mitsudomi T, Taube JM, Galffy G, Hochmair M, Winder T, Zukov R, Garbaos G, Gao S, Kuroda H, Ostros G, Tran TV, You J, Lee KY, Antonuzzo L, Papai-Szekely Z, Akamatsu H, Biswas B, Spira A, Crawford J, Le HT, Aperghis M, Doherty GJ, Mann H, Fouad TM, Reck M; AEGEAN Investigators. Perioperative Durvalumab for Resectable Non-Small-Cell Lung Cancer. [N Engl J Med.](#) 2023 Nov 2;389(18):1672-1684. doi: 10.1056/NEJMoa2304875. Epub 2023 Oct 23. PMID: 37870974

Hosoda H, Izumi H, Tukada Y, Takagiwa J, Chiaki T, Yano M, Arai H. Plasma hepatocyte growth factor elevation may be associated with early metastatic disease in primary lung cancer patients. *Ann Thorac Cardiovasc Surg.* 2012;18(1):1-7. doi: 10.5761/atcs.oa.09.01522. Epub 2011 Sep 29. PMID: 21959198

Hill W, Lim EL, Weeden CE, Lee C, Augustine M, Chen K, Kuan FC, Marongiu F, Evans EJ Jr, Moore DA, Rodrigues FS, Pich O, Bakker B, Cha H, Myers R, van Maldegem F, Boumelha J, Veeriah S, Rowan A, Naceur-Lombardelli C, Karasaki T, Sivakumar M, De S, Caswell DR, Nagano A, Black JRM, Martínez-Ruiz C, Ryu MH, Huff RD, Li S, Favé MJ, Magness A, Suárez-Bonnet A, Priestnall SL, Lüchtenborg M, Lavelle K, Pethick J, Hardy S, McRonald FE, Lin MH, Troccoli CI, Ghosh M, Miller YE, Merrick DT, Keith RL, Al Bakir M, Bailey C, Hill MS, Saal LH, Chen Y, George AM, Abbosh C, Kanu N, Lee SH, McGranahan N, Berg CD, Sasieni P, Houlston R, Turnbull C, Lam S, Awadalla P, Grönroos E, Downward J, Jacks T, Carlsten C, Malanchi I, Hackshaw A, Litchfield K; TRACERx Consortium; DeGregori J, Jamal-Hanjani M, Swanton C. Lung adenocarcinoma promotion by air pollutants. *Nature.* 2023 Apr;616(7955):159-167. doi: 10.1038/s41586-023-05874-3. Epub 2023 Apr 5. PMID: 37020004

Himuro H, Nakahara Y, Igarashi Y, Kouro T, Higashijima N, Matsuo N, Murakami S, Wei F, Horaguchi S, Tsuji K, Mano Y, Saito H, Azuma K, Sasada T. Clinical roles of soluble PD-1 and PD-L1 in plasma of NSCLC patients treated with immune checkpoint inhibitors. *Cancer Immunol Immunother.* 2023 Aug;72(8):2829-2840. doi: 10.1007/s00262-023-03464-w. Epub 2023 May 16. PMID: 37188764

Ilie M., Long-Mira E., Bence C., Butori C., Lassalle S., Bouhlel L., Fazzalari L., Zahaf K., Lalvée S., Washetine K., et al. Comparative study of the PDL1 status between surgically resected specimens and matched biopsies of NSCLC patients reveal major discordances: A potential issue for anti-PD-L1 therapeutic strategies. *Ann. Oncol.* 2016;27:147–153. doi: 10.1093/annonc/mdv489.

Incorvaia L, Fanale D, Badalamenti G, Porta C, Olive D, De Luca I, Brando C, Rizzo M, Messina C, Rediti M, Russo A, Bazan V, Iovanna JL. Baseline plasma levels of soluble PD-1, PD-L1, and BTN3A1 predict response to nivolumab treatment in patients with metastatic renal cell carcinoma: a step toward a biomarker for therapeutic decisions. *Oncoimmunology.* 2020 Oct 27;9(1):1832348. doi: 10.1080/2162402X.2020.1832348. PMID: 33178494

Iveson T, Donehower RC, Davidenko I, Tjulandin S, Deptala A, Harrison M, Nirni S, Lakshmaiah K, Thomas A, Jiang Y, Zhu M, Tang R, Anderson A, Dubey S, Oliner KS, Loh E. Rilotumumab in combination with epirubicin, cisplatin, and capecitabine as first-line treatment for gastric or oesophagogastric junction adenocarcinoma: an open-label, dose de-escalation phase 1b study and a double-blind, randomised phase 2 study. *Lancet Oncol.* 2014 Aug;15(9):1007-18. doi: 10.1016/S1470-2045(14)70023-3. Epub 2014 Jun 22. PMID: 24965569

Jäne PA, Riely GJ, Gadgeel SM, Heist RS, Ou SI, Pacheco JM, Johnson ML, Sabari JK, Leventakos

K, Yau E, Bazhenova L, Negrao MV, Pennell NA, Zhang J, Anderes K, Der-Torossian H, Kheoh T, Velastegui K, Yan X, Christensen JG, Chao RC, Spira AI. Adagrasib in Non-Small-Cell Lung Cancer Harboring a KRAS(G12C) Mutation. *N Engl J Med.* 2022 Jul 14;387(2):120-131. doi: 10.1056/NEJMoa2204619. Epub 2022 Jun 3. PMID: 35658005

Jhunjhunwala S, Hammer C, Delamarre L. Antigen presentation in cancer: insights into tumour immunogenicity and immune evasion. *Nat Rev Cancer* 2021;21:298–312.

Jia Y, Li X, Zhao C, Ren S, Su C, Gao G, Li W, Zhou F, Li J, Zhou C. Soluble PD-L1 as a Predictor of the Response to EGFR-TKIs in Nonsmall Cell Lung Cancer Patients With EGFR Mutations. *Front Oncol.* 2020 Aug 25;10:1455. doi: 10.3389/fonc.2020.01455. eCollection 2020. PMID: 32983977

Jovanović D, Roksandić-Milenković M, Kotur-Stevuljević J, Ćeriman V, Vukanić I, Samardžić N, Popević S, Ilić B, Gajić M, Simon M, Simon I, Spasojević-Kalimanovska V, Belić M, Mirkov D, Šumarac Z, Milenković V. Soluble sPD-L1 and Serum Amyloid A1 as Potential Biomarkers for Lung Cancer. *J Med Biochem.* 2019 May 11;38(3):332-341. doi: 10.2478/jomb-2018-0036. eCollection 2019 Jul. PMID: 31156344

**K**amada T, Togashi Y, Tay C, Ha D, Sasaki A, Nakamura Y, Sato E, Fukuoka S, Tada Y, Tanaka A, Morikawa H, Kawazoe A, Kinoshita T, Shitara K, Sakaguchi S, Nishikawa H. PD-1(+) regulatory T cells amplified by PD-1 blockade promote hyperprogression of cancer. *Proc Natl Acad Sci U S A.* 2019 May 14;116(20):9999-10008. doi: 10.1073/pnas.1822001116. Epub 2019 Apr 26. PMID: 31028147

Karasrides M, Cogdill AP, Robbins PB, Bowden M, Burton EM, Butterfield LH, Cesano A, Hammer C, Haymaker CL, Horak CE, McGee HM, Monette A, Rudqvist NP, Spencer CN, Sweis RF, Vincent BG, Wennerberg E, Yuan J, Zappasodi R, Lucey VMH, Wells DK, LaVallee T. Hallmarks of Resistance to Immune-Checkpoint Inhibitors. *Cancer Immunol Res.* 2022 Apr 1;10(4):372-383. doi: 10.1158/2326-6066.CIR-20-0586. PMID: 35362046

Kikuchi E, Yamazaki K, Torigoe T, Cho Y, Miyamoto M, Oizumi S, Hommura F, Dosaka-Akita H, Nishimura M. HLA class I antigen expression is associated with a favorable prognosis in early stage non-small cell lung cancer. *Cancer Sci.* 2007 Sep;98(9):1424-30. doi: 10.1111/j.1349-7006.2007.00558.x. Epub 2007 Jul 23. PMID: 17645781

Kim JH, Kim HS, Kim BJ. Prognostic value of MET copy number gain in non-small-cell lung cancer: an updated meta-analysis. *J Cancer.* 2018 Apr 23;9(10):1836-1845. doi: 10.7150/jca.24980. eCollection 2018. PMID: 29805710

Kim S., Kim M.Y., Koh J., Go H., Lee D.S., Jeon Y.K., Chung D.H. Programmed death-1 ligand 1 and 2 are highly expressed in pleomorphic carcinomas of the lung: Comparison of sarcomatous and carcinomatous areas. *Eur. J. Cancer.* 2015;51:2698–2707. doi: 10.1016/j.ejca.2015.08.013.

Kincaid EZ, Che JW, York I, Escobar H, Reyes-Vargas E, Delgado JC, Welsh RM, Karow ML, Murphy AJ, Valenzuela DM, Yancopoulos GD, Rock KL. Mice completely lacking immunoproteasomes show major changes in antigen presentation. *Nat Immunol.* 2011 Dec 25;13(2):129-35. doi: 10.1038/ni.2203.PMID: 22197977

Klebe S, Leigh J, Henderson DW, Nurminen M. Asbestos, Smoking and Lung Cancer: An Update. *Int J Environ Res Public Health.* 2019 Dec 30;17(1):258. doi: 10.3390/ijerph17010258.PMID: 31905913

Kluger H, Barrett JC, Gainor JF, Hamid O, Hurwitz M, LaVallee T, Moss RA, Zappasodi R, Sullivan RJ, Tawbi H, Sharon E. Society for Immunotherapy of Cancer (SITC) consensus definitions for resistance to combinations of immune checkpoint inhibitors. *J Immunother Cancer.* 2023 Mar;11(3):e005921. doi: 10.1136/jitc-2022-005921.PMID: 36918224

Kong-Beltran M, Stamos J, Wickramasinghe D. The Sema domain of Met is necessary for receptor dimerization and activation. *Cancer Cell.* 2004 Jul;6(1):75-84. doi: 10.1016/j.ccr.2004.06.013.PMID: 15261143

Korkolopoulou P, Kaklamani L, Pezzella F, Harris AL, Gatter KC. Loss of antigen-presenting molecules (MHC class I and TAP-1) in lung cancer. *Br J Cancer.* 1996 Jan;73(2):148-53. doi: 10.1038/bjc.1996.28.PMID: 8546899

Krebs M, Spira AI, Cho BC. Amivantamab in patients with NSCLC with MET exon 14 skipping mutation: updated results from the CHRYSLIS study *J Clin Oncol.* 40 (suppl 16) (2022) 9008–9008

Krishnakumar S, Abhyankar D, Sundaram AL, Pushparaj V, Shanmu-gam MP, Biswas J. Major histocompatibility antigens and antigen-processing molecules in uveal melanoma. *Clin Cancer Res.* 2003;9:4159-64; PMID:1451964012.

Kubo Y, Fukushima S, Inamori Y, Tsuruta M, Egashira S, Yamada-Kanazawa S, Nakahara S, Tokuzumi A, Miyashita A, Aoi J, Kajihara I, Tomita Y, Wakamatsu K, Jinnin M, Ihn H. Serum concentrations of HGF are correlated with response to anti-PD-1 antibody therapy in patients with metastatic melanoma. *J Dermatol Sci.* 2019 Jan;93(1):33-40. doi: 10.1016/j.jdermsci.2018.10.001. Epub 2018 Oct 6.PMID: 30318169

Kuroasaki T, Chamoto K, Suzuki S, Kanemura H, Mitani S, Tanaka K, Kawakami H, Kishimoto Y, Haku Y, Ito K, Sato T, Suminaka C, Yamaki M, Chiba Y, Yaguchi T, Omori K, Kobayashi T, Nakagawa K, Honjo T, Hayashi H. The combination of soluble forms of PD-1 and PD-L1 as a predictive marker of PD-1 blockade in patients with advanced cancers: a multicenter retrospective study. *Front Immunol.* 2023 Dec 11;14:1325462. doi: 10.3389/fimmu.2023.1325462. eCollection 2023.PMID: 38149256

**L**arrinaga G, Solano-Iturri JD, Errarte P, Unda M, Loizaga-Iriarte A, Pérez-Fernández A, Echevarría E, Asumendi A, Manini C, Angulo JC, López JI. Soluble PD-L1 Is an Independent Prognostic Factor in Clear Cell Renal Cell Carcinoma. *Cancers (Basel)*. 2021 Feb 7;13(4):667. doi: 10.3390/cancers13040667. PMID: 33562338

Li BT, Smit EF, Goto Y, Nakagawa K, Udagawa H, Mazières J, Nagasaka M, Bazhenova L, Saltos AN, Felip E, Pacheco JM, Pérol M, Paz-Ares L, Saxena K, Shiga R, Cheng Y, Acharyya S, Vitazka P, Shahidi J, Planchard D, Jänne PA; DESTINY-Lung01 Trial Investigators. Trastuzumab Deruxtecan in HER2-Mutant Non-Small-Cell Lung Cancer. *N Engl J Med*. 2022 Jan 20;386(3):241-251. doi: 10.1056/NEJMoa2112431. Epub 2021 Sep 18. PMID: 34534430

Li C., Huang C., Mok T.S., Zhuang W., Xu H., Miao Q., Fan X., Zhu W., Huang Y., Lin X., et al. Comparison of 22C3 PD-L1 Expression between Surgically Resected Specimens and Paired Tissue Microarrays in Non-Small Cell Lung Cancer. *J Thorac Oncol*. 2017;12:1536–1543. doi: 10.1016/j.jtho.2017.07.015.

Li G, Choi JE, Kryczek I, Sun Y, Liao P, Li S, Wei S, Grove S, Vatan L, Nelson R, Schaefer G, Allen SG, Sankar K, Fecher LA, Mendiratta-Lala M, Frankel TL, Qin A, Waninger JJ, Tezel A, Alva A, Lao CD, Ramnath N, Cieslik M, Harms PW, Green MD, Chinnaiyan AM, Zou W. Intersection of immune and oncometabolic pathways drives cancer hyperprogression during immunotherapy. *Cancer Cell*. 2023 Feb 13;41(2):304-322.e7. doi: 10.1016/j.ccr.2022.12.008. Epub 2023 Jan 12. PMID: 36638784

Li X, Du H, Zhan S, Liu W, Wang Z, Lan J, PuYang L, Wan Y, Qu Q, Wang S, Yang Y, Wang Q, Xie F. The interaction between the soluble programmed death ligand-1 (sPD-L1) and PD-1 + regulator B cells mediates immunosuppression in triple-negative breast cancer. *Front Immunol*. 2022 Jul 22;13:830606. doi: 10.3389/fimmu.2022.830606. eCollection 2022. PMID: 35935985

Liang Z, Chen W, Guo Y, Ren Y, Tian Y, Cai W, Bao Y, Liu Q, Ding P, Li Y. Soluble monomeric human programmed cell death-ligand 1 inhibits the functions of activated T cells. *Front Immunol*. 2023 May 17:14:1133883. doi: 10.3389/fimmu.2023.1133883. eCollection 2023.

Liao G, Zhao Z, Qian Y, Ling X, Chen S, Li X, Kong F. Prognostic Role of Soluble Programmed Death Ligand 1 in Non-Small Cell Lung Cancer: A Systematic Review and Meta-Analysis. *Front Oncol*. 2021 Dec 23;11:774131. doi: 10.3389/fonc.2021.774131. eCollection 2021. PMID: 35004295

Lim S.H., Hong M., Ahn S., Choi Y.L., Kim K.M., Oh D., Ahn Y.C., Jung S.H., Ahn M.J., Park K., et al. Changes in tumour expression of programmed death-ligand 1 after neoadjuvant concurrent chemoradiotherapy in patients with squamous oesophageal cancer. *Eur. J. Cancer*. 2016;52:1–9. doi: 10.1016/j.ejca.2015.09.019.

Lim SM, Kim HR, Lee JS, Lee KH, Lee YG, Min YJ, Cho EK, Lee SS, Kim BS, Choi MY, Shim HS, Chung JH, La Choi Y, Lee MJ, Kim M, Kim JH, Ali SM, Ahn MJ, Cho BC. Open-

Label, Multicenter, Phase II Study of Ceritinib in Patients With Non-Small-Cell Lung Cancer Harboring ROS1 Rearrangement. *J Clin Oncol.* 2017 Aug 10;35(23):2613-2618. doi: 10.1200/JCO.2016.71.3701. Epub 2017 May 18.PMID: 28520527

Lin JJ, Horan JC, Tangpeerachaikul A, Swalduz A, Valdivia A, Johnson ML, Besse B, Camidge DR, Fujino T, Yoda S, Nguyen-Phuong L, Mizuta H, Bigot L, Nobre C, Lee JB, Yu MR, Mente S, Sun Y, Kohl NE, Porter JR, Shair MD, Zhu VW, Felip E, Cho BC, Friboulet L, Hata AN, Pelish HE, Drilon A. NVL-655 Is a Selective and Brain-Penetrant Inhibitor of Diverse ALK-Mutant Oncoproteins, Including Lorlatinib-Resistant Compound Mutations.

Lo Russo G, Moro M, Sommariva M, Cancila V, Boeri M, Centonze G, Ferro S, Ganzinelli M, Gasparini P, Huber V, Milione M, Porcu L, Proto C, Pruneri G, Signorelli D, Sangaletti S, Sfondrini L, Storti C, Tassi E, Bardelli A, Marsoni S, Torri V, Tripodo C, Colombo MP, Anichini A, Rivoltini L, Balsari A, Sozzi G, Garassino MC. Antibody-Fc/FcR Interaction on Macrophages as a Mechanism for Hyperprogressive Disease in Non-small Cell Lung Cancer Subsequent to PD-1/PD-L1 Blockade. *Clin Cancer Res.* 2019 Feb 1;25(3):989-999. doi: 10.1158/1078-0432.CCR-18-1390. Epub 2018 Sep 11.PMID: 30206165

Lou Y, Vitalis TZ, Basha G, Cai B, Chen SS, Choi KB, Jeffries AP, Elliott WM, Atkins D, Seliger B, Jefferies WA. Restoration of the expression of transporters associated with antigen processing in lung carcinoma increases tumor-specific immune responses and survival. *Cancer Res.* 2005 Sep 1;65(17):7926-33. doi: 10.1158/0008-5472.CAN-04-3977.PMID: 16140964

Lu S, Kato T, Dong X, Ahn MJ, Quang LV, Soparattanapaisarn N, Inoue T, Wang CL, Huang M, Yang JC, Cobo M, Özgüroğlu M, Casarini I, Khiem DV, Sriuranpong V, Cronemberger E, Takahashi T, Runglodvatana Y, Chen M, Huang X, Grainger E, Ghiorghiu D, van der Gronde T, Ramalingam SS; LAURA Trial Investigators. Osimertinib after Chemoradiotherapy in Stage III EGFR-Mutated NSCLC. *N Engl J Med.* 2024 Aug 15;391(7):585-597. doi: 10.1056/NEJMoa2402614. Epub 2024 Jun 2.PMID: 38828946

Lu S, Fang J, Li X, Cao L, Zhou J, Guo Q, Liang Z, Cheng Y, Jiang L, Yang N, Han Z, Shi J, Chen Y, Xu H, Zhang H, Chen G, Ma R, Sun S, Fan Y, Li J, Luo X, Wang L, Ren Y, Su W. Once-daily savolitinib in Chinese patients with pulmonary sarcomatoid carcinomas and other non-small-cell lung cancers harbouring MET exon 14 skipping alterations: a multicentre, single-arm, open-label, phase 2 study. *Lancet Respir Med.* 2021 Oct;9(10):1154-1164. doi: 10.1016/S2213-2600(21)00084-9. Epub 2021 Jun 21.PMID: 34166627

**M**achiraju D, Wiecken M, Lang N, Hülsmeyer I, Roth J, Schank TE, Eurich R, Halama N, Enk A, Hassel JC. Soluble immune checkpoints and T-cell subsets in blood as biomarkers for resistance to immunotherapy in melanoma patients.. *Oncoimmunology.* 2021 May 25;10(1):1926762. doi: 10.1080/2162402X.2021.1926762.PMID: 34104542

Mahoney KM, RossMacdonald P, Yuan L, Song L, Veras E, Wind-Rotolo M, McDermott DF,

Stephen Hodi F, Choueiri TK, Freeman GJ. Soluble PD-L1 as an early marker of progressive disease on nivolumab. *J Immunother Cancer.* 2022 Feb;10(2):e003527. doi: 10.1136/jitc2021-003527. PMID: 35131863

Mansfield A.S., Aubry M.C., Moser J.C., Harrington S.M., Dronca R.S., Park S.S., Dong H. Temporal and spatial discordance of programmed cell death-ligand 1 expression and lymphocyte tumor infiltration between paired primary lesions and brain metastases in lung cancer. *Ann. Oncol.* 2016;27:1953–1958. doi: 10.1093/annonc/mdw289.

Marant Micallef C, Shield KD, Baldi I, Charbotel B, Fervers B, Gilg Soit Ilg A, Guénél P, Olsson A, Rushton L, Hutchings SJ, Straif K, Soerjomataram I. Occupational exposures and cancer: a review of agents and relative risk estimates. *Occup Environ Med.* 2018 Aug;75(8):604-614. doi: 10.1136/oemed-2017-104858. Epub 2018 May 7. PMID: 29735747

Mazzaschi G, Minari R, Zecca A, Cavazzoni A, Ferri V, Mori C, Squadrilli A, Bordi P, Buti S, Bersanelli M, Leonetti A, Cosenza A, Ferri L, Rapacchi E, Missale G, Petronini PG, Quaini F, Tiseo M. Soluble PD-L1 and Circulating CD8+PD-1+ and NK Cells Enclose a Prognostic and Predictive Immune Effector Score in Immunotherapy Treated NSCLC patients. *Lung Cancer.* 2020 Oct;148:1-11. doi: 10.1016/j.lungcan.2020.07.028. Epub 2020 Aug 2. PMID: 32768804

Mehlman C, Takam Kamga P, Costantini A, Julié C, Dumenil C, Dumoulin J, Ouaknine J, Giraud V, Chinet T, Emile JF, Giroux Leprieur E. Baseline Hedgehog Pathway Activation and Increase of Plasma Wnt1 Protein Are Associated with Resistance to Immune Checkpoint Inhibitors in Advanced Non-Small-Cell Lung Cancer. *Cancers (Basel).* 2021 Mar 5;13(5):1107. doi: 10.3390/cancers13051107. PMID: 33807552

Michalek MT, Grant EP, Gramm C, Goldberg AL, Rock KL. A role for the ubiquitin-dependent proteolytic pathway in MHC class I-restricted antigen presentation. *Nature.* 1993 Jun 10;363(6429):552-4. doi: 10.1038/363552a0. PMID: 8389422

Milner RE, et al. Calreticulin, and not calsequestrin, is the major calcium binding protein of smooth muscle sarcoplasmic reticulum and liver endoplasmic reticulum. *J. Biol. Chem.* 1991;266:7155–7165.

Mohapatra B, Ahmad G, Nadeau S, Zutshi N, An W, Scheffe S, Dong L, Feng D, Goetz B, Arya P, Bailey TA, Palermo N, Borgstahl GE, Natarajan A, Raja SM, Naramura M, Band V, Band H. Protein tyrosine kinase regulation by ubiquitination: critical roles of Cbl-family ubiquitin ligases. *Biochim Biophys Acta.* 2013 Jan;1833(1):122-39. doi: 10.1016/j.bbamcr.2012.10.010. Epub 2012 Oct 17. PMID: 23085373

Mok T, Camidge DR, Gadgeel SM, Rosell R, Dziadziszko R, Kim DW, Pérol M, Ou SI, Ahn JS, Shaw AT, Bordogna W, Smoljanović V, Hilton M, Ruf T, Noé J, Peters S. Updated overall survival and final progression-free survival data for patients with treatment-naïve advanced ALK-positive non-

small-cell lung cancer in the ALEX study. Ann Oncol. 2020 Aug;31(8):1056-1064. doi: 10.1016/j.annonc.2020.04.478. Epub 2020 May 11. PMID: 32418886

Molga-Magusiak M, Rzepakowska A, Żurek M, Kotuła I, Demkow U, Niemczyk K. Prognostic and predictive role of soluble programmed death ligand-1 in head and neck cancer. Braz J Otorhinolaryngol. 2023 May-Jun;89(3):417-424. doi: 10.1016/j.bjorl.2023.02.005. Epub 2023 Feb 21. PMID: 36868994

Moosavi F, Giovannetti E, Saso L, Firuzi O. HGF/MET pathway aberrations as diagnostic, prognostic, and predictive biomarkers in human cancers. Crit Rev Clin Lab Sci. 2019 Dec;56(8):533-566. doi: 10.1080/10408363.2019.1653821. Epub 2019 Sep 12. PMID: 31512514

Moro-Sibilot D, Cozic N, Pérol M, Mazières J, Otto J, Souquet PJ, Bahleda R, Wislez M, Zalcman G, Guibert SD, Barlesi F, Mennecier B, Monnet I, Sabatier R, Bota S, Dubos C, Verriele V, Haddad V, Ferretti G, Cortot A, De Fraipont F, Jimenez M, Hoog-Labouret N, Vassal G. [Crizotinib in c-MET-or ROS1-positive NSCLC: results of the AcSe phase II trial.](#) Ann Oncol. 2019 Dec;30(12):1985-1991. doi: 10.1093/annonc/mdz407. PMID: 31584608

Murakami S, Shibaki R, Matsumoto Y, Yoshida T, Goto Y, Kanda S, Horinouchi H, Fujiwara Y, Yamamoto N, Ohe Y. Association between serum level soluble programmed cell death ligand 1 and prognosis in patients with non-small cell lung cancer treated with anti-PD-1 antibody. Thorac Cancer. 2020 Dec;11(12):3585-3595. doi: 10.1111/1759-7714.13721. Epub 2020 Oct 27. PMID: 33108686

Murata S, Takahama Y, Kasahara M, Tanaka K. [The immunoproteasome and thymoproteasome: functions, evolution and human disease.](#) Nat Immunol. 2018 Sep;19(9):923-931. doi: 10.1038/s41590-018-0186-z. Epub 2018 Aug 13. PMID: 30104634

**N**akamura T., Nawa K., Ichihara A. Partial purification and characterization of hepatocyte growth factor from serum of hepatectomized rats. Biochem. Biophys. Res. Commun. 1984;122:1450–1459. doi: 10.1016/0006-291X(84)91253-1

Naumnik W, Naumnik B, Niklińska W, Ossolińska M, Chyczewska E. Clinical Implications of Hepatocyte Growth Factor, Interleukin-20, and Interleukin-22 in Serum and Bronchoalveolar Fluid of Patients with Non-Small Cell Lung Cancer. Adv Exp Med Biol. 2016;952:41-49. doi: 10.1007/5584\_2016\_66. PMID: 27573644

**O**'Brien M, Paz-Ares L, Marreaud S, Dafni U, Osolin K, Havel L, Esteban E, Isla D, Martinez-Marti A, Faehling M, Tsuboi M, Lee JS, Nakagawa K, Yang J, Samkari A, Keller SM, Mauer M, Jha N, Stahel R, Besse B, Peters S; EORTC-1416-LCG/ETOP 8-15 – PEARLS/KEYNOTE-091 Investigators. Pembrolizumab versus placebo as adjuvant therapy for completely resected stage IB-IIIA non-small-cell lung cancer (PEARLS/KEYNOTE-091): an interim analysis of a randomised, triple-blind,

phase 3 trial. Lancet Oncol. 2022 Oct;23(10):1274-1286. doi: 10.1016/S1470-2045(22)00518-6. Epub 2022 Sep 12. PMID: 36108662

Ogino T, Bandoh N, Hayashi T, Miyokawa N, Harabuchi Y, Ferrone S. Association of tapasin and HLA class I antigen down-regulation in primary maxillary sinus squamous cell carcinoma lesions with reduced survival of patients. Clin Cancer Res 2003; 9:4043-51; PMID:1451962513.

Ogino T, Shigyo H, Ishii H, Katayama A, Miyokawa N, Harabuchi Y, Ferrone S. HLA class I antigen down-regulation in primary laryngeal squamous cell carcinoma lesions as a poor prognostic marker. Cancer Res 2006; 66:9281-9; PMID:16982773; <http://dx.doi.org/10.1158/0008-5472.CAN-06-048814>.

Oh SY, Kim S, Keam B, Kim TM, Kim DW, Heo DS. Soluble PD-L1 is a predictive and prognostic biomarker in advanced cancer patients who receive immune checkpoint blockade treatment..Sci Rep. 2021 Oct 5;11(1):19712. doi: 10.1038/s41598-021-99311-y. PMID: 34611279

Okuma Y, Hosomi Y, Nakahara Y, Watanabe K, Sagawa Y, Homma S. High plasma levels of soluble programmed cell death ligand 1 are prognostic for reduced survival in advanced lung cancer. Lung Cancer. 2017 Feb;104:1-6. doi: 10.1016/j.lungcan.2016.11.023. Epub 2016 Dec 5. PMID: 28212990

Okuma Y, Wakui H, Utsumi H, Sagawa Y, Hosomi Y, Kuwano K, Homma S. Soluble Programmed Cell Death Ligand 1 as a Novel Biomarker for Nivolumab Therapy for Non-Small-cell Lung Cancer. Clin Lung Cancer. 2018 Sep;19(5):410-417.e1. doi: 10.1016/j.cllc.2018.04.014. Epub 2018 May 5. PMID: 29859759

Organ SL, Tsao MS. An overview of the c-MET signaling pathway. Ther Adv Med Oncol. 2011 Nov;3(1 Suppl):S7-S19. doi: 10.1177/1758834011422556. PMID: 22128289

**P**aik PK, Felip E, Veillon R, Sakai H, Cortot AB, Garassino MC, Mazieres J, Viteri S, Senellart H, Van Meerbeeck J, Raskin J, Reinmuth N, Conte P, Kowalski D, Cho BC, Patel JD, Horn L, Griesinger F, Han JY, Kim YC, Chang GC, Tsai CL, Yang JC, Chen YM, Smit EF, van der Wekken AJ, Kato T, Juraeva D, Stroh C, Bruns R, Straub J, Johne A, Scheele J, Heymach JV, Le X. [Tepotinib in Non-Small-Cell Lung Cancer with MET Exon 14 Skipping Mutations.](#) N Engl J Med. 2020 Sep 3;383(10):931-943. doi: 10.1056/NEJMoa2004407. Epub 2020 May 29. PMID: 32469185

Panaretakis T, Kepp O, Brockmeier U, Tesniere A, Bjorklund AC, Chapman DC, Durchschlag M, Joza N, Pierron G, van Endert P, Yuan J, Zitvogel L, Madeo F, Williams DB, Kroemer G. Mechanisms of pre-apoptotic calreticulin exposure in immunogenic cell death. EMBO J. 2009 Mar 4;28(5):578-90. doi: 10.1038/emboj.2009.1. Epub 2009 Jan 22. PMID: 19165151

Pasello G, Fabricio ASC, Del Bianco P, Salizzato V, Favaretto A, Piccin L, Zustovich F, Fabozzi A, De Rossi C, Pigozzo J, De Nuzzo M, Cappelletto E, Bonanno L, Palleschi D, De Salvo GL, Guarneri V,

Gion M, Chiarion-Silni V. Sex-related differences in serum biomarker levels predict the activity and efficacy of immune checkpoint inhibitors in advanced melanoma and non-small cell lung cancer patients. *S J Transl Med.* 2024 Mar 5;22(1):242. doi: 10.1186/s12967-024-049206.PMID: 38443899

Passlick B, Izbicki JR, Simmel S, Kubuschok B, Karg O, Habekost M, Thetter O, Schweiberer L, Pantel K. Expression of major histocompatibility class I and class II antigens and intercellular adhesion molecule-1 on operable non-small cell lung carcinomas: frequency and prognostic significance. *Eur J Cancer.* 1994;30A(3):376-81. doi: 10.1016/0959-8049(94)90259-3.PMID: 8204362

Paz-Ares L, Luft A, Vicente D, Tafreshi A, Gümuş M, Mazières J, Hermes B, Çay Şenler F, Csőzzi T, Fülöp A, Rodríguez-Cid J, Wilson J, Sugawara S, Kato T, Lee KH, Cheng Y, Novello S, Halmos B, Li X, Lubiniecki GM, Piperdi B, Kowalski DM; KEYNOTE-407 Investigators. Pembrolizumab plus Chemotherapy for Squamous Non-Small-Cell Lung Cancer. *N Engl J Med.* 2018 Nov 22;379(21):2040-2051. doi: 10.1056/NEJMoa1810865. Epub 2018 Sep 25.PMID: 30280635

Peaper DR, Wearsch PA, Cresswell P. Tapasin and ERp57 form a stable disulfide-linked dimer within the MHC class I peptide-loading complex. *EMBO J.* 2005 Oct 19;24(20):3613-23. doi: 10.1038/sj.emboj.7600814. Epub 2005 Sep 29.PMID: 16193070

Pennacchietti S, Michieli P, Galluzzo M, Mazzone M, Giordano S, Comoglio PM. Hypoxia promotes invasive growth by transcriptional activation of the met protooncogene. *Cancer Cell.* 2003 Apr;3(4):347-61. doi: 10.1016/s1535-6108(03)00085-0.PMID: 12726861

Peters J M, Franke W W, Kleinschmidt J A. Distinct 19 S and 20 S subcomplexes of the 26 S proteasome and their distribution in the nucleus and the cytoplasm. *J Biol Chem.* 1994 Mar 11;269(10):7709-18.

Peters S, Gadgeel SM, Mok T, Nadal E, Kilickap S, Swalduz A, Cadranell J, Sugawara S, Chiu CH, Yu CJ, Moskovitz M, Tanaka T, Nersesian R, Shagan SM, MacLennan M, Mathisen M, Bhagawati-Prasad V, Diarra C, Assaf ZJ, Archer V, Dziadziuszko R. Entrectinib in ROS1-positive advanced non-small cell lung cancer: the phase 2/3 BFAST trial. *Nat Med.* 2024 Jul;30(7):1923-1932. doi: 10.1038/s41591-024-03008-4. Epub 2024 Jun 19.PMID: 38898120

Pinato D.J., Shiner R.J., White S.D., Black J.R., Trivedi P., Stebbing J., Sharma R., Mauri F.A. Intra-tumoral heterogeneity in the expression of programmed-death (PD) ligands in isogenic primary and metastatic lung cancer: Implications for immunotherapy. *Oncoimmunology.* 2016;5:e1213934.  
doi: 10.1080/2162402X.2016.1213934. eCollection 2016.

Planchard D, Besse B, Groen HJM, Souquet PJ, Quoix E, Baik CS, Barlesi F, Kim TM, Mazieres J, Novello S, Rigas JR, Upalawanna A, D'Amelio AM Jr, Zhang P, Mookerjee B, Johnson BE. Dabrafenib plus trametinib in patients with previously treated BRAF(V600E)-mutant metastatic

non-small cell lung cancer: an open-label, multicentre phase 2 trial. Lancet Oncol. 2016 Jul;17(7):984-993. doi: 10.1016/S1470-2045(16)30146-2. Epub 2016 Jun 6. PMID: 27283860

Planchard D, Jänne PA, Cheng Y, Yang JC, Yanagitani N, Kim SW, Sugawara S, Yu Y, Fan Y, Geater SL, Laktionov K, Lee CK, Valdiviezo N, Ahmed S, Maurel JM, Andrasina I, Goldman J, Ghiorgiu D, Rukazenkova Y, Todd A, Kobayashi K; FLAURA2 Investigators. Osimertinib with or without Chemotherapy in EGFR-Mutated Advanced NSCLC. N Engl J Med. 2023 Nov 23;389(21):1935-1948. doi: 10.1056/NEJMoa2306434. Epub 2023 Nov 8. PMID: 37937763

Planchard D, Smit EF, Groen HJM, Mazieres J, Besse B, Helland Å, Giannone V, D'Amelio AM Jr, Zhang P, Mookerjee B, Johnson BE. Dabrafenib plus trametinib in patients with previously untreated BRAF (V600E)-mutant metastatic non-small-cell lung cancer: an open-label, phase 2 trial. Lancet Oncol. 2017 Oct;18(10):1307-1316. doi: 10.1016/S1470-2045(17)30679-4. Epub 2017 Sep 11. PMID: 28919011

Ponzetto C, Bardelli A, Zhen Z, Maina F, dalla Zonca P, Giordano S, Graziani A, Panayotou G, Comoglio PM. [A multifunctional docking site mediates signaling and transformation by the hepatocyte growth factor/scatter factor receptor family.](#) Cell. 1994 Apr 22;77(2):261-71. doi: 10.1016/0092-8674(94)90318-2. PMID: 7513258

Raffaghello L, Prigione I, Bocca P, Morandi F, Camoriano M, Gam-bini C, Wang X, Ferrone S, Pistoia V. Multiple defects of the anti-gen-processing machinery components in human neuroblastoma:immunotherapeutic implications. Oncogene 2005; 24:4634-44;PMID:15897905; <http://dx.doi.org/10.1038/sj.onc.1208594e1274476-10> Y.

Rami-Porta R, Nishimura KK, Giroux DJ, Detterbeck F, Cardillo G, Edwards JG, Fong KM, Giuliani M, Huang J, Kernstine KH Sr, Marom EM, Nicholson AG, Van Schil PE, Travis WD, Tsao MS, Watanabe SI, Rusch VW, Asamura H; Members of the IASLC Staging and Prognostic Factors Committee and of the Advisory Boards, and Participating Institutions. The International Association for the Study of Lung Cancer Lung Cancer Staging Project: Proposals for Revision of the TNM Stage Groups in the Forthcoming (Ninth) Edition of the TNM Classification for Lung Cancer. J Thorac Oncol. 2024 Jul;19(7):1007-1027. doi: 10.1016/j.jtho.2024.02.011. Epub 2024 Mar 4. PMID: 38447919

Ramnath N, Tan D, Li Q, Hylander BL, Bogner P, Ryes L, Ferrone S. Is downregulation of MHC class I antigen expression in human non-small cell lung cancer associated with prolonged survival? Cancer Immunol Immunother. 2006 Aug;55(8):891-9. doi: 10.1007/s00262-005-0085-7. Epub 2005 Sep 27.

Reck M, Rodríguez-Abreu D, Robinson AG, Hui R, Csőzsi T, Fülöp A, Gottfried M, Peled N, Tafreshi A, Cuffe S, O'Brien M, Rao S, Hotta K, Leiby MA, Lubiniecki GM, Shentu Y, Rangwala R, Brahmer

JR; KEYNOTE-024 Investigators. Pembrolizumab versus Chemotherapy for PD-L1-Positive Non-Small-Cell Lung Cancer. *N Engl J Med.* 2016 Nov 10;375(19):1823-1833. doi: 10.1056/NEJMoa1606774. Epub 2016 Oct 8. PMID: 27718847

Remon J, Hendriks LEL, Mountzios G, García-Campelo R, Saw SPL, Uprety D, Recondo G, Villacampa G, Reck M. MET alterations in NSCLC-Current Perspectives and Future Challenges. *J Thorac Oncol.* 2023 Apr;18(4):419-435. doi: 10.1016/j.jtho.2022.10.015. Epub 2022 Oct 29. PMID: 36441095

Riedel R, Fassunke J, Scheel AH, Scheffler M, Heydt C, Nogova L, Michels S, Fischer RN, Eisert A, Scharpenseel H, John F, Ruge L, Schaufler D, Siemanowski J, Ihle MA, Wagener-Ryczek S, Pappesch R, Rehker J, Bunck A, Kobe C, Keil F, Merkelbach-Bruse S, Büttner R, Wolf J. MET Fusions in NSCLC: Clinicopathologic Features and Response to MET Inhibition. *J Thorac Oncol.* 2024 Jan;19(1):160-165. doi: 10.1016/j.jtho.2023.06.020. Epub 2023 Jul 8. PMID: 37429463

Riely GJ, Smit EF, Ahn MJ, Felip E, Ramalingam SS, Tsao A, Johnson M, Gelsomino F, Esper R, Nadal E, Offin M, Provencio M, Clarke J, Hussain M, Otterson GA, Dagogo-Jack I, Goldman JW, Morgensztern D, Alcasid A, Usari T, Wissel P, Wilner K, Pathan N, Tonkoyd S, Johnson BE. Phase II, Open-Label Study of Encorafenib Plus Binimetinib in Patients With *BRAF<sup>V600</sup>*-Mutant Metastatic Non-Small-Cell Lung Cancer. *J Clin Oncol.* 2023 Jul 20;41(21):3700-3711. doi: 10.1200/JCO.23.00774. Epub 2023 Jun 4. PMID: 37270692

Rock KL, Goldberg AL. Degradation of cell proteins and the generation of MHC class I-presented peptides. *Annu Rev Immunol.* 1999;17:739-79. doi: 10.1146/annurev.immunol.17.1.739. PMID: 10358773

Rock KL, Gramm C, Rothstein L, Clark K, Stein R, Dick L, Hwang D, Goldberg AL. Inhibitors of the proteasome block the degradation of most cell proteins and the generation of peptides presented on MHC class I molecules. *Cell.* 1994 Sep 9;78(5):761-71. doi: 10.1016/s0092-8674(94)90462-6.

Ros M, Nguyen AT, Chia J, Le Tran S, Le Gueennec X, McDowall R, Vakhrushev S, Clausen H, Humphries MJ, Saltel F, Bard FA. ER-resident oxidoreductases are glycosylated and trafficked to the cell surface to promote matrix degradation by tumour cells. *Nat Cell Biol.* 2020 Nov;22(11):1371-1381. doi: 10.1038/s41556-020-00590-w. Epub 2020 Oct 19. PMID: 33077910

Rossille D, Gressier M, Damotte D, Maucort-Boulch D, Pangault C, Semana G, Le Gouill S, Haioun C, Tarte K, Lamy T, Milpied N, Fest T; Groupe Ouest-Est des Leucémies et Autres Maladies du Sang; Groupe Ouest-Est des Leucémies et Autres Maladies du Sang. High level of soluble programmed cell death ligand 1 in blood impacts overall survival in aggressive diffuse large B-Cell lymphoma: results from a French multicenter clinical trial. *Leukemia.* 2014 Dec;28(12):2367-75. doi: 10.1038/leu.2014.137. Epub 2014 Apr 15. PMID: 24732592

**S**choenfeld AJ, Hellmann MD. Acquired Resistance to Immune Checkpoint Inhibitors. *Cancer Cell.* 2020 Apr 13;37(4):443-455. doi: 10.1016/j.ccr.2020.03.017. PMID: 32289269

Scirocchi F, Strigari L, Di Filippo A, Napoletano C, Pace A, Rahimi H, Botticelli A, Rughetti A, Nuti M, Zizzari IG. Soluble PD-L1 as a Prognostic Factor for Immunotherapy Treatment in Solid Tumors: Systematic Review and Meta-Analysis. *Int J Mol Sci.* 2022 Nov 21;23(22):14496. doi: 10.3390/ijms232214496.

Seliger B, Atkins D, Bock M, Ritz U, Ferrone S, Huber C, Storkel S. Characterization of human lymphocyte antigen class I antigen-processing machinery defects in renal cell carcinoma lesions with special emphasis on transporter-associated with antigen-processing down-regulation. *Clin Cancer Res* 2003; 9:1721-7; PMID:1273872615.

Sezer A, Kilickap S, Gümüş M, Bondarenko I, Özgüröglu M, Gogishvili M, Turk HM, Cicin I, Bentsion D, Gladkov O, Clingan P, Sriuranpong V, Rizvi N, Gao B, Li S, Lee S, McGuire K, Chen CI, Makharadze T, Paydas S, Nechaeva M, Seebach F, Weinreich DM, Yancopoulos GD, Gullo G, Lowy I, Rietschel P. Cemiplimab monotherapy for first-line treatment of advanced non-small-cell lung cancer with PD-L1 of at least 50%: a multicentre, open-label, global, phase 3, randomised, controlled trial. *Lancet.* 2021 Feb 13;397(10274):592-604. doi: 10.1016/S0140-6736(21)00228-2. PMID: 33581821 Clinical Trial.

Sharma P, Hu-Lieskovan S, Wargo JA, Ribas A. Primary, Adaptive, and Acquired Resistance to Cancer Immunotherapy. *Cell.* 2017 Feb 9;168(4):707-723. doi: 10.1016/j.cell.2017.01.017. PMID: 28187290

Shaw AT, Solomon BJ, Chiari R, Riely GJ, Besse B, Soo RA, Kao S, Lin CC, Bauer TM, Clancy JS, Thurm H, Martini JF, Peltz G, Abbattista A, Li S, Ou SI. Lorlatinib in advanced ROS1-positive non-small-cell lung cancer: a multicentre, open-label, single-arm, phase 1-2 trial. *Lancet Oncol.* 2019 Dec;20(12):1691-1701. doi: 10.1016/S1470-2045(19)30655-2. Epub 2019 Oct 25. PMID: 31669155

Shen L, Rock KL. Cellular protein is the source of cross-priming antigen in vivo. *Proc Natl Acad Sci U S A.* 2004 Mar 2;101(9):3035-40. doi: 10.1073/pnas.0308345101. Epub 2004 Feb 20. PMID: 14978273

Sheng J., Fang W., Yu J., Chen N., Zhan J., Ma Y., Yang Y., Huang Y., Zhao H., Zhang L. Expression of programmed death ligand-1 on tumor cells varies pre and post chemotherapy in non-small cell lung cancer. *Sci. Rep.* 2016;6:20090. doi: 10.1038/srep20090.

Shigemori T, Toiyama Y, Okugawa Y, Yamamoto A, Yin C, Narumi A, Ichikawa T, Ide S, Shimura T, Fujikawa H, Yasuda H, Hiro J, Yoshiyama S, Ohi M, Araki T, Kusunoki M. Soluble PD-L1 Expression

in Circulation as a Predictive Marker for Recurrence and Prognosis in Gastric Cancer: Direct Comparison of the Clinical Burden Between Tissue and Serum PD-L1 Expression. *Ann Surg Oncol.* 2019 Mar;26(3):876-883. doi: 10.1245/s10434-018-07112-x. Epub 2018 Dec 18. PMID: 30565045

Shimizu T, Inoue E, Ohkuma R, Kobayashi S, Tsunoda T, Wada S. Soluble PD-L1 changes in advanced non-small cell lung cancer patients treated with PD-1 inhibitors: an individual patient data meta-analysis. *Front Immunol.* 2023 Nov 23;14:1308381. doi: 10.3389/fimmu.2023.1308381. eCollection 2023. PMID: 38115995

Shionoya Y, Kanaseki T, Miyamoto S, Tokita S, Hongo A, Kikuchi Y, Kochin V, Watanabe K, Horibe R, Saijo H, Tsukahara T, Hirohashi Y, Takahashi H, Sato N, Torigoe T. Loss of tapasin in human lung and colon cancer cells and escape from tumor-associated antigen-specific CTL recognition. *Oncoimmunology.* 2017 Jan 3;6(2):e1274476. doi: 10.1080/2162402X.2016.1274476. eCollection 2017. PMID: 28344889

Siegel RL, Miller KD, Wagle NS, Jemal A. Cancer statistics, 2023..CA Cancer J Clin. 2023 Jan;73(1):17-48. doi: 10.3322/caac.21763. PMID: 36633525

Smith CJ, Perfetti TA, Garg R, Hansch C. IARC carcinogens reported in cigarette mainstream smoke and their calculated log P values. *Food Chem Toxicol.* 2003 Jun;41(6):807-17. doi: 10.1016/s0278-6915(03)00021-8. PMID: 12738186

Solomon BJ, Liu G, Felip E, Mok TSK, Soo RA, Mazieres J, Shaw AT, de Marinis F, Goto Y, Wu YL, Kim DW, Martini JF, Messina R, Paolini J, Polli A, Thomaidou D, Toffalorio F, Bauer TM. Lorlatinib Versus Crizotinib in Patients With Advanced ALK-Positive Non-Small Cell Lung Cancer: 5-Year Outcomes From the Phase III CROWN Study. *J Clin Oncol.* 2024 May 31;JCO2400581. doi: 10.1200/JCO.24.00581. Online ahead of print. PMID: 38819031

Soria JC, Ohe Y, Vansteenkiste J, Reungwetwattana T, Chewaskulyong B, Lee KH, Dechaphunkul A, Imamura F, Nogami N, Kurata T, Okamoto I, Zhou C, Cho BC, Cheng Y, Cho EK, Voon PJ, Planchard D, Su WC, Gray JE, Lee SM, Hodge R, Marotti M, Rukazekov Y, Ramalingam SS; FLAURA Investigators. Osimertinib in Untreated EGFR-Mutated Advanced Non-Small-Cell Lung Cancer. *N Engl J Med.* 2018 Jan 11;378(2):113-125. doi: 10.1056/NEJMoa1713137. Epub 2017 Nov 18. PMID: 29151359

Spicer JD, Garassino MC, Wakelee H, Liberman M, Kato T, Tsuboi M, Lee SH, Chen KN, Dooms C, Majem M, Eigendorff E, Martinengo GL, Bylicki O, Rodríguez-Abreu D, Chafft JE, Novello S, Yang J, Arunachalam A, Keller SM, Samkari A, Gao S; KEYNOTE-671 Investigators. Neoadjuvant pembrolizumab plus chemotherapy followed by adjuvant pembrolizumab compared with neoadjuvant chemotherapy alone in patients with early-stage non-small-cell lung cancer (KEYNOTE-671): a randomised, double-blind, placebo-controlled, phase 3 trial. *Lancet.* 2024 Sep 28;404(10459):1240-1252. doi: 10.1016/S0140-6736(24)01756-2. Epub 2024 Sep 14. PMID: 39288781

Spigel DR, Faivre-Finn C, Gray JE, Vicente D, Planchard D, Paz-Ares L, Vansteenkiste JF, Garassino MC, Hui R, Quantin X, Rimner A, Wu YL, Özgüroğlu M, Lee KH, Kato T, de Wit M, Kurata T, Reck M, Cho BC, Senan S, Naidoo J, Mann H, Newton M, Thiagarajah P, Antonia SJ. Five-Year Survival Outcomes From the PACIFIC Trial: Durvalumab After Chemoradiotherapy in Stage III Non-Small-Cell Lung Cancer. *J Clin Oncol.* 2022 Apr 20;40(12):1301-1311. doi: 10.1200/JCO.21.01308. Epub 2022 Feb 2. PMID: 35108059

Sucker A, Zhao F, Pieper N, Heeke C, Maltaner R, Stadtler N, Real B, Bielefeld N, Howe S, Weide B, Gutzmer R, Utikal J, Loquai C, Gogas H, Klein-Hitpass L, Zeschnigk M, Westendorf AM, Trilling M, Horn S, Schilling B, Schadendorf D, Griewank KG, Paschen A. Acquired IFNgamma resistance impairs anti-tumor immunity and gives rise to T-cell-resistant melanoma lesions. *Nat Commun.* 2017 May 31;8:15440. doi: 10.1038/ncomms15440. PMID: 28561041

Sui X, Jiang L, Teng H, Mi L, Li B, Shi A, Yu R, Li D, Dong X, Yang D, Yu H, Wang. Prediction of Clinical Outcome in Locally Advanced Non-Small Cell Lung Cancer Patients Treated With Chemoradiotherapy by Plasma Markers. *Front Oncol.* 2021 Feb 17;10:625911. doi: 10.3389/fonc.2020.625911. eCollection 2020. PMID: 33680949

Széles Á, Fazekas T, Váncsa S, Váradi M, Kovács PT, Krafft U, Grünwald V, Hadaschik B, Csizmarik A, Hegyi P, Váradi A, Nyirády P, Szarvas T. Pre-treatment soluble PD-L1 as a predictor of overall survival for immune checkpoint inhibitor therapy: a systematic review and meta-analysis. *Cancer Immunol Immunother.* 2023 May;72(5):1061-1073. doi: 10.1007/s00262-02203328-9. Epub 2022 Nov 16. PMID: 36385210

Takahashi N, Iwasa S, Sasaki Y, Shoji H, Honma Y, Takashima A, Okita NT, Kato K, Hamaguchi T, Yamada Y. Serum levels of soluble programmed cell death ligand 1 as a prognostic factor on the first-line treatment of metastatic or recurrent gastric cancer. *J Cancer Res Clin Oncol.* 2016 Aug;142(8):1727-38. doi: 10.1007/s00432-016-2184-6. Epub 2016 Jun 2. PMID: 27256004

Takam Kamga P, Mayenga M, Sebane L, Costantini A, Julie C, Capron C, Parent F, Seferian A, Guettier C, Emile JF, Giroux Leprieur E. Colony stimulating factor-1 (CSF-1) signalling is predictive of response to immune checkpoint inhibitors in advanced non-small cell lung cancer. *Lung Cancer.* 2024 Feb;188:107447. doi: 10.1016/j.lungcan.2023.107447. Epub 2023 Dec 24. PMID: 38176297

Tan AC, Tan DSW. Targeted Therapies for Lung Cancer Patients With Oncogenic Driver Molecular Alterations. *J Clin Oncol.* 2022 Feb 20;40(6):611-625. doi: 10.1200/JCO.21.01626. Epub 2022 Jan 5. PMID: 34985916

Tanaka H, Kimura T, Kudoh S, Mitsuoka S, Watanabe T, Suzumura T, Tachibana K, Noguchi M, Yano S, Hirata K. Reaction of plasma hepatocyte growth factor levels in non-small cell lung cancer patients treated with EGFR-TKIs. *Int J Cancer.* 2011 Sep 15;129(6):1410-6.

doi: 10.1002/ijc.25799. Epub 2011 Feb 26.PMID: 21128242

Tarhini AA, Rafique I, Floros T, Tran P, Gooding WE, Villaruz LC, Burns TF, Friedland DM, Petro DP, Farooqui M, Gomez-Garcia J, Gaither-Davis A, Dacic S, Argiris A, Socinski MA, Stabile LP, Siegfried JM. Phase 1/2 study of rilotumumab (AMG 102), a hepatocyte growth factor inhibitor, and erlotinib in patients with advanced non-small cell lung cancer. *Cancer*. 2017 Aug 1;123(15):2936-2944. doi: 10.1002/cncr.30717. Epub 2017 May 4.PMID: 28472537

Teramoto K, Igarashi T, Kataoka Y, Ishida M, Hanaoka J, Sumimoto H, Daigo Y. Prognostic impact of soluble PD-L1 derived from tumor-associated macrophages in non-small-cell lung cancer. *Cancer Immunol Immunother*. 2023 Nov;72(11):3755-3764. doi: 10.1007/s00262-023-03527-y. Epub 2023 Aug 30.PMID: 37646826

Trusolino L, Bertotti A, Comoglio PM. MET signalling: principles and functions in development, organ regeneration and cancer. *Nat Rev Mol Cell Biol*. 2010 Dec;11(12):834-48. doi: 10.1038/nrm3012.PMID: 21102609

Tovar EA, Graveel CR. MET in human cancer: germline and somatic mutations. *Ann Transl Med*. 2017 May;5(10):205. doi: 10.21037/atm.2017.03.64.PMID: 28603720

Tsuji T, Sakamori Y, Ozasa H, Yagi Y, Ajimizu H, Yasuda Y, Funazo T, Nomizo T, Yoshida H, Nagai H, Maeno K, Oguri T, Hirai T, Kim YH. Clinical impact of high serum hepatocyte growth factor in advanced non-small cell lung cancer. *Oncotarget*. 2017 May 16;8(42):71805-71816. doi: 10.18632/oncotarget.17895. eCollection 2017 Sep 22.PMID: 29069748

Tiako Meyo M, Jouinot A, Giroux-Leprieur E, Fabre E, Wislez M, Alifano M, Leroy K, Boudou-Rouquette P, Tlemsani C, Khoudour N, Arrondeau J, Thomas-Schoemann A, Blons H, Mansuet-Lupo A, Damotte D, Vidal M, Goldwasser F, Alexandre J, Blanchet B. Predictive Value of Soluble PD-1, PD-L1, VEGFA, CD40 Ligand and CD44 for Nivolumab Therapy in Advanced Non-Small Cell Lung Cancer: A Case-Control Study. *Cancers (Basel)*. 2020 Feb 18;12(2):473. doi: 10.3390/cancers12020473.PMID: 32085544

Tokunou M., Niki T., Eguchi K., Iba S., Tsuda H., Yamada T., Matsuno Y., Kondo H., Imamura H., Hirohashi S. c-MET expression in myofibroblasts: Role in autocrine activation and prognostic significance in adenocarcinoma. *Am. J. Pathol.* 2001;158:1451–1463. doi: 10.1016/S0002-9440(10)64096-5.

Trujillo JA, Luke JJ, Zha Y, Segal JP, Ritterhouse LL, Spranger S, Matijevich K, Gajewski TF. Secondary resistance to immunotherapy associated with beta-catenin pathway activation or PTEN loss in metastatic melanoma. *J Immunother Cancer*. 2019 Nov 8;7(1):295. doi: 10.1186/s40425-019-0780-0.PMID: 31703593

Umeguchi H, Sueoka-Aragane N, Kobayashi N, Nakamura T, Sato A, Takeda Y, Hayashi S, Sueoka E, Kimura S. Usefulness of plasma HGF level for monitoring acquired resistance to EGFR tyrosine kinase inhibitors in non-small cell lung cancer. *Oncol Rep.* 2015 Jan;33(1):391-6. doi: 10.3892/or.2014.3560. Epub 2014 Oct 22. PMID: 25338771

**U**ruga H., Bozkurtlar E., Huynh T.G., Muzikansky A., Goto Y., Gomez-Caraballo M., Hata A.N., Gainor J.F., Mark E.J., Engelman J.A., et al. Programmed Cell Death Ligand (PD-L1) Expression in Stage II and III Lung Adenocarcinomas and Nodal Metastases. *J. Thorac. Oncol.* 2017;12:458–466. doi: 10.1016/j.jtho.2016.10.015.

**V**uong HG, Ho ATN, Altibi AMA, Nakazawa T, Katoh R, Kondo T. Clinicopathological implications of MET exon 14 mutations in non-small cell lung cancer - A systematic review and meta-analysis. *Lung Cancer.* 2018 Sep;123:76-82. doi: 10.1016/j.lungcan.2018.07.006. Epub 2018 Jul 6. PMID: 30089599

**W**akelee H, Liberman M, Kato T, Tsuboi M, Lee SH, Gao S, Chen KN, Dooms C, Majem M, Eigendorff E, Martinengo GL, Bylicki O, Rodríguez-Abreu D, Chafit JE, Novello S, Yang J, Keller SM, Samkari A, Spicer JD; KEYNOTE-671 Investigators. Perioperative Pembrolizumab for Early-Stage Non-Small-Cell Lung Cancer. *N Engl J Med.* 2023 Aug 10;389(6):491-503. doi: 10.1056/NEJMoa2302983. Epub 2023 Jun 3. PMID: 37272513

Wang L, Wang H, Chen H, Wang WD, Chen XQ, Geng QR, Xia ZJ, Lu Y. Serum levels of soluble programmed death ligand 1 predict treatment response and progression free survival in multiple myeloma. *Oncotarget.* 2015 Dec 1;6(38):41228-36. doi: 10.18632/oncotarget.5682. PMID: 26515600

Wang Y, He H. Prognostic value of soluble programmed cell death ligand-1 in patients with non-small cell lung cancer: a meta-analysis.. *Immunotherapy.* 2022 Aug;14(12):945-956. doi: 10.2217/imt-2021-0238. Epub 2022 Jul 13. PMID: 35822688

Waqar SN, Redman MW, Arnold SM, Hirsch FR, Mack PC, Schwartz LH, Gandara DR, Stinchcombe TE, Leighl NB, Ramalingam SS, Tanna SH, Raddin RS, Minichiello K, Bradley JD, Kelly K, Herbst RS, Papadimitrakopoulou VA. A Phase II Study of Telisotuzumab Vedotin in Patients With c-MET-positive Stage IV or Recurrent Squamous Cell Lung Cancer (LUNG-MAP Sub-study S1400K, NCT03574753). *Clin Lung Cancer.* 2021 May;22(3):170-177. doi: 10.1016/j.cllc.2020.09.013. Epub 2020 Oct 14. PMID: 33221175

Wearsch PA, Cresswell P. Selective loading of high-affinity peptides onto major histocompatibility complex class I molecules by the tapasin-ER $\alpha$  heterodimer. *Nat Immunol.* 2007 Aug;8(8):873-81. doi: 10.1038/ni1485. Epub 2007 Jul 1. PMID: 17603487

Wei J, Zanker D, Di Carluccio AR, Smelkinson MG, Takeda K, Seedhom MO, Dersh D, Gibbs JS, Yang N, Jadhav A, Chen W, Yewdell JW. Varied Role of Ubiquitylation in Generating MHC Class I Peptide Ligands. *J Immunol.* 2017 May 15;198(10):3835-3845. doi: 10.4049/jimmunol.1602122. Epub 2017 Mar 31. PMID: 28363906

Weidner KM, Di Cesare S, Sachs M, Brinkmann V, Behrens J, Birchmeier W. Interaction between Gab1 and the c-Met receptor tyrosine kinase is responsible for epithelial morphogenesis. *Nature.* 1996 Nov 14;384(6605):173-6. doi: 10.1038/384173a0. PMID: 8906793

Weng J, Mohan RR, Li Q, Wilson SE. IL-1 upregulates keratinocyte growth factor and hepatocyte growth factor mRNA and protein production by cultured stromal fibroblast cells: interleukin-1 beta expression in the cornea.. *Cornea.* 1997 Jul;16(4):465-71. PMID: 9220246

Wilding B, Woelflingseder L, Baum A, Chylinski K, Vainorius G, Gibson N, Waizenegger IC, Gerlach D, Augsten M, Spreitzer F, Shirai Y, Ikegami M, Tilandyova S, Scharn D, Pearson MA, Popow J, Obenauf AC, Yamamoto N, Kondo S, Opdam FL, Bruining A, Kohsaka S, Kraut N, Heymach JV, Solca F, Neumuller RA. Zongertinib (BL 1810631), an irreversible HER2 TKI, spares EGFR signaling and improves therapeutic response in preclinical models and patients with HER2-driven cancers. *Cancer Discov.* 2024 Sep 9. doi: 10.1158/2159-8290.CD-24-0306. Online ahead of print. PMID: 39248702

Wolf J, Hochmair M, Han JY, Reguart N, Souquet PJ, Smit EF, Orlov SV, Vansteenkiste J, Nishio M, de Jonge M, Akerley W, Garon EB, Groen HJM, Tan DSW, Seto T, Frampton GM, Robeva A, Carbini M, Le Mouhaer S, Yovine A, Boran A, Bossen C, Yang Y, Ji L, Fairchild L, Heist RS. Capmatinib in MET exon 14-mutated non-small-cell lung cancer: final results from the open-label, phase 2 GEOMETRY mono-1 trial. *Lancet Oncol.* 2024 Oct;25(10):1357-1370. doi: 10.1016/S1470-2045(24)00441-8. PMID: 39362249

Wolf J, Seto T, Han JY, Reguart N, Garon EB, Groen HJM, Tan DSW, Hida T, de Jonge M, Orlov SV, Smit EF, Souquet PJ, Vansteenkiste J, Hochmair M, Felip E, Nishio M, Thomas M, Ohashi K, Toyozawa R, Overbeck TR, de Marinis F, Kim TM, Laack E, Robeva A, Le Mouhaer S, Waldron-Lynch M, Sankaran B, Balbin OA, Cui X, Giovannini M, Akimov M, Heist RS; GEOMETRY mono-1 Investigators. Capmatinib in MET Exon 14-Mutated or MET-Amplified Non-Small-Cell Lung Cancer. *N Engl J Med.* 2020 Sep 3;383(10):944-957. doi: 10.1056/NEJMoa2002787. PMID: 32877583

Wu YL, Dziadziszko R, Ahn JS, Barlesi F, Nishio M, Lee DH, Lee JS, Zhong W, Horinouchi H, Mao W, Hochmair M, de Marinis F, Migliorino MR, Bondarenko I, Lu S, Wang Q, Ochi Lohmann T, Xu T, Cardona A, Ruf T, Noe J, Solomon BJ; ALINA Investigators. Alectinib in Resected ALK-Positive Non-Small-Cell Lung Cancer. *N Engl J Med.* 2024 Apr 11;390(14):1265-1276. doi: 10.1056/NEJMoa2310532. PMID: 38598794

Wu YL, Tsuboi M, He J, John T, Grohe C, Majem M, Goldman JW, Laktionov K, Kim SW, Kato T, Vu HV, Lu S, Lee KY, Akewanlop C, Yu CJ, de Marinis F, Bonanno L, Domine M, Shepherd FA, Zeng L, Hodge R, Atasoy A, Rukazenkov Y, Herbst RS; ADAURA Investigators. Osimertinib in Resected EGFR-Mutated Non-Small-Cell Lung Cancer. *N Engl J Med.* 2020 Oct 29;383(18):1711-1723. doi: 10.1056/NEJMoa2027071. Epub 2020 Sep 19. PMID: 32955177

**Y**aguchi T, Goto Y, Kido K, Mochimaru H, Sakurai T, Tsukamoto N, Kudo-Saito C, Fujita T, Sumimoto H, Kawakami Y. Immune suppression and resistance mediated by constitutive activation of Wnt/beta-catenin signaling in human melanoma cells. *J Immunol.* 2012 Sep 1;189(5):2110-7. doi: 10.4049/jimmunol.1102282. Epub 2012 Jul 18. PMID: 22815287

Yang K, Halima A, Chan TA. Antigen presentation in cancer - mechanisms and clinical implications for immunotherapy. *Nat Rev Clin Oncol.* 2023 Sep;20(9):604-623. doi: 10.1038/s41571-023-00789-4. Epub 2023 Jun 16. PMID: 37328642

Yang Q, Chen M, Gu J, Niu K, Zhao X, Zheng L, Xu Z, Yu Y, Li F, Meng L, Chen Z, Zhuo W, Zhang L, Sun J. Novel Biomarkers of Dynamic Blood PD-L1 Expression for Immune Checkpoint Inhibitors in Advanced Non-Small-Cell Lung Cancer Patients. *Front Immunol.* 2021 Apr 16;12:665133. doi: 10.3389/fimmu.2021.665133. eCollection 2021. PMID: 33936103

Yi L, Wang X, Fu S, Yan Z, Ma T, Li S, Wei P, Zhang H, Wang J. Association between response to anti-PD-1 treatment and blood soluble PD-L1 and IL-8 changes in patients with NSCLC. *Discov Oncol.* 2023 Mar 29;14(1):35. doi: 10.1007/s12672-023-00641-2. PMID: 36991160

**Z**amora Atenza C, Anguera G, Riudavets Melià M, Alserawan De Lamo L, Sullivan I, Barba Joaquin A, Serra Lopez J, Ortiz MA, Mulet M, Vidal S, Majem M. The integration of systemic and tumor PD-L1 as a predictive biomarker of clinical outcomes in patients with advanced NSCLC treated with PD-(L)1blockade agents. *Cancer Immunol Immunother.* 2022 Aug;71(8):18231835. doi: 10.1007/s00262-021-03107-y. Epub 2022 Jan 5. PMID: 34984538

Zaretsky JM, Garcia-Diaz A, Shin DS, Escuin-Ordinas H, Hugo W, Hu-Lieskovan S, Torrejon DY, Abril-Rodriguez G, Sandoval S, Barthly L, Saco J, Homet Moreno B, Mezzadra R, Chmielowski B, Ruchalski K, Shintaku IP, Sanchez PJ, Puig-Saus C, Cherry G, Seja E, Kong X, Pang J, Berent-Maoz B, Comin-Anduix B, Graeber TG, Tumeh PC, Schumacher TN, Lo RS, Ribas A. Mutations Associated with Acquired Resistance to PD-1 Blockade in Melanoma. *N Engl J Med.* 2016 Sep 1;375(9):819-29. doi: 10.1056/NEJMoa1604958. Epub 2016 Jul 13. PMID: 27433843

Zarling AL, Luckey CJ, Marto JA, White FM, Brame CJ, Evans AM, Lehner PJ, Cresswell P, Shabanowitz J, Hunt DF, Engelhard VH. Tapasin is a facilitator, not an editor, of class I MHC peptide binding. *J Immunol.* 2003 Nov 15;171(10):5287-95. doi:10.4049/jimmunol.171.10.5287. PMID: 14607930

Zhang J, Babic A. Regulation of the MET oncogene: molecular mechanisms. *Carcinogenesis*. 2016 Apr;37(4):345-55. doi: 10.1093/carcin/bgw015. Epub 2016 Feb 10. PMID: 26905592

Zhang J, Gao J, Li Y, Nie J, Dai L, Hu W, Chen X, Han J, Ma X, Tian G, Wu D, Shen L, Fang J. Circulating PD-L1 in NSCLC patients and the correlation between the level of PD-L1 expression and the clinical characteristics. *Thorac Cancer*. 2015 Jul;6(4):534-8. doi: 10.1111/1759-7714.12247. Epub 2015 Mar 5. PMID: 26273411

Zhao F, Xiao C, Evans KS, Theivanthiran T, DeVito N, Holtzhausen A, Liu J, Liu X, Boczkowski D, Nair S, Locasale JW, Hanks BA. Paracrine Wnt5a-beta-Catenin Signaling Triggers a Metabolic Program that Drives Dendritic Cell Tolerization. *Immunity*. 2018 Jan 16;48(1):147-160.e7. doi: 10.1016/j.jimmuni.2017.12.004. PMID: 29343435

Zhao J, Zhang P, Wang J, Xi Q, Zhao X, Ji M, Hu G. Plasma levels of soluble programmed death ligand-1 may be associated with overall survival in nonsmall cell lung cancer patients receiving thoracic radiotherapy. *Medicine (Baltimore)*. 2017 Feb;96(7):e6102. doi: 10.1097/MD.0000000000006102. PMID: 28207525

Zhou C, Tang KJ, Cho BC, Liu B, Paz-Ares L, Cheng S, Kitazono S, Thiagarajan M, Goldman JW, Sabari JK, Sanborn RE, Mansfield AS, Hung JY, Boyer M, Popat S, Mourão Dias J, Felip E, Majem M, Gumus M, Kim SW, Ono A, Xie J, Bhattacharya A, Agrawal T, Shreeve SM, Knoblauch RE, Park K, Girard N; PAPILLON Investigators. Amivantamab plus Chemotherapy in NSCLC with EGFR Exon 20 Insertions. *N Engl J Med*. 2023 Nov 30;389(22):2039-2051. doi: 10.1056/NEJMoa2306441. Epub 2023 Oct 21. PMID: 37870976

Zhou S, Yang H. Immunotherapy resistance in non-small-cell lung cancer: From mechanism to clinical strategies. *Front Immunol*. 2023 Apr 6;14:1129465. doi: 10.3389/fimmu.2023.1129465. eCollection 2023. PMID: 37090727

Zhu HB, Song X. Analysis of soluble programmed death-1 ligand-1 of lung cancer patients with different characteristics. *Eur Rev Med Pharmacol Sci*. 2023 Sep;27(18):8690-8696. doi: 10.26355/eurrev\_202309\_33792. PMID: 37782182

Zingg D, Arenas-Ramirez N, Sahin D, Rosalia RA, Antunes AT, Haeusel J, et al. . The histone methyltransferase Ezh2 controls mechanisms of adaptive resistance to tumor immunotherapy. *Cell Rep* 2017;20:854-67

Zizzari IG, Di Filippo A, Scirocchi F, Di Pietro FR, Rahimi H, Ugolini A, Scagnoli S, Vernocchi P, Del Chierico F, Putignani L, Rughetti A, Marchetti P, Nuti M, Botticelli A, Napoletano C. Soluble Immune Checkpoints, Gut Metabolites and Performance Status as Parameters of Response to Nivolumab Treatment in NSCLC Patients. *J Pers Med*. 2020 Nov 4;10(4):208. doi: 10.3390/jpm10040208. PMID: 33158018

<https://ecog-acrin.org/resources/ecog-performance-status/>

<https://clinicaltrials.gov/study/NCT04928846>, accessed 14<sup>th</sup> of October 2024

<https://gco.iarc.fr/today/en>

<https://sante.gouv.fr/fichiers/bo/2003/03-40/a0403145a2.pdf>

<https://www.cancer.gov/publications/dictionaries/cancer-terms/def/immune-checkpoint-inhibitor>

[ourworldindata.org/cancer](http://ourworldindata.org/cancer)

[https://www.has-sante.fr/jcms/p\\_3471682/fr/opdivo-nivolumab-cbnpc-cancer-bronchique-non-a-petites-cellules](https://www.has-sante.fr/jcms/p_3471682/fr/opdivo-nivolumab-cbnpc-cancer-bronchique-non-a-petites-cellules),

[https://www.has-sante.fr/upload/docs/application/pdf/2024-06/avis\\_anسم\\_opdivo\\_juin\\_2024.drd\\_refus.pdf](https://www.has-sante.fr/upload/docs/application/pdf/2024-06/avis_anسم_opdivo_juin_2024.drd_refus.pdf)

[Https://www.santepubliquefrance.fr/maladies-et-traumatismes/cancers#:~:text=L'estimation%20du%20nombre%20total,9%20000%20et%208%20000](https://www.santepubliquefrance.fr/maladies-et-traumatismes/cancers#:~:text=L'estimation%20du%20nombre%20total,9%20000%20et%208%20000)